THE CLINICAL IMPACT OF INTRAVASCULAR ULTRASOUND DERIVED VIRTUAL HISTOLOGY ON PERCUTANEOUS CORONARY INTERVENTION.

A thesis submitted in accordance with the requirements of the University of Liverpool for the degree of Doctor of Medicine

Scott Warnock Murray

Student ID: 200639283

March 2016

For Sylvia, Alexander and Ewan

In memory of: *James "Jimmy" Murray*

Euphaemia Murray

Moses Warnock

Agnes Warnock

.

"A blind man knows he cannot see, and is glad to be led; but he that is blind in his understanding, believes he sees best and scorns guidance"

Samuel Butler (1835-1902)

"A recipe for ignorance is to be satisfied with your opinions and content with your knowledge, but the greatest ignorance is to reject something you know nothing about"

Elbert Hubbard (1856-1915)

"Experience is what you get, when you don't get what you want"

Dan Stanford

Abstract

It has been shown that early interventional treatment of patients with high risk acute coronary syndromes (ACS) has a favourable effect on mortality. It is also known that coronary plaque rupture and atherothrombosis creates a mileu of necrotic and thrombotic material, which is difficult to treat. Moreover, angiographic assessment of coronary artery disease is highly flawed; 2-dimensional luminal silhouettes are not ideal templates to guide very important interventions. Intravascular ultrasound (IVUS) is the gold standard imaging tool able to delineate vessel dimensions, plaque burden, length and now with virtual histology (VH) - plaque composition. Despite optimal medical care and urgent revascularisation, 12-20% of ACS patients will suffer a further major adverse cardiac event (MACE) at 30 months.

Our aim was to evaluate the angiographic treatment of high risk ACS patients by performing IVUS-VH pre and post-intervention, with the operators blinded to the images. Our hypotheses for this work were as follows:

1. Significant compositional and structural differences exist between culprit, non-culprit and stable plaques when analysed by Virtual Histology.

2. The histologically most unstable plaque does not occur at the site of maximum angiographic stenosis (in culprit lesions).

3. Angiographically guided stent length selection and positioning is flawed, leaving unstable plaque behind in the reference segments.

Following recruitment, 135 lesions split into: 70 ACS culprit; 20 ACS non-culprit and 35 Stable lesions underwent analysis for inter-observer and intra-observer variability. We were able to show good standard markers of correlation but a large repeatability co-efficent, for some outputs from the analysis. This has raised questions with regard to the ability of the technique to detect differences between plaque types.

In relation to our main hypothesis, we have been able to show structural and compositional volume differences between "active" ACS plaques (n=70) and "stable" angina plaques (n=35). We have used the most important of these to generate a plaque risk score based upon ROC statistics and logistic regression. The most important discriminators were: Remodelling index at the minimum lumen area; Plaque Burden; Presence of VH-TCFA; minimum lumen area (MLA) $<4mm^2$ and necrotic core to dense calcium ratio (NC/DC). The subsequent risk model was tested on an independent, blinded cohort of plaques from the Thoraxcentre, Rotterdam (n=50). This confirmed good discriminatory power for the equation (AUC – 0.71). Within this hypothesis we also explored the differences in individual areas of plaque. At two separate sites (MLA and MAX NC) in each lesion type (ACS and stable) n=210, we showed that the MAX NC site lies proximal to the MLA in most cases and contains more positively remodelled plaque disease with less calcification. This is important as positively remodeled plaque disease is often not visible on a plain coronary angiogram when treating ACS lesions.

Finally, as a follow on from thie previous chapter, we examined the treatment of ACS lesions by blinded IVUS examination. The operator completed their stent procedure with only angiographic guidance. We were able to show in 56 ACS lesions that systematic errors of judgement occur related to sizing of the vessel, the choice of stent sizes and the subsequent stent deployment. 36%, 40% and 65.5% of stents met three separate standard criteria for good stent deployment. Moreover, between 5-40% of stents had some form of significant abnormality. With regard to the sizing of stents to the vessel, the mean reference vessel size was 10.58mm^2 ($\pm$2.51) yet the minimum stent area achieved was only 6.79mm^2 ($\pm$2.43). If the stent that was chosen had been symmetrically deployed to its nominal size (e.g 2.5; 3.0; 3.5) then the stent area achievable should have been 8.87mm^2 ($\pm$2.68). This has allowed us to calculate for the first time an estimated "under deployment area". This was 2.08mm^2 ($\pm$1.87).

In conclusion we have shown that IVUS-VH can help discriminate active ACS plaques from stable angina plaques and can formulate a plaque risk score to aid plaque identification in the future. We have characterized the longitudinal anatomy of the ACS plaque and how this impacts on the percutaneous treatment of these lesions. We have also confirmed that angiography alone, as a guide for the treatment of ACS lesions, leads to systematic sizing and placement errors. These could have an affect on long term outcomes, in both the stent and the stented vessel. Our findings have added to the literature on this subject and provided some hypothesis generating conclusions that could be taken forward to improve the recognition and appropriate treatment of high risk plaques in the future.

Acknowledgements

It was in 2004 during my time as a Clinical Fellow in Cardiology, that I attended an evening symposium concerned with the treatment of Acute Coronary Syndromes. The speaker that night was Dr Nick Palmer and as he showed slides of IVUS and talked about the flaws of angiography, my interest was immediate. The final slide showed the "next big step" in lesion assessment – Virtual Histology. This could give us the ability to become pathologists (*in-vivo*) and to use this information to potentially identify plaques prone to rupture.

I therefore reserve the greatest of my thanks for Nick. He above everyone else supported my aggressive, weekly enquiries about starting research in this area. He put forward our proposals for the research post and believed in me as the best person for the job. Nick, for all of your direction, supervision, encouragement and friendship, I thank you whole-heartedly. I am also indebted to Prof George Hart for early supervision and sound academic advice. Major thanks must also go to Dr Rod Stables for constant advice, support and teaching. Rod, you continue to be an inspiration – it has been a great privilege to work with you and learn the right way to do things. This work would not have been possible without the support that came from The Liverpool Heart and Chest Hospital and the other operators and teams in the cardiac catheter labs.

The unrelenting love from my parents reminds me of what is truly important in life and without you, I am nothing. You gave me life and an environment in which I

could flourish, I owe you everything. I must also thank my in-laws, Heather and Glyn Foulkes, for all their encouragement over the years and for letting me work (in peace) above their garage in Norfolk.

Lastly, but certainly not least, the majority of the thanks must go to my wife, Sylvia. Thanks for putting up with me and my job. Without your support, patience, companionship and love; this thesis would never have been written. You, Alexander and Ewan remain to be my reason for living and striving to succeed.

March 2016

I confirm that, under the supervision of Dr Nicholas D Palmer, Dr Rodney H Stables and Professor George Hart, I was responsible for the design and completion of all the theory and studies contained within this thesis. This thesis was written by myself and has not been submitted for any other degree or professional qualification.

Dr Scott W Murray **Student I.D. 200639283** **March 2016**

Chapter I: Background: IVUS in Interventional cardiology

1.1.1 Introduction

1.1.2 Coronary artery disease

1.1.3 Epidemiology

1.1.4 Pathophysiology

1.2 Interventional cardiology

1.2.1 Initial developments

1.2.1.1 Problems with "plain old balloon angioplasty" (POBA)

1.2.1.2 Stent Technology

1.2.1.3 Problems with Stents

1.3.1.1 IVUS

1.3.1 Background

1.3.2 Adjunct to stent implantation

1.3.3 Grey-scale IVUS guidance in the bare metal stent era.

1.3.4. IVUS guidance of drug-eluting stent placement.

1.3.5 Rccent updates to the IVUS evidence

1.3.6 IVUS based tissue characterisation

Chapter II: Introduction: Virtual Histology and Acute Coronary Syndromes

2.1 Introduction

2.1.1 The Technology

2.1.2 Validity

2.1.3 Tissue Types

2.1.3.1 Fibrous

2.1.3.2 Fibrofatty

2.1.3.3 Necrotic core

2.1.3.4. Dense calcium

2.2 How can IVUS-VH improve our knowledge about coronary disease?

- 2.2.1 Plaque Risk Assessment
- 2.2.2 Adaptive and Pathological intimal thickening (AIT)/(PIT)
- 2.2.3 Fibroatheroma (FA)
- 2.2.4 Fibrocalcific plaque

2.2.5 Thin Cap Fibroatheroma (TCFA): The vulnerable plaque.

2.3 Can IVUS-VH influence coronary intervention?

2.4 Investigating the utility of IVUS-VH analysis in ACS.

2.5 Previous clinical studies assessing and utilising IVUS-VH in ACS

2.6 IVUS-VH Current Limitations

2.7 More recent large trials in IVUS-VH utility

2.7.1 Prospect, VIVA, Atheroemo and VIVA sub-studies

3.4 Exclusion Criteria

3.5 Procedural Methods

3.5.1 Statistics

3.6 Recruitment

3.6.1 Methods

3.6.2 Limitations

Chapter IV – Study I: The intra and inter-observer agreement of IVUS-VH analyses for qualitative and quantitative lesion assessment

Chapter V - Study II: The Creation and Validation of a Plaque Discrimination Score from the Anatomical and Histological Differences in Coronary Atherosclerosis.

Chapter VI - Study III: Observable patterns of site-specific plaque morphologies by IVUS-VH: The relationship between maximum necrotic core site and minimum lumen area with implications for the identification of vulnerable plaque phenotypes.

6.1 Introduction

6.2 Methods

6.2.1 Methods of detailed plaque analysis using Virtual Histology

6.2.2 Statistics and power calculation

6.3 Results

6.4 Discussion

6.5 Limitations

6.6 Conclusion

Chapter VII - Study IV: The Intravascular Relationship of Proximal Unstable Plaque Components to the Minimum Lumen Area Stenosis: Implications for Coronary Stent Implantation.

7.1 Introduction

7.2 Study Objectives

7.2.1 Hypotheses:

7.3 Methods

7.4 Statistics and Power

7.5 Results

7.6 Discussion

7.7 Limitations

7.8 Conclusions

Chapter VIII – Study V: Observations of angiographically guided stent selection and placement during percutaneous coronary intervention for acute coronary syndromes: The potential influence of IVUS-VH assessment.

Chapter IX - Final Summary Discussion and Conclusion

Bibliography

Appendices

FIGURES

CHAPTER I

CHAPTER II

CHAPTER IV

CHAPTER V

CHAPTER VI

CHAPTER VII

TABLES

CHAPTER I

CHAPTER II

CHAPTER IV

CHAPTER V

CHAPTER VI

CHAPTER VII

Publications from the work in this thesis

The work involved for this thesis has produced the following publications:

1. Virtual Histology Imaging in Acute Coronary Syndromes: Useful or just a research tool?

   Murray SW, Stables RH, Palmer ND

   J Invas Cardiol 2010; 22: 84-91

2. Virtual Histology Imaging in Acute Coronary Syndromes.

   Murray SW, Stables RH, Palmer ND

   Cath Lab Digest May 2010 Vol 8.

3. From Patient to Plaque: Contemporary Coronary Imaging

   Part 1: IVUS derived Virtual Histology

   Murray SW, Rathore S, Stables RH, Palmer ND

   Br J Cardiol 2010; 17:129-32

4.. How to Treat? A spontaneously reperfused STEMI with plaque involving left main stem and proximal LAD.

   Murray SW, Periaswamy V, Ramsdale DR

   Eurointervention 2010 Feb;6(7):895-9

5. Measuring the magnitude of measurement error in the virtual histology analysis of acute coronary syndrome plaques.

   Murray SW, Stables RH, Hart GW, Palmer ND

   European Heart J Cardiovas Imaging *2013 Vol. 62(2)167-74*

6. Construction and validation of a plaque discrimination score from the anatomical and histological differences in coronary atherosclerosis: The Liverpool *IVUS-V-HEART* Study (*I*ntra *V*ascular *U*ltra*S*ound-*V*irtual-*H*istology *E*valuation of *A*therosclerosis *R*equiring *T*reatment)

   Murray SW, Stables RH, Garcia-Garcia HM, Grayson AD, Shaw MA, Perry RA, Serruys PW, Palmer ND.

   Eurointervention, 2014 – Published online ahead of print

7. Site Specific Intravascular Ultrasound analysis of remodelling index and calcified necrosis patterns reveals novel blueprints for coronary plaque instability.

   Murray SW; Patel B; Stables RH; Perry RA; Palmer ND

   Cardiovasc Diagn Ther, 2014 vol. 4 (4) pp. 287-98

Publications (Abstracts)

1. Operator Blinded Virtual histology Intravascular ultrasound Observations of Usual Stenting practice in Acute Coronary Syndromes: The OBVIOUS-ACS study.
   SW Murray, RH Stables, G Hart, RA Perry, ND Palmer

   J Am Coll Cardiol 2013 (TCT Supplement)

2. Defining the True Threshold Of Measurement Error in the Volumetric Virtual Histology Analysis of High Risk Plaques: Important Implications for the Serial Study of Plaque Composition
   SW Murray, RH Stables, G Hart, RA Perry, ND Palmer

   J Am Coll Cardiol 2010 56: B82

3. The Prevalence of Luminal Stress Interface Mismatch Points On Virtual Histology Analysis is an Accurate Indicator Of Plaque Vulnerability: Insights From the ***V-HEART*** Study
   SW Murray, RH Stables, G Hart, RA Perry, ND Palmer
   J Am Coll Cardiol 2010 56: B15-B16

4. Are non-culprit coronary lesions safe? Preliminary results from the ***V-HEART*** observational study.
   SW Murray, RH Stables, G Hart, RA Perry, ND Palmer

   European Heart Journal, Aug 2010; 31. 797

5. Plaque vulnerability is an important feature of chronic stable coronary disease: A comparison of lesion characteristics in stable angina patients and acute coronary syndromes using Virtual Histology.
   SW Murray, RH Stables, G Hart, RA Perry, ND Palmer

   European Heart Journal, Aug 2010 (31) 613-614.

6. Finding the culprit of the culprit lesion: The relationship between maximum necrotic core site and minimum lumen area using virtual histology.
   SW Murray, RH Stables, G Hart, RA Perry, ND Palmer

   Heart, June 2010; 96 (11) supp 1 A62

7. The Plaque Vulnerability Index calculated by Necrotic Core to Dense Calcium Ratio differs across the spectrum of Coronary Artery Disease: Insights from Intravascular Ultrasound Tissue Characterisation
   SW Murray, RH Stables, G Hart, RA Perry, ND Palmer

   Eurointervention, May 2010; 8(6) H55

8. Is Volumetric Plaque Characterisation By Intravascular Ultrasound Based Virtual Histology (IVUS-VH) Reliable In Serial Studies? An Analysis Of Intra And Inter-observer Variability In The Culprit Lesion Assessment Of Acute Coronary Syndrome Patients.
   SW Murray, Hamilton C, Perry RA, Palmer ND.

   Catheterization and Cardiovascular Interventions*, May 2009 volume 73, pg 61 D-8*

Publications (Letters/Case Reports/Editorials)

1. The Intravascular Ultrasound and Virtual Histology Interpretation of Plaque Rupture and Thrombus in Acute Coronary Syndromes.

Murray SW, Palmer ND

Heart 2009;**95**:1494

2. What is behind the calcium? The relationship between calcium and necrotic core on virtual histology analyses.

Murray SW, Palmer ND

EHJ 2009 30, 125-126

3. Segmental coronary endothelial dysfunction in patients with minimal atherosclerosis is associated with necrotic core plaques.

Murray SW, Palmer ND

Heart 2010;96:550-551

4. "Seek and you shall find": Angiographically silent left main stem plaque rupture with residual filamentous LAD thrombus (found by IVUS and Pronto extraction)

Murray SW, Kunadian B, Fisher M

EuroIntervention 2009 Vol 5; No 5

7. A peculiar case of very late re-stenosis in a drug eluting stent.

S W Murray, M Andron, R A Perry and N D Palmer.

Am Heart Hosp J. 2011; 9(1):63-4

8. Double Jeopardy: Multi-modality imaging of monozygotic "twin cap" atherosclerosis.

Murray SW; Cooper RM; Appleby C; McCann C; Binukrishnan S; Radu M; Stables RH

Atherosclerosis; 2014 vol. 237 (1) pp.264-267

9. Evading the fate of Pheidippidies: Coronary thrombosis in a young marathon runner with minimal atherosclerosis but sickle cell trait.
Murray SW; Cooper RM; Mills JD; Palmer ND.
Cardiovasc Diagn Ther, 2015 – In press

Abbreviations/Glossary

ACS	acute coronary syndromes
AMI	acute myocardial infarction
AVID	Angiography Versus Intravascular ultrasound Directed coronary stent placement [study]
CABG	coronary artery bypass grafting
CCS	Canadian Cardiovascular Society
CI	confidence interval
CRUISE	Can Routine Ultrasound Influence Stent Employment [study]
CSA	cross-sectional area
CT	computed tomography
CUDA	calculated under deployment area
EEM	external elastic membrane
ICC	intra class correlation co-efficient
IDDM	insulin-dependent diabetes mellitus
IVUS	intravascular ultrasound
LAD	left anterior descending [coronary artery]
LCx	left circumflex coronary artery
LMS	left main coronary artery
LMWH	low molecular weight heparin
LVEF	left ventricular ejection fraction
MACE	major adverse cardiac event
MI	myocardial infarction
MLA	minimum lumen area
MLD	minimal lumen diameter

MSA	minimum stent area
MRI	magnetic resonance imaging
MUSIC	Multicenter Ultrasound Stenting in Coronaries [study]
NIDDM	non-insulin dependent diabetes mellitus
NIRS	near infra-red spectroscopy
OCT	optical coherence tomography
OPTICUS	Optimization with ICUS to reduce stent restenosis [study]
PCI	percutaneous coronary intervention
POBA	plain old balloon angioplasty
QCA	quantitative coronary angiography
RCA	right coronary artery
RCO	repeatability co-efficient
RCT	randomised controlled trial
RR	relative risk
SD	standard deviation
SE	standard error
TLR	target lesion revascularisation
VH	Virtual Histology
WSSD	within subject standard deviation

Chapter I

Background

IVUS in Interventional cardiology

1.1.1 Introduction

Intravascular ultrasound (IVUS) is the generic name for any ultrasound technology used *in-vivo* within blood vessels. IVUS has evolved into an adjunct to interventional cardiology and it is this role that forms the basis for investigation in this thesis. This introductory information describes the technology from its inception and places it in its current clinical context, especially in relation to contemporary interventional cardiology. Initially, background descriptions are provided of coronary artery disease and the development of invasive cardiology. This will allow a more adequate understanding of the basis for the main research questions. Chapter II will then deal with an overview of the latest technology, as IVUS continues to evolve.

1.1.2 Coronary artery disease

The coronary arteries are the blood vessels that carry oxygenated blood to the myocardium (the muscle of the heart) and they arise from the aorta just above the aortic valve. There are usually two, the left and the right. The left divides into two branches, the left anterior descending (LAD) and the circumflex (LCx), and these further subdivide into a series of branches that supply predominantly the left ventricle. The initial part of the left coronary artery before it divides is known as the left main stem (LM). The right coronary artery (RCA) supplies the right ventricle and a variable amount of the inferior surface of the left ventricle. Coronary artery disease is the development of narrowings (stenoses) in the walls of the coronary arteries caused by deposits of atheroma (a collection of lipid, collagen and inflammatory cells in the artery wall) that eventually leads to partial or complete obstruction of normal

blood flow and the development of myocardial ischaemia. Atheroma of the coronary arteries presents in a variety of ways, including stable or unstable angina, acute myocardial infarction (AMI) or sudden death. These events can be described by the acronym MACE (major adverse cardiac event) and are: death, ST elevation myocardial infarction (STEMI), non-ST elevation myocardial infarction (NSTEMI) and revascularisation. The pain of myocardial ischaemia is characterised by a heavy, pressing chest pain that may be mistaken for indigestion, but also typically radiates to the jaw or left arm. The major difference between unstable angina and MI is the presence of myocardial cell death or necrosis with infarction, usually defined by blood analysis for the myocyte protein troponin. In recent years it has become increasingly clear that these are different expressions of the same underlying pathophysiological process, namely plaque rupture or erosion and partial or total coronary occlusion, which may be transient or permanent [Falk et al 1983, Virmani et al 2000]. Atherosclerosis is a lipoprotein-driven disease that leads to plaque formation at specific sites of the arterial tree through intimal inflammation, necrosis, fibrosis, and calcification. After decades of indolent progression, such plaques may suddenly cause life-threatening coronary thrombosis presenting as an acute coronary syndrome. Most often, the culprit morphology is plaque rupture with exposure of highly thrombogenic, red cell–rich necrotic core material. The permissive structural requirement for this to occur is an extremely thin fibrous cap, and thus, ruptures occur mainly among lesions defined as thin-cap fibroatheromas. Also common are thrombi forming on lesions without rupture (plaque erosion), most often on

pathological intimal thickening or fibroatheromas. However, the mechanisms involved in plaque erosion remain largely unknown, although coronary spasm is suspected. The calcified nodule has been suggested as a rare cause of coronary thrombosis in the highly calcified arteries of older individuals.

However, It is clear from autopsy studies that these manifestations of coronary artery disease form part of a spectrum, with substantial overlap. [Burke et al 1997; Kolodgie et al 2004]

1.1.3 Epidemiology

Heart and circulatory disease is the UK's biggest killer. In 2007, cardiovascular disease (CVD) caused 34% of deaths in the UK and killed just over 193,000 people. Coronary heart disease, the main form of CVD, causes over 90,000 deaths a year in the UK: approximately one in five deaths in men and one in six deaths in women. Although death rates for CHD have been falling rapidly in the UK since the late 1970s, they are still amongst the highest in Western Europe [Allender *et al* BHF statistics 2008]**.** Data from the 2006 Health Survey for England suggest the prevalence of CHD in England was 6.5% in men and 4.0% in women. Prevalence rates increase with age, with more than 1 in 3 men and around 1 in 4 women aged 75 and over living with CHD. Although recently deaths from heart and circulatory disease are falling, it remains the biggest killer in the UK.

- Almost 1 in 5 men and 1 in 8 women die from heart disease.
- Heart Disease is responsible for 82,000 deaths in the UK each year, an average of 224 people each day.
- More than 26,000 people under the age of 75 in the UK died from Heart Disease in 2009
- There are nearly 2.7 million people living with heart disease in the UK.
- There are more than 1.6 million men and more than a million women with heart disease in the UK.
- Death rates from heart disease are highest in Scotland and northern England and lowest in southern England.
- The UK spends 3.2 billion each year on healthcare costs for heart disease.
- Most deaths from heart disease are caused by a heart attack.
- There are around 124,000 heart attacks in the UK each year.
- Around 62,000 men and 39,000 women in England suffer a heart attack each year.
- In England, around 11% of men and 15% of women who were admitted to hospital with a heart attack die within 30 days.
-

- The chances of dying from a heart attack increases with age and is higher in women than men.
- We estimate there are around 1,000,000 men and nearly 500,000 women living in the UK who have had a heart attack. More than 900,000 of these are under the age of 75.
- In Scotland, the number of heart attacks each year has decreased by around 25 per cent between 2000 and 2009 in both men and women, but is between 20 per cent and 35 per cent higher than England's incidence level.
- Every six minutes someone dies of a heart attack in the UK.
- One in three people who have a heart attack die before reaching hospital.

1.1.4 Pathophysiology

The fundamental processes underlying coronary atheroma are endothelial dysfunction, lipid accumulation and smooth muscle cell proliferation [*Yusuf S et al 2001, Virmani et al 2006*]. As the atheromatous plaque enlarges, the vessel grows to accommodate this by remodelling positively. This process is an attempt to prevent luminal narrowing and blood flow disturbance. This growth, highlighted first by *Glagov et al* in 1987, (figure 1.1) can continue until the vessel has grown by 40% of its original size. Further plaque enlargement, at this stage, results in luminal encroachment and eventually blood flow is restricted. A stenosis of more than 50% can be of haemodynamic significance, with compromise to coronary flow with effort. As myocardial work increases, for example, with exercise, myocardial oxygen demand increases. This is normally accommodated by an increase in coronary blood flow. However, as demand exceeds supply, the myocardium becomes ischaemic and angina is the symptomatic expression of this. Nevertheless, not all ischaemia causes angina. The threshold at which ischaemia causes pain varies between patients and most have episodes of silent ischaemia that are unaccompanied by pain. In some patients all ischaemic episodes may be silent. The acute coronary syndromes (NSTEMI and STEMI) occur when coronary plaque erodes or ruptures. The lining of the coronary artery overlying the plaque (the endothelium) tears and exposes the plaque core to the flowing blood. The plaque core contains a variety of highly thrombogenic substances and through the processes of platelet aggregation and fibrin formation, the lumen becomes acutely narrowed or occluded.

This causes a sudden severe reduction in blood flow with resultant myocardial ischaemia at rest, presenting as unstable angina. If the vessel becomes partially or completely occluded or distal embolisation of plaque occurs, and this is sustained, then myocardial tissue may die. This is MI (NSTEMI or STEMI). The precise process of atherogenesis is multiple and complex but is being unlocked slowly be scientific and molecular advances. However, a variety of factors are associated with an increased risk of developing coronary artery disease. [*Dawber et al 1959, Lloyd-Jones et al 2010*] The best characterised of these are smoking, diabetes mellitus, hypertension, hypercholesterolaemia and a family history of premature coronary artery disease. Patients with one or more of these abnormalities are more likely to develop angina or have a myocardial infarction. Based on the Framingham data [*Wilson et al 1998, D'Agostino et al 2000*], there are now risk functions by which the possibility of death or non-fatal MI can be estimated over a 10-year period for patients with various constellations of risk factors. [*Wilson et al 1998*]

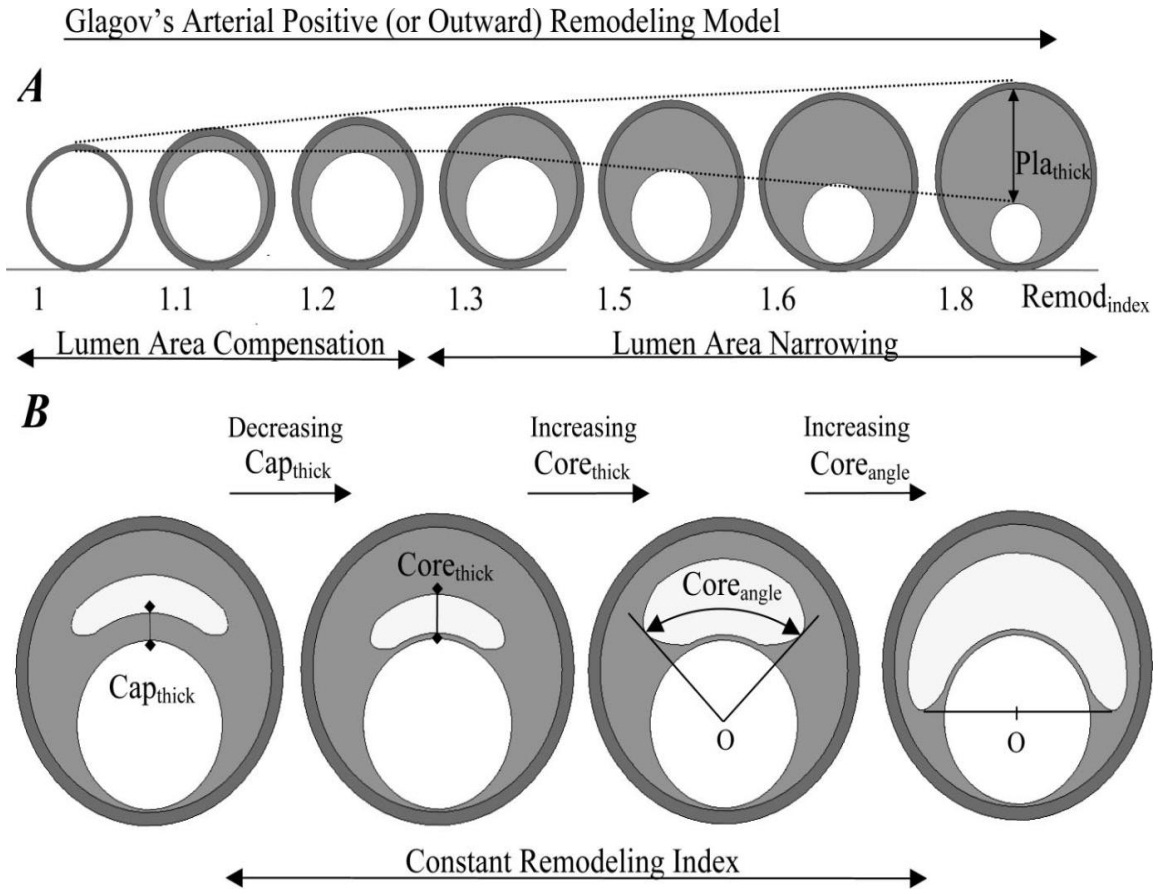

Figure 1.1: Graphical representation of the Glagov phenomenon. (Adapted from Volcano Corporation Slide set (permission granted))

1.2 Interventional cardiology

1.2.1 Initial developments

Mason Sones first carried out selective coronary angiography in October 1958. Some 20 years later, in September 1977, Andreas Gruentzig carried out the first percutaneous transluminal coronary angioplasty (PTCA) in Zurich, Switzerland. Subsequently, there has been an exponential growth, both in the range of techniques and their indications. The number of percutaneous coronary interventions (PCI) carried out annually in the UK is now 94,000 nearly five times more than a decade ago. This number is currently increasing at a rate of 5% per year. [*Ludlam et al 2009*].

The concept of PCI is fundamentally simple. The coronary artery is selectively engaged with a guide catheter (a one metre length of tubing with a diameter slightly over 2 mm), which has been introduced into the arterial circulation via either the femoral or radial artery. A guide wire (0.014 inches or 0.36 mm in diameter) is passed up the catheter to the coronary artery and steered into the artery and across the stenosis. An appropriately sized balloon catheter is then passed over the wire so that it follows into the narrowing. The balloon is inflated to somewhere between 4 and 16 atmospheres. The aim is for the stenosis to have been reduced following dilatation and to remove haemodynamic significance.

As originally conceived by Gruentzig [*Gruentzig et al 1987*], this was applied to patients with limiting chronic stable angina and discrete stenoses in a single coronary artery (usually the LAD). In subsequent years, the complexity and number of lesions

and vessels subjected to angioplasty have expanded. Interventions are now undertaken in saphenous vein grafts, multivessel disease and chronic total occlusions (CTOs). They are also undertaken urgently in patients with acute STEMI and NSTEMI. Even some unprotected left main stem disease with concomitant three vessel disease is able to be treated safely now by the interventional cardiologist.[*Serruys et al 2009*] This diversification has only been possible because of the dramatic improvements and research into the technology of interventional cardiology, with improved guide catheters and balloons, steerable guidewires and additional devices, such as bare metal and drug eluting stents, rotational atherectomy, thrombus aspiration and better imaging with digital systems and IVUS.

1.2.2 Problems with "plain old" balloon angioplasty (POBA)

As experience grew, it became apparent that there were problems such as acute recoil and restenosis associated with POBA. IVUS development helped address these issues and provide solutions [*Mintz et al 1996, Stone et al 1997*]. It became apparent that lesion characteristics influence the outcome of POBA [*Kornowski et al 1997, Gil R et al 1996, Baptista et al 1996*]. For example, Short discrete concentric lesions are more likely to respond successfully to angioplasty than long, eccentric calcified ones [*Tenaglia et al 1992, Jain et al 1994*]. Lesion dissection, recoil and acute occlusion was common. A variety of devices were therefore developed to deal with some of these problems. This often involved some form of 'debulking' in which the burden of atheroma in the vessel is reduced prior to angioplasty.The choice of

device might have been guided, back then, by information acquired using IVUS [*Weissman et al 1995, Mintz et al 1994*].

1.2.3 Stent Technology

The introduction of intra-coronary stents has revolutionised the practice of interventional cardiology. Stents are endoprosthetic scaffolding devices, usually metallic and based on a slotted tube or a coil design. They are deployed on a balloon and inflation of the balloon expands the stent against the wall of the coronary artery. Stents seal dissections, provide radial strength to combat recoil and create a rounder, smoother channel within the vessel, enlarging the lumen. In the early days, stents had limited application because they were unwieldy and not easily deployed into tortuous vessels or complex lesions. However, there has been exponential development in stent design and they now come in a range of diameters and lengths, pre-mounted on dedicated balloons. Initially, stents were used to treat arteries that had become acutely occluded during angioplasty (bail-out stenting) [*Sigwart et al 1987 and 1988, de Feyter et al 1991*]. Subsequently, in 1994, they were shown to reduce restenosis rates in certain lesion subsets in both the BENESTENT and STRESS trials [*Serruys et al 1994, Fischman et al 1994*] Stenting practice was again modified when IVUS was used to evaluate the success of stent deployment [*Goldberg et al 1994, Hall et al 1994*]. IVUS demonstrated that many stents were not fully deployed at conventional dilation pressures (6–8 atmospheres). A subsequent high-pressure deployment strategy, with bigger post-dilatation balloons, achieved better results,

reducing stent thrombosis and in-stent restenosis. [*Colombo et al 1995, Werner et al 1997*] and this has now become standard practice.

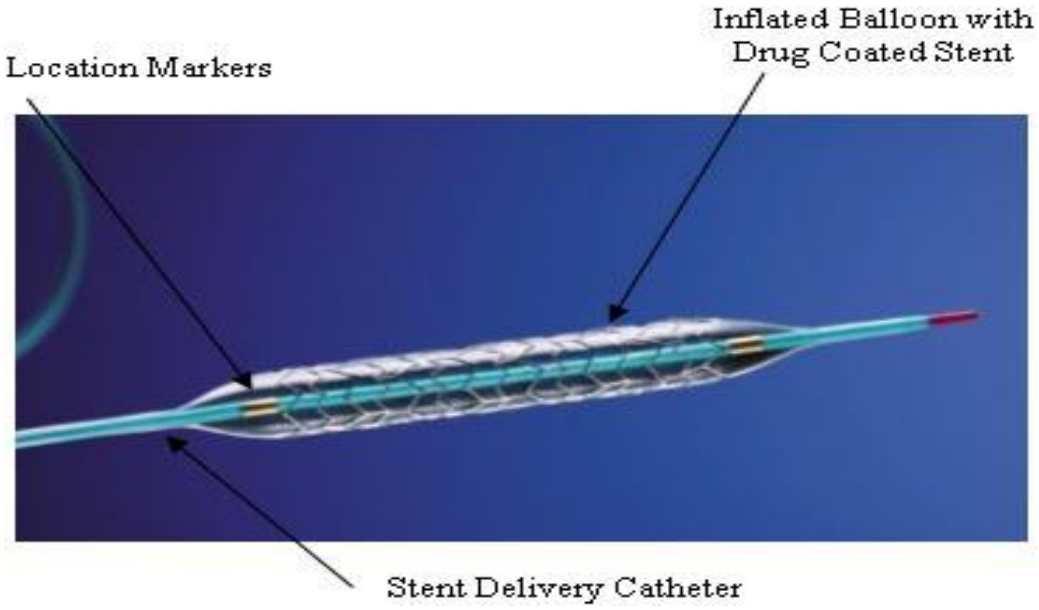

Figure 1.2: Example of an inflated coronary stent on the delivery balloon (adapted from Wikipedia)

1.2.4 Problems with Stents

While Bare Metal Stents (BMS) reduced the re-stenosis rate in appropriate lesion subsets, they did not abolish it [*Hoffman et al 1996 and 1997, Kastrati et al 1995*]. The subsequent reduction in MLD due to new tissue growth (neo-intimal hyperplasia) within the stent created the phenomenon of "late loss" in around one third of patients at six months. Unfortunately, when it does occur, in-stent re-stenosis is more difficult to treat than re-stenosis after angioplasty alone.

This led to the development of the Drug Eluting Stents (DES), which revolutionised the outcome of PCI by blocking the proliferation of re-stenosis and reducing rates

down to single figures. These improved late angiographic outcomes and reduction in future intervention for re-stenosis were shown in the first randomised trials utilising the Cypher stent [*RAVEL, SIRIUS, C-SIRIUS and E-SIRIUS 2002-2003*]. As time passed and utilisation of DES rose, it was clear that in solving the re-stenosis problem, a new problem had emerged, - *late* stent thrombosis [*Pfisterer et al 2006, Lagerqvist et al 2007]* As DES prevents neo-intimal proliferation and remains seen as a "foreign body" for sometime in the patient, thrombotic activation around this site is common. This especially seems to happen in relation to other patient factors such as anti-platelet discontinuation or resistance and inter-current illness or surgery.

In the last few years, IVUS has been utilised again and again to solve the problems generated by coronary intervention. The precise understanding of intra-vascular pathology both pre and post-stenting, will allow us to take the next step in identifying plaques and stents with vulnerable features, that are likely to create future problems.

Figure 1.3 Schematic of an IVUS catheter in a blood vessel

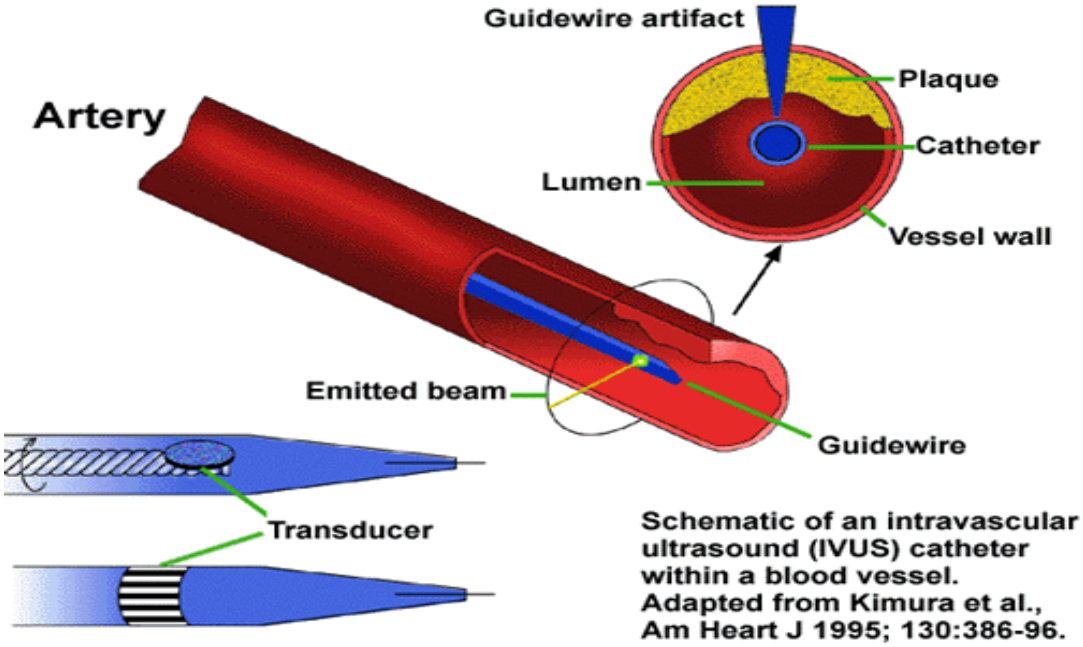

1.3 IVUS

1.3.1 Background

Contrast angiography has been the gold standard in the assessment of coronary artery disease for over four decades. However, angiography only provides a 2-D sillouhette of the coronary lumen and gives no insight into the degree of atheroma in the vessel wall. As discussed above, pathological studies reveal that before atherosclerosis encroaches on the lumen, there is compensatory enlargement of the coronary artery, the Glagov phenomenon. [*Glagov et al 1987*] Lumen area is not compromised until plaque area exceeds 40% of the total vessel cross-sectional area. IVUS has enabled this phenomenon to be studied *in-vivo* and confirmed its existence [*Gerber et al 1993, Ge et al 1994 , Hermiller et al, 1993 Mintz et al 1996*]. IVUS also highlights that, in some cases, vessel size could reduce in the presence of atheroma (negative remodelling or reverse Glagov) [*Pasterkamp et al 1995*]. IVUS has been the most useful tool (over the years) to improve and facilitate knowledge of the intra-vascular anatomy, that surrounds the interventional treatment of coronary disease. These ongoing insights have led to IVUS being seen as a tool that can assist the interventionalist and push forward the improvement of intra-vascular procedures.

Figure 1.4: Angiographically patent vessels containing variation in IVUS plaque burden at points A/B/C/D, despite the normal angiographic calibre (Adapted from Volcano Corporation, permission granted)

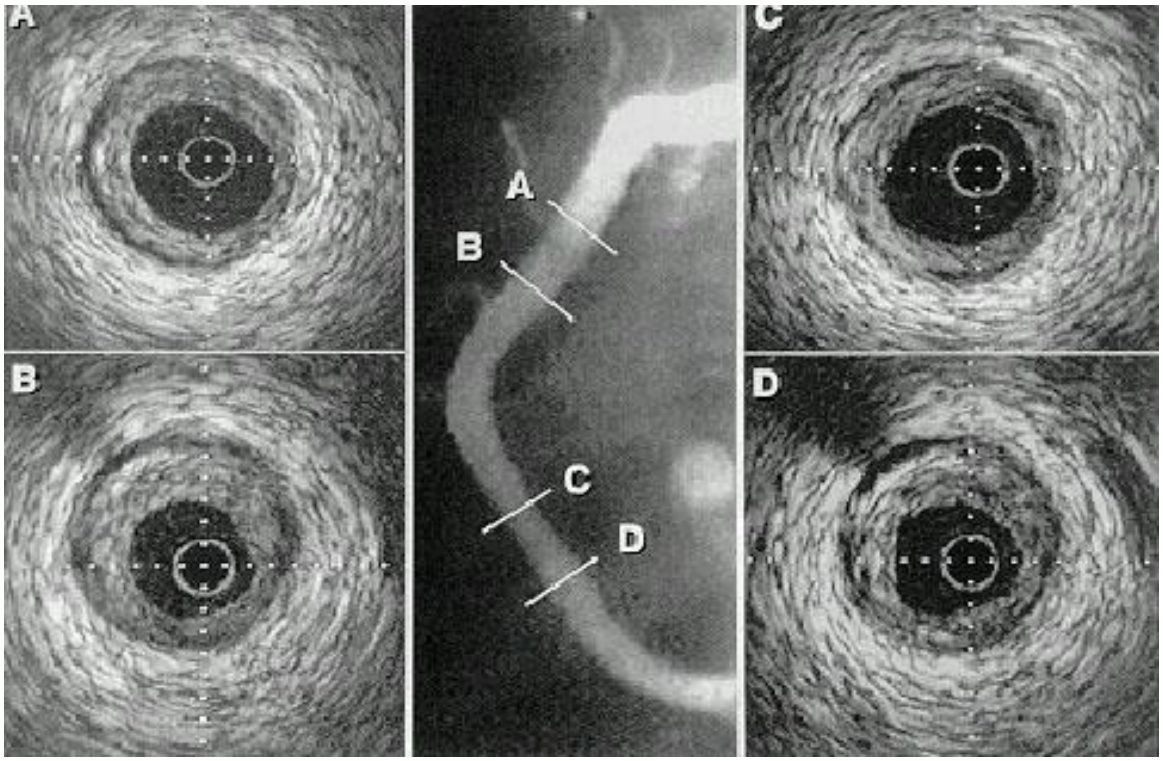

IVUS uses the principles of echocardiography by generating very high frequency sound waves (ultrasound) from electrically stimulated piezo-electric crystals in the transducer. These ultrasound waves bounce off the various types of tissue structures in the body and the amplitude of the returned signal is used to generate the image. Intravascular Ultrasound transducers have been miniaturized to less than four hundredths of an inch and placed on the tip of a catheter. This catheter can be placed into the coronary arteries over the same guidewire that is used to position the

angioplasty balloons or stents. It becomes, in effect, a tiny camera that gives us a cross-sectional view of the artery, a view that shows distinct circular layers, using shades of grey, the major ones being:

Figure 1.5: A typical cross-sectional frame of IVUS (courtesy of Volcano)

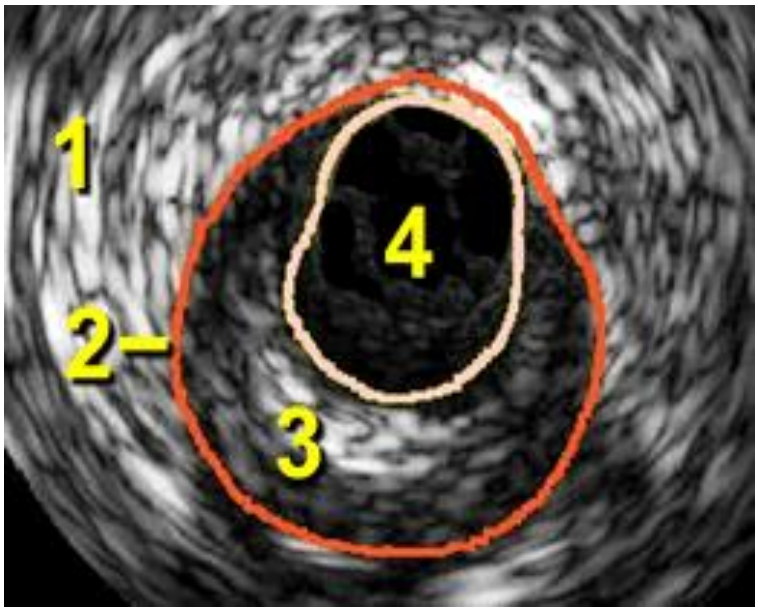

1. The adventitia or outer muscular covering of the artery
2. The media or wall of the artery
3. The intima or layer of endothelial and other cells that make direct contact with the blood inside the artery. In normal arteries this layer is very thin. However, in diseased arteries (as shown) the intima is thickened by atheromatous plaque in an eccentric or asymmetrical manner.

4. The lumen, the actual channel of the artery through which the blood flows.

Figure 1.6: A more complex cross-sectional frame of IVUS. (Source Medscape)

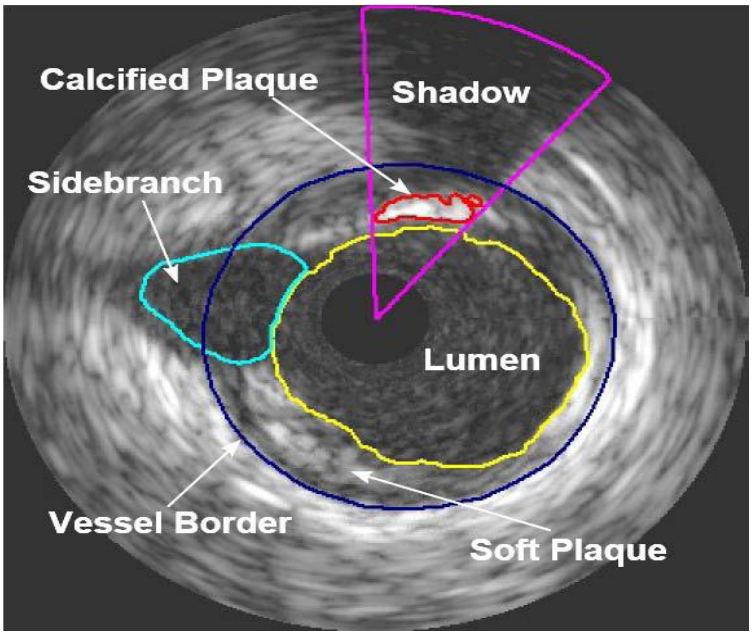

1.3.2 Adjunct to stent implantation

Theoretically, IVUS guidance can facilitate optimal long-term results from stenting in three ways: first, by ensuring that significant residual stenosis or dissection at the stent margins is dealt with; second, by ensuring that plaque calcification that might limit stent expansion is identified and removed, for example, by Rotablation; third, by ensuring that an optimal lumen gain has been achieved in the stented segment. Criteria have been developed that define the achievement of optimal stenting (The 'MUSIC' criteria) [*De Jaegere et al 1996 and 1998*]. These are based on a comparison of the lumen within the stent with the lumen of proximal stent and distal stent reference segments. This is together with the presence of complete stent apposition

to the vessel wall and a symmetrical stent expansion index related to the ratio of minimal to maximal stent lumen diameter. The lessons of bigger post-dilatation balloons and high pressure inflations that have been gleaned from the many early IVUS studies such as: AVID; OPTICUS; CLOUT; RESIST; WEST-2; STRUT; STARS and CRUISE are now used in most centres to improve angiographic results. It is known from the POST registry [*Uren et al 2002*] that in cases of stent thrombosis there was retrospective evidence of an abnormal IVUS in 94% of the cases.

1.3.3 Grey-scale IVUS guidance in the bare metal stent era.

In the studies mentioned above, the use of intravascular ultrasound as an adjunct to percutaneous coronary intervention, using bare metal stents, produced the following general findings:

1. IVUS guidance resulted in a significantly larger mean post-intervention angiographic minimal lumen diameter compared to angiographic guidance alone.

2. IVUS guidance resulted in a reduction in the odds of target lesion revascularization (repeat percutaneous coronary intervention or coronary bypass graft) compared to angiographic guidance alone. The reduction was statistically significant at a follow-up period of 6 months to 2 years.

3. Total revascularization rate (either target lesion or target vessel revascularization) was significantly lower for IVUS-guided patients at 18

months to 2.5 years after intervention. The main benefits were seen in long lesions and smaller calibre vessels.

4. There were no statistically significant differences in the odds of death or myocardial infarction between IVUS-guidance and angiographic guidance alone at up to 2.5 years of follow-up.

5. The odds of having a major cardiac event (defined as death, myocardial infarction, and target lesion or target vessel revascularization) were significantly lower for patients with IVUS guidance compared to angiographic guidance alone during follow-up periods of up to 2.5 years.

However, in these studies, the reduction in the odds of combined events, reflects mainly the reduction in revascularization rates.

1.3.4. IVUS guidance of drug-eluting stent placement.

The MAIN-COMPARE registry [*Park et al 2010*] shows that IVUS guidance of left-main procedures using DES can have a profound impact on mortality. The risk of 3 year mortality was 60% lower in the IVUS arm versus angiography (**figure 1.7**).

Other studies such as *Roy et al 2007*, have also proposed that IVUS guidance during PCI may reduce the rate of DES thrombosis. The JSAP trial (*Nigishaki et al 2008*) showed that PCI guided by IVUS in stable angina provided better outcomes than medical therapy alone, which is different from all previous stable angina trials comparing medical therapy with PCI.

One-year data from the Washington Hospital Center (WHC) IVUS vs. No IVUS DES Study show that patients in the IVUS group had:

- 65% lower stent thrombosis
- 29% lower TLR
- The study concluded that using IVUS during DES implantation has the potential to influence treatment strategy and affect both DES thrombosis and the need for repeat procedures.
-

Figure 1.7 – Results of the MAIN-COMPARE IVUS in LMS study (adapted from Volcano Corp slideset)

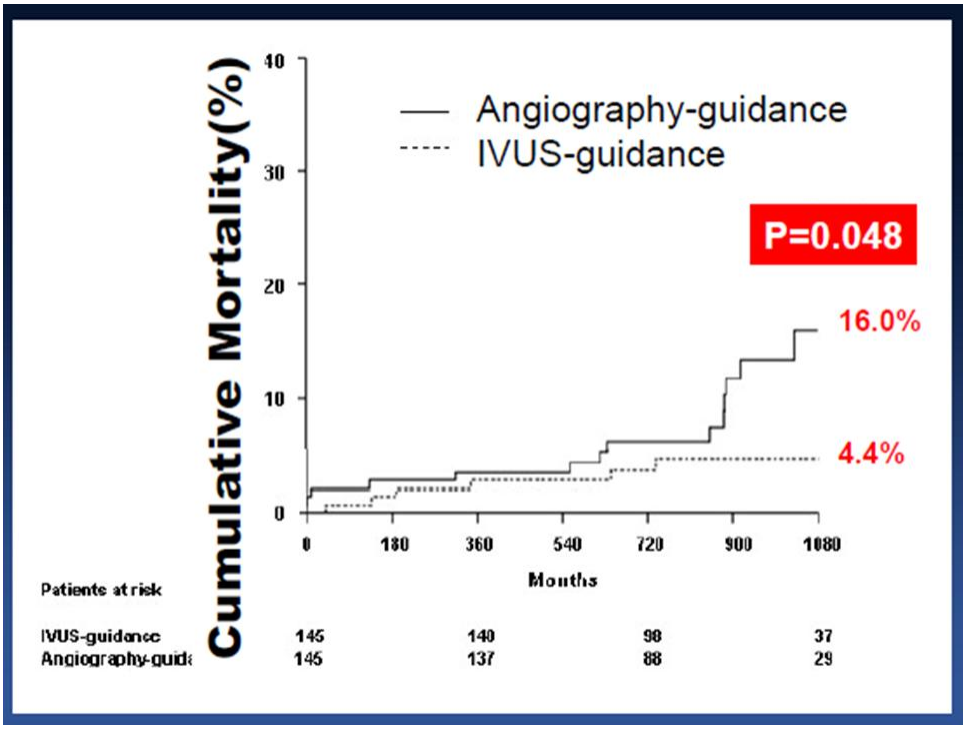

Moreover, as reported by *Costantini et al 2008*, patients in the IVUS group had the following lower rates compared to those in the non-IVUS group:

- 62% lower Stent Thrombosis
- 29% lower Target Vessel Failure (TVF)

Figure 1.8 – Results from Costantini et al (adapted from Volcano Corp slideset)

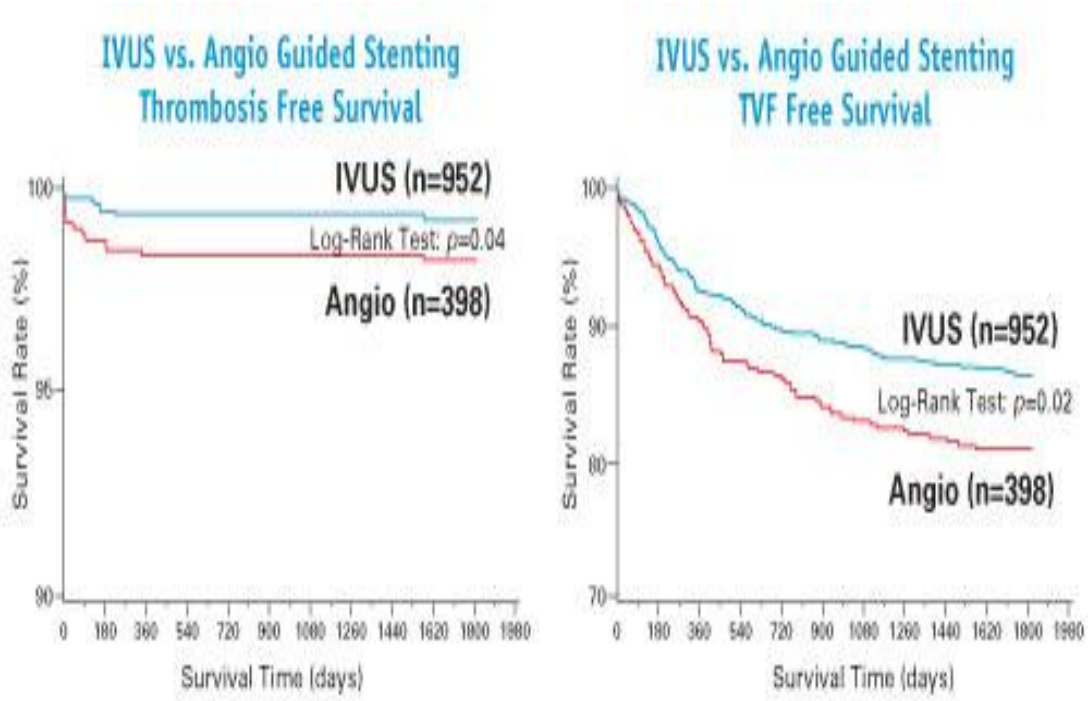

Compared with angiography, IVUS has the unique ability to assess suboptimal results of stenting, which may be associated with the occurrence of stent thrombosis. Previously, IVUS evaluations of stent under-expansion, incomplete lesion coverage, small stent areas, large residual plaque, and poor apposition have been found to

predict stent thrombosis after DES placement [*Okabe et al 2007, Sonoda et al 2004. Fuji et al 2005, Costa et al 2005*].

1.3.5 Recent updates to the IVUS evidence

Figure 1.9.1 – Final results of ADAPT DES

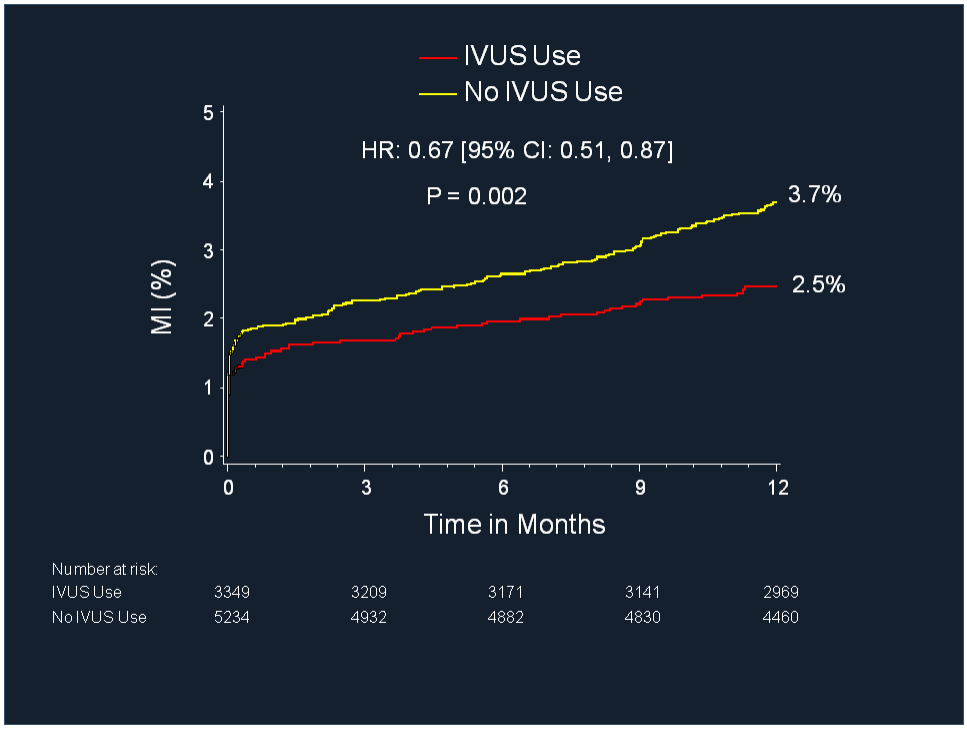

Recently, the largest ever study conducted with IVUS guidance [*Witzenbichler et al 2014*] has reported its findings. In the ADAPT-DES (Assessment of Dual AntiPlatelet Therapy with Drug-Eluting Stents) trial, over 8500 real-world patients (no clinical or anatomic exclusions) underwent PCI and received at least one drug-eluting stent. IVUS guidance was prospectively examined with 5200 cases not using IVUS and 3300 cases using IVUS. The results shed new light in favor of IVUS

use: as IVUS guidance improved clinical outcomes both acute (<30 Days) and at 1 year with both:

- **33% reduction in MI.**

- **50% reduction in subacute and late stent thrombosis.**

These results are despite 40% more IVUS patients initially presenting with STEMI. IVUS guidance changed the procedure 75% of the time. Longer, more appropriately sized stents, bigger balloons (pre/post dilatation) were used at higher pressures with no negative impact on outcomes.

Table 1.1 - Basic comparative results from ADAPT-DES

	IVUS group (n=3343)	Non IVUS group (n=5233)	P value
Any ST within 1 year	0.52%	1.04%	**0.01**
- Acute (< 24 hours)	0.06%	0.04%	0.66
- Subacute (1-30 days)	0.27%	0.56%	**0.05**
- Late (31 days – 1 year)	0.25%	0.48%	0.1
All-cause death/MI within 1 year	3.96%	5.35%	**0.004**
Cardiac death within 1 year	0.84%	1.17%	0.1384
Peri-procedural MI	1.26%	1.53%	0.3
Non peri-procedural MI within 1 year	1.23%	2.17%	**0.002**

Overall, In **ADAPT-DES**, operators who used IVUS pre and post-procedure were found to achieve greater maximal lumen areas for proximal reference lumen area (8.9 vs. 7.6 mm^2), in-stent lumen area (6.3 vs. 5.8 mm^2) and distal reference lumen areas (6.5 vs. 6.1mm^2, P<.0001 for all measures). Greater maximum lumen area is identified as a key procedural factor to reduce the risk for stent thrombosis with DES.

In addition, a recent large meta-analysis by *Zhang et al 2014*, has shown in 19,619 patients from both randomised and observational studies that a mortality benefit exists for IVUS guided stent implantation. It seems that by improving acute stent results we can improve event-free survival compared to angiographic guidance alone

Figure 1.9.2 Forrest plots from Zhang et al 2014 – Permission requested

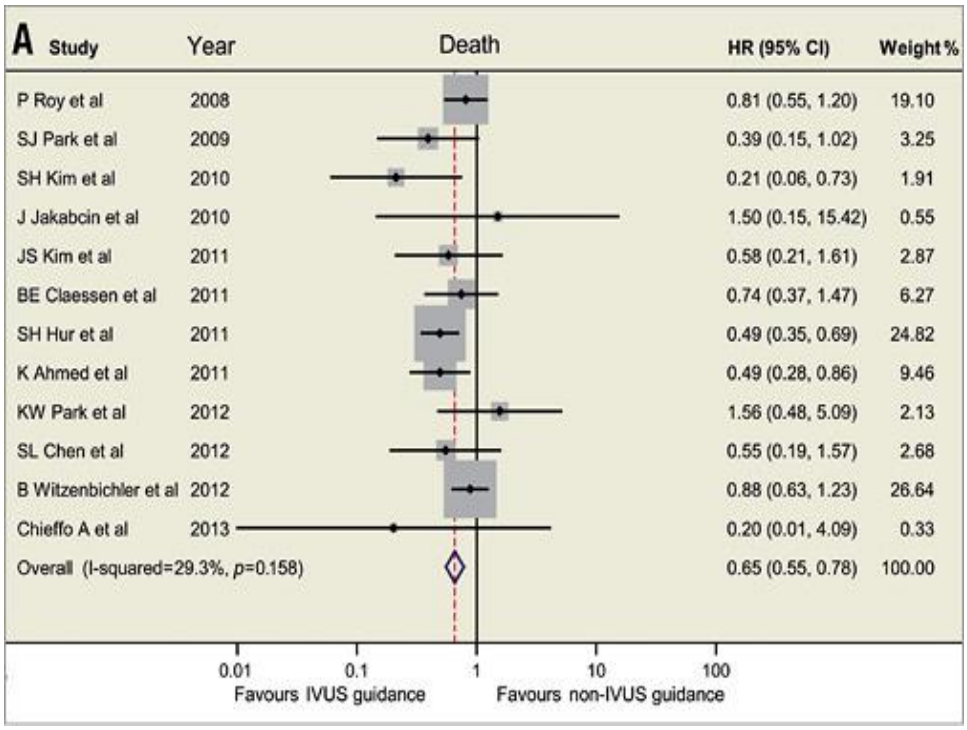

1.3.6 IVUS based tissue characterisation

The development of plaque tissue characterisation with IVUS in 1990s [*Moore et al 1998, Nair et al 2002*] heralded a new way of thinking about the percutaneous treatment of atherosclerosis, with more thought being put into the vulnerability of plaque. The study of plaque composition in different groups of patients appears to be the only current way to improve our knowledge about the natural history of this disease. In order to solve the problem of plaque progression, plaque rupture and re-stenosis, we must observe plaque with these new techniques to hopefully develop a strategy to improve plaque recognition and subsequent treatment strategies. The natural progression from grey-scale plaque characterisation was realised with the introduction of crude grey scale correlations and eventually a computer based algorithm generating a colour coded map, developed from the backscattered ultrasound signals taken from the plaque. This leap forward was made with the help of expert pathologists and is now called Virtual Histology.

Chapter II - Introduction

Virtual Histology and Acute Coronary Syndromes

2.1 Introduction

Acute coronary syndromes (ACS) frequently cause considerable morbidity and mortality with a high risk of further events within the following year despite the use of optimal medical therapy and percutaneous coronary intervention (PCI) [*Eagle et al 2004*]. Numerous studies have described the concept of acute, partial or complete, thrombotic occlusion of the coronary artery which occurs at the site of a friable atherosclerotic plaque with a lipid-rich necrotic core and a ruptured overlying thin fibrous cap ('culprit lesion') [*Kolodgie et al 2004, Surmely et al 2006*]. Moreover, this process initially appeared independent of the severity of the underlying stenosis [*Falk et al 2005]*. Most of our initial knowledge about the morphological characteristics of culprit lesions has been obtained from necropsy studies of lesions at the extreme end of the ACS spectrum [*Uemura et al 2006*]. The development of Intravascular Ultrasound (IVUS) with Virtual Histology™ (VH), using spectral analysis of the radiofrequency ultrasound backscatter signals to identify the components of atherosclerotic plaque, has allowed some in-vivo delineation of the relative contributions of necrotic core and fibrous atheroma in unstable lesions [*Nasu et al 2006, Surmely et al 2007, Fujii et al 2005]*. This evidence suggests that there may be variations in the morphology of plaques which rupture and promote thrombosis in ACS, rather than the traditionally accepted view that a common pathological mechanism is at play. This imaging modality therefore provides great potential for *in vivo* information about the culprit lesion {*Konig et al 2007*].

The spectrum of coronary heart disease is heterogenous. Most acute events arise from lesions which were originally non-flow limiting [*Virmani et al 2000*]. Precise lesion characteristics or lesion staging could influence interventional and medical treatment but currently this has not been evaluated. Clinically, ACS presentations vary from unstable angina to non-ST/ST elevation myocardial infarction (NSTEMI, STEMI). Considerable variation exists in the degree of myocardial injury, assessed by troponin release and the extent of myocardial ischaemia, as demonstrated by patient symptoms and electrocardiographic changes. Moreover, the response of patients to conventional pharmacological therapy with respect to the resolution of myocardial ischaemia is variable, ranging from a single episode of chest pain to prolonged, intractable symptoms. This variation is multifactorial and, as well as clinical factors, includes the extent of coronary disease at the culprit lesion site. However, contemporary medical treatment is not lesion or patient specific, largely due to the inability to accurately characterise the lesion. Current IVUS-VH data suggests significant variations exist in the lipid-rich, necrotic core content of the culprit lesion [*Surmely, Uemura, Nasu, Fujii et al*]. We examined the ability of IVUS-VH as an investigational tool in the treatment of coronary artery disease. The work contained in this thesis hopes to contribute important knowledge to this growing field and examine the clinical utility of IVUS-VH in the field of coronary intervention for ACS lesions.

2.1.1 The Technology

As previously described, grayscale intravascular ultrasonography (IVUS) is a tomographic imaging tool that can visualise coronary atherosclerosis *in vivo*, elucidating plaque area, plaque distribution, lesion length and coronary remodeling. IVUS has demonstrated discrepancies between the extent of atherosclerosis seen by coronary angiography and the actual extent of atherosclerotic disease.[*Nissen et al 2001*] Angiography or "Lumenography" is able to determine only whether there is adequate space for blood to flow well, but it cannot assess the underlying vessel changes and "hidden" plaque burden. Quantitative assessment of this plaque composition within a lesion has not been possible with grayscale IVUS analysis, until now.[*Nissen et al 2002*] IVUS-VH uses advanced analysis of ultrasound backscatter signals by processing the power, frequency and amplitude to overcome the limitations of grayscale IVUS and provide a detailed analysis of plaque morphology.[*Nair A et al 2002*] In addition, IVUS-VH has the potential to provide *in-vivo* patient-specific plaque analysis to determine the range of characteristics in relation to clinical factors and risk, rather than making assumptions from a highly selected autopsy population.

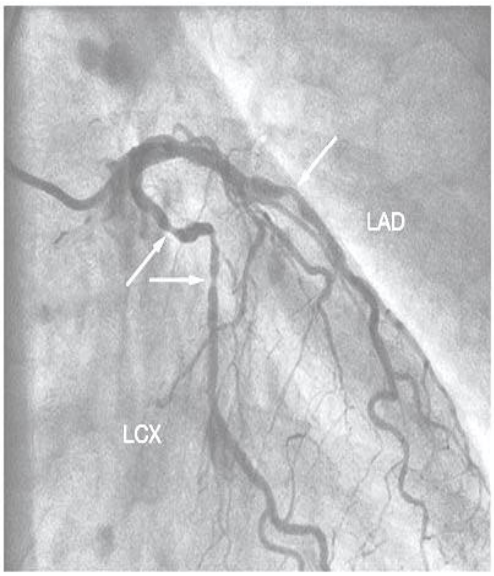

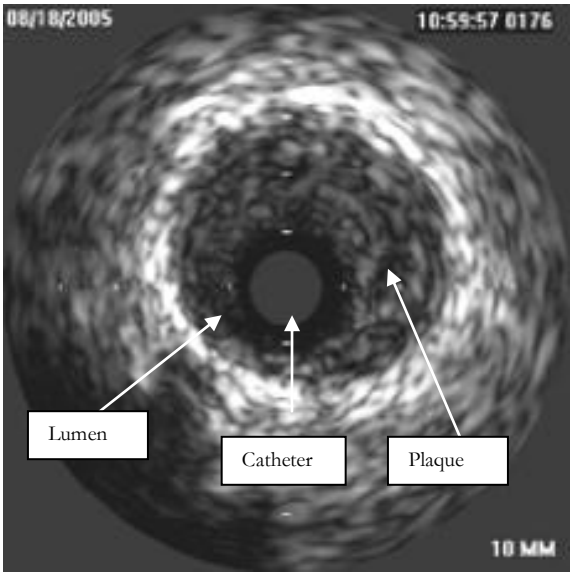

Angiography **IVUS Greyscale**

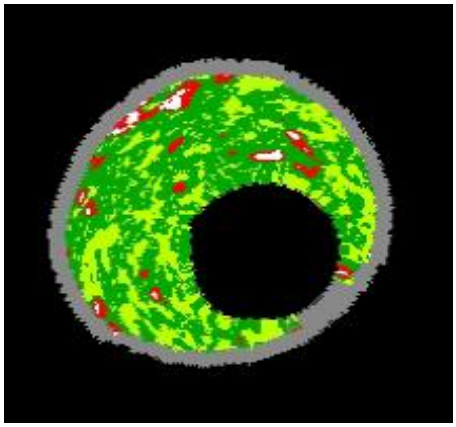

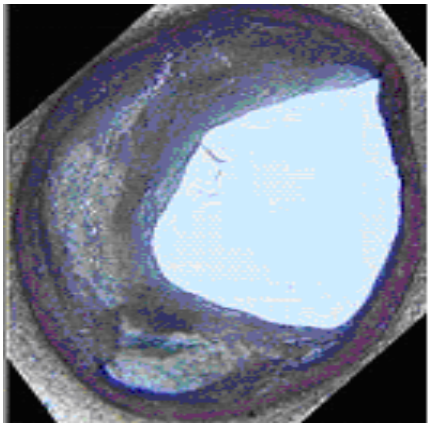

IVUS-VH **Traditional Histology**

Figure 2.1: IVUS-VH Production of a colour map of the atherosclerotic plaque

Obviously many different cell and tissue types are commonly found in atherosclerotic plaques analysed pathologically. To simplify image interpretation and because of the fundamental resolution limitations of the underlying ultrasound signal, plaque components are grouped into four basic tissue types during IVUS-VH imaging. These components are displayed on the image as different colour pixels. This technique is based on advanced radiofrequency analysis of reflected ultrasound signals in a frequency domain analysis and displays the reconstructed color-coded tissue map of plaque composition superimposed on cross-sectional mages of the coronary artery obtained by grayscale IVUS.[Nair et al 2002] Basic IVUS enables real-time, high-resolution tomographic visualization of the coronary arteries. Both lumen and vessel dimensions and the distribution of plaques can be analyzed. In addition, grayscale IVUS can be used to assess the presence of intraluminal thrombus and plaque rupture.[Potkin et al 1990] Grayscale IVUS has demonstrated the multiplicity of plaque ruptures seen in patients with ACS.[Tanaka et al 2005, Rioufol et al 2002, Schoenhagen 2003] In 2002 a study demonstrated that the number of vulnerable plaques with less than 75% luminal obstruction identified by IVUS had a positive correlation with future cardiovascular events.[Yamagishi et al 2000] Of note, serial IVUS analysis of a small patient cohort showed that 50% of ruptured coronary plaques detected on first ACS event had spontaneously healed at 22 months' follow-up.[Rioufol et al 2004]

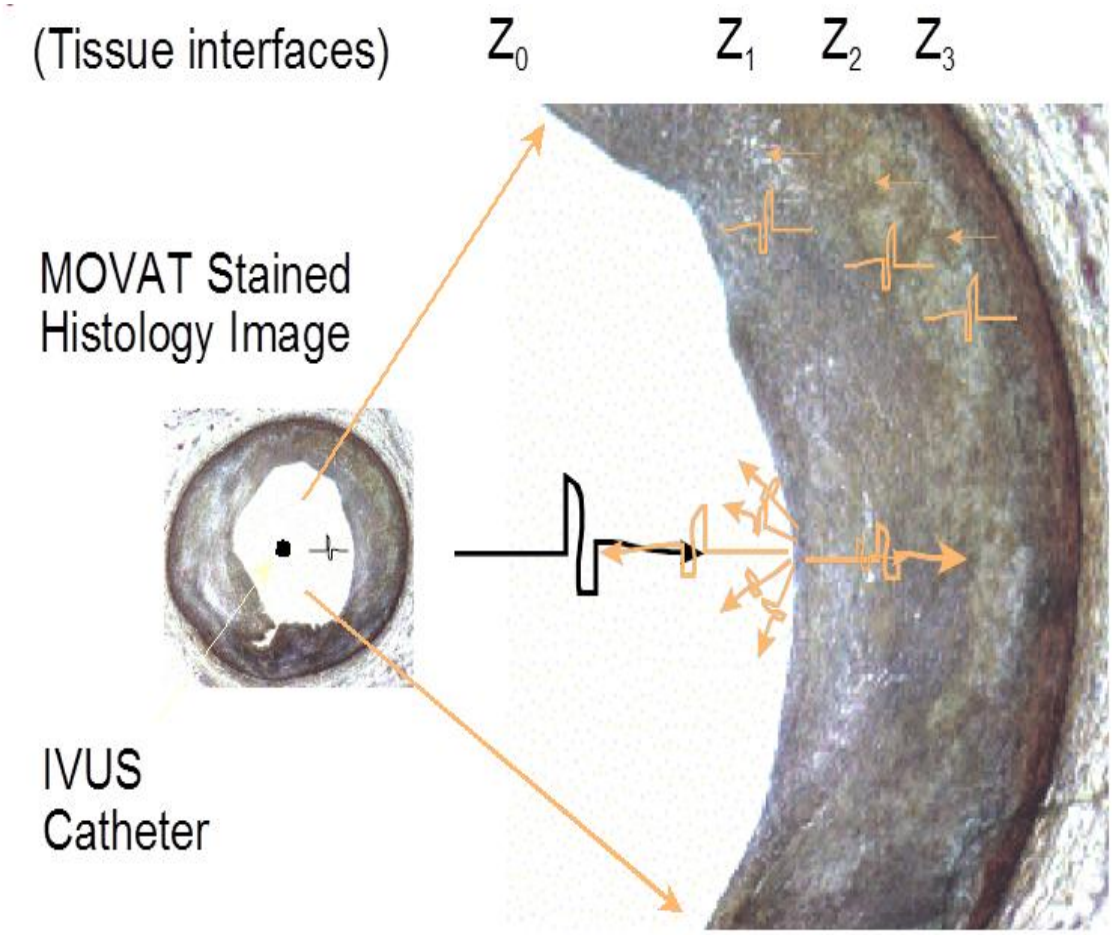

Figure 2.2: Path of the ultrasound signal into the tissue interface (adapted from Volcano slide set – permission granted)

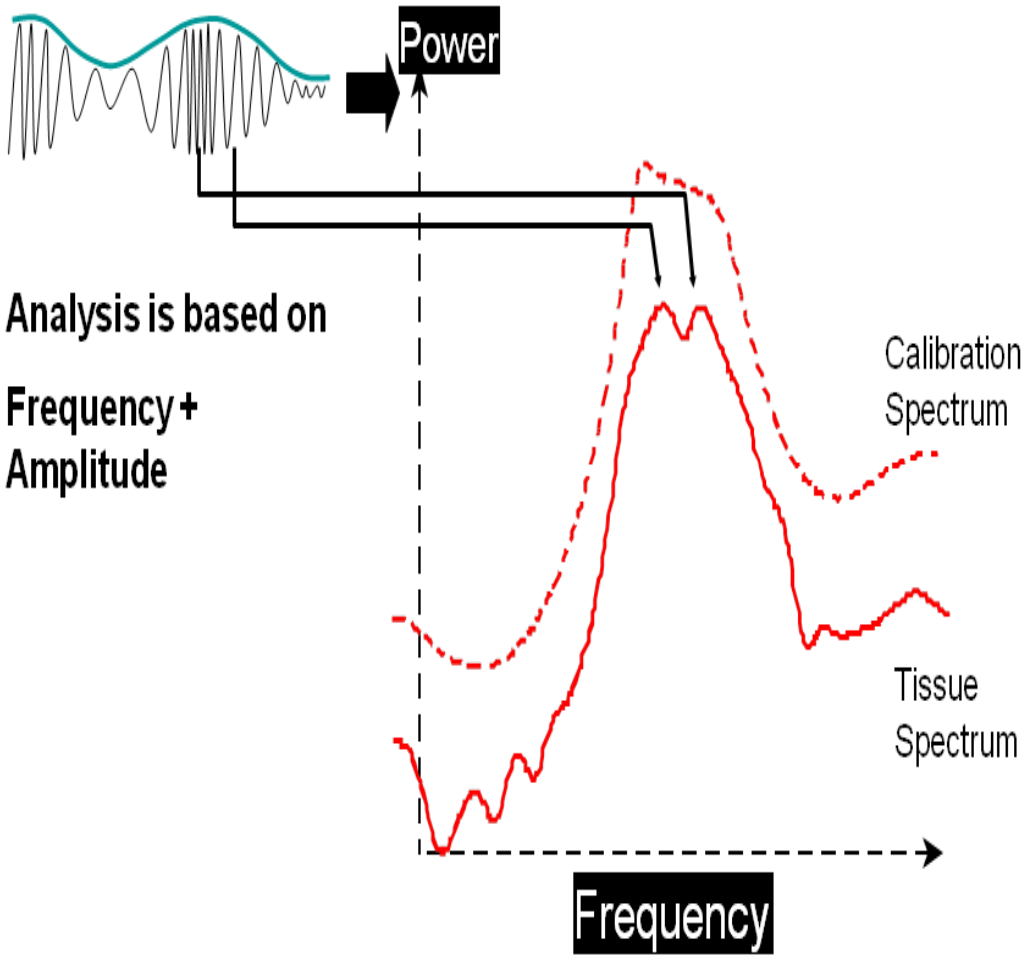

Figure 2.3: The backscattered ultrasound signal frequency and amplitude related to previously known tissue calibration spectra (Adapted from Volcano Corp slideset)

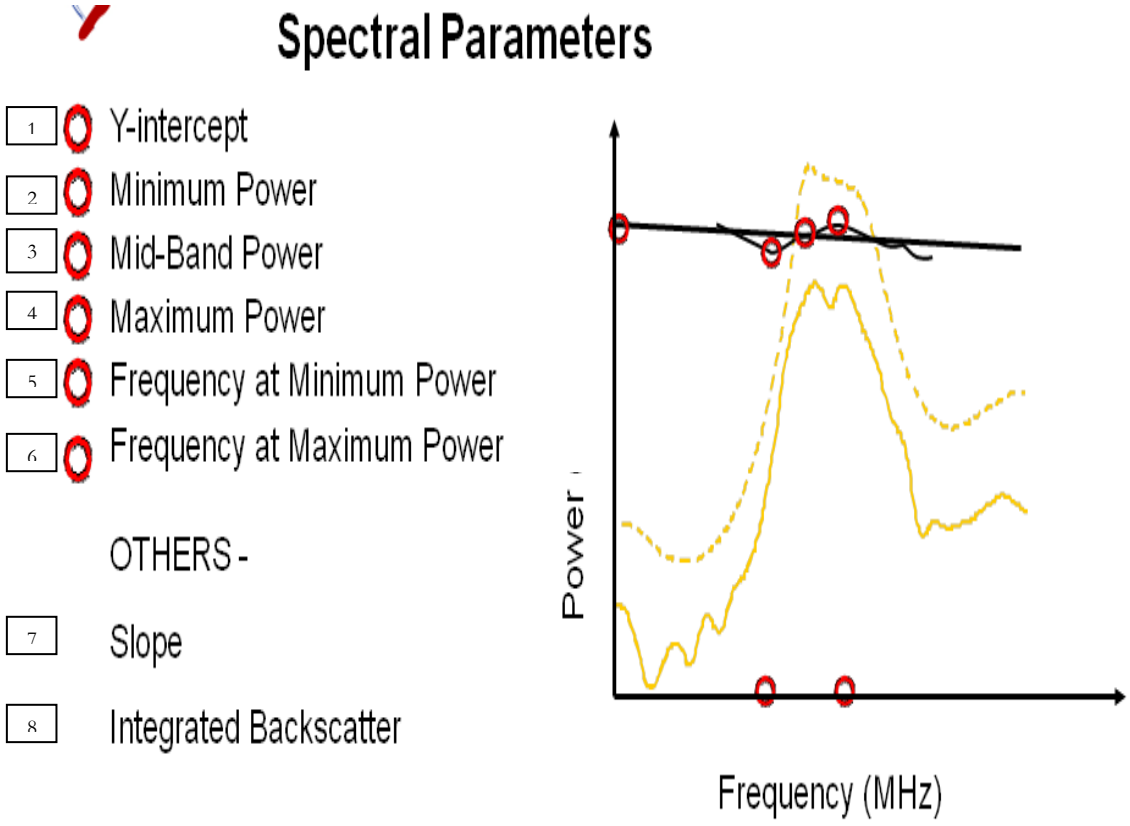

Figure 2.4: The eight spectral parameters taken from the ultrasound signal that are used in decision tree for VH tissue types

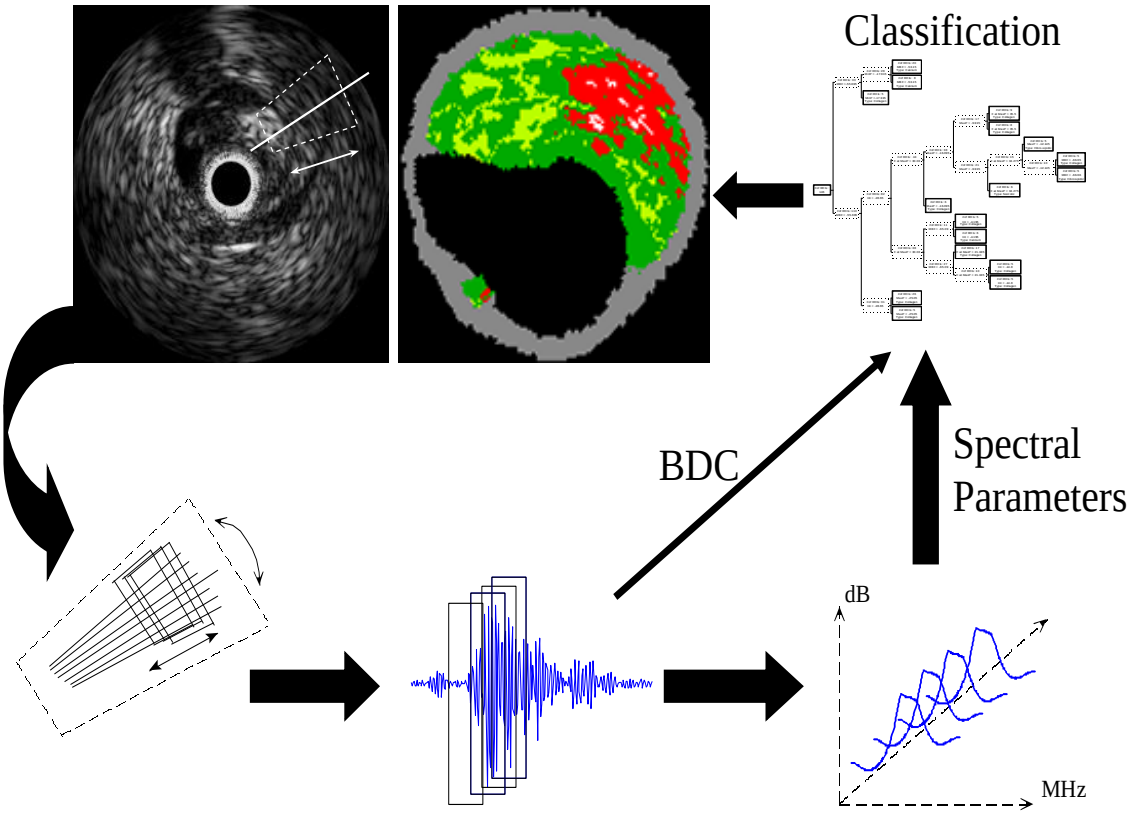

Figure 2.5: The process of spectral analysis generating tissue classification

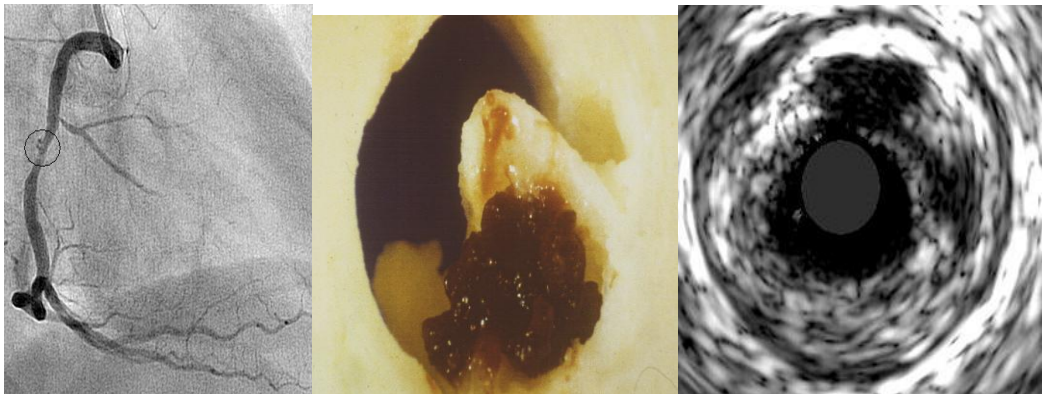

Figure 2.6: Plaque rupture shown angiographically, histologically and on IVUS.

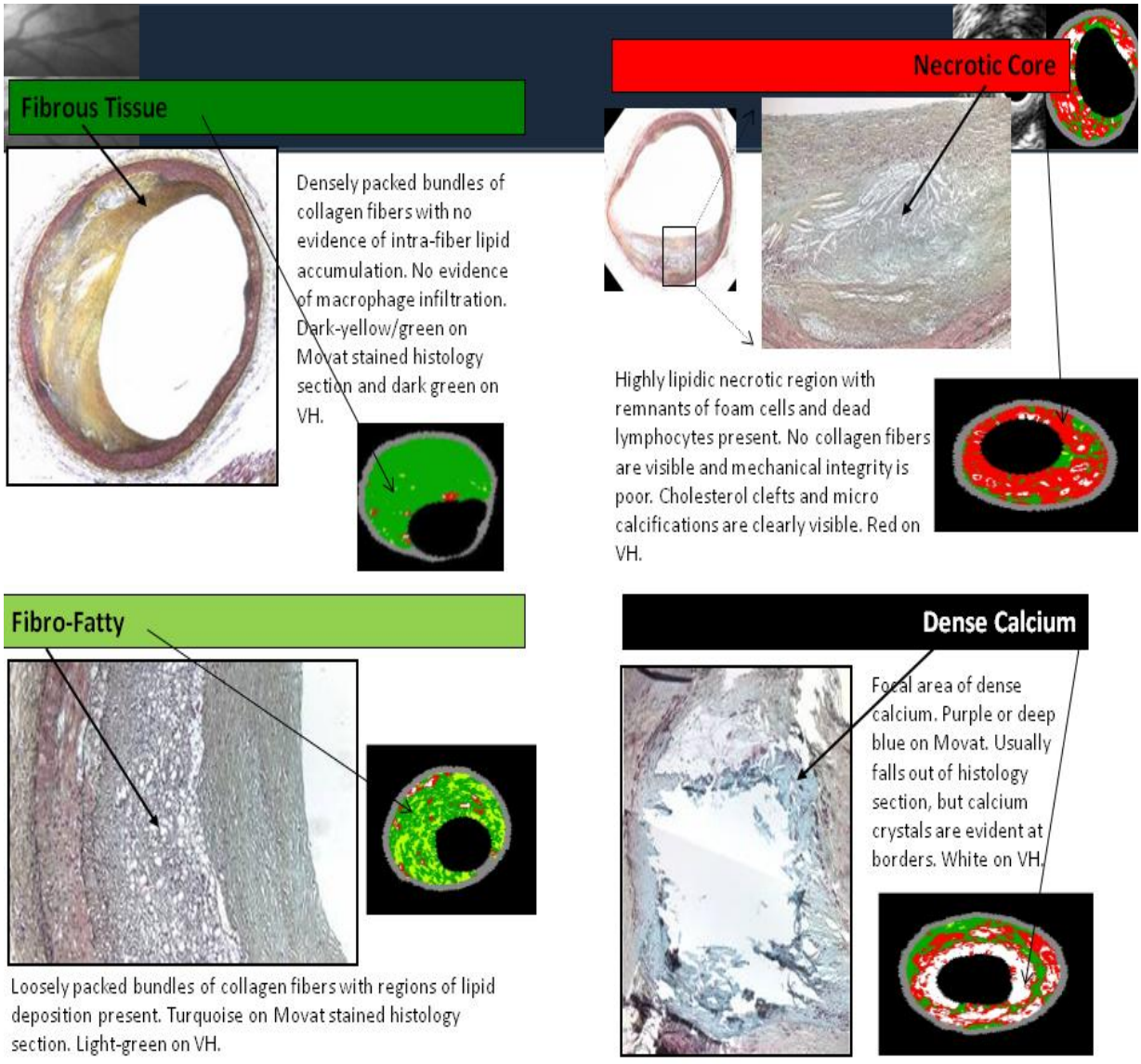

Figure 2.7 – VH tissue types with examples and descriptions of the corresponding histology.

Grayscale IVUS imaging is, however, limited with regards to analysis of plaque composition. Both calcified and dense fibrotic tissues, such as those found in plaques, have strong echoreflections with lateral shadowing and are, therefore, not easy to differentiate. Currently, VH can better distinguish between areas with low echoreflection than grayscale IVUS. Nevertheless, quantification of hypoechogenicity is important, as it has been related to an adverse event rate. [*Mathiesen et al 2001, Gronholdt et al 2001*]

2.1.2 Validity

There have been issues over the best way to validate IVUS-VH as ex-vivo analysis removes blood attenuation, ECG gating and coronary contraction/motion. To assess validity in-vivo, VH-IVUS backscatter data from 51 *ex vivo* left anterior descending coronary arteries were recorded and compared with histological interpretation of the same sites. [*Nair A et al 2007*] The overall predictive accuracies were 93.5% for fibrotic tissue, 94.1% for fibrofatty tissue, 95.8% for necrotic core and 96.7% for dense calcium. This demonstrated the potential of this imaging tool for the specific analysis of plaque vulnerability. In the Carotid Artery Plaque Virtual Histology Evaluation (CAPITAL) study there was a strong correlation between plaque characterisation and that following true histological examination of the plaque following endarterectomy. [*Diethrich et al 2007*] The predictive accuracy for TCFA was 99.4% and 96.1% for calcified TCFA. *In vivo* studies using IVUS-VH have shown that presumed vulnerable plaques (TCFAs according to IVUS criteria) occur more often in patients with ACS than in patients with stable

angina.[*Rodriguez-Granillo et al 2005*] Patients who are stable at clinical presentation show more intimal thickening and plaque composition with considerably more fibrotic tissue than that typically seen in vulnerable plaques.

VH Plaque Component	Predictive Accuracy	Sensitivity		Specificity	
		%	CI	%	CI
FT (*n* = 471)	93.5%	95.7%	94 – 98	90.9%	88 – 94
FF (*n* = 130)	94.1%	72.3%	65 – 80	97.9%	97 – 99
NC (*n* = 132)	95.8%	91.7%	87 – 96	96.6%	95 – 98
DC (*n* = 156)	96.7%	86.5%	81 – 92	98.9%	98 – 100

Table 2.1: Histological validation of IVUS-VH.

2.1.3Tissue Types

2.1.3.1 Fibrous

Fibrous tissue is represented by dark green pixels. Histologically, this tissue is collagenous with no lipid. [*Burke et al 2002, Nair et al 2007*] On grayscale IVUS, these tissues tend to be medium-bright regions.

2.1.3.2 Fibrofatty

Fibrofatty tissue is denoted in VH by light green pixels. This tissue is loosely packed collagen, but it can have a cellular quality with potential for foam cells to start invading. [*Nair et al 2007*] There is usually no necrotic core and even cholesterol products are rare**.** If thrombus or plaque rupture is included as plaque during analysis, then it appears as fibrofatty plaque [*Murray et al 2009*].

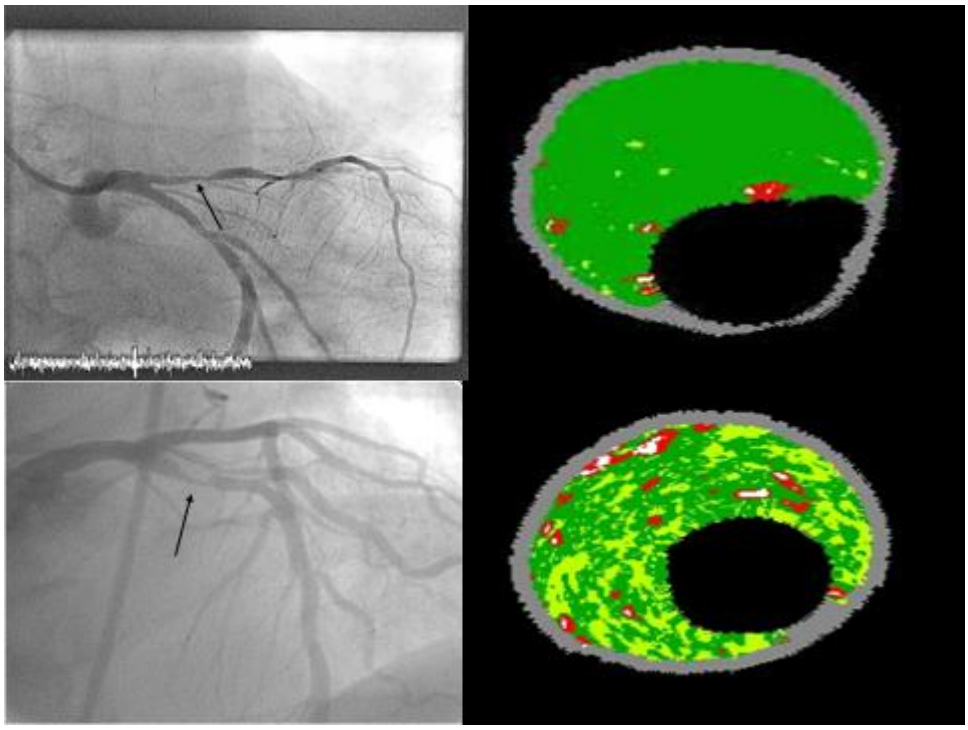

Figure 2.8: IVUS-VH characterisation of Fibrous and Fibrofatty lesions

2.1.3.3 Necrotic core

In VH the necrotic core is seen as red. This tissue is a mixture of soft, lipid-like dead cells, foam cells and trapped blood cells.[*Burke at al 2002*] Most of any real structure is lost and with some areas producing micro-calcification as a by-product (from the dead cells) this leads to a recipe for gross instability and rupture with friable areas next to sharp calcification.

2.1.3.4. Dense calcium

White pixels represent dense calcium. These calcified regions can be lost during histology processing but on plain grayscale IVUS, they act as extremely strong reflectors of signal and appear as bright white with a "red" shadow behind. There is ongoing debate amongst the IVUS-VH research community about how much information can safely be derived behind various types of calcium [*Murray et al 2010*]. Stent struts may also appear as calcium, if included in plaque analysis.

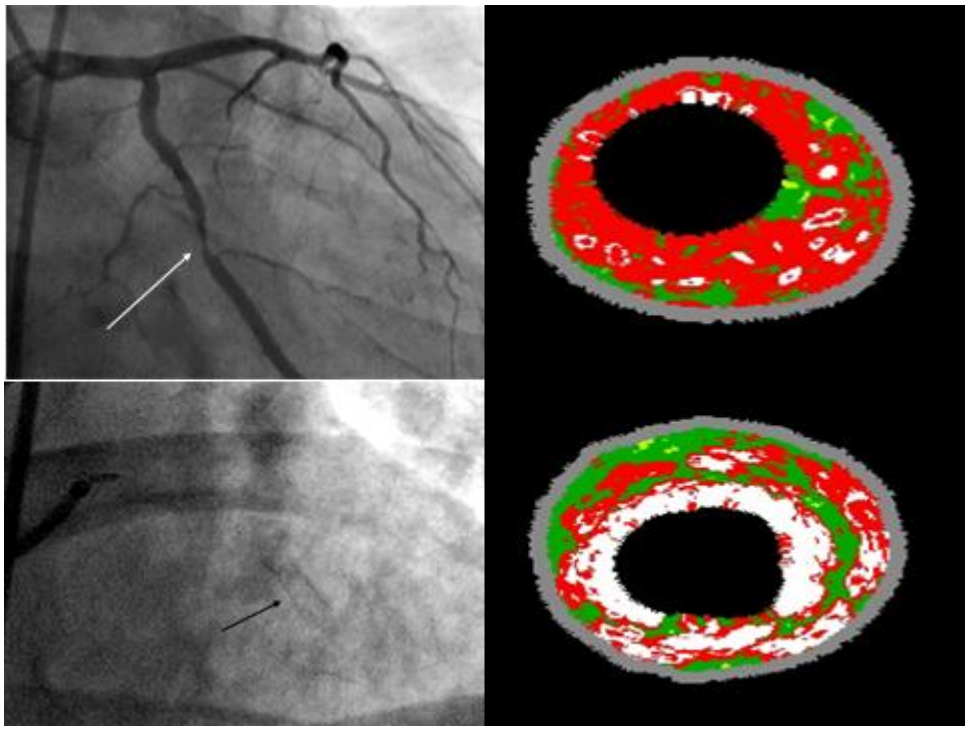

Figure 2.9: IVUS-VH analysis of necrotic core and dense calcium within lesions

2.2 How can IVUS-VH improve our knowledge about coronary disease?

2.2.1 Plaque Risk Assessment

In-vivo plaque classification with VH-IVUS is based on a histopathological classification system developed by *Virmani et al. in 2000*. From this system, coronary lesions seen on VH can be classified as adaptive intimal thickening, pathologic intimal thickening, fibroatheroma, fibrocalcific and TCFA plaques. For risk stratification or the likelihood of lesion rupture, it may be important to distinguish between the above-mentioned plaque types. This classification system represents the development of atherosclerosis through to atherothrombosis.

2.2.2 Adaptive and Pathological intimal thickening (AIT) + (PIT)

In adaptive intimal thickening, the intimal tissue largely comprises smooth muscle cells within a collagen matrix. In pathological intimal thickening, the intimal tissue comprise of mixed fibrous and fibrofatty plaque (lipid pools) with very little or no necrotic core. There can be microcalcification but this occurs in less than 10% of the plaque [*Nakashima et al 2007*].

2.2.3 Fibroatheroma (FA)

Fibroatheromatous plaques have a true necrotic core greater than 10% of total plaque volume and this contains cholesterol products. The fibrous cap that protects the coronary lumen from the necrotic core is significant. As the lesions progresses, the fibrous cap is assumed to diminish to a thickness less than 65 μm, which would

increase vulnerability and allow classification as a TCFA. The limited resolution of IVUS-VH (approx 150μm) means the cap can be measured only if greater than 150 μm thick. IVUS-VH cannot determine true TCFA and therefore VH-TCFA is only a surrogate measure and not a definitive term.

2.2.4 Fibrocalcific plaque

Fibrocalcific plaques are mainly fibrous plaques that are dense in calcium (>10%) and some have a small amount of confluent necrotic core (<10%). Fibrocalcific plaques are increasingly found in plaques at advanced stages of development and therefore likely represent the late stages of atherosclerosis. [*Falk et al 1995*]

2.2.5 Thin Cap Fibroatheroma (TCFA): The vulnerable plaque.

TCFA have a confluent necrotic core (>10%) in direct contact with the lumen (no evidence of a fibrous cap) and a minor amount of calcium (<10%). If this is present on three consecutive IVUS-VH cross-sectional frames, this confers an increase in vulnerability. It is currently thought that the higher the extent of surface contact the necrotic core has with the lumen, produces the highest risk of rupture. From some post-mortem data, a TCFA with a narrow lumen, confluent necrotic core greater than 20% at an angle of more than 35 degrees, with speckly calcification and a positive remodeling index or high plaque burden confers the most-vulnerable plaque [*Burke et al 2001*]. This appears to be in some ways different from the commonly taught theory that non-significant plaques are the ones which are more likely to

rupture [*Kolodgie et al 2003*]. It may simply be that non-significant plaques are just more frequent along a given coronary segment.

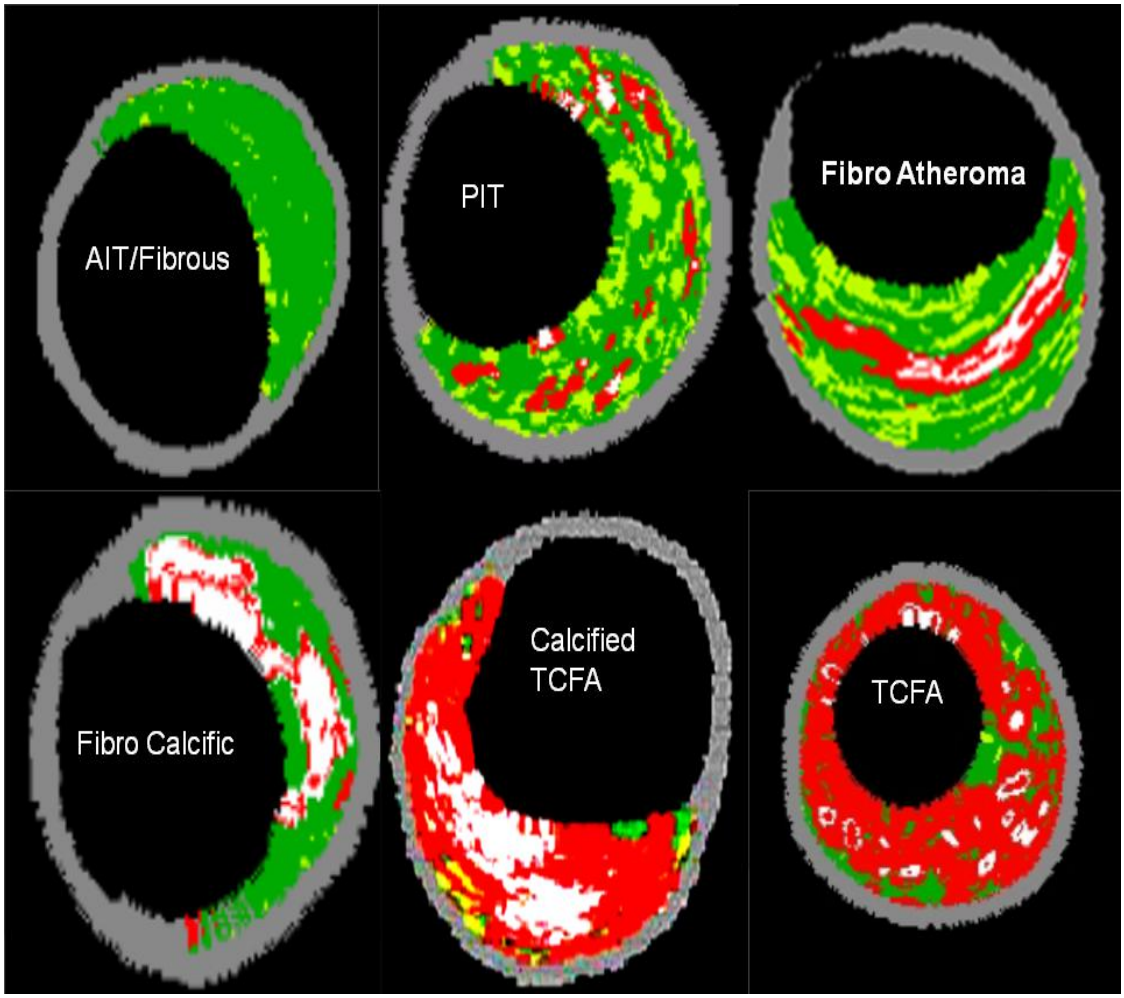

Figure 2.9.1 – Virmani classification of VH Plaque types with examples.

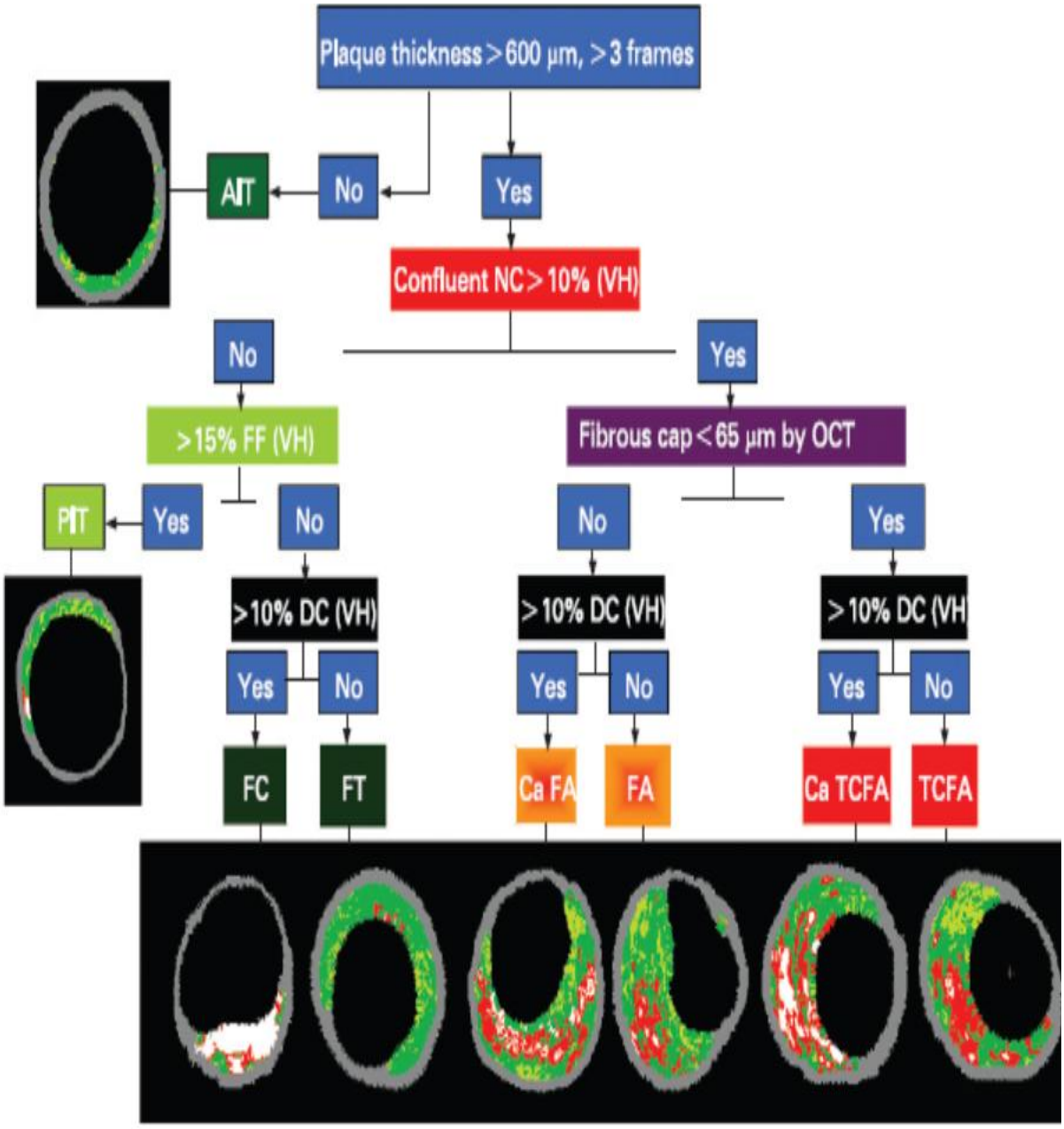

Figure 2.9.2 – Flow chart to allow full plaque diagnostics to a histological standard using OCT and IVUS-VH. OCT is used to confirm TCFA presence.

2.3 Can IVUS-VH influence coronary intervention?

The majority of acute coronary events are triggered by plaque rupture. [*Rioufol et al 2002, Schoenhagen et al 2003*] Therefore, defining the anatomic features that lead to plaque rupture should be of central importance to lesion imaging. Post-mortem analyses have shown that thin-cap fibroatheroma (TCFA) is probably the main precursor lesion for plaque rupture.[*Kolodgie et al 2004*] TCFAs are characterized by a large necrotic core separated from the coronary lumen by a thin fibrous cap. According to histological studies, the size of the necrotic core and the thickness of the fibrous cap have a critical influence on plaque stability. In addition, other characteristics of vulnerable lesions include localized expansive enlargement of the vessel wall ('positive remodeling') and microcalcification within the lesion. The location of the lesion within the coronary tree, the length of the lesion and the narrowing of the artery relative to healthy reference lumen size are also important parameters for the evaluation of plaque vulnerability. Coronary dimensions and elements of plaque composition such as the presence and amount of necrotic core, the degree of calcification and coronary remodeling are all anatomic features visualized by IVUS and IVUS-VH, but not by traditional angiography. The reconstruction of IVUS-VH images in a longitudinal view, enables a comprehensive analysis of the total length of the plaque and its complete orientation to the rest of the coronary tree. Within this thesis we are concerned with the complete understanding and treatment of vulnerable plaque by PCI. Angiography may highlight the minimum lumen diameter and allow successful stent placement in this

area, but it gives no account of potential positively remodelled, unstable plaque lurking within the reference segments. Unfortunately, it is in these reference segments that stent edges are placed and therefore this may potentially result in a failure to treat all unstable plaque or indeed directly disturb the inflow and outflow of the stented segment. Theortically, this may contribute to the previously quoted future MACE and repeat revascularisation rate of around 20% in ACS patients previously treated with PCI [*Eagle et al 2004*].

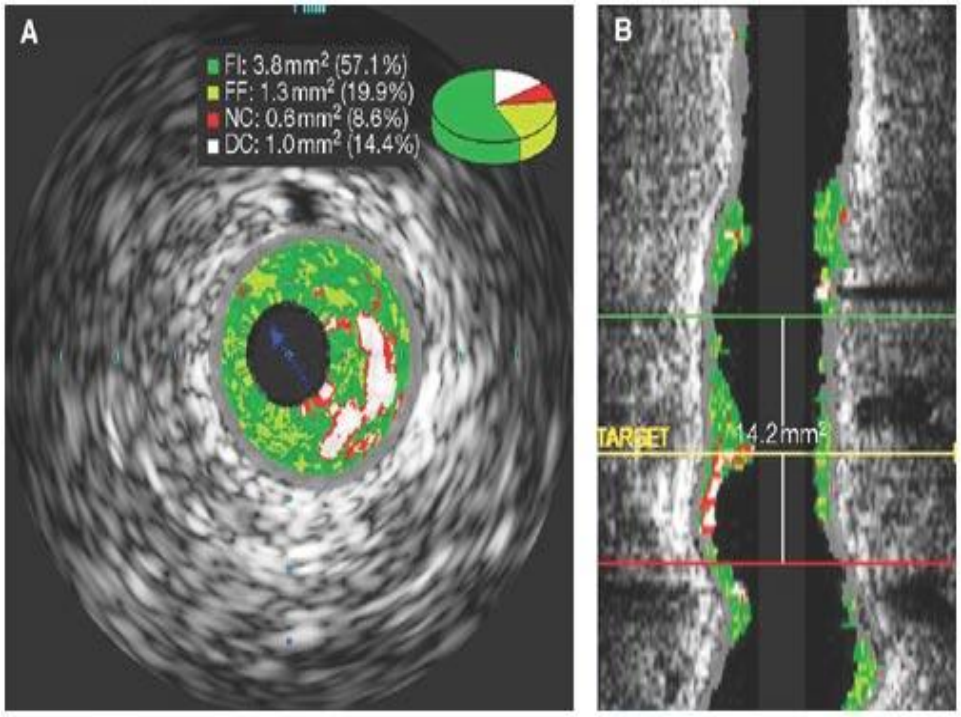

Figure 2.9.3: Longitudinal view of IVUS-VH pullback showing available information.

2.4 Investigating the utility of IVUS-VH analysis in ACS.

The longitudinal IVUS-VH view of the target segment provides detailed information about the length of the plaque and its general composition. According to post-mortem data, plaque composition is a better predictor of ACS events than the degree of coronary stenosis. [*Kolodgie et al 2003*] The formation of intraluminal thrombus after plaque rupture or erosion has a central role in the clinical course of ACS. Coronary thrombosis is a dynamic process and the culprit thrombus can assume different degrees of organization. With repeated thrombosis, the imaging of lesions becomes increasingly difficult. As the plaque ruptures, the lesion site is covered with thrombus and the underlying plaque and necrotic core is filled by intramural hemorrhage.[*Nissen et al 2000*] An intraluminal thrombus tail, rich in red blood cells, can form proximal or distal to the site of plaque rupture, especially in the presence of slow blood flow. Pharmacological therapy at this stage can aid to partially clear the thrombotic debris. However, any residual thrombotic tissue can become organised over time to become fibrotic tissue, causing luminal narrowing further to that at the rupture site. This can only be assessed completely by IVUS-VH analysis before PCI.

Post-mortem studies have clearly shown that repeated plaque ruptures have a key role in plaque progression. Pathologic studies have detected complex plaques with previous ruptures concentrating at one site, suggesting that certain sites are chronically vulnerable.[*Burke et al 2003*] Subclinical episodes of plaque disruption followed by healing is considered a mechanism by which plaque burden increases

and leads to inward remodelling processes and finally luminal narrowing.[*Burke et al 2001*] .The origin or focus of the plaque rupture can be proximal or distal to the minimum lumen of the lesion.[*Nissen et al 2004*] Hence, assessment of atherosclerotic lesions should include the whole length of the lesion to ensure detection of the site of plaque rupture, which might not necessarily be the site of the minimum lumen cross-sectional area. This phenomenon has been seen, but not fully investigated earlier in IVUS studies. [*Valgimiglii et al 2006*] As a follow on from this idea of culprit plaques being remote from the angiographic stenosis, we aim to measure the distance between plaque types in our cohort of ACS patients, with the hypothesis that different sites within the culprit artery will contain significantly different types of plaque.

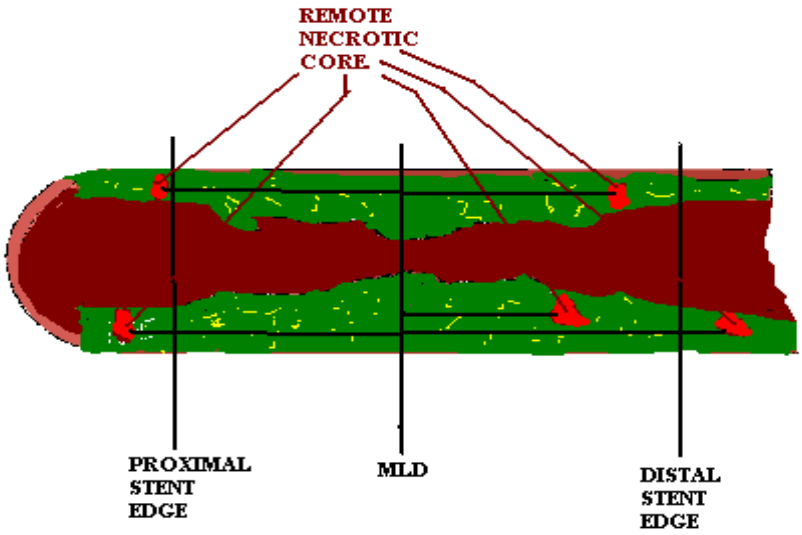

Figure 2.9.4: Schematic diagram of potential multiple necrotic core positions**.**

In ACS patients, despite pharmacology and early PCI, significant numbers of patients have a recurrent event which raises the question of whether procedural factors influence the outcome. The mechanism of angioplasty in acute plaques is poorly understood [*Wei Hu et al 2001*]. In a recent first in man paper, Wei and Schiele reported in 20 ACS patients undergoing pre-dilatation that 35% of lumen enlargement was due to an increase in vessel area and 65% to a decrease in plaque area. They concluded that fibrous and fibro-fatty elements re-distribute into the reference segments and one third of necrotic tissue was "lost" potentially supporting a theory of embolisation. It is possible that in this ACS group that fibrous and fibro-fatty "plaque" is actually thrombus or thrombo-fibrotic material coded as "fibrous" within the VH classification tree. This may suggest that incomplete lesion treatment could leave behind either a thrombotic or necrotic burden at the stent edges. For this reason, we will image the culprit vessel after stent implantation to ascertain both the stent deployment and the prevalence of reference segment or stent edge residual disease. Utilising VH observations, we will then be able to analyse this disease to assess its relative composition and geometry.

Angiographically guided stent placement is an imperfect but realistic compromise in the setting of 'real world' PCI. Many subtle forms of stent placement abnormalities exist and unfortunately these may contribute to long-term adverse events, such as stent thrombosis and in-stent re-stenosis. The S.T.L.L.R (Prospective Evaluation of the Impact of Stent Deployment Techniques on Clinical Outcomes of Patient

Treated With the CYPHER® Stent) [*Costa et al 2005*] used QCA evaluation of stent placement to show that suboptimal placement (or "geographic miss") is widespread and confers a "three times increased chance of heart attack and twice the chance of a repeat procedure". The types of geographic miss range from longitudinal miss with the stent being too short or too proximal/distal to cover the lesion, to axial miss which means the stent is under/over sized. The use of IVUS-VH before and after interventions allows further inspection and measurement of the vessel size, plaque length and inspection of side-branch anatomy and plaque constituents (e.g. significant calcification) This extra information will form part of our aim to follow the patients' clinical course after discharge to ascertain if it has any impact on future MACE or hospitalisation.

Another area of interest is in the angiographic placement of stents directly into necrotic areas of plaque, which are thought not to occur at the MLA of the culprit plaque [*Hong et al 2007*]. Stent struts embedded within necrotic tissue delay endothelialisation and adversely effect tissue level homeostasis and thrombotic status [*Joner et al 2006*] This is a very important area where IVUS-VH could positively influence stent placement in ACS patients. This would ensure that not only the MLA is covered but also the more unstable necrotic shoulder of the distal / proximal plaque, which may prevent further late thrombotic sequelae. We therefore aim to record evidence within our observational study of whether angiographically guided stent placement may cause stent edges to be close or within necrotic core.

As post-mortem data have demonstrated, longitudinal analysis of the target lesion using IVUS-VH can show the site of plaque rupture which are often proximal to the site of the minimal lumen area. As a consequence, only just covering the minimum lumen site might not be sufficient to fully treat the site of the problem. This could reduce the rate of future events related to reoccurring ruptures of an uncovered lesion. The prevalence of stent length to lesion length mismatch will also be recorded in our observations with the end point being the absolute rate of geographic miss within the culprit lesion.

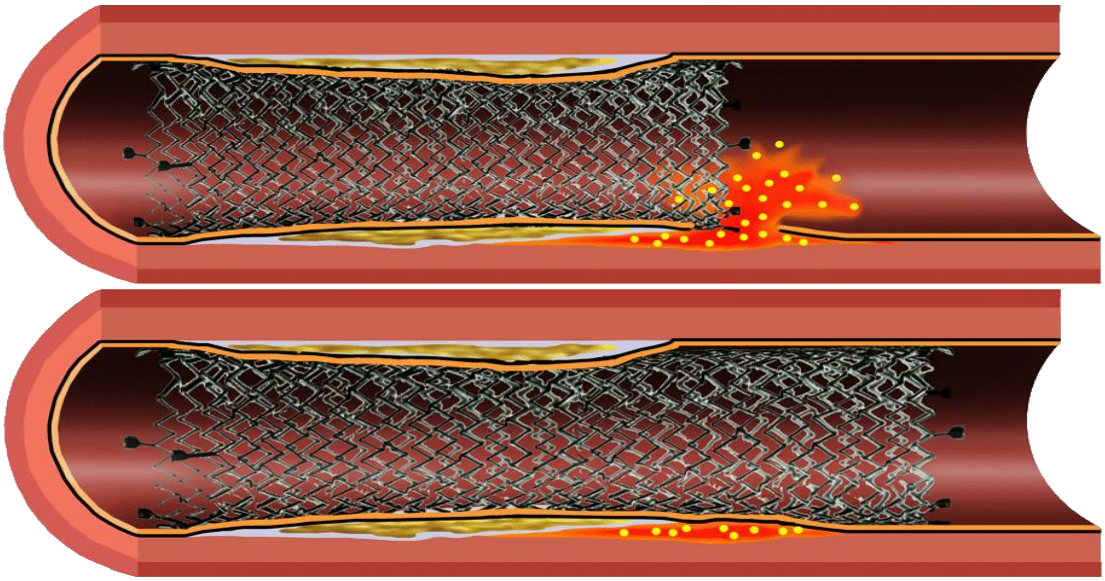

Figure 2.9.5: The theoretical benefits of entire lesion coverage in ACS.

2.5 Previous clinical studies assessing and utilising IVUS-VH in ACS

Recent studies have confirmed that plaque composition has a nonuniform distribution along the coronary arteries. [*Valgimigli et al 2005*] Depending on the distance from the coronary ostium, the proximal segments show a significantly larger necrotic core, but no change in other plaque components. As the proportion of necrotic core is related to overall lesion vulnerability, these findings could explain the higher incidence of plaque ruptures in the proximal segments of the coronary tree.

According to previous studies, IVUS-VH analysis could confirm the relation of outward (positive) and inward (negative) remodeling processes to plaque composition. In a small, *in vivo* study, plaque composition and morphology assessed using IVUS radiofrequency analysis were shown to relate to coronary remodelling, supporting a role of plaque composition in vessel remodelling. [*Rodriguez-Granillo et al 2006*] The size of necrotic core is significantly larger in lesions with positive remodeling; fibrous plaque burden, however, appears to have a significant inverse relationship with remodeling index. Positive remodelling is, therefore, associated with presumed high-risk lesions such as fibroatheromata and TCFAs, while negative remodeling is associated with less-vulnerable lesion types such as those with pathologic intimal thickening and fibrotic stable plaques. Recently IVUS-VH analyses were performed in the first 990 patients enrolled in the 3,000+ patient global IVUS-VH Registry to assess the impact of gender and age on in vivo plaque characterization. The 990 patients were divided into 3 age group terciles (<58, 58 to

68, and >68 years) and again divided according to gender. Naturally, both women and men had an increase in plaque with increasing age and at any age, men had more plaque than women. The percentages of dense calcium and necrotic core increased with increasing patient age and diabetic status. In both men and women and gender differences were lowest in the oldest tercile (>68 years). [*Qian et al 2009*]

In December 2008 a group from Korea found no re-flow/slow flow in 12 of 57 patients (21%) undergoing PCI for ACS. [*Bae et al*] Having performed pre-PCI IVUS-VH they found that fibro-fatty plaque volume across the entire lesion length correlated with slow flow which appears to incriminate this type of plaque (or more likely thrombus) as the main culprit for reduction in TIMI flow following lesion treatment. This suggests that IVUS-VH in ACS can identify angiographically silent thrombus burden and potentially facilitate thrombus aspiration before balloon angioplasty or stent implantation. However other authors looking at post thrombus aspiration STEMI patients and stable angina patients, appear to suggest that only the necrotic core volume is the independent predictor of no-reflow. [*Hong et al 2009; Kawaguchi et al 2007; Kawamoto et al 2007*].

Over time a growing evidence base is accumulating to support optimum lesion assessment and stent deployment during PCI procedures, to ensure the clinical benefit is passed on to patients. We aim to show within our observational studies, the difference between plaque geometry and components in different clinical situations and the effect of angiographically guided PCI on lesion outcome (as

assessed by IVUS-VH) We hope that the information gained in this area will not only enhance our knowledge of unstable coronary disease but provide insight and evidence for the continued use of IVUS-VH to improve invasive coronary procedures. Our knowledge of the natural history of atherosclerosis including lesion classification relies on post-mortem histology data. As IVUS-VH enables *in vivo* identification of four different plaque characteristics and their location, this technique may enable a more accurate classification of lesions with regard to progression and regression. With time, we may even be able to determine with high accuracy which lesions should be treated immediately with intervention and which with long-term systemic medical therapy.

2.6 IVUS-VH Current Limitations

The limitations of this technique are described elsewhere. [*Konig et al 2008*] The most crucial aspect of any IVUS examination is a steady pullback. However, accurate observer manual border detection is critical when post-processing the images. The virtual histology software produces an automated border detection which is very variable in its accuracy. Poor detection of vessel landmarks can seriously influence composition results and plaque risk assessment. Therefore our first study within this thesis aims to fully determine not only the intra and inter-observer variability of VH analyses but to define the thresholf of measurement error for future longitudinal studies in this area.

The axial resolution of IVUS-VH (150 μm) is too low to detect thin fibrous cap thickness, which is currently defined as 65 μm. This threshold for critical cap thickness has, however, been established for ruptured plaques and not TCFAs. Histopathological studies apparently demonstrate a higher thickness for caps in TCFAs. [*Konig et al 2008*] This is related to the dehydration produced when preparing specimens.

As previously discussed and shown, thrombus detection could help localize the extent and also origin of the plaque rupture in patients with ACS. Thrombus as the primary surrogate for acute coronary thrombosis cannot yet be assigned a colour classification and therefore it should be spotted on grey-scale IVUS to ensure it is documented within the analyses. More attention should be paid to rupture and thrombus associated plaque (TAP) as this effectively represents the ruptured plaque that has been involved directly in an atherothrombotic episode. In a similar situation plaque rupture is visible on grey-scale IVUS but is not traceable by the current software and has to be included within the plaque burden (increasing fibrofatty proportions).

There also remains a concern with regard to the true ability of the IVUS-VH classification tree algorithm to accurately predict what is behind areas of significant calcification within plaques [*Murray et al 2010*].

There are evolving techniques using OCT (optical coherence tomography) and NIRS (near-infrared spectroscopy) which may help delineate the vessel architecture and composition. Optical coherence tomography (OCT) uses near-infrared electromagnetic radiation, and cross-sectional images are generated by measuring the echo time delay and intensity of light that is reflected or back-scattered from internal structures in the tissue.

Current OCT images are obtained at the peak wavelength in the 1,280–1,350 nm band that enables a 10–15 μm tissue axial resolution, 94 μm lateral resolution at 3 mm, and maximal scan diameter of 6–8 mm (about 10 times resolution as compared with IVUS. 'Lipiscan™' IVUS has now been cleared for sale in the USA and uses NIRS to detect areas of lipid core providing a 'chemogram™' linked to the IVUS pullback. This NIRS is based upon the different absorption of light at different wavelengths by different chemicals. This allows co-registration of coronary anatomy and true lipid composition. This technique not only advances our knowledge of atherosclerosis but appears to show promise in determining which patients may sustain a peri-procedural myocardial infarction. It may also become useful in judging the length of stent to place in order to prevent landing edges into unstable lipid cores.

2.7 Recent large trials in IVUS-VH utility

2.7.1 Prospect, VIVA, Atheroemo and VIVA sub-studies

Interestingly, all of these trials (both independent and industry sponsored) have reported surprisingly similar results. In patients undergoing coronary angiography, the presence of IVUS virtual histology-derived TCFA lesions in a non-culprit coronary artery is strongly and independently predictive for the occurrence of MACE within 1 year, particularly of death and ACS. Thin-cap fibroatheroma lesions with a large plaque burden carry higher risk than small TCFA lesions, especially in the short term.

Moreover, lesions lacking necrotic core (non-fibroatheromatous lesions) were found to be clinically stable and were rarely associated with clinical events during 3 years of follow-up.

In summary, the common finding from these trials was that the following were predictive of future MACE in non-culprit arteries (The culprits were stented before IVUS-VH was performed):

1. Plaque Burden >70%
2. Presence of TCFA
3. Minimum Lumen Area <4mm^2

The most recent trial Atheroemo [*Garcia-Garcia et al 2012*] confirmed the findings of Prospect [*Stone et al 2010*] and VIVA [*Calvert et al 2011*]. In >500 patients, 6% had a high risk plaque that fits all of thse criteria and these patients had a 10% rate of death, ACS or revascularisation at 1 year. This end-point was driven by revascularisation events. Unfortunately this trial subdivided TCFA into small and large. This is something that was never done before and not within the previous guidelines on how to analyse VH [*Garcia-Garcia et al 2008*]. The lack of hard events adjudicated in all these trials is related to the general methodology. Unfortunately when a stent is placed in the culprit lesion and non-culprit disease is then imaged for follow up, the natural history of this disease process is profoundly attenuated by the patients being placed upon DAPT, Statin, ACE and B-blocker in as treatment for their culprit event. The only way to study this as a true natural history study would be to intravascularly image asymptomatic patients (on no primary preventative medication) and follow them up for events. There are serious questions about whether this would ever be ethical in the light of current findings.

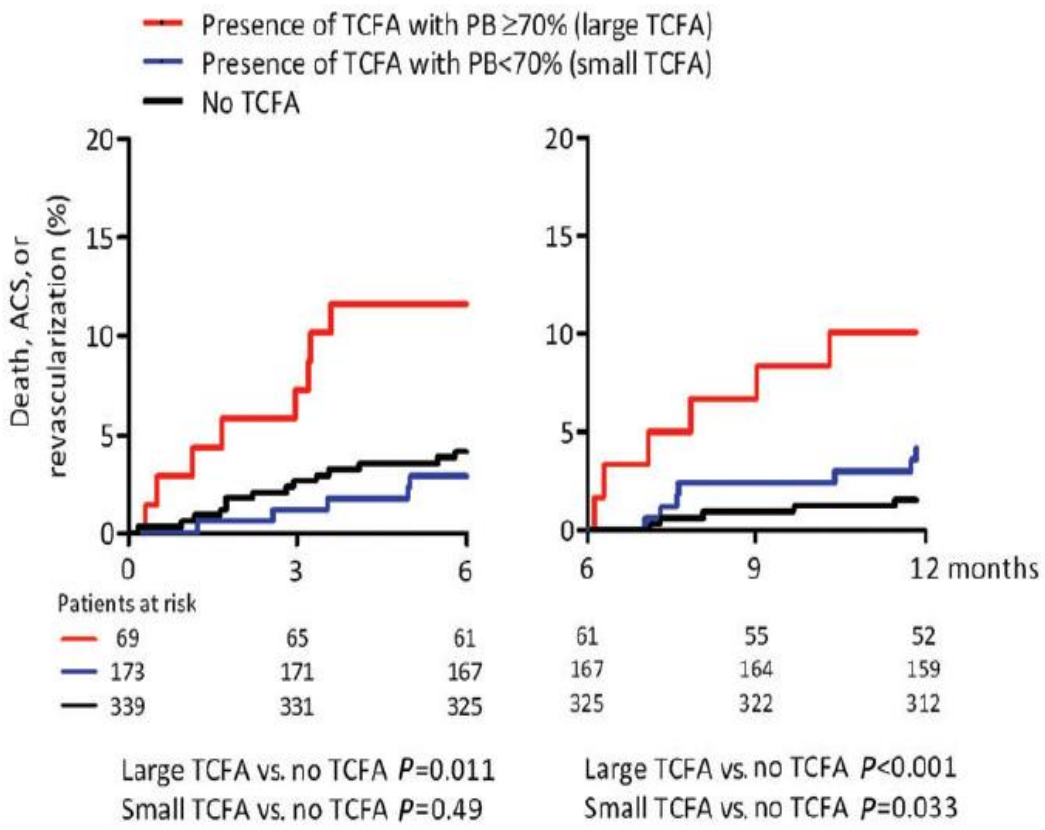

Figure 2.9.6 – Results of Atheroemo study into plaque features and subsequent events

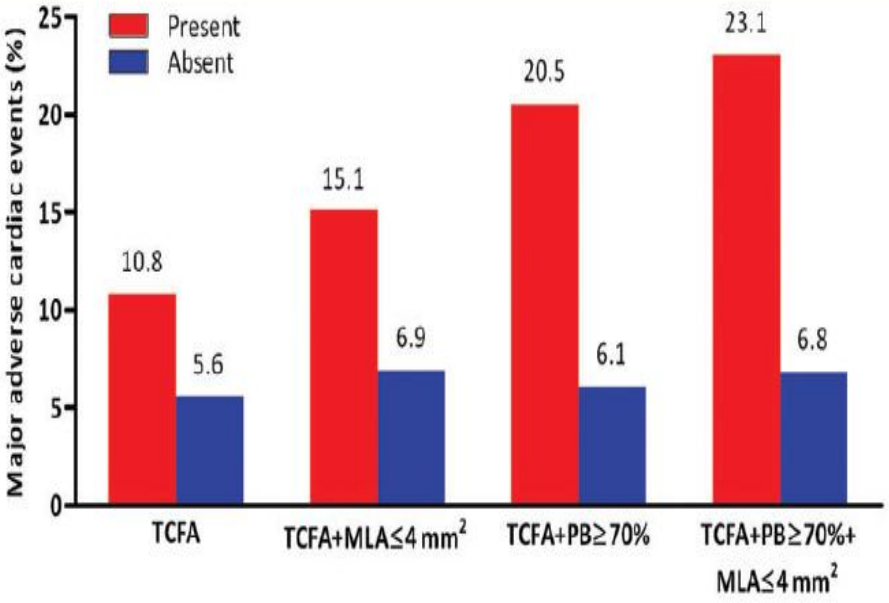

95% CI lower limit (%)	6.9	3.1	6.1	4.7	10.9	3.9	9.0	4.6
95% CI upper limit (%)	14.7	8.1	24.1	9.1	30.1	8.3	37.2	9.0
Prevalence (%)	41.7	58.3	10.5	89.5	11.9	88.1	6.0	94.0
No. at risk at 1 year (n)	211	312	50	473	52	471	52	471
Hazard ratio (95% CI)	1.96 (1.08-3.53)		2.26 (1.09-4.69)		3.47 (1.86-6.49)		3.70 (1.72-7.95)	
P-value	0.024		0.025		<0.001		<0.001	

Figure 2.9.7 – Most recent data on plaque features and % MACE. This may allow prognostication and plaque staging in the future.

2.8 Counter arguments to the "vulnerable plaque theory"

The vulnerable plaque theory (like any theory) has lots of issues. Principally, a "biologically active" plaque can change over time (possibly even as short as a few months). Notwithstanding this major issue, we must start to consider the whole problem in more detail and attempt to understand "the perfect storm". A recent review by *Renu Virmani and Valentin Fuster et al 2014*, has highlighted six major areas that can help us map out the array of variables that are responsible for these arterial natural disasters.

1. **Plaque Characteristics** (location, endothelial dysfunction, composition, vessel remodelling)

2. **Blood Flow** (shear stress, hypertension, viscosity etc)

3. **Haemostasis** (platelet function, tissue factor, PAI-1, thrombin, coagulation factors etc)

4. **Inflammation/metabolic conditions** (Infection, CKD, diabetes, metabolic syndrome etc)

5. **Neuro-hormonal** (mental stress, depression etc)

6. **Environmental** (diet, smoking, drugs, sedentary lifestyle, extreme exertion etc)

I would add to this a seventh: **Genetics** (A genetic pre-disposition that may encompass all of the above other factors, but is currently poorly understood).

2.9 Conclusions and subsequent hypotheses

IVUS-VH is a promising imaging tool with potential for clinical application in PCI. However, several issues have yet to be adequately addressed by the current literature. Some of these issues are addressed in our hypotheses for this work. These are as follows:

1. Is the intra and inter-observer measurement variability for the technique (in both area and volume analyses) sufficient to allow differences in plaque variables to actually be detected?

2. Are there detectable difference in IVUS-VH plaque variables between culprit and stable patient presentations? Can we predict the clinical implications of a plaque from morphology alone? Are there site-specific differences in plaque morphology across the spectrum of coronary artery disease?

3. Does the minimum lumen area of a coronary plaque contain the most vulnerable plaque as classified by IVUS-VH? What is the relationship and difference between plaque at the MLA and the site of maximum Necrotic Core.

4. What is the subsequent prevalence of stent abnormalities, geographic miss and residual vulnerable plaque when PCI is performed for ACS under angiographic guidance?

Chapter III

Methodology

3.1 Introduction

The use of IVUS in the clinical setting has previously been restricted, in our centre, to the evaluation of left main stem disease, in-stent restenosis and visualisation of indeterminate narrowings or strange angiographic appearances. We sought during this study, with ethical approval, to expand the indications for IVUS-VH use to encompass the treatment of Acute Coronary Syndrome patients.

3.1.1 Study design

The following methods provide the study protocol for the initial investigation into the use of virtual histology in the observation of acute coronary syndromes. This study protocol has been designed as a single centre, prospective, observational cohort study.

3.1.2 Specific research objectives

A comprehensive background to the field and literature review has been presented in the previous chapters. The specific research objectives of this thesis are to examine the use of virtual histology in four specific areas.

1) The intra- and inter-observer variability of plaque compositional measurements.
2) The quantification and difference in plaques types across the spectrum of coronary artery disease. Can these generate a plaque risk model?
3) The measurement of the distance and compositional differences between the angiographic culprit stenosis and the most unstable plaque in the target vessel seen on virtual histology.

4) The observation of angiographically guided stent placement and the rate of failure to treat unstable plaques and to gain good stent results.

3.1.4 Sample size calculation

Using the hypothesis that the mean necrotic core volume will be variable between the three groups and based upon data from our interim analysis showing a large mean SD for volumetric plaque components of +/- 30mm^3 a sample size of 70 ACS lesions and 50 comparator lesions (non-culprit and stable) has been calculated. From this we can expect 80% power to detect a 10mm^3 difference in plaque components with a 95% confidence interval. This will permit the relative differences in the mean of these continuous variables to be calculated using a one-tailed *t* test between the ACS group and the stable angina control group. A p-value of <0.05 will be considered significant.

3.1.5 Statistical analysis

The clinical, procedural and IVUS-VH data were analyzed using Stats Direct statistical software (version 2.7.7). The continuous variables were expressed as mean ± SD and the categorical data were expressed as proportions. Continuous data were compared using Student's t-test for normally distributed data and a Mann–Whitney U test for skewed data. Intra-individual comparisons were performed using the Wilcoxon test. Comparison of categorical data and frequency of occurrence was performed with Fisher's exact test. A P value of less than 0.05 was considered statistically significant.

3.1.6 Protocol Development

Protocol development for this study began in August 2007 between SM and NDP after extensive literature analysis and previous background work in the field (NDP). The final draft was accepted through the hospital research development committee in 2008 and also was processed through the local ethics committee at that time. Following discussion with Prof G Hart at the University of Liverpool, an amendment was made to the protocol and this was then accepted and registered for the degree of MD. The protocol revision was passed by the regional ethics committee thereafter in 2008. There was a delay of around one year during this process due to political issues at the University which substantially affected the flow of the study in terms of initial recruitment.

3.2 Ethical approval

3.2.1 Good clinical practice

The study was conducted in compliance with accepted standards of the International Conference on Harmonisation Good Clinical Practice guidelines, and conformed with all national and local laws, rules and regulations relating to study conduct. The protocol was approved by the local Cheshire Research Ethics Committee.

3.2.2 Informed consent

During the patient visit an unambiguous written patient information sheet in simple language was provided, with sufficient time to fully read this information. The study was then discussed in greater detail, allowing for specific questions and providing additional information regarding the study. Each potential subject was adequately informed of the aims, methods, anticipated benefits and potential risks of the study and any discomfort it may entail. Patients were informed of their liberty to abstain from participation in the study and freedom to withdraw consent to participation at any time. Freely given written informed consent was obtained from all subjects before enrolment. A further verbal consent was taken in all patients on entering the cardiac catheterisation lab to ensure they still agreed on IVUS examination of their coronary arteries before and after the procedure. See Appendix for consent form.

3.2.3 Confidentiality

Patients were assigned an individual participant number immediately after providing written informed consent and database details were cut to hospital number, initials and age in years. All other electronic documents pertaining to personal data, study protocol and results were stored securely by the investigator on home and laptop personal computers, solely accessible by the investigator and password protected.

3.2.4 Monitoring

Continuous monitoring was undertaken throughout by supervisors Dr ND Palmer, Dr RH Stables and Prof G Hart. The study was subject to review at any time by the Cheshire Research Ethics Committee.

3.2.5 Amendments

A notice of amendment was submitted to the Research Ethics Committee in the event of any substantial amendment to the protocol. Full approval was gained from the committee chair before further continuation of the study

3.3 Inclusion Criteria

1. Active acute coronary syndrome requiring PCI.
2. Able to provide informed consent.
3. Coronary anatomy suitable for IVUS introduction and pullback.

3.4 Exclusion Criteria

1. Significant angiographic left main stem disease.
2. Significant vessel calcification.
3. Significant three vessel disease.
4. Cardiogenic shock or left ventricular failure.
5. Acute or chronic renal impairment (Creat>200).

6. Reduced flow (TIMI II) in the culprit vessel.
7. Heavy thrombus likely to embolise on passage of IVUS.
8. Previous PCI in the culprit vessel.

3.5 General Procedural Methods

We performed IVUS-VH analysis along defined proximal coronary segments incorporating the entire lesion prior to PCI using motorised (0.5mm/sec) pullbacks. Each segment for study was greater than 20mm in length to enable sufficient acquisition of data per segment and therefore replicate the current research and clinical application of IVUS-VH in lesion assessment. The same data was analysed off-line at an interval of two weeks by one independent operator (***A+B***) to compare for intra-observer variability and once by a second independent operator to compare for inter-observer variability (***C***). Individual regions of interest (ROIs) will be selected by the operator, guided by agreed anatomical landmarks such as side-branches or localised calcium deposits. Automated, followed by manual, lumen and vessel contour detection is performed by each operator prior to computer-based calculation of plaque constituent and plaque/vessel volumes, expressed as mm^3.

IVUS-VH analysis of a culprit vessel containing a lesion (which is thought to be clinically and angiographically the cause for ischaemia and infarction in ACS) deemed suitable for PCI and an angiographic non-culprit (unlikely to be responsible for ECG changes or ischaemia) lesion was undertaken in ACS patients (n=100

lesions). Lesions identified for PCI in elective patients with stable angina were also studied in a similar way (n=35 lesions). The three groups were compared with respect to measurements of remodelling index (RI), total plaque volume in mm^3 and the volumes and percentages for the individual plaque components: Fibrous; Fibro-fatty; Dense Calcium and Necrotic Core.

Each culprit lesion was also analysed from a predefined point within the distal reference segment to a similar position within the proximal reference segment. The length of the segment incorporating the culprit lesion was measured using computer-generated calipers incorporated within the IVUS-VH system. Along the length of each lesion, each IVUS-VH individual frame was analysed. Necrotic core was identified by the IVUS-VH classification tree and felt to be significant if it is responsible for >20% of the plaque. Over a number of frames the maximum point of the necrotic core (NC) was selected, defined as the IVUS cross-section with the largest area of confluent necrotic core expressed as a percentage. Finally the distance from the maximum NC site to the MLD site was measured in mm. A direct comparison was made between the MLD site and maximum NC site, which will include the relative constituents of all four plaque components, total plaque burden and the remodelling index.

The selection of non-culprit plaques was operator determined and in 16 cases these lesions were interrogated distal to the site of a culprit plaque (same vessel). Four non-culprit plaques came from a different (non-culprit) vessel.

Comparisons of IVUS and IVUS-VH analysis before and after stent deployment were also undertaken. In accordance with conventional clinical practice, operators had the option of utilizing the grey-scale IVUS to determine vessel size and therefore stent size selection. However, IVUS-VH information regarding lesion composition and length was not made available, as this was not a conventional clinical application during PCI in our institution. Following stent deployment and angiographic evaluation, a further blinded IVUS-VH assessment was undertaken to assess stent deployment and geographic miss. Particular importance was placed on the distance in mm from stent edges to sites of proximal and distal necrotic core. This required accurate determination of proximal and distal anatomical segment markers in the initial phase of the study protocol with which to reproducibly determine accurate distances to necrotic core and stent edge sites.

Therefore, the first blinded IVUS-VH determined the lesion length and sites of necrotic core rich vulnerable areas. The second blinded (post-stent) IVUS-VH determined whether the angiographic stent strategy had:

1. Covered the full length of the culprit plaque and adjacent vulnerable areas.
2. Covered all sites of lumen reduction with plaque burden >40%
3. Adequately expanded the stent to MUSIC and AVID criteria.
4. Measure the length and dimensions of residual uncovered plaque.
5. Calculate the prevalence of unstable plaque left behind.

3.5.1 Statistics

We compared relative distances in mm between the stent edges and necrotic core sites or residual plaque. Comparisons were also made between the proportions of stents that provide complete lesion coverage and those that leave plaque or unstable disease uncovered (described as percentages). In the stent group that failed to cover disease or adequately deploy, an analysis of the mechanism was undertaken i.e. proportions with stent length underestimation, stent misplacement, underexpansion or a combination of these factors. Simple descriptive statistics were employed. An unpaired *t* test was made to compare the angiographic stent length selection in mm against the subsequent IVUS-VH based full lesion length in mm.

A more detailed statistical methodology is included during each chapter to remind the reader of what was done at each investigative stage.

3.6 Recruitment

3.6.1 Methods

Patients suitable to participate in the study were identified by screening the transfer lists for urgent PCI. Each patient who was transferred from a district general hospital had a referral form detailing their presentation, ECG changes, diagnosis and in some cases, diagnostic coronary angiograpy. Further suitability was taken from existing case notes and inclusion and exclusion criteria were directly applied at this

stage. Following a formal approach, the nature of the study was verbally explained and patients were asked if they were interested in participating. Those expressing an interest were invited to read the patient information leaflet and then re-approached for informed consent.

3.6.2 Limitations

Recruitment was a challenge for a number of reasons. Many patients being transferred had an extensive cardiac history including various exclusion criteria. Many patients were not keen to undergo any further procedures than were absolutely necessary (in the circumstances). Many patients, after enrollment, were subsequently found to have anatomy unsuitable for IVUS such as: heavy thrombotic load, significant left main stem disease, heavy calcification and surgical 3VD. In some cases, the IVUS would not pass the culprit lesion. Occasionally on passing the IVUS catheter, significant ECG ischaemia and symptoms of chest pain, meant the IVUS had to be abandoned in favour of urgent PCI. Following completion of the case, there were further technical factors related to problems with pullback quality. A number of pullbacks were of poor quality and unable to provide meaningful data. Media related issues also occurred related to capture of virtual histology data and the ability to analyse the data on the given software. A breakdown of the recruitment is shown in fig 3.1 below.

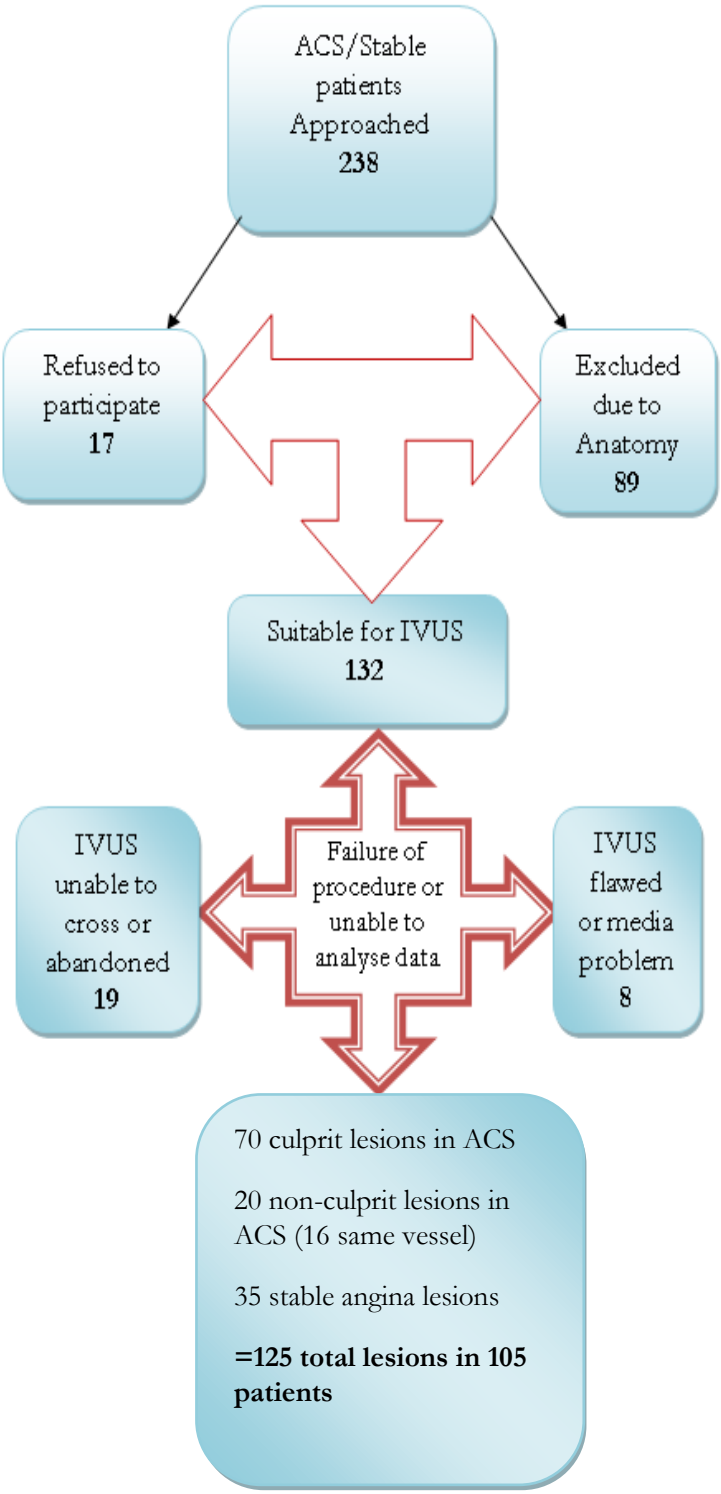

Figure 3.1: Flow diagram of recruitment with patient/lesion numbers.

Chapter IV

Study I

The intra and inter-observer agreement of IVUS-VH analyses for qualitative and quantitative lesion assessment.

4.1 Introduction

Coronary plaque imaging with Virtual Histology (VH) allows estimation of the quantitative composition of atherosclerotic plaques *in-vivo* and has already been used as a surrogate outcome measure [*Serruys et al 2008*]. However, there is currently no consensus on appropriate VH endpoints for clinical trials or for accurate power calculations, to ensure a true difference is being detected. Repeat measurements of plaque composition can be subject to both reproducibility (inter-catheter and inter-pullback) error and variability (human measurement) error - introduced in the following ways:

• Inconsistent definition by the operator of the surfaces to be measured (lumen, vessel).

• Inconsistent selection of the segment to be measured (proximal and distal marker frames).

• Difficulty in distinguishing plaque margins, for example blood from thrombus and tissue.

• Difficulty in distinguishing plaque components such as calcification from adventitia or artefact.

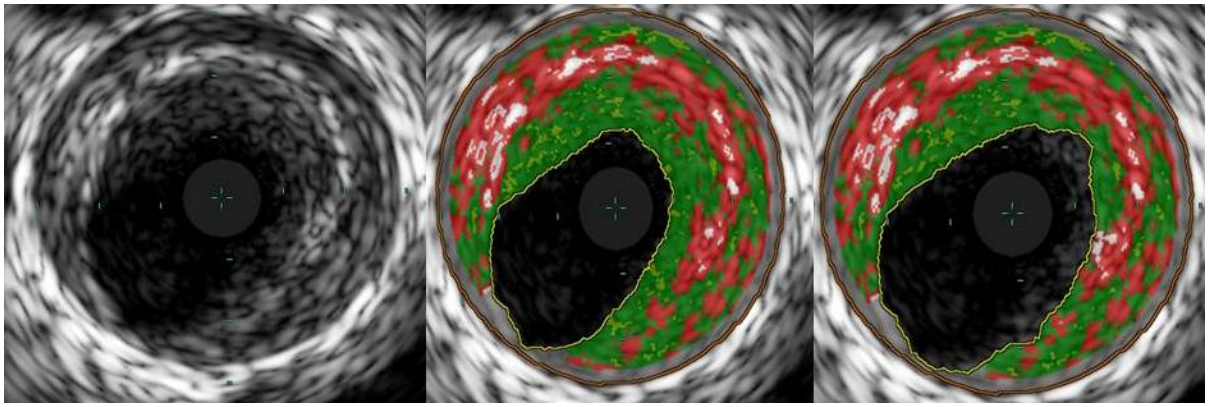

Figure 4.1: An example of differing IVUS-VH border detection between operators.

Recent serial clinical IVUS-VH studies, such as the IBIS-2 trial [*Serruys et al 2008*] have revealed only small changes in plaque volume and its relative composition following pharmacological intervention. The measurement variability of volumetric IVUS-VH analyses is therefore an important scientific issue. In the past there has been a distinct lack of published literature documenting variability or reproducibility for volumetric IVUS-VH measurements in the clinical setting [*Hartmann et al 2008; Huisman et al 2010; Prasad et al 2008*]. Previous validation studies have been confined to single frame area analysis or volumetric analysis in pre-defined, short coronary segments with mild disease in stable patients. These patients were generally not scheduled for coronary intervention [*Rodriguez-Granillo et al 2006*]. To date, assessments of the level of agreement have been based upon calculating the paired differences in data and applying a token rule of less than 10% difference in mean values as being clinically acceptable. This does not take into account the inherent

standard deviation within the data which has a dramatic effect on final numerical calculations of individual plaque measurements.

The knowledge of the observer variability of any measurement is essential for validation of scientific techniques and in this case, it is required to ensure a high predictive accuracy in serial plaque measurement and composition.

Therefore, in this study, we assessed the intra and inter-observer variability of individual plaque areas, volumes and segment length selection in a single pullback of acute coronary syndrome plaques. We utilised a selection of detailed statistical tests of measurement error including the repeatability co-efficient. Our aim was to comprehensively determine the limits of human variability error for this proposed clinical tool.

4.2 Methods

This was a single centre, prospective, observational study that received ethical approval from a regional National Health Service (NHS) ethics committee in the UK. Patients presenting with ACS gave written informed consent and were studied prior to percutaneous revascularisation. IVUS-VH imaging of the culprit lesion (CL) was undertaken using a phased array catheter (EagleEye catheter, 2.9 F/20 MHz; Volcano Corp). Marker frames were chosen in keeping with a consensus document on how to analyse both IVUS and VH [*Garcia-Garcia et al 2009; Di Mario et al 1998; Mintz et al 2001*]. The IVUS transducer was advanced beyond the presumed culprit

lesion and beyond the next distal side-branch which would be used as a marker for localisation during IVUS image assessment. A proximal border for image assessment was established in a similar fashion using another side branch or the mouth of the guide catheter. Following administration of 1mg of Isosorbide Dinitrate (ISDN) intra-arterially, a continuous motorized pull-back at 0.5 mm/s was performed (Volcano R100 pullback device) until the probe had passed the proximal segment marker. The plaque composition and other analyses were performed by off-line IVUS-VH analysis (S5i Tower and PC VIAS 3.0.394 software; Volcano Corporation) following manual adjustment of border contours. The data were analysed off-line at intervals of two weeks by two independent operators (SM and NDP), to compare for intra (SM1 and SM2) and inter-observer variability (SM1 and NDP).

Segment length was initially determined by the operator choice of distal and proximal VH reference frames. This decision was made after consultation of angiographic images (if required), the grey-scale IVUS runs and a written description of the pullback segment markers. Short pullbacks (<10mm) or pullbacks containing significant calcification or large side-branches (obscuring adequate vessel delineation) were not included in the final analysis. Thrombus-laden or ruptured plaques were included, as they are a common feature in high risk ACS patients. A separate cohort of high risk ACS lesions with a fixed length (n=300 frames) were also individually analysed by each operator to provide comparative data on area and volume calculations from a fixed length model. Following individual observer manual

adjustment of borders in keeping with previous consensus statements, plaque variables and constituents were then calculated by the VH algorithm over the entire length of a lesion [*Von Birglen et al 1997*]. Data was collected to include: Lumen area; Vessel area; Plaque area; Media area; Fibrous (**F**); Fibro-fatty (**FF**); Necrotic core (**NC**); Dense calcium (**DC**) area are as well as total plaque burden. The total volume of fibrous (**F**); fibro-fatty (**FF**); dense calcium (**DC**) and necrotic core (**NC**) plaque was also quantified in mm^3. The technique and validation of IVUS-VH has been described elsewhere [*Garcia-Garcia et al 2009; Nasu et al 2006/2008; Nair et al 2002/2007*] and in a single human study, histological verification has shown accuracy [*Nasu et al 2006*].

4.3 Statistical Methods

There are limited previous studies discussing the calculation of power for variability analyses. In 2008 Bartlett *et al* published a paper focussed purely on measurement errors in continuous variables; we used the statistical methods from this to calculate our provisional limits of agreement for each measurement involved in this work. Using necrotic core data from our first 5 patients, the mean of the paired difference was $0.74mm^3$ with a standard deviation (SD) of +/- $0.82mm^3$. To calculate the limits of agreement for a Bland Altman plot of variability we used these results in the previously verified formula [*Bland et al 1986; Altman et al 1991*].

$$\textbf{Limits of Agreement} = \textbf{mean difference} +/- 1.96 \times \textbf{SD}$$

From these data, the worked limits of agreement are from -0.867 to 2.34mm^3. To calculate the standard error of these limits and the subsequent 95% confidence intervals (CI), we used our standard deviation and n=5 in the formula:

$$\textbf{Standard error} = \frac{\textbf{1.71 x SD}}{\sqrt{\textbf{(n)}}}$$

This produces a standard error of 0.63 and in turn 95% CIs of (-2.09, 0.36) and (1.12, 3.58) respectively. This data for five patients produces a standard error of 0.63 which is reduced to 0.31 by increasing the sample size to 20 patients (assuming the SD remains relatively constant). A standard error of 0.31 ensures 95% confidence intervals around our limits of agreement, which is also within the previously acceptable Bland Altman variability of 10%.

4.3.1 Intra-class correlation co-efficient

A 10% variability limit, as in previous studies, without considering the inherent standard deviation and the limits of agreement, under-estimates error. Therefore, we have chosen to calculate the intra and inter-observer agreement using intra class correlation co-efficient (ICC) as well as displaying the overall within subject standard deviation (WSSD). ICC was used over Kappa because our data is mainly continuous. ICC is effectively equivalent to a weighted Kappa statistic [*Bonett et al 2002*]. We have included Bland-Altman plots for visual illustration of variability. Optimal sample sizes for ICC are based on the desired power level, the magnitude of the predicted ICC and the lower confidence limit. Bonnett *et al* in 2002, investigated sample size

issues for ICC, concluding that the optimum sample size is a function of the size of the ICC and the number of ratings per subject, as well as the desired significance level (alpha) and desired width (w) of the confidence interval. Bonnett concluded that the optimal sample size for two ratings varied from 15 for ICC=.9 to 378 for ICC = 0.1. Our sample size of 20 is therefore adequate in this context.

4.3.2 The repeatability co-efficient

In order to find the maximum magnitude of measurement error during the analysis of these cases, we expanded our analysis to include the repeatability co-efficient (RCO). This is calculated from the within subject standard deviation as follows:

$$\mathbf{RCO = \sqrt{m}\, Z\, (x_w)}$$

Where **m** is the number of observations per subject, **Z** is a quantile from the standard normal distribution (usually taken as the 5% two tailed quantile of 1.96) and **Xw** is the estimated within-subjects standard deviation (calculated previously).

The repeatability coefficient (RCO) is a precision measure. It can be thought of as a confidence interval for error. It represents the value, below which, the absolute difference between two repeated tests results may be expected to lie, with a probability of 95%. This is the definition adopted by the British Standards Institution [BSI BS5497 1979]. We can therefore say that 95% of our potential future measurement errors, in this cohort, should not be beyond the figure calculated by

the RCO. Therefore, any change greater than this level is likely to represent a true change in the measured variable of the plaque.

4.3.3 Statistical analysis

Statistical analysis was performed using the agreement function within Stats Direct statistical software version 2.7.7. Quantitative data are expressed as mean ±1SD or within subject standard deviation (WSSD) in mm, mm^2 or mm^3. The repeatability co-efficient is presented as a calculated area or volume in mm^2 or mm^3 and is also expressed as a proportion of the total measured area or volume. Bland Altman plots provide a visual display of the agreement within ±2SD of the mean between measurements. An intra-class correlation co-efficient of >0.90 is considered excellent indicating that less than 10% of the error is due to operator variability.

4.4 Results

20 lesions from 20 patients generated 1080 frames of IVUS-VH. Each frame was analysed three times (SM1, SM2, NDP) n=3240. A further 300 fixed frames were analysed twice (SM1, NDP) to provide data on individual area and volume variability from a fixed length. Therefore, a total of 3840 frames were analysed on both the S5i platform and PC VIAS 3.0.394.

4.4.1 Patient Characteristics

The basic patient clinical data is documented below in table 4.1.

Table 4.1: Patient clinical characteristics

Characteristic Prevalence	Value or Percentage
Age(±SD)	**61.2 (±9.7)**
Male	**80%**
LAD/Diagonal	**42.3%**
RCA	**36%**
Circumflex/OM	**21.7%**
NSTEMI	**60%**
STEMI (Thrombolysed)	**16%**
ACS	**24%**
Mean Troponin µg/ml (±SD)	**12.14 (±24.4)**
Median Troponin µg/ml (IQR)	**1.4 (0.04-13.7)**
Local modified TIMI Risk Score	**8.5 (±2.3)**
Hypertension	**64%**
Diabetes	**24%**
Current Smoker	**36%**
Ex-smoker	**16%**
Family History CAD	**60%**
Hypercholesterolaemia	**44%**
CKD	**4%**
Previous MI	**12%**
Previous PCI	**0%**
Previous CABG	**0%**

4.4.2 IVUS-VH analysis and data

The mean segment length analysed in this study was 27.14±9.1mm, (range 13 to 45mm). The results of these analyses are presented in tables 4.2-4.4 and displayed graphically with Bland Altman plots of inter-observer variability (figure 4.1). The details of the separate individual area analyses and fixed length volume analyses are displayed in table 4.5.

Table 4.2: Calculated observer means ± Standard Deviation (SD), per variable.

Vessel Variable	SM(1)* Mean ±SD	SM(2) Mean ±SD	NDP* Mean ±SD
Segment Length (mm)	27.02±9.1	27.29±8.7	27.12±9.4
Total Plaque Volume (mm^3)	212.63±103	212.68±102.9	212.90±103.6
Fibrous Volume (mm^3)	78.99±38.9	79.66±39.2	79.40±39.8
Fibro-fatty Volume (mm^3)	15.13±8.6	15.73±8.7	16.05±9.1
Necrotic Core Volume (mm^3)	29.10±32.3	28.93±32.1	28.51±32
Dense Calcium Volume (mm^3)	14.68±18.8	14.62±18.6	15.03±18.3

*SM=Observer 1; NDP=Observer 2.

Table 4.3: Paired differences between individual observers and the relative percentages of the variable total.

Vessel Variable	SM (1+2) Mean ±SD	NDP Mean ±SD	Paired Difference ±SD (% total)
Segment length (mm)	27.2±8.9	27.1±9.4	0.1±0.5 (0.36 %)
Total plaque volume (mm^3)	212.66±103	212.90±103.6	0.24±0.6 (0.11%)
Fibrous volume (mm^3)	79.33±39.1	79.40±39.8	0.07±0.7 (0.09%)
Fibro-fatty volume (mm^3)	15.43±8.7	16.05±9.1	0.62±0.4 (4%)
Necrotic vore Volume (mm^3)	29.02±32.2	28.51±32	0.51±0.2 (1.8%)
Dense calcium volume (mm^3)	14.70±18.7	15.03±18.3	0.33±0.4 (2.2%)

Figure 4.2: Bland-Altman plots for the variables measured between different operators with solid lines representing the 95% limits of agreement.

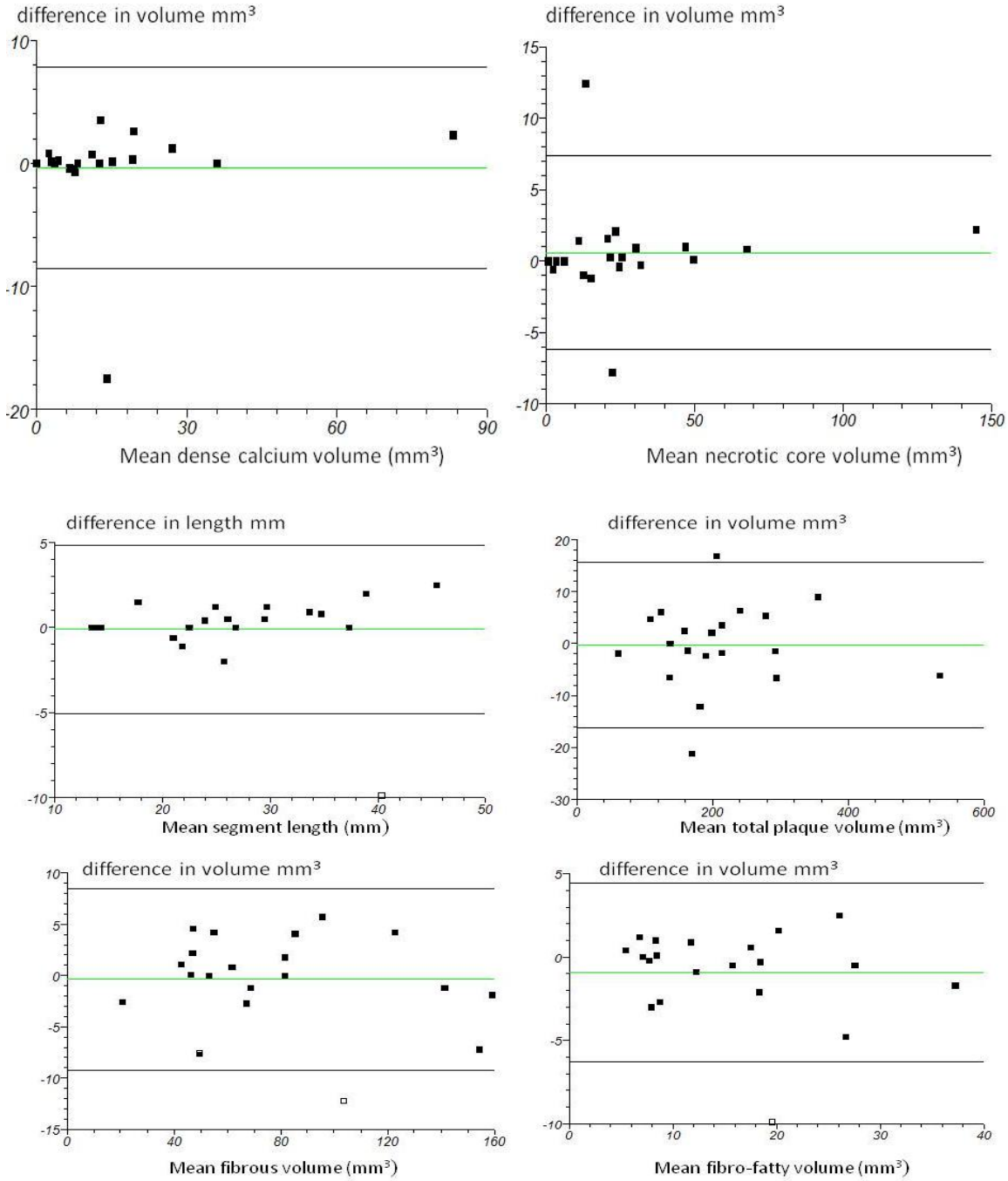

Table 4.4: Observer measures of agreement, precision and repeatability with the relative percentages of the variable total.

	INTRA-OBSERVER				**INTER-OBSERVER**		
Vessel	ICC*	WSSD¥ (% total)	RCOδ (%total)		**ICC**	**WSSD** (% total)	**RCO** (% total)
Segment length (mm)	0.986	1.01 **(3.7%)**	2.81 **(10.3%)**		0.96	1.74 **(6.4%)**	4.82 **(17.7%)**
Plaque volume (mm^3)	1	1.2 **(0.56%)**	3.32 **(1.6%)**		0.997	5.59 **(2.6%)**	15.51 **(7.3%)**
Fibrous volume (mm^3)	0.998	1.85 **(2.3%)**	5.12 **(6.5%)**		0.993	3.14 **(4%)**	8.71 **(11%)**
Fibro-fatty volume (mm^3)	0.969	1.49 **(9.7%)**	4.13 **(26.8%)**		0.947	1.99 **(12.9%)**	5.52 **(35.8%)**
Necrotic core volume (mm^3)	1	0.37 **(1.3%)**	1.04 **(3.6%)**		0.994	2.42 **(8.3%)**	6.71 **(23.1%)**
Dense calcium volume (mm^3)	1	0.26 **(1.8%)**	0.73 **(5%)**		0.974	2.89 **(19.7%)**	8.01 **(54%)**

*ICC – intra-class correlation co-efficient; ¥ WSSD – within subject standard deviation; δRCO – repeatability co-efficient.

Figure 4.3: The magnitude of the repeatability co-efficient error between observers.

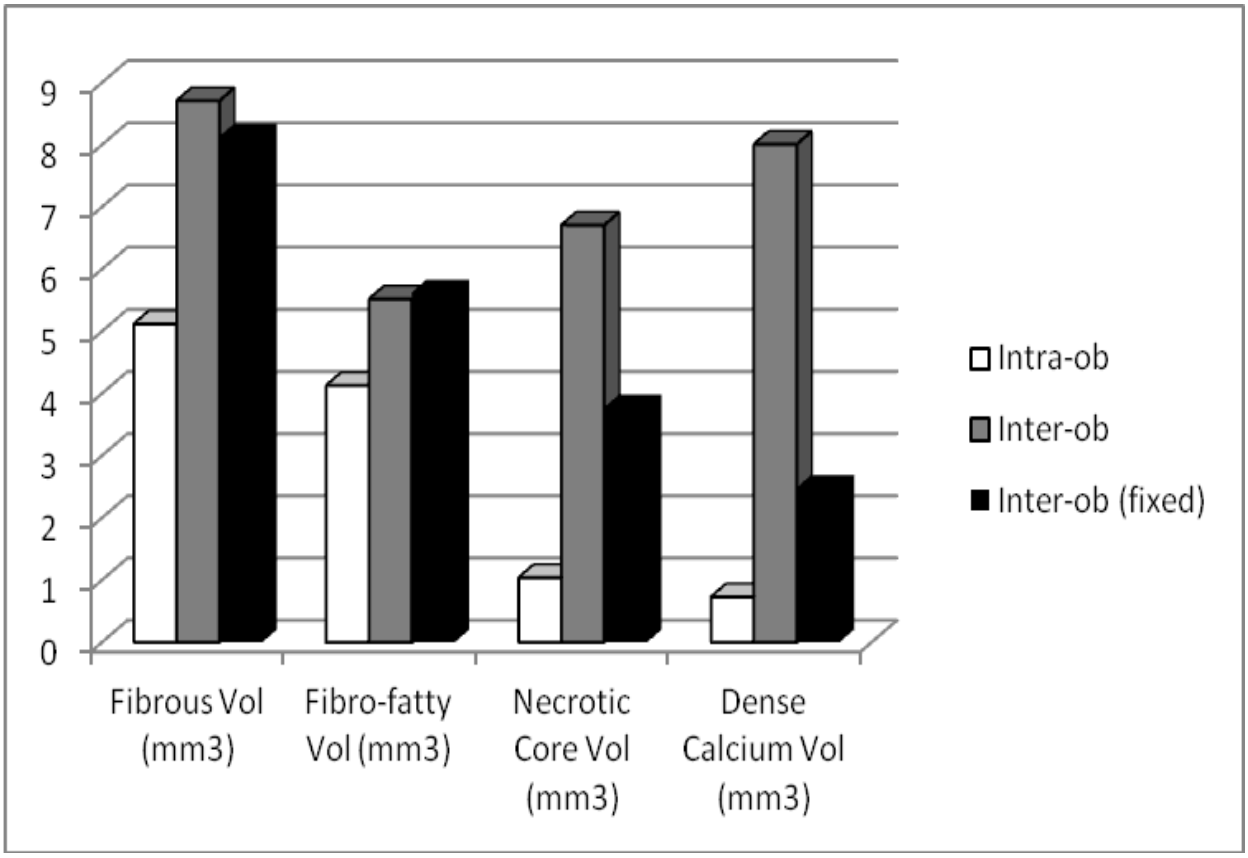

4.4.3 Segment length

Despite this being an operator based judgement where large amounts of variability could be introduced; the ICC remained above 0.90 at 0.986 for intra-observer and 0.96 for inter-observer. However, this equated to a RCO of 2.81mm for intra and 4.81mm for inter-observer. This represented 10.4% and 17.4% of the total segment length analysed. For comparative assessment, the results from a fixed length assessment of 300 frames (147.9mm) are also displayed within table 5.

Table 4.5: Fixed length Inter-Observer measurement of 300 VH frames

Variable Mean (mm^2 or mm^3)	Observer 1 (SM) ±SD	Observer 2 (NDP) ±SD	Paired Difference ±SD (%total)	ICC *	WSSD ¥ (%total)	RCO δ (%total)
Lumen Area	6.58±4.1	6.24±3.4	0.34±0.7	0.96	0.74 (11%)	**2.06 (31.3%)**
Vessel Area	14.99±6.17	14.98±6.13	0.01±0.04	0.99	0.78 (5%)	**2.1 (14%)**
Plaque Area	8.41±3.94	8.75±4.42	0.34±0.48	0.94	1.05 (12%)	**2.92 (33.3%)**
Media Area	2.95±0.64	2.96±0.59	0.01±0.05	0.92	0.17 (5.7%)	**0.48 (16.2%)**
Plaque Burden %	56.46±15	57.39±14.28	0.93±0.72	0.94	3.72 (6.5%)	**10.31 (17.9%)**
Fibrous Area	2.55±1.46	2.77±1.69	0.22±0.23	0.86	0.59 (21.3%)	**1.64 (59%)**
Fibro-fatty Area	0.32±0.34	0.35±0.34	0.03±0.00	0.72	0.18 (51.4%)	**0.49 (140%)**
Necrotic Core Area	1.73±0.62	1.83±0.74	0.1±0.12	0.96	0.18 (9.8%)	**0.39 (21.3%)**

Dense Calcium Area	0.86±0.83	0.84±0.84	0.02±0.01	0.98	0.10 (11.6%)	**0.29 (33.7%)**
Fibrous Volume	82.39±41.3	83.15±44.05	0.76±2.75	0.99	2.94 (3.5%)	**8.14 (9.9%)**
FibroFatty Volume	9.65±5.8	10.45±6.17	0.80±0.37	0.87	2.03 (19.4%)	**5.63 (53.8%)**
Necrotic Core Volume	54.77±44.8	54.98±45.6	0.21±0.8	0.99	1.36 (2.5%)	**3.78 (6.9%)**
Dense Calcium Volume	25.87±18.4	25.22±17.7	0.65±0.70	0.99	0.89 (3.4%)	**2.49 (9.6%)**

*ICC – intra-class correlation co-efficient; ¥ WSSD – within subject standard deviation; δRCO – repeatability co-efficient.

4.4.4 Total Plaque Volume

Results for this variable (along with % plaque burden – table 4.5) show how heavily diseased our analysed segments were. The actual variability between operators was small considering the amount of plaque. ICC was greater than 0.99 for both intra and inter-observer, with paired differences between operators of only 0.24±0.6mm^3. This represents only 0.1% of the total plaque volume. However, due to the wide SD and resultant 95% limits of agreement, the repeatability error between operators is calculated at 15.51mm^3 (7.3% of total plaque volume). This error is reduced to 3.32mm^3 (1.6%) by single operator repeat analysis.

Figure 4.4: The repeatability co-efficient as a percentage of the total measured plaque between observers.

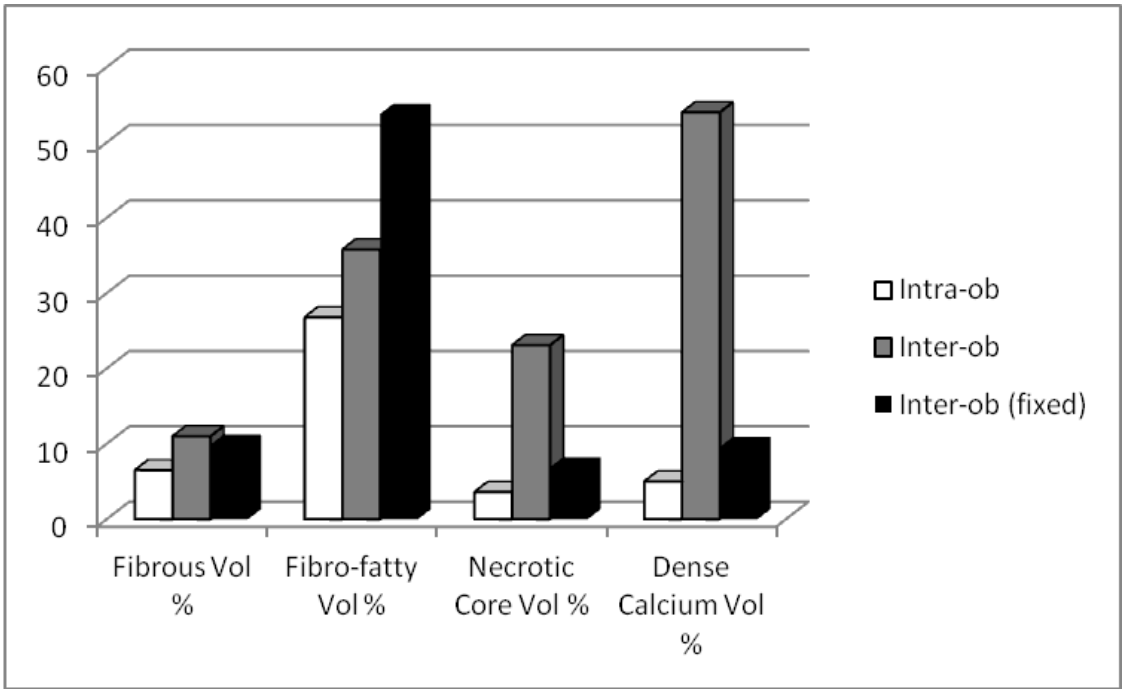

4.4.5 Composition

IVUS-VH assessments of composition were highly correlated in the majority of plaque variables with ICC>0.92 (i.e. less than 8% error between operators). From our fixed data in ACS lesions - Fibrous area (ICC=0.86); Fibro-fatty area (ICC=0.72) and Fibro-fatty volume (ICC=0.87) show less agreement between operators and this appears to be related to the placement of luminal borders around soft plaques and thrombus. It is also clear that one of the reasons for the large limits of agreement and repeatability co-efficient is the large SD of the data. This is secondary to the large spread of plaque values and the large variation seen between individual plaque

components. The relevant results for plaque composition are displayed in tables 4.2-4.5 and figures 4.2-4.3.

4.5 Discussion

We have investigated and reported the intra and inter-observer variability for volumetric virtual histology analyses, in coronary lesions implicated in an acute coronary syndrome presentation. From the results, it is clear that variability in segment length selection between operators exists. This is one of the most important limitations of IVUS technology and serial studies in the "real world" (as reliance is placed on local landmarks such as side branches and calcium deposits). Moreover, assessing a long segment of disease requires analysis of multiple serial tomographic slices recorded during a pullback sequence. These slices must be manually corrected by the individual and the area of the lumen and external elastic membrane (EEM) must be traced accurately to ensure viable results. Although the ICC appears to state that our variability error for tracing lumen and vessel areas is acceptable between 1-4% (ICC 0.99-0.96), when calculating the more quantifiable RCO, we appear to have differences between operators up to 14% for vessel area and 31% for lumen area.

Interestingly, the analysis of 300 individual frames between operators has revealed significant differences with regard to plaque areas (see table 4.5). Although the paired difference of the mean appears very small (as documented in other studies) by calculating the within subjects standard deviation and repeatability co-efficient, we

see that maximum error levels for fibro-fatty plaque area can be greater than the measured area itself (RCO=0.49mm^2 = 140% of the fibro-fatty area 0.32mm^2).

Although on first consideration the inherent variability of volume measurements should be higher as subsequent area errors are multiplied by length, the opposite appears to be true. Volume measurements appear to "smooth out" the individual frame errors over the length of the lesion. This could be because one operator may measure a greater area than the other operator in one frame, but the reverse may be true on the next and over a large lesion this may balance out some of the volume variability. This is the first report to highlight that there could be a regression-type phenomenon within the values seen for volume measurement error.

In our cohort, the use of fixed length analysis improved the errors seen in the measurement of necrotic core and dense calcium components. However, the measurement of fibrous and fibro-fatty components did not change greatly and this may be due to the severe nature of the plaques analysed with thrombus, plaque rupture and difficult luminal border interpretations. The main source of error in all of these cases is a direct reflection of the difficulties in selecting the true lumen-blood interface (fibrous and fibro-fatty plaque calculations). ACS plaques have a high thrombus burden (usually coded as fibrofatty plaque in VH) and this has affected our ability to distinguish blood-speckle from true plaque or thrombus.

Despite the above results and as in previous studies [*Hartmann et al 2009; Huismann et al 2010; Prasad et al 2008*], the classical markers of agreement such as ICC and paired difference of the mean, prove that basic IVUS-VH data can be well matched. Our ICC correlation is in keeping with all previously published results, including a recent multi-centre IVUS-VH reproducibility registry [*Huismann et al 2010*] which reported values of ICC>0.9 for all plaque components and total plaque volume. These results were in mild-moderately diseased coronary segments without a culprit stenosis and this is clear when comparing the maximum total plaque volume and maximum necrotic core volume between their study (**A**) and ours (**B**): **A** - TPV 91.9±27.3; NC 9.2±8.8. **B** - TPV 212.66±103; NC 54.98±45.6.

It appears from these figures that we have examined the severe end of the spectrum of coronary disease with necrotic core and plaque volumes being up to six times greater, from relatively similar pullback lengths. There is no doubt that with increasing plaque burden comes increasing standard deviations and subsequently statistical variability errors.

The previous benchmark reproducibility and variability study was performed in 15 patients undergoing IVUS-VH before PCI. In this study from 2006, Rodriguez-Granillo *et al*, used two independent observers from a well established core-lab and focused on geometrical and compositional elements of IVUS-VH output and reported "acceptable reproducibility with less than 10% error". They published the limits of agreement around the measurement of necrotic core area. An inter-

observer range between +0.16mm^2 and -0.20mm^2 was seen, indicating a potential for maximum error values of around 0.36mm^2 for necrotic core across individual frame analyses (between operators). This is very similar to what we have calculated with the RCO for necrotic core area (0.39mm^2). Although this inter-observer variability appears reasonable and suggests an overall mean 6% change in necrotic core area measurement, if it were applied to a 50 frame volume analysis, then it may produce "worst case" errors up to a maximum of 18mm^3 necrotic core. However, as we have demonstrated in our volume analyses, subsequent over or under estimations can cancel each other out over the full lesion length. This may explain our relatively accurate error results of 6.7mm^3 for necrotic core volume in variable segment lengths and 3.78mm^3 for fixed length assessments.

Importantly, a recent *inter-catheter* reproducibility study by Prasad *et al* in 2008 showed that in a subgroup of volumetric analyses, involving only 12 segments with a mean length of 11mm, the repeatability co-efficient for *inter-catheter* error produced large compositional differences of: Fibrous 13.89mm^3; Fibrofatty 2.95mm^3; Necrotic core 10.46mm^3 and Dense calcium 14.16mm^3. These results and a warning in the discussion chapter of other papers [*Hartman et al 2009; Huisman et al 2010; Rodriguez-Granillo et al 2006*] state that, between catheters and pullbacks, volumetric VH analysis produces high levels of measurement error. Despite these known issues, papers rarely document clearly (in mm^3) the volumetric change that could be expected purely from total measurement error. They opt to only report percentages

or statistical analyses of paired differences, which may grossly under-estimate true errors in compositional volumes. The IBIS-2 trial [*Serruys et al 2008*] used data from the aforementioned Rodriguez-Granillo *et al* 2006 (single frame ***area*** analysis) to justify adequate reproducibility and variability of IVUS-VH ***volume*** analyses. In this study, change in necrotic core **volume** was used as a surrogate end-point to evaluate pharmacotherapy. The final absolute difference between placebo and darapladib treatment was a 5.2mm^3 reduction in necrotic core volume. Unfortunately, this endpoint value lies within the inter-catheter reproducibility error for necrotic core in the study by Prasad *et a*l (10.46mm^3). This endpoint value of 5.2mm^3 does appear to be measurable between operators on a *single* pullback, as it lies above our inter-observer variability RCO of 3.78mm^3. Moreover, the power calculation for the IBIS II trial was initially based upon primary endpoint palpography and HS-CRP data. 239 patients were analysed by VH-IVUS but if a repeat power calculation is performed based on the data from the paper (Mean NC volumes around 22-26mm^3 with a standard deviation of 25), then 1200-1600 patients would have been required at a standard power (80%; α=0.5) to prove a real difference due to the drug alone. Clearly, these findings impact greatly on the validity of some serial studies in this field. Also, a very recent variability analysis by [*Obaid et al 2011*] has shown that in comparison to core-lab analysis there can be significant errors in judgement when identifying plaque sub-types (VH-TCFA etc) between operators. This further reduces the clinical utility of this tool and has implications for studies where different observers make judgements about plaque types.

4.6 Limitations

This study was performed in a single centre, by two experienced operators, without the aid of an industry sponsored core-lab. Some of our analyses were performed by an operator purely on the S5i platform and in some cases these were compared with results from an operator on PC VIAS 3.0.394. Potential differences in the classification tree or software may therefore have influenced plaque components. However, it is hoped that there are not further variability errors to consider between software packages as well as operators, catheters and pullbacks.

Studying high-risk ACS plaques introduces large variations between individual plaque components and therefore creates large SD values. This in turn affects the calculation of limits of agreement and the RCO. It may be that the inherent variability in these plaque types precludes them from future serial study or that the spread of this data makes the RCO less sensitive. Furthermore, our results can only be applied to this cohort of patients, examined by these operators and will therefore not be representative of future measurements made by other operators in non-ACS patients. Our aim has been to provide a cautionary guide to the potential for measurement error with this technique, even in experienced hands. This will hopefully forewarn future result interpretation by operators in a clinical setting.

4.7 Conclusions

As in previous studies, there appears to be good agreement between IVUS-VH observers. However, when the standard deviation of the data is taken into account, this can occasionally represent large measurement error values and percentages. These findings could impact on the interpretation of previous studies and influence future studies using IVUS-VH measurements as endpoints.

CHAPTER V

STUDY II

The Creation and Validation of a Plaque Discrimination Score from the Anatomical and Histological Differences in Coronary Atherosclerosis.

5.1 Introduction

Post-mortem pathological studies have shown that a "vulnerable" plaque is the dominant pathophysiological mechanism responsible for Acute Coronary Syndromes (ACS) [*Falk et al 1995; Virmani et al 2000/2001*]. One way to try and image these plaques *in-vivo* is by using histological "surrogates" created by intravascular ultrasound derived virtual histology (IVUS-VH) [*Sawada et al 2008*]. IVUS-VH has been validated in human pathological studies and atherectomy specimens [*Nasu et al 2006*]. The recent publication of the VIVA (Virtual Histology in Vulnerable Atherosclerosis) study [*Calvert et al 2011*]; has created a new interest in this potential role for IVUS-VH. This is because the study findings replicated the final results of the landmark PROSPECT (Providing Regional Observations to Study Predictors of Events in the Coronary Tree) study [*Stone et al 2011*]. Both studies concluded that important *non-culprit* lesion-specific characteristics are: Plaque Burden > 70%; VH-Thin Cap Fibroatheroma (VH-TCFA – a virtual surrogate for unstable plaque) and a Minimum Lumen Area (MLA) < 4mm^2

IVUS-VH is based upon the analysis of ultrasound backscatter as different plaque components produce a particular spectrum [*Nasu K et al 2006; Van Herck et al 2009; Rodriguez-Granillo et al 2005*]. The power, amplitude and frequency of the signal undergo de-convolution through a trained classification tree. This process transforms signals into four colour-coded pixels: fibrous (green); fibro-fatty tissue (light green); necrotic core (red) and dense calcium (white). This has been found to

correlate with histopathology and atherectomy specimens (predictive accuracy = 87.1%, 87.1%, 88.3%, and 96.5% for fibrous, fibro-fatty, necrotic core, and dense calcium, respectively) [*Nasu K et al 2006; Van Herck et al 2009; Rodriguez-Granillo et al 2005*].

Numerous other studies have analysed ACS and stable *culprit* plaques with IVUS-VH [*Garcia-Garcia et al 2006; Hong et al 2008; Qian et al 2009; Rodriguez-Granillo et al 2006; Surmely et al 2006; Nakamura et al 2006*], however none have attempted to construct a discriminatory score based upon the specific anatomical and compositional changes seen in "active" culprit ACS plaques.

5.2 Study Objectives

We designed a prospective, observational study that would examine active culprit (AC) plaques from patients with an ACS presentation and stable culprit (SC) plaques from patients with clinically stable angina. The research aims were:

1. To define the anatomical and histological differences between ACS and stable disease.

2. To use these differences in a multiple logistic regression model that can assign a numerical value to each associated variable.

3. To test the ability of this model to discriminate between plaque types in another independent cohort.

5.3 Study specific methods

This was a single centre, prospective, observational cohort study that received ethical approval from the Cheshire National Health Service (NHS) ethics committee in the UK. Patients with a Troponin positive ACS diagnosed by a general Cardiologist were transferred urgently to our tertiary centre for PCI. These cases were screened and gave written informed consent to be involved in the study. The main exclusion criteria were: ST elevation MI; unsuitable anatomy for PCI; left main stem disease; chronic kidney disease; previous PCI in the target vessel and heavily calcified or visibly thrombotic vessels. Active Culprit plaques (AC) were defined as those meeting electrocardiographic (ECG) criteria for the ACS culprit vessel and where intervention was performed. Stable Culprit (SC) plaques were those requiring PCI for progressive symptoms and failure of medical therapy in an elective setting. All vessels were studied *prior* to any percutaneous revascularisation. Imaging of the vessel in each group was undertaken as described in our methodology section. The plaque composition and other analyses were performed by off-line IVUS-VH analysis by a single individual blinded to the patient details and mode of presentation. Single operator analysis of ACS plaques produces less measurement error as shown in our validation work, which has been previously published [*Murray et al 2013*].

5.3.1 Study specific statistics and power calculation

To guide the initial sample size for this study, we used the hypothesis that the mean necrotic core volume will be variable between the two groups. Previous studies in ACS patients and our own variability study suggested that the mean would be around 35mm^3 with a standard deviation (SD) for necrotic core +/- 28mm^3. A sample size of 100 lesions was calculated. From this we expect 80% power to detect a 7mm^3 difference in plaque components with an alpha of .05. This permitted the relative differences in the mean to be tested for statistical significance using a student's *t* test. A p-value of <0.05 was considered significant. Continuous variables are expressed as means +/- standard error of the mean (SEM). Statistically significant variables in culprit plaques were entered into a multivariate logistic regression analysis, with the forward stepwise technique [*Hosmer et al 1989*], to identify independent associations between plaque variables, with AC lesion phenotype being the dependant variable. Those variables that were strongest in the output from the regression each have a logistic regression co-efficient (**Table 5.4**). This co-efficient is then used to multiply each numerical value for that variable. (i.e 0.675 X NC/DC ratio =0.675 X 3.5=2.363). The summation of the output for each associated variable then creates the overall "Liverpool Active Plaque Score" (LAPS). To assess model performance, receiver operating characteristics (ROC) data were examined. The area under the curve (AUC) and 95% confidence intervals (CI) were then estimated. A larger area under the ROC curve reflects better performance

of a discriminatory test. An AUC of greater than 0.5 suggests that the discriminatory power of the variable in question is superior to that of natural chance.

5.3.2 Validation

Following construction of the score, the diagnostic equation was taken to the Thoraxcentre, Rotterdam and applied to an independent cohort of 50 plaques taken from a previous three vessel IVUS-VH study [*Garcia-Garcia et al 2006*]. Each plaque score was initially calculated with the operator blinded to the independent lesion status, until the final ROC curve was calculated.

5.3.3 Sample size considerations for logistic regression

Sample size calculation for logistic regression is complex, but based on the work of Peduzzi *et al* from 1996 the following guideline for a minimum number of cases can be suggested: With **p** as the smallest of the proportions of negative or positive cases for the total population and **k** the number of covariates (the number of independent variables). The minimum number of cases to include is: **N = 10 k / p.** For our total population, p = 0.44 (68 stable (35 construction and 33 validation)/ 155 total lesions (105 construction and 50 validation) and k = 4 variables. Therefore from this equation: **N =4x10/0.44; N=91 plaques.** We have analysed a total of 155 plaques in our overall model and therefore should have statistical power.

5.4 Results

Two hundred and thirty eight patients were approached after urgent ACS transfer and case note review. Seventeen patients refused to participate and two hundred and twenty one were formally consented and enrolled *before* angiography. Eighty nine were excluded after angiography due to fulfilment of exclusion criteria. The majority of exclusions were due to the presence of surgical disease and/or heavy thrombus burden with reduced TIMI flow in the culprit vessel. One hundred and thirty two lesions were suitable for IVUS. However, in 19 cases the IVUS failed to cross or was abandoned and in 8 cases the IVUS pullback was not sufficient for analysis or there were media problems preventing full analysis. Therefore, a total of one hundred and five lesions were analysed; seventy culprit lesions in ACS patients and a further thirty five culprit lesions from stable angina patients undergoing PCI.

The patient baseline characteristics are displayed in **table 5.1** Of note, there was a statistically significant difference in the vessel interrogated between plaque types with more left anterior descending or diagonal (LAD/D1) arteries imaged in the stable cohort and a more even distribution in the ACS group: LAD/D1 (41%); Circumflex (25%); Right Coronary (34%). There were no significant differences in conventional risk factors for coronary artery disease; however the ACS cohort were more likely to have had a previous myocardial infarction (16% Vs. 7% p=0.02).

Characteristic	ACS N=70 active culprit (AC)	Stable angina N=35 stable culprit (SC)	*p*-value
Mean age (±SD)	59.2±11.0	60.1±7.8	*p*=ns
Male %	73%	60%	*p*=ns
LAD/diagonal	41%	74%	*p*=0.03
Circumflex/OM	25%	12%	*p*=0.01
Right coronary	34%	14%	*p*=0.01
Mean troponin (±SD)	14.8±27.2	n/a	n/a
Median troponin (IQR)	1.4 (0.1-13.7)	n/a	n/a
Hypertension	51%	59%	*p*=ns
Diabetes	24%	18%	*p*=ns
Current smoker	54%	57%	*p*=ns
Hypercholesterolaemia	60%	52%	*p*=ns
Family history	70%	65%	*p*=ns
Chronic kidney disease	3%	1%	*p*=ns
Previous MI	16%	7%	*p*=0.02

Table 5.1 Patient baseline characteristics

A comprehensive observational assessment of plaque anatomy and virtual histology is presented in **tables 5.2 and 5.3**. Total plaque length is statistically greater in the ACS culprit group, combined with a greater total plaque volume and burden, which heavily influences the relative volume calculations for individual VH plaque components displayed in **table 5.3.** Plaque volumes are therefore corrected for length by displaying the measured percentage contribution of each plaque type. Subsequently, the only VH variable that shows a statistical difference between groups is dense calcium plaque, being increased within stable plaques. Creating a ratio between important plaque types also corrects for volume differences and we have shown that there is a statistical difference in the Necrotic Core volume/Dense Calcium volume (NC/DC) ratio between ACS culprit and Stable plaques.

Mean measurement variable (±SEM)	ACS (N=70) active culprit (AC)	Stable angina (N=35) stable culprit (SC)	*p*-value
Length of disease mm	30.6 (±1.4)	21.8 (1.8)	*p*=0.003
Lumen volume mm^3	189.5 (±12.8)	163.3 (±15.6)	NS
Vessel volume mm^3	473.6 (±32.0)	328.1 (±29.9)	*p*=0.0044
Plaque volume mm^3	285.3 (±21.7)	164.8 (±15.4)	*p*<0.0001
Vessel plaque burden	57.6 (±0.8) %	49.9 (±1.5) %	*p*<0.0001
Min lumen diam. mm	1.6 (±0.03)	1.8 (±0.05)	*p*=0.002
Max lumen diam. mm	4.4 (±0.11)	4.3 (±0.16)	NS
Min vessel diam. mm	3.4 (±0.07)	2.9 (±0.08)	*p*=0.0012
Max vessel diam. mm	5.6 (±0.10)	5.4 (±0.15)	*p*=0.046
Min lumen area (MLA) mm^2	2.8 (±0.15)	3.5 (±0.23)	*p*<0.001
Remodelling index at MLA	1.2 (±0.02)	0.95 (±0.02)	*p*<0.001

Table 5.2 Plaque anatomical analysis (grayscale IVUS).

Mean measurement variable (±SEM)	ACS (N=70) active culprit (AC)	Stable angina (N=35) stable culprit (SC)	*p*-value
Fibrous vol (mm^3)	111.0 (±9.6)	50.5 (±5.3)	$p<0.0001$
Fibro-fatty vol (mm^3)	19.5 (±1.9)	9.2 (±1.2)	$p<0.0001$
Necrotic core vol (mm^3)	50.9 (±5.9)	21.3 (±2.5)	$p<0.0001$
Dense calcium vol (mm^3)	20.6 (±3.1)	13.5 (±2.0)	$p=0.014$
Fibrous %	57.2 (±1.2)	55.4 (±1.9)	ns
Fibro-fatty %	10.8 (±1.4)	9.9 (±0.9)	ns
Necrotic core %	23.2 (±1.2)	21.7 (±1.2)	ns
Dense calcium %	9.1 (±0.8)	13.1 (±1.3)	$p=0.02$
NC/DC volume	4.2 (±0.3)	2.1 (±0.2)	$p<0.0001$
VH-TCFA	1.4 (±0.09)	0.8 (±0.1)	$p< 0.0001$
Plaque rupture n (%)	45 (64%)	7 (20%)	$p<0.0001$
Thrombus n (%)	49 (70%)	4 (11%)	$p<0.0001$

SEM: standard estimate of the mean; VH-TCFA: virtual histology thin-cap fibroatheroma

Table 5.3 – Plaque Histological analysis (Virtual Histology)

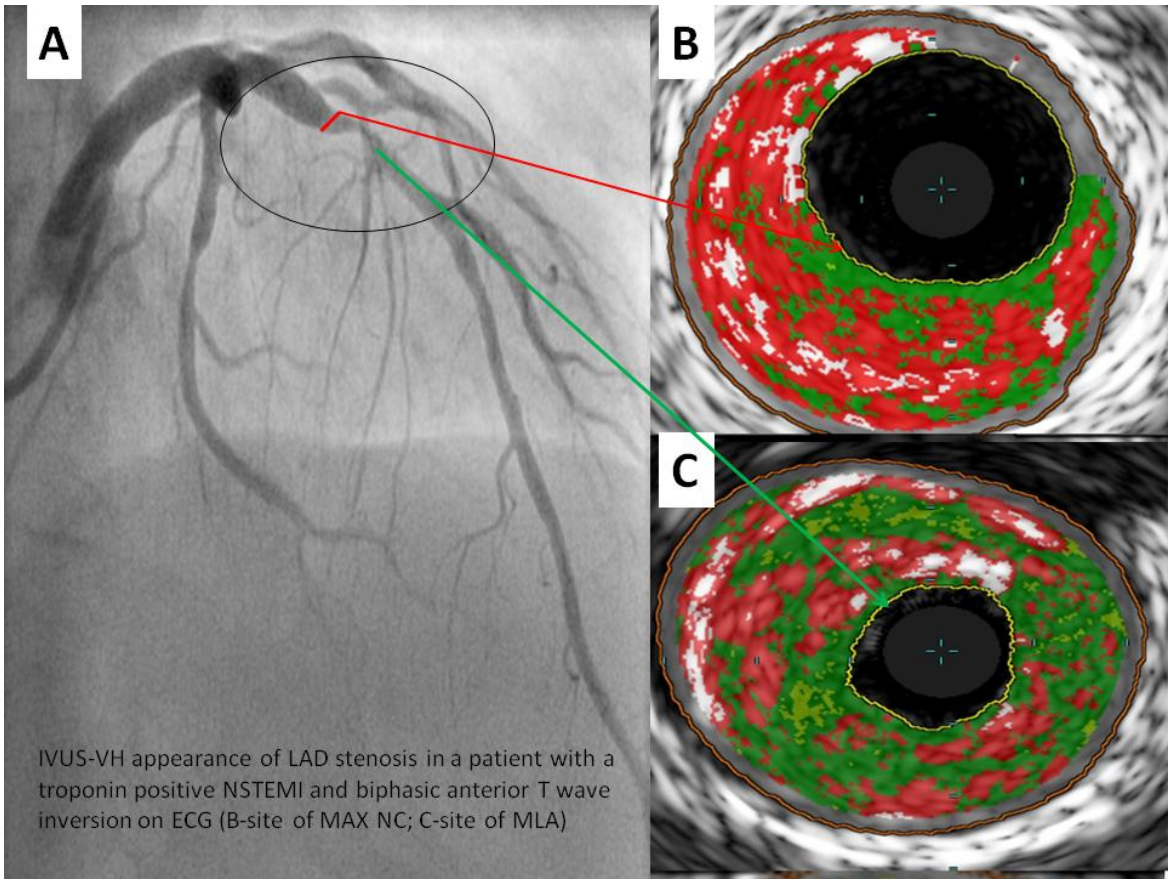

Figure 5.1 above, shows the angiographic appearance of a culprit ACS plaque **(Frame A)** with VH frames shown at both the site of maximum necrotic core **(Frame B)** and the minimum lumen area (MLA) **(Frame C)**. This highlights the eccentric nature and positively remodelled disease typically seen in ACS culprit plaques.

In comparison **Figure 5.2 (below)** shows the angiographic image of a stable culprit coronary lesion in the proximal RCA. The minimum lumen area **(Frame B)** shows a significant amount of circumferential calcification and relative negative remodelling. **Frame C** shows the maximum necrotic core frame confirming disease that is less eccentric and mixed in composition.

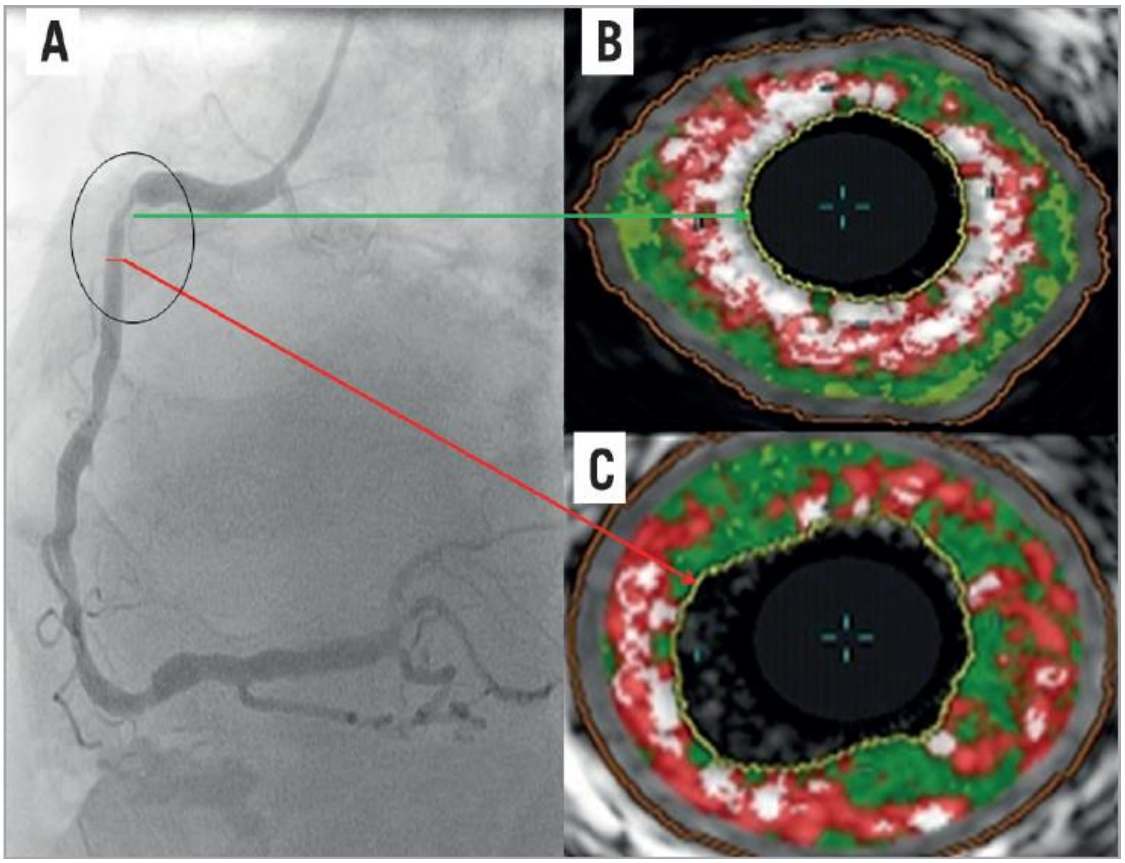

Figure 5.3 (below) displays the ROC analysis for each plaque variable that was statistically significant in the construction logistic regression. Interestingly this shows the relative importance of the remodelling index at the minimum lumen area (RI@MLA) and the necrotic core to dense calcium ratio (NC/DC) in comparison to minimum lumen area <4mm² (MLA<4) and VH-TCFA.

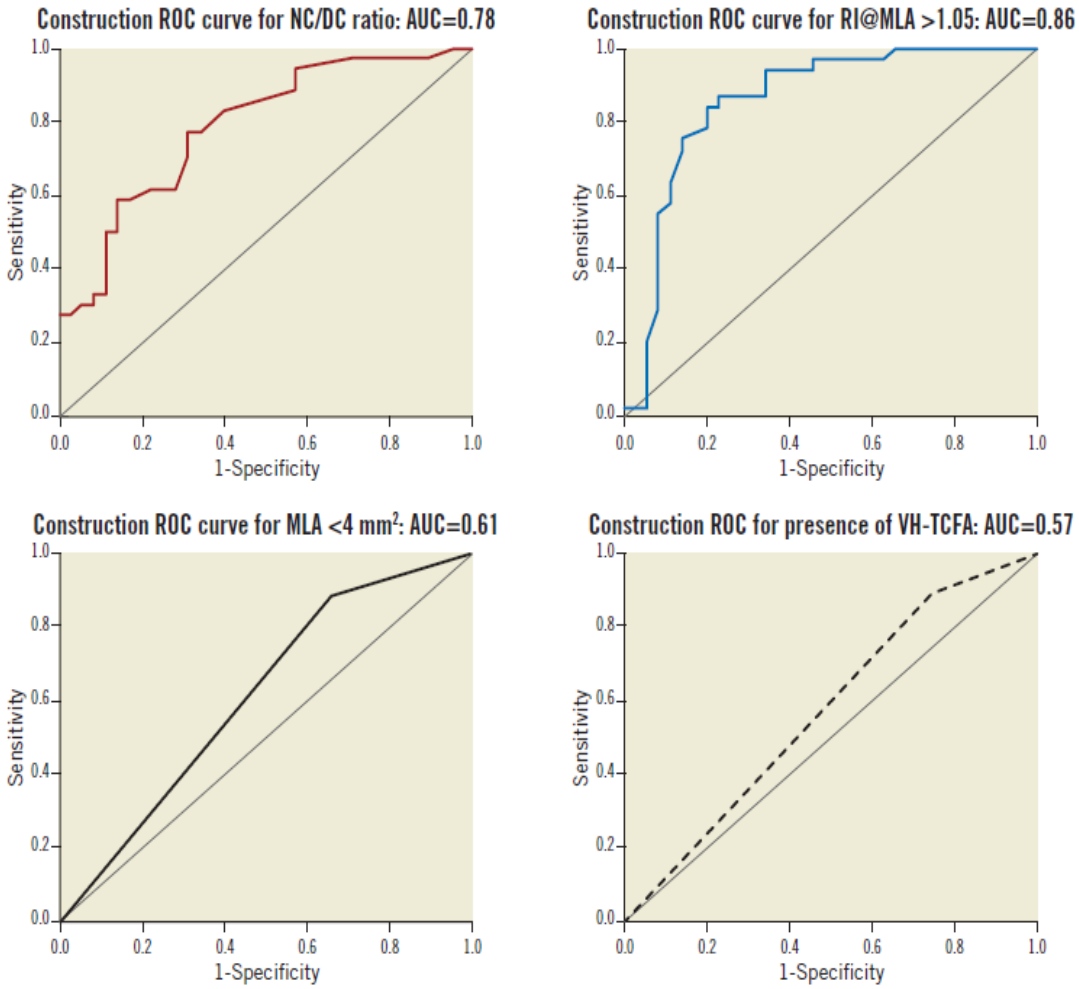

Figure 5.3: ROC curve analyses for each statistically significant variable

Table 5.4 (below) shows the output from the regression analysis and the relevant calculated co-efficients that make up the score.

Characteristic	Regression coefficient	Standard error	*p*-value
Remodelling Index @ MLA (>1.05)	5.1	1.41	<0.001
NC/DC ratio	0.68	0.24	0.004
VH-TCFA	3.7	1.32	0.005
MLA <4 mm^2	3.39	1.16	0.003
Intercept	–2.149	0.45	<0.001

Figure 5.4 (below) displays the regression equation that calculates the Liverpool Active Plaque Score (LAPS) and the ROC curve showing the strong discriminatory power for an active plaque phenotype (in the construction cohort).

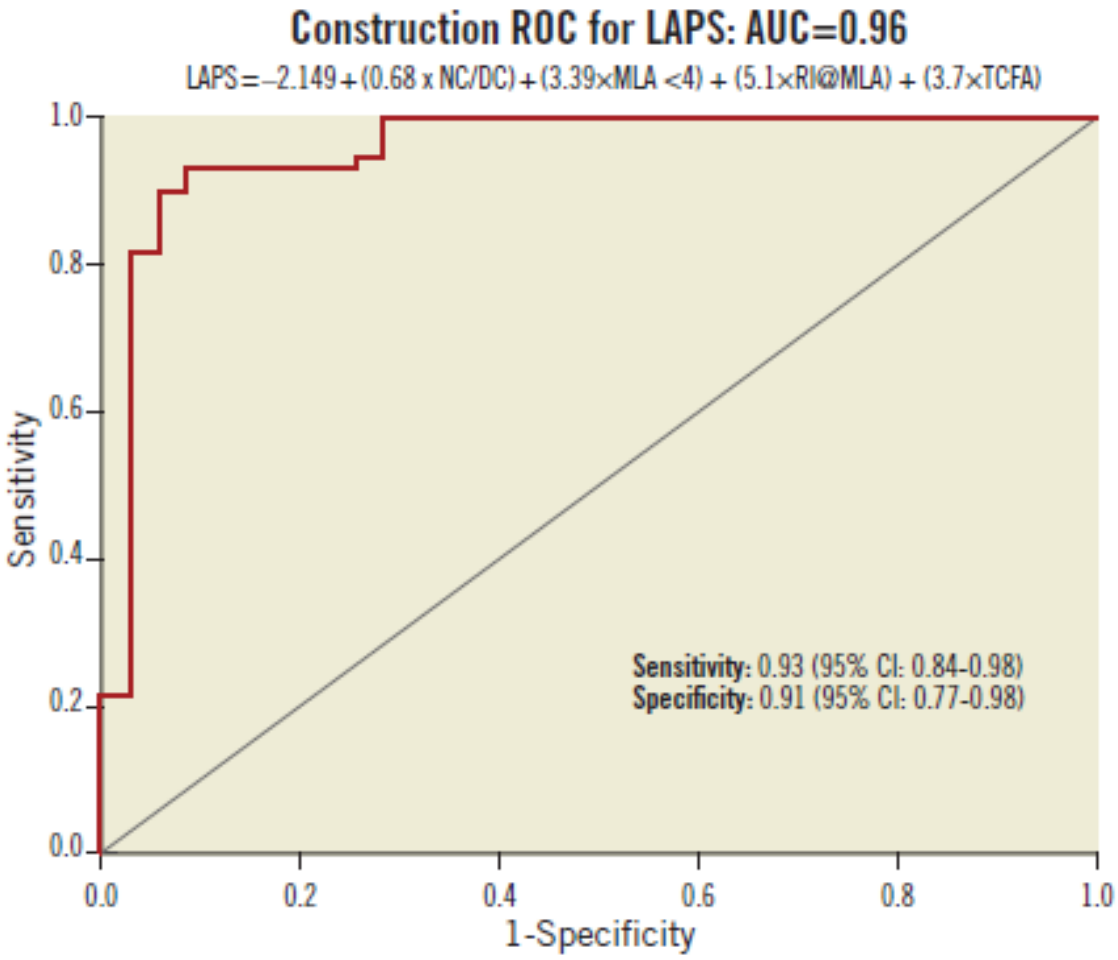

Figure 5.5 (below) is the ROC curve derived when the LAPS was applied to an independent cohort of plaques analysed at the Thoraxcentre, Rotterdam. As expected, the discriminatory ability of the score is reduced. However, the AUC value of 0.71 confirms that the score maintains some predictive discriminatory ability for active (AC) plaque phenotypes.

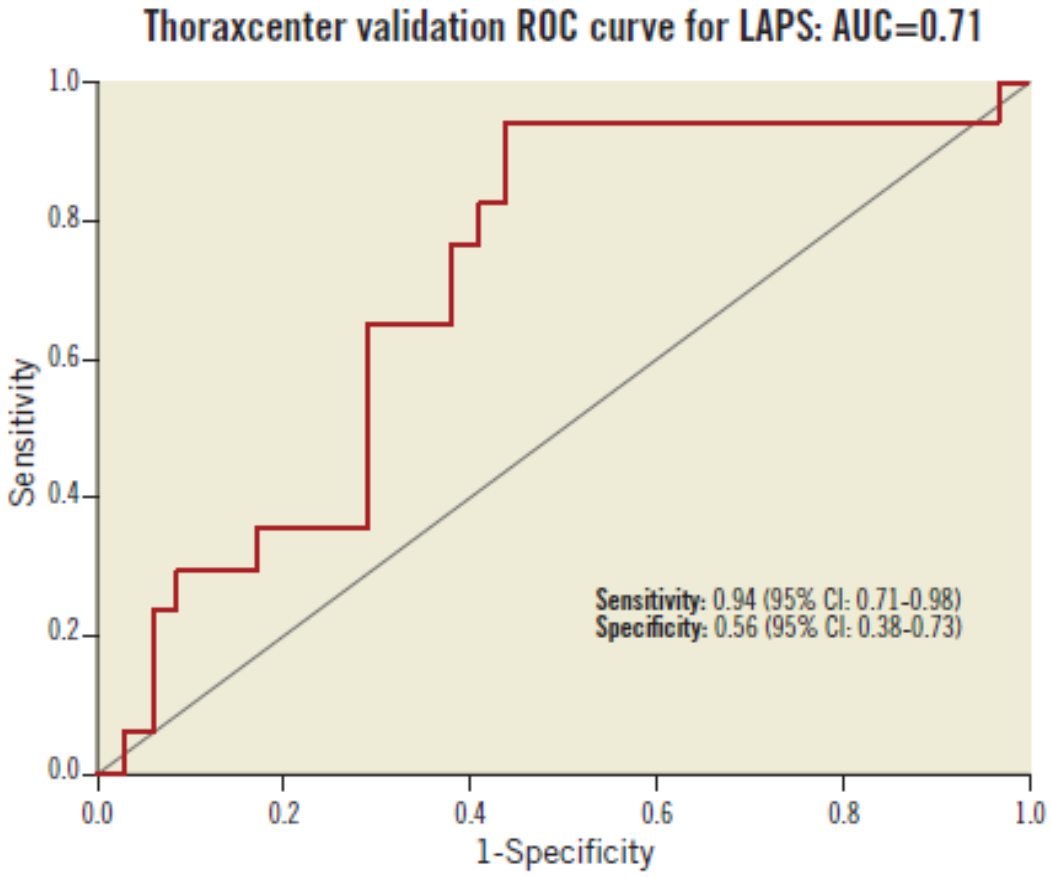

Figure 5.6 (below) is a box and whisker plot showing the differences and full descriptive distribution of the LAPS between AC and SC presentations in 155 plaques.

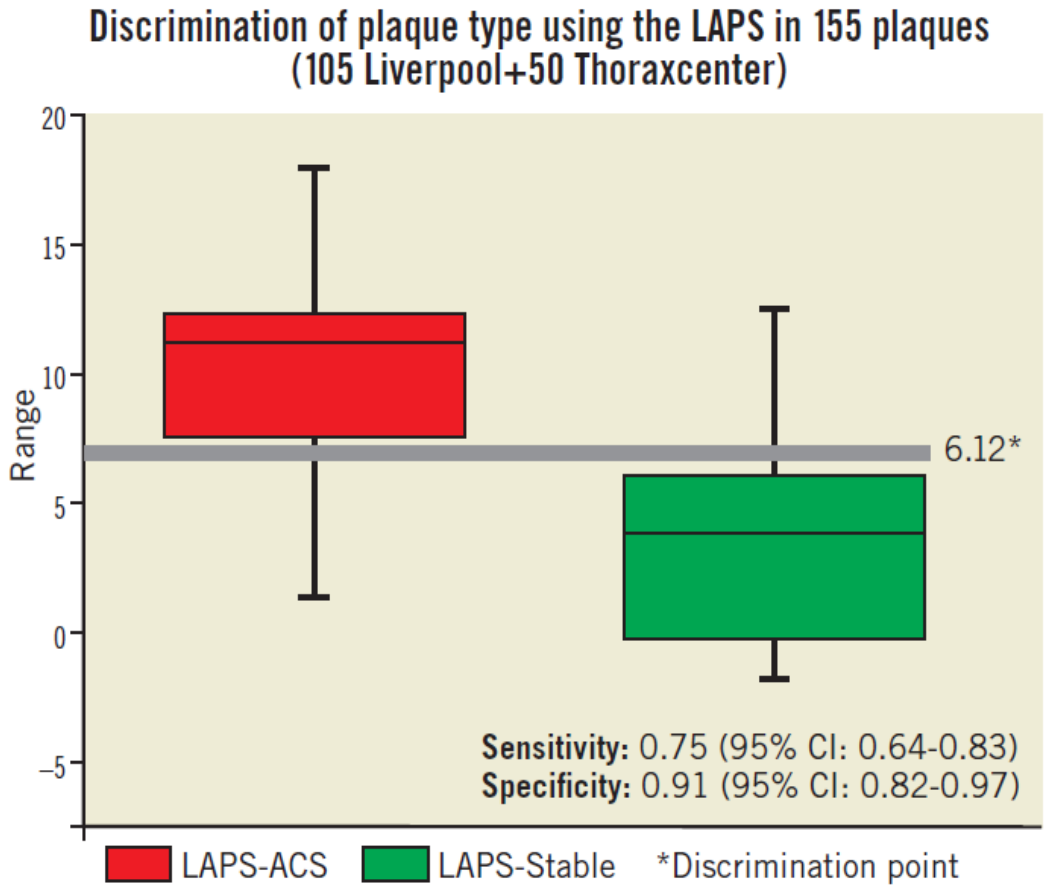

Figure 5.7 (below) is a visual illustration of the results from the application of the LAPS, where a score >6 is more typical of an active phenotype and a score <6 is more likely to represent a stable presentation. This is shown to emphasise how the score could be applied to stratify coronary artery plaques.

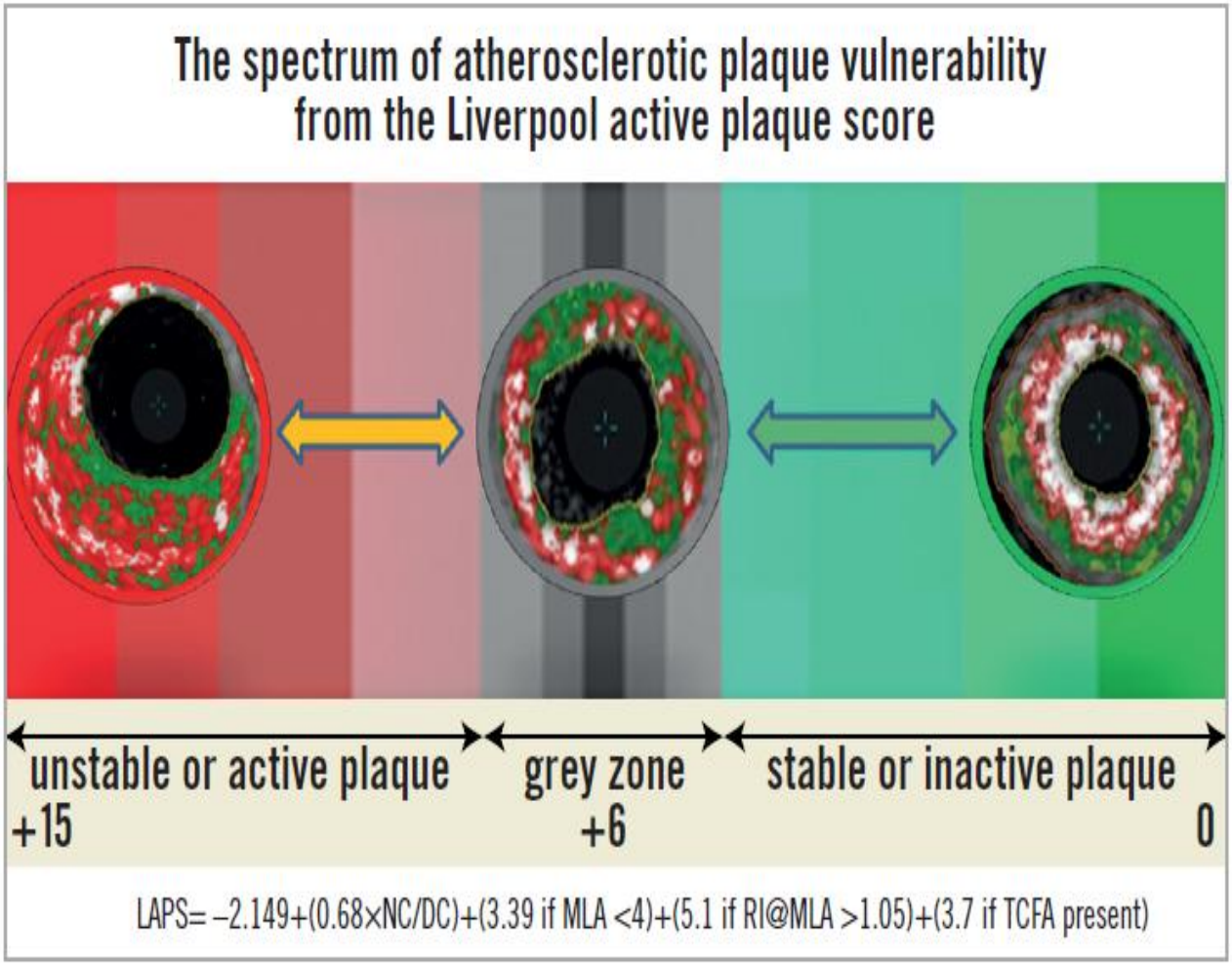

5.5 Discussion

The *in-vivo* assessment of high-risk atherosclerotic plaque characteristics may help improve our understanding and accuracy to reliably identify vulnerable plaques in the future. We have analysed the differences between the anatomical and virtual histological features in culprit coronary plaques from both unstable and stable presentations. Using logistic regression we have both determined the important features found in plaques responsible for ACS events and assigned a numerical value to these, allowing the calculation of a summative score with discriminatory power. Although many of the features within our score have been previously discussed in the IVUS-VH literature [*Garcia-Garcia et al 2006; Hong et al 2008; Qian et al 2009; Rodriguez-Granillo et al 2006; Surmely et al 2006; Nakamura et al 2006*] and found to be more prevalent in culprit plaques, this is the first attempt at modelling a plaque score from IVUS and VH data. The aim of this was to generate a concept that could be taken forward in larger trials and applied to future lesions and studies, possibly with more advanced imaging techniques such as: Coronary CT; Optical Coherence Tomography (OCT) and Near Infra-Red Spectroscopy (NIRS). Identifying the high risk features of plaques that have been shown to correlate with future MACE in previous studies [*Calvert et al 2011; Stone et al 2011*] is of paramount importance from both a preventative and an interventional point of view. Moreover, creating a reproducible score could allow both proper validation and invasive assessment of pharmacological agents aiming to modify vulnerable plaque features [*Rodriguez-*

Granillo et al 2005]. It may also be conceivable that in the future a "master" plaque risk score could be produced following further studies. The overall aim of this concept would be to guide cardiologists towards "staging" plaques where the risk of a future event occurring may be greater than the risk of treatment with a particular drug or device, such as: high dose statins, PCSK9 inhibition, darapladib or bioabsorbable vascular scaffolds (BVS) [*Wykrzykowska et al 2012*]. The variables that have formed our score and are associated with culprit ACS plaque presentations include similar findings from both VIVA and PROSPECT [*Calvert et al ; Stone et al 2011*] with MLA and VH-TCFA found again to be important. However, given our study focussed on culprit plaque morphologies, we add to this the remodelling index at the MLA (RI@MLA) and the necrotic core/dense calcium ratio (NC/DC). Both of these findings have previously been found to indicate an unstable lesion phenotype [*Garcia-Garcia et al 2006; Pasterkamp et al 1998; Missel et al 2008*] and even been linked to sudden death [*Missel, Mintz et al 2008*].

Our study examined the most pathologically important part of the vessel, responsible for the ACS event, *before PCI*. This has allowed us to observe vital information about residual plaque characteristics in a contemporary setting. The PROSPECT trial examined the VH appearance of non-culprit, angiographically insignificant, lesions that eventually caused re-admission to hospital with unstable angina. The actual myocardial infarction (MI) rate in the follow-up cohort was low at 1%. This is a direct reflection of the study protocol, which required all significant

angiographic lesions to undergo PCI *before* IVUS-VH analysis. Therefore, the results of PROSPECT do not inform us about the composition of culprit plaques implicated in a confirmed MI presentation. The VIVA study acquired three vessel IVUS in both unstable and stable atherosclerosis *before* PCI, but again the rate of MI during follow up was low, with end points being driven by revascularisation not MI. Although the total number of plaques analysed in this study is small compared to PROSPECT and VIVA, the number imaged in the context of a confirmed MACE event (n=70 (construction) + n=17 (validation) = 87) is greater than in PROSPECT (n=55) and VIVA (n=19) combined.

The inclusion of the NC/DC ratio within the score does merit some discussion as previously in the literature, the impact of dense calcium measurement on necrotic core coding on VH has been investigated [*Murray et al 2009; Sales et al 2010*]. We found that stable culprit (SC) plaques have statistically higher values for dense calcium but not for necrotic core. It has previously been shown on some analyses [*Kubo et al 2010*] that dense calcium in VH analysis begets the identification of necrotic core behind the calcium signal. Although this is certainly observed in some situations, it does not seem to have statistically influenced our overall *volume* measurements. Moreover, calcium in a spotty distribution within relatively larger necrotic cores (i.e. a high NC/DC level) appears to be a more important phenotype and this has previously been observed, pathologically, in sudden coronary death victims [Virmani et al 2000].

The NC/DC ratio in our cohort proved to be a significant independent predictor of a culprit lesion phenotype alone with an individual construction AUC of 0.78.

The influence of positive remodelling at the site of the MLA was very strong in our cohort (individual AUC – 0.83). This may be explained by the eccentric plaque burden seen in culprit ACS plaques or that extensively remodelled plaques are biologically active and have an increased tendency to weaken at the luminal surface, when the fibrous cap thins or an unknown Glagovian expansive limit is reached [*Garcia-Garcia et al 2006; Pasterkamp et al 1998; Nakamura et al 2001; Schoenhagen et al 2000; Kaple et al 2009; Rodriguez-Granillo et al 2006; Fuji et al 2005; Kroner et al 2011 and Missel et al 2008*]. The presence of more negatively remodelled plaques with greater dense calcium, in stable angina, may be explained by plaque contraction as necrotic core and macrophages "burn-out" and undergo calcification.

Further interesting insights from our data relate to the influence of the vulnerable plaque surrogate VH-TCFA in plaque diagnostics. This has previous been linked with future MACE events [*Calvert et al 2011; Stone et al 2011*]. In our cohort, VH-TCFA presence within the interrogated plaque disease was greater in the culprit ACS plaques compared to stable angina. However, on a discriminatory level, VH-TCFA has an individual AUC of 0.57, suggesting it has modest diagnostic ability. The limitations of the VH-TCFA concept have been described elsewhere before [*Rodriguez-Granillo et al 2005; Garcia-Garcia et al 2009; Kubo et al 2010*]. IVUS-VH cannot define true thin-caps, due to the resolution of a 20MHZ IVUS catheter being

in the order of 150μm. Also, VH-TCFA lesions are found within culprit stable angina lesions and this therefore weakens their discriminatory power. Moreover, it has been shown that these lesions are dynamic and fleeting in nature with around 75% "healing" over a year [*Kubo et al 2010*], this weakens their overall influence on culprit ACS lesion diagnosis, In addition, a recent study from the VIVA group has shown unacceptable variability in VH-TCFA recognition and the process of individually naming plaque sub-types (such as Thick fibrous Cap Atheroma (ThCFA) etc) [*Obaid et al 2012*]. This leads us critically to the concept generated by this investigation. It is clear that our work provides a basic "pilot" idea in this field, that could be taken forward in future investigations, hopefully with additional information gained from other imaging tools such as OCT (which can define true thin caps <65 μm) and NIRS (highly sensitive for lipid core). More importantly, most of the plaque variables we have found in this investigation can now be measured by non-invasive cardiac computerised tomography. Therefore, there may be a role for this theory in the preventative screening of asymptomatic plaques found in individuals with familial hazard or abnormal conventional risk factors.

5.5 Limitations

This is a single centre, observational study with the inherent limitations of this design. Although efforts were made to blind the analysing operator to the presentation type, it can occasionally be clear when a plaque is a culprit, due to the presence of residual thrombus and plaque rupture. This is a potential source of bias.

The analysis of MLA<4cm², RI>1.05 and VH-TCFA with logistic regression required these datasets to be converted to binary responses, which may not be representative of what is reported in the real world. In this study we imaged the full volume data from culprit plaques a few days after an event had occurred within the plaque. Although this is as close as we can realistically come to phenotyping event associated unstable plaques, we still cannot say with certainty what the pinpoint anatomy and histology was at the point of rupture/erosion. Analysis of high-risk ACS culprit plaques required interrogation of IVUS images containing rupture cavities and thrombus at varying stages of progression and therefore we followed previously published guidance by including thrombus in the plaque analysis where possible [*Garcia-Garcia et al 2009*]. This is notoriously difficult and previous studies have shown a difference between independent IVUS-VH measurements and measurements performed in a core-lab facility [*Obaid et al 2012; Huisman et al 2010/2012*]. However, we have published our magnitude of measurement variability in high risk ACS plaques, following a previous in-depth study [*Murray et al 2013*] and also have three previous peer-reviewed publications involving the identification of thrombus on IVUS [*Murray et al 2009/2010*].

5.6 Conclusion

We have found four features on IVUS and VH that can predict and discriminate active ACS culprit lesion phenotypes from those that are clinically stable. Subsequently, we have constructed and validated the Liverpool Active Plaque Score based upon these features. Although the main outcome of this study is concept generating, it is hoped that in the future a similar score may allow the prospective identification, staging and aggressive treatment of active coronary plaques to prevent major adverse cardiac events.

CHAPTER VI

STUDY III

Observable patterns of site-specific plaque morphologies by IVUS-VH: The relationship between maximum necrotic core site and minimum lumen area with implications for the identification of vulnerable plaque phenotypes.

6.1 Introduction

Numerous other studies have analysed atherosclerosis with IVUS-VH [*Calvert et al 2011; Stone et al 2011; Garcia-Garcia et al 2006; Hong et al 2007/2008; Qian et al 2009; Surmely et al 2006; Nakamura et al 2009*]. The main focus of these studies has been on conventional parameters and outputs from a standard Virtual Histology (VH) analysis. However, no study has focussed on remodelling index and the relationship that exists between necrosis and calcification. We have analysed this to try and find patterns or "blueprints" that might explain the progression of individual plaque phenotypes from stable disease to those seen in acute coronary syndromes. This may involve differential plaque growth, eccentricity, distance between minimum lumen area and a migrating or fluctuating presence of necrotic core.

Moreover, the process of plaque calcification is incompletely understood and documentation or measurements of calcification patterns are difficult. It is not completely clear what role progressive calcification plays in plaque instability [*Joshi et al 2014; Ehara et al 2004; Fujii et al 2005*]. Recently, a novel nuclear tracer of active calcification (^{18}F-NaF) has been found to highlight both ruptured and high risk plaques using Positron Emission Computed Tomography (PET CT) [*Joshi et al 2014*]. The Virtual Histology analysis of the tracer positive plaques appeared to show more evidence of positive remodelling and micro-calcification.

We therefore examined, in an observational study, culprit plaques implicated in a troponin positive acute coronary syndrome (ACS) and stable plaques responsible for symptomatic angina pectoris. The research aims were:

1. To define site-specific differences in atherosclerosis between ACS and stable disease.

2. To identify differences in remodelling and calcification patterns at:

   a) Minimum Lumen Area (**MLA**)

   b) Site of maximum necrotic core content (**Max NC**).

3. To create novel markers of vulnerability and/or plaque "blueprints" from frequent patterns or observable recurrent characteristics.

6.2 Methods

These have been described within the main methodology chapter and within the previous chapter.

6.2.1 Study specific methods of detailed plaque analysis using VH.

From the previously published chapter, looking at entire plaques and the volume of plaque components, we have shown that certain measurable factors can help distinguish "active" plaques present in acute coronary syndromes [*Murray et al 2014*]. In particular, minimum lumen area (MLA), plaque burden (PB), necrotic core to dense calcium ratio (NC/DC) and remodelling index (RI) were the most important factors in a multivariate prediction model. For this current work we have applied these findings to site-specific points within plaques (MLA and MAX NC) to explore in more detail the relationship between remodelling, necrosis and calcification. Necrotic Core to Dense Calcium ratio (NC/DC) was therefore calculated for individual plaque areas. However, we also calculated (NC+DC/DC) area in an attempt to quantify mathematically a surrogate for the amount of interfacial connection between NC and DC. We have named this measurement the Calcified Interface Area (CIA). Also, DC/NC area X 100 was calculated as a representation of the calcification that has developed respective to the necrotic core; this has been given the term Plaque Calcification Equipoise (PCE). A single previous study has defined micro-calcification as being evidence of "spotty" calcification on three frames or more with no evidence of acoustic shadowing behind the calcium [Joshi *et al* 2014]. However, our view was that calculating the PCE and CIA provides more continuous and reproducible variables that can better define the relationships within calcifying necrosis. The remodelling index was defined as the ratio between the

external elastic membrane cross-sectional area of the specific site (MAX NC or MLA) and the average of the proximal and distal reference regions in the same vessel. The maximum necrotic core frame (MAX NC) was defined as the frame with the highest percentage of necrotic core on a single frame.

6.2.2 Study specific statistics and power calculation

To ensure significant power was available for this sub-study, a retrospective post-hoc analysis was made using the results achieved for calcium interface area (CIA). The mean for one group was 3.58 (±2.26) and for the other 5.38 (±2.71). Therefore, for an Alpha of 0.05 over 105 plaque sites, the power to detect a statistical difference was calculated at 94.8%. Continuous variables are expressed as means +/- standard deviation (SD).

On comparing plaque sites a Student's t-test was used when the data was normally distributed, however if variances were unequal or a two sided F test was significant a Mann-Whitney U test was performed to ensure statistical significant was met for median values. A P value of **<**0.05 was taken as indicating a statistically significant result. Receiver operator characteristics were used again to test the discriminatory ability of certain plaque variables, this was done with the binary classification: 1= (**CP** ACS culprit/Troponin +); 0 = (**SP** Stable Plaque). Plaque variables that have shown statistical differences between these groups were also explored by simple linear regression to determine any correlation.

6.3 Results

Two hundred and thirty eight patients were approached after urgent ACS transfer and case note review. Seventeen patients refused to participate and two hundred and twenty one were formally consented and enrolled *before* angiography. Eighty nine were excluded after angiography due to fulfilment of exclusion criteria. The majority of exclusions were due to the presence of surgical disease and/or heavy thrombus burden with reduced TIMI flow in the culprit vessel. One hundred and thirty two lesions were suitable for IVUS. However, in 19 cases the IVUS failed to cross or was abandoned and in 8 cases the IVUS pullback was not sufficient for analysis or there were media problems preventing full analysis. Therefore, a total of one hundred and five lesions were analysed; seventy culprit lesions in ACS patients and a further thirty five culprit lesions from stable angina patients undergoing PCI.

The patient characteristics are below in Table 6.1

Characteristic	ACS (N=70) culprit (CP)	Stable angina (N=35) stable (SP)	P value
Mean age (± SD)	59.2±11.0	60.1±7.8	ns
Male, %	73	60	ns
LAD/diagonal	41%	74%	0.03
Circumflex/OM	25%	12%	0.01
Right coronary	34%	14%	0.01
Mean troponin (± SD)	14.8±27.2	n/a	n/a
Median troponin (IQR)	1.4 (0.1-13.7)	n/a	n/a
Hypertension	51%	59%	ns
Diabetes	24%	18%	ns
Current smoker	54%	57%	ns
Hypercholesterolaemia	60%	52%	ns
Family history	70%	65%	ns
Chronic kidney disease	3%	1%	ns
Previous MI	16%	7%	0.02

6.3.1 Site comparisons within the same plaque (CP or SP)

Following the analysis of 2 separate sites (MAX NC and MLA) in each individual plaque (n =70 x 2 CP and n=35 x 2 SP); a total of n=210 separate plaque sites were analysed and measured. In general, more left anterior descending arteries were examined in the stable group with more right coronary and circumflex arteries being involved in the ACS group. More ACS patients had suffered a previous myocardial event. An overview of the focussed IVUS and VH comparisons for each plaque type and site is present in Tables 6.2-6.5.

Table 6.2 – Site Comparisons within Stable Plaques (SP) n=70

Variables	Plaque at Maximum Necrotic Core Site (MAX NC)	Plaque at Minimum lumen area Site (MLA)	P-Value
Lumen Area	6.04 (±2.97)	3.61 (±1.34)	<0.001
Plaque Burden %	59%	68%	0.004
NC/DC	2.57 (±2.25)	2.74 (±2.82)	0.79 (NS)
Remodelling Index	1.1 (±0.17)	0.95 (±0.14)	<0.001
Calcium Interface Area (CIA)	3.58 (±2.26)	2.36 (±1.07)	0.005
Plaque Calcification Equipoise (PCE) %	54%	56%	0.68 (NS)

Within each particular type of plaque (**CP/SP**) there are statistically significant differences at specific points within the plaque. Table 6.2 shows that in stable plaques (SP) n=70, despite the obvious differences in lumen area (MAX NC 6.04 mm (±2.97) Vs MLA 3.61mm (±1.34)), there remains a substantial plaque burden at

the MAX NC site (59%). As expected, plaque burden is greater at both the MLA and CP sites. This appears to be accommodated by a greater amount of positive remodelling (1.1 (±0.17) Vs 0.95 (±0.14)) sparing luminal integrity. The MLA point of a stable plaque is more likely to display negative remodelling (RI 0.95 (±0.14)). Also, each of these individual plaque sites appears to have similar values for NC/DC ratios (2.57 (±2.25) Vs 2.74 (±2.82)). However, the pattern of this differs at the MAX NC site, having a greater calcified interface area (CIA) (MAX NC 3.58 (±2.26) Vs MLA 2.36 (±1.07).

Table 6.3 – Site Comparisons within culprit ACS plaques (CP) n=140

Variables	Plaque at Maximum Necrotic Core Site (MAX NC)	Plaque at Minimum lumen area Site (MLA)	P-Value
Lumen Area	5.93 (±2.67)	2.98 (±1.27)	<0.001
Plaque Burden %	66%	79%	<0.001
NC/DC	4.38 (±2.72)	3.46 (±3.48)	0.08 (NS)
Remodelling Index	1.34 (±0.18)	1.20 (±0.13)	<0.001
Calcium Interface Area (CIA)	5.38 (±2.72)	4.33 (±3.61)	0.001
Plaque Calcification Equipoise (PCE) %	30%	43%	0.004

Table 6.3 shows the results for culprit ACS plaques (CP) n=140, and interestingly a similar pattern emerges. However, these plaques appear to have less calcification and greater amounts of positive remodelling both at the MLA and MAX NC site.

Moreover, the MAX NC site within a culprit plaque has the greatest amount of positive remodelling (RI 1.20 (±0.13) Vs 1.34 (±0.18) P<0.001).

6.3.2 Site comparisons between CP and SP (n=210)

Table 6.4 – MAX NC site comparisons between stable and ACS plaques.

Variables	Plaque at Maximum Necrotic Core Site (MAX NC) - **STABLE**	Plaque at Maximum Necrotic Core Site (MAX NC) - **ACS**	P-Value
Lumen Area	6.04 (±2.97)	5.93 (±2.67)	0.85
Plaque Burden %	59%	66%	0.012
NC/DC	2.57 (±2.25)	4.38 (±2.72)	<0.001
Remodelling Index	1.1 (±0.17)	1.34 (±0.18)	<0.001
Calcium Interface Area (CIA)	3.58 (±2.26)	5.38 (±2.72)	=0.001
Plaque Calcification Equipoise (PCE) %	54%	30%	<0.001

On direct comparison between CP and SP at these specific points in the plaque (Table 6.4 and 6.5) we can again observe statistical differences. With regard to the MAX NC site; there is generally more necrosis than calcification. This is shown by PCE values less than 50% and subsequently higher calcified interface areas (smaller amounts of calcification) with greater amounts of positive remodelling. At the MLA in stable plaques, there appears to be an increasing amount of calcification (PCE>50% and lower CIA <3) coupled with more negative remodelling (RI < 1). This is the opposite of what is occurring in ACS culprit plaques (PCE <50%, CIA > 4 and RI >1).

Table 6.5 – MLA comparisons between Stable and ACS plaques (n=210)

Variables	Plaque at Minimum Lumen Area Site (MLA) - **STABLE**	Plaque at Minimum Lumen Area Site (MLA) - **ACS**	P-Value
Lumen Area	3.61 (±1.34)	2.98 (±1.27)	0.021
Plaque Burden %	68%	79%	<0.001
NC/DC	2.74 (±2.82)	3.46 (±3.48)	0.26 (NS)
Remodelling Index	0.95 (±0.14)	1.20 (±0.13)	<0.001
Calcium Interface Area (CIA)	2.36 (±1.07)	4.33 (±3.61)	<0.001
Plaque Calcification Equipoise (PCE) %	56%	43%	0.068

Figure 6.1 – Virtual Histology evolution of plaque from primitive necrosis and spotty calcium through to calcium arcs. Each stage shows values for NC/DC ratio, PCE (plaque calcification equipoise) and CIA (calcified interface area).

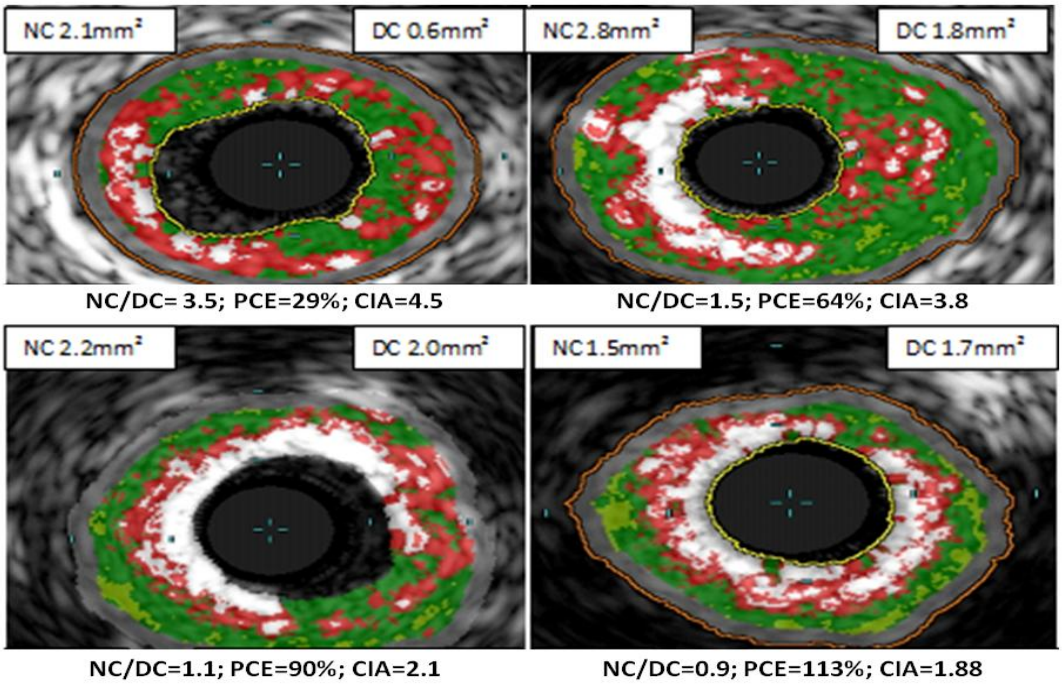

These results, demonstrated visually in figure 6.1, shed some light on the intricate pathological changes that are occurring in plaques at different stages of atherosclerosis. Graphical explanations of the results (as an aid to comprehension) are displayed in Figures 6.2, 6.3 and 6.4.

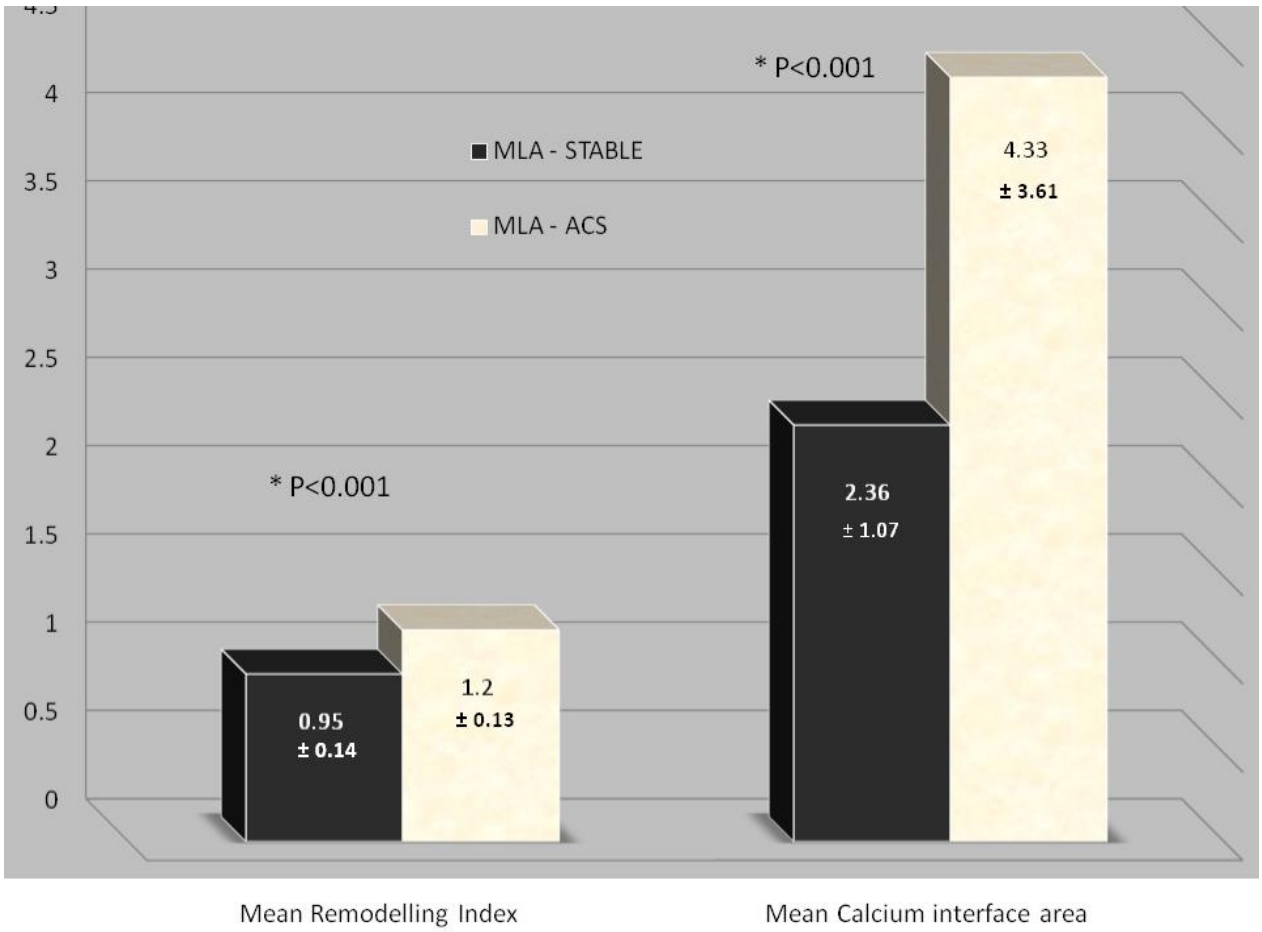

FIGURE 6.2: Histogram showing significant differences in remodelling index and calcified interface area at the minimum lumen area (MLA) in both ACS and stable plaques.

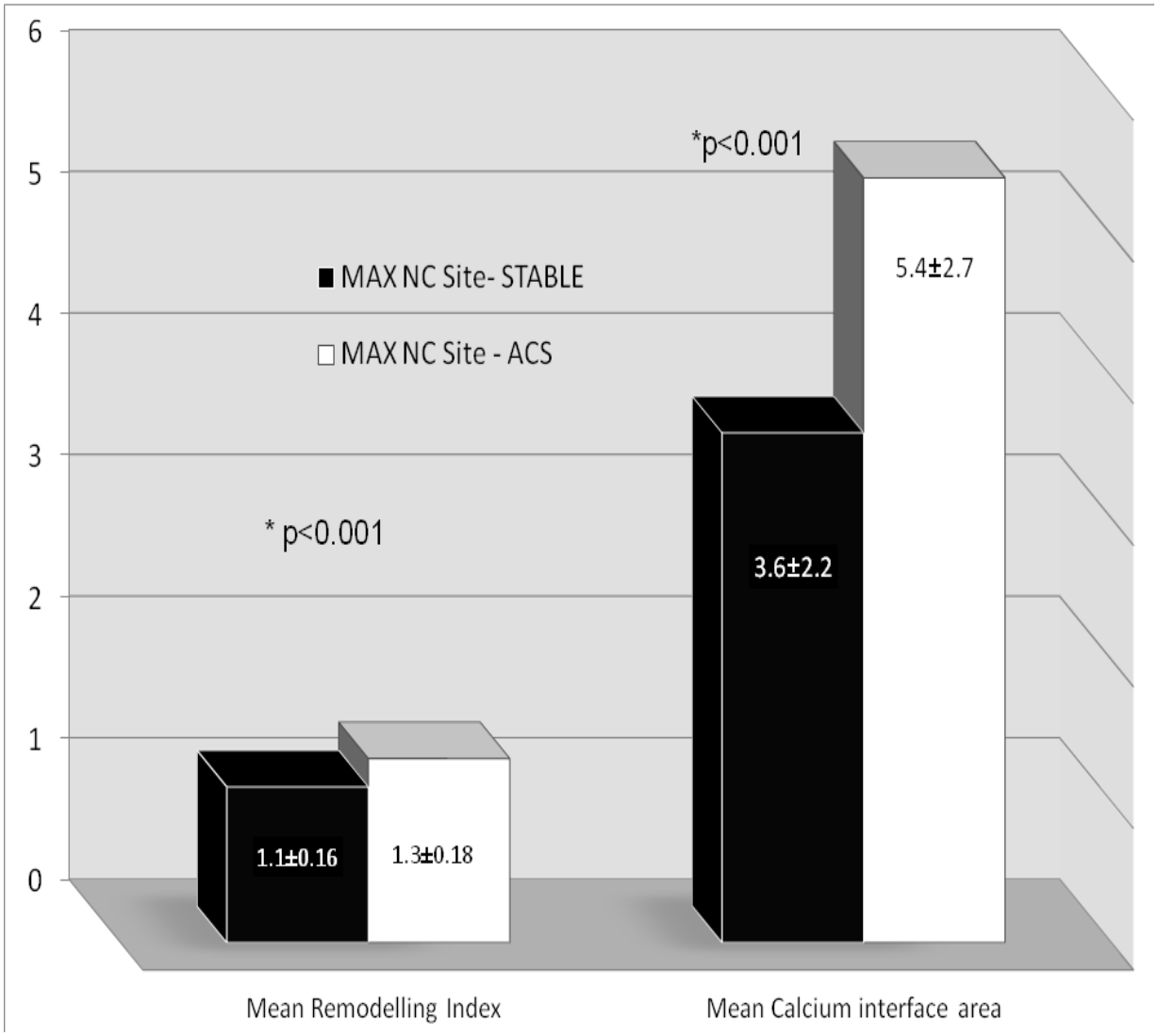

Figure 6.3: Histogram showing significant differences in remodelling index and calcified interface area at the Maximum Necrotic Core (MAX NC) site in both ACS and Stable plaques.

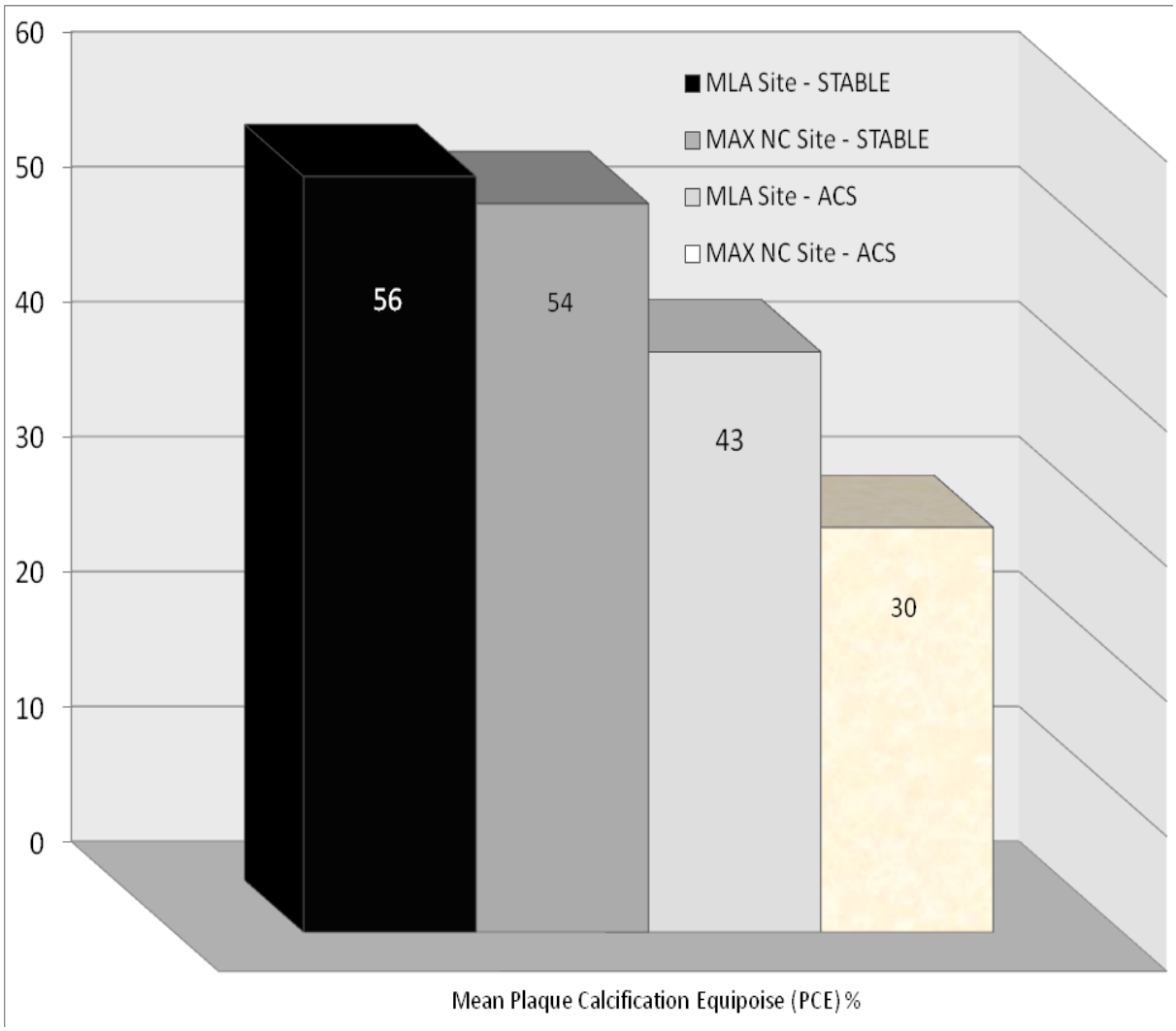

Figure 6.4: Histogram showing mean PCE across the major plaque sites in both ACS and Stable plaques. This displays the change in percentage calcification between different clinical presentations.

These site-specific statistical differences have been explored using ROC analysis to look for discriminatory ability. This is shown in figures 5 and 6. Although the area under the curve (AUC) and sensitivity/specificity vary somewhat (0.86-0.65 and 97%-51%) the best cut-off values to determine"culprit plaque-like" morphologies are: RI @ MLA>1.12; RI @ MAX NC>1.22; PCE @ MLA<47.1%; PCE @MAX NC<47.3%; CIA @ MLA>2.6; CIA @ MAX NC>3.1.

Analysis of the data, to look for correlations between remodelling index and patterns of atherosclerosis/calcification, shows the following:

1. There does not appear to be a statistically significant direct correlation between remodelling index and PCE. However, there is a weak negative trend ($p<0.09$) in stable plaques; as plaque calcification increases the remodelling index can decrease. (Figure 6.7)

2. Although not significant ($p=0.07$), there is a trend in stable plaques towards a positive correlation between CIA and remodelling index (Figure 6.7).

3. There is a statistically significant negative correlation between Calcified Interface Area (CIA) and Plaque Calcification Equipoise (PCE) in 3 out of 4 measurements in both CP and SP, suggesting that as plaque calcification increases the interface area decreases. This relationship is shown in Figure 6.8 and 6.9.

Figure 6.5: ROC Curve for predictive ability of RI for ACS (Trop +) plaque

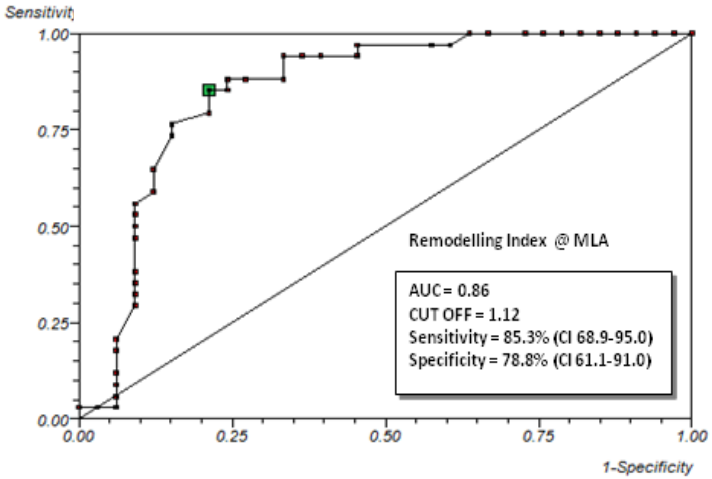

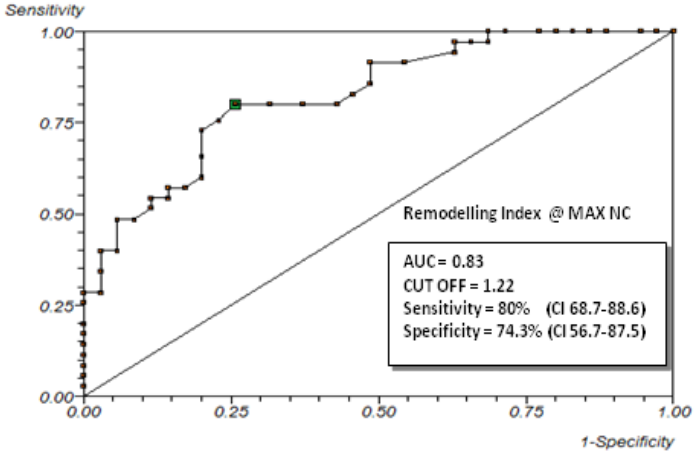

[178]

ROC Curve for the predictive ability of PCE for ACS (Trop +) plaque

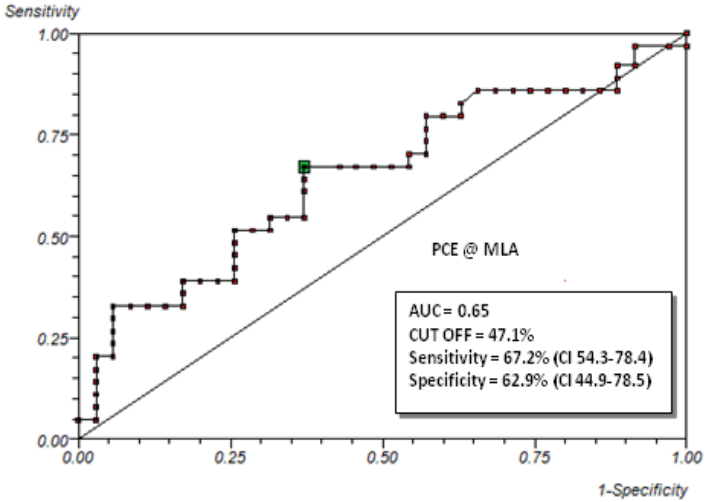

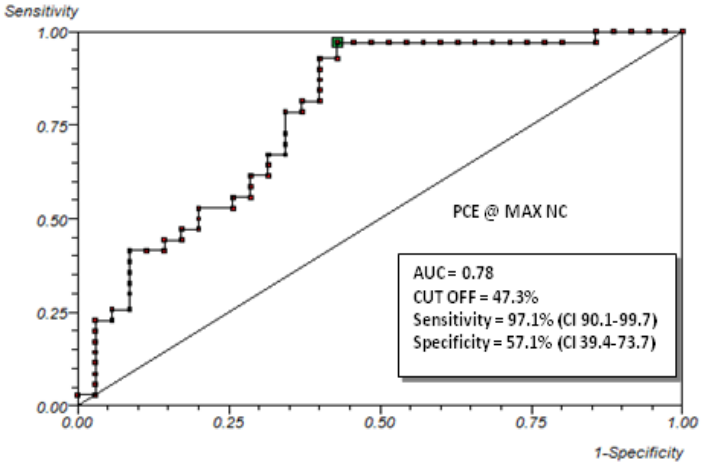

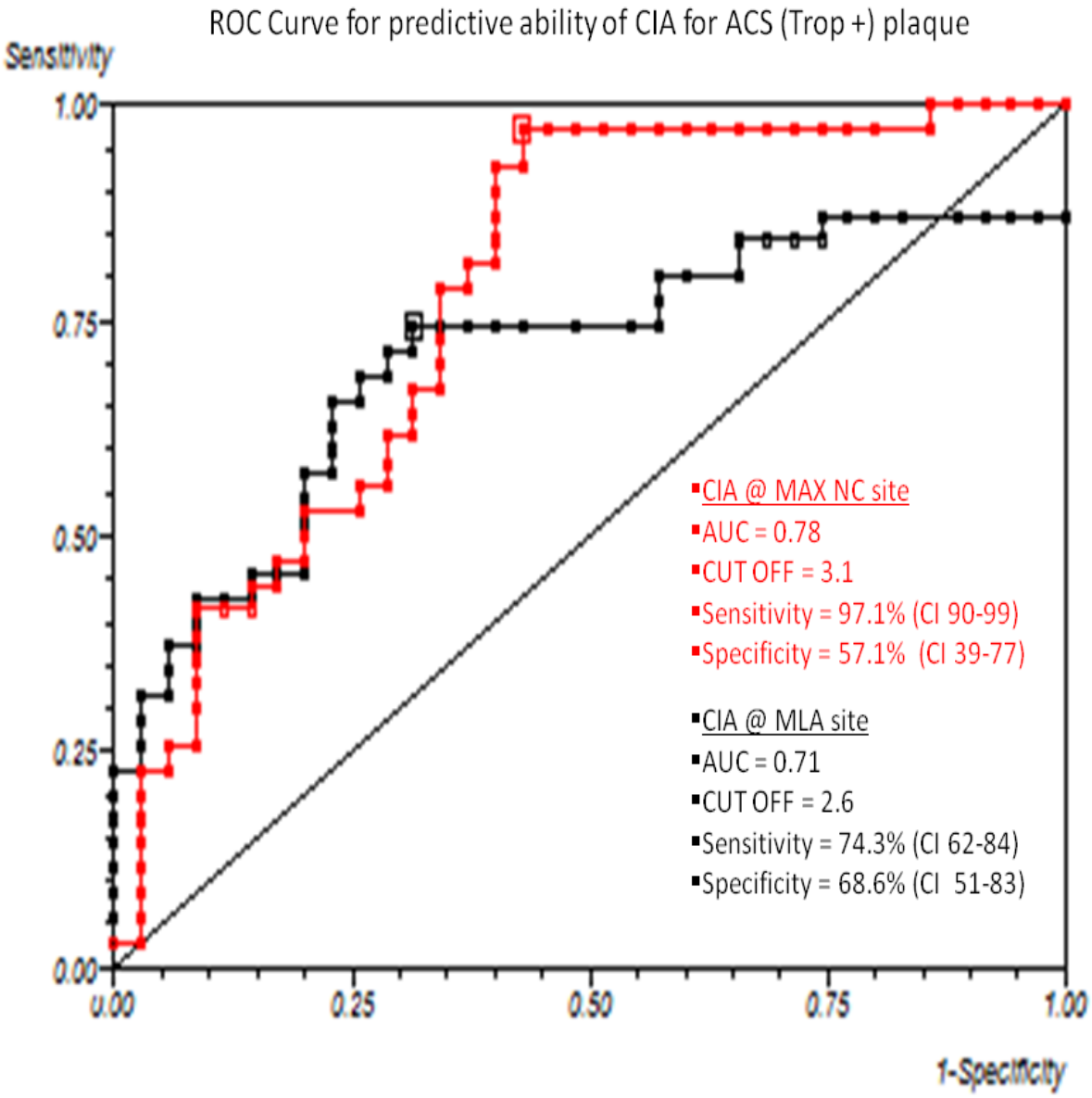

Figure 6.6: ROC curve for CIA showing reasonable discriminatory ability for ACS plaques using this measurement obtained both at MLA and MAX NC sites.

Figure 6.7: Scatter plots of linear regression looking for a correlation between Remodelling Index and both PCE and CIA. Weak trends are seen at stable plaque MLA.

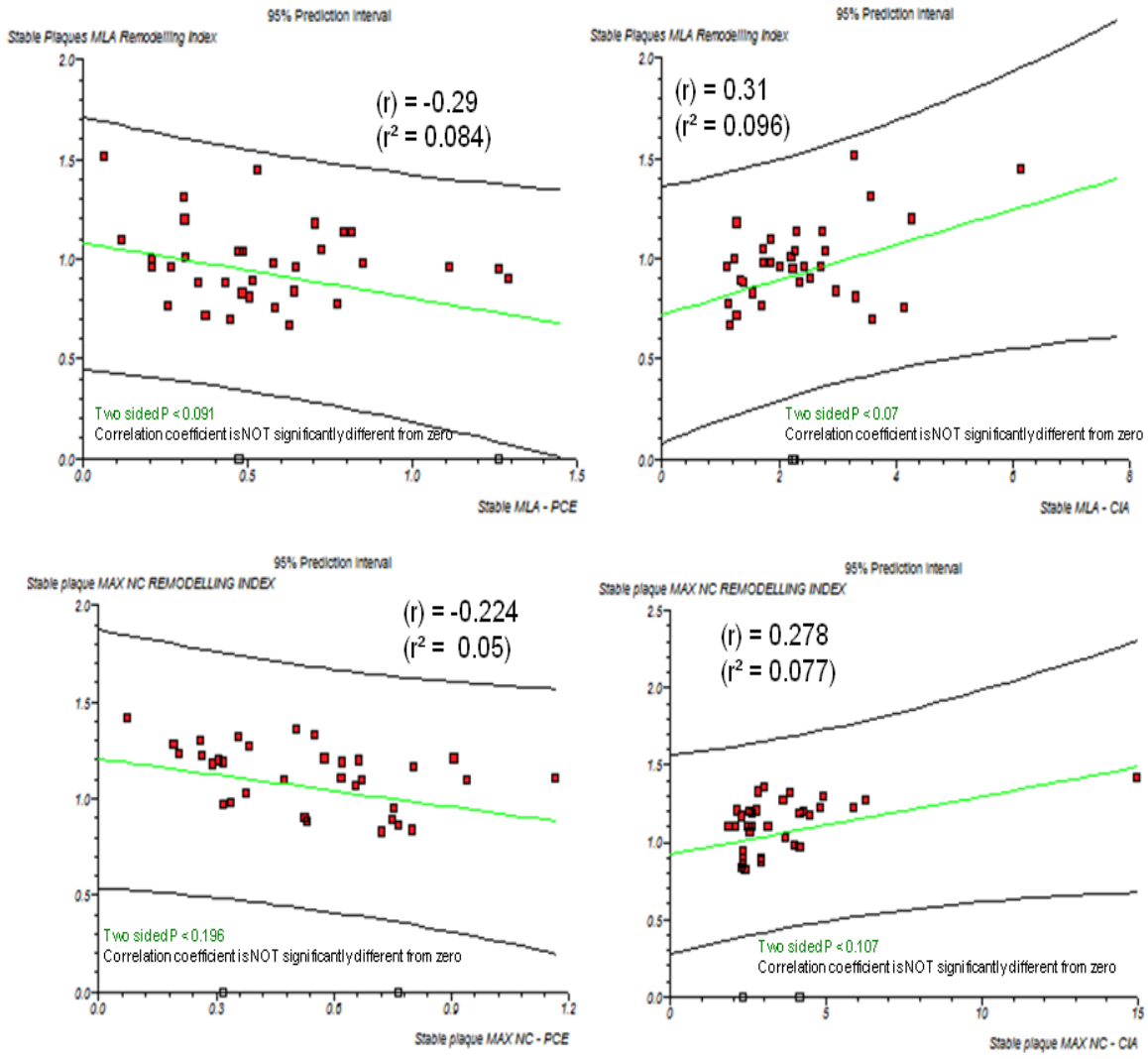

6.8: Scatter plots of linear regression showing a confirmed correlation between CIA and PCE in both stable and ACS plaques. Stable lesions at the MLA site (Panel B) do not have such a smooth curvilinear relationship due to the fact that these sites are the most heavily calcified already and therefore have a low baseline CIA (Y-axis) compared to other sites.

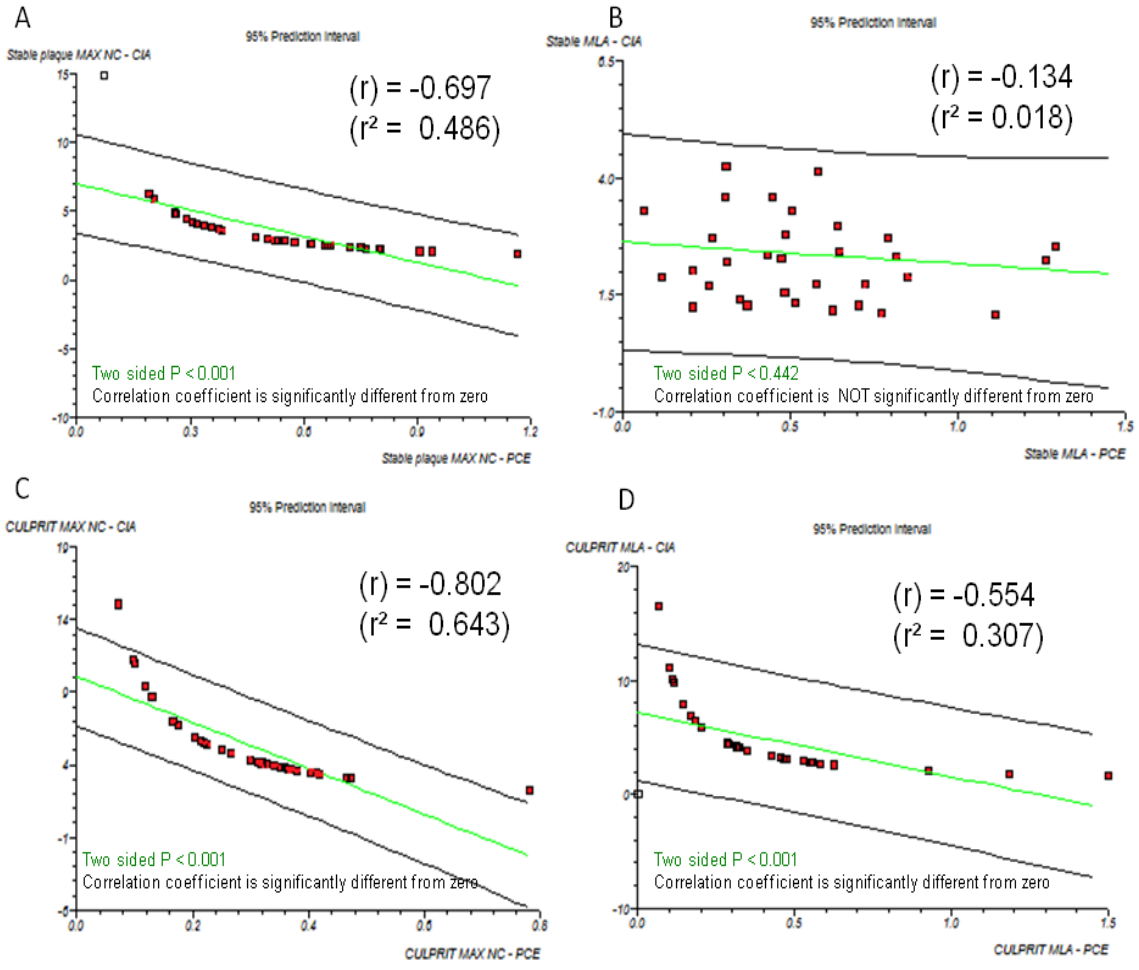

6.4 Discussion

New indices and to assess plaque vulnerability and suggest possible instability, *before* a fatal event, are urgently called for. We have presented a series of novel observational virtual histology IVUS findings gathered from the analysis of 210 plaque sites across the spectrum of stable and unstable coronary disease. VH characterisation reveals (in ACS culprit plaques) the striking feature of positive remodelling and primitive "spotty" calcification within the necrotic core (CIA↑ PCE↓). We have also shown via our calculations that stable phenotypes tend to have a greater extent of calcification as measured by the PCE (>47%). This cut off value (close to 50% calcification of necrotic core) is the "equipoise point" where a plaque is in calcific transition from a potentially unstable (spotty-type) to a more organised stable form, hence the term PCE. Also, through calculating the CIA, we have shown that potentially different patterns of calcification can exist despite similar values for NC, DC, NC/DC ratio or PCE. This has been evident when comparing MAX NC and MLA sites within a stable plaque and also when comparing the MLA point of a culprit plaque (CIA <3) with that of a stable plaque (CIA >3). Our data also suggests a correlation between PCE and CIA (PCE↑, CIA↓). As a reference, NC/DC ratio was only statistically different when comparing the MAX NC site between SP and CP, whereas PCE, CIA and remodelling index were statistically different at five out of six sites between SP and CP.

Previously, the NC/DC ratio on VH analyses has been shown to correlate with risk factors for sudden cardiac death and high risk ACS presentations

[*Missel and Mintz et al 2008*]. With regard to the process and role of plaque calcification, it is interesting to discuss this based on a "friend or foe" analogy. Coronary calcium correlates with plaque burden [*Missel et al 2008; Maehara et al 2002*] but its effect on plaque instability is less evident. Beckman *et al* in 2001 demonstrated that the maximal arc of calcium decreased progressively from patients with stable angina (91±10°), to those with unstable angina (59±8°) and finally to those with myocardial infarction (49±11°, p =0.014). Ehara *et al* in 2004 reported that the average number of calcium deposits (within an arc of 90°) decreased progressively in patients with acute myocardial infarction, compared with unstable angina and those with stable angina. Calcium deposits were also longer in patients with stable angina. Fujii *et al* in 2005 showed that ruptured plaques also had quantitatively less calcium but a larger number of small calcium deposits when compared with non-ruptured plaques. It appears that primitive spots of calcification within the necrotic core may be our foe but as calcification progresses there is a point where it may have a stabilising effect. The individual nuances behind these previous findings can again be explained by our calculations of CIA and PCE (figure 6.1 and 6.9). As the PCE increases towards 50% and the CIA falls below 4, a certain amount of "plaque contraction" appears to occur as the biologically active necrotic core is "consumed" by calcification. The vessel remodelling in stable plaques with these features is more negative and a trend towards this has been shown on linear regression (figure 6.8). This is in keeping with multiple previous analyses highlighting that positive

remodelling is more prevalent in acute coronary syndrome plaques [*Virmani et al 2000; Garcia-Garcia et al 2006; Hong et al 2007; Joshi et al 2014; Murray et al 2014*].

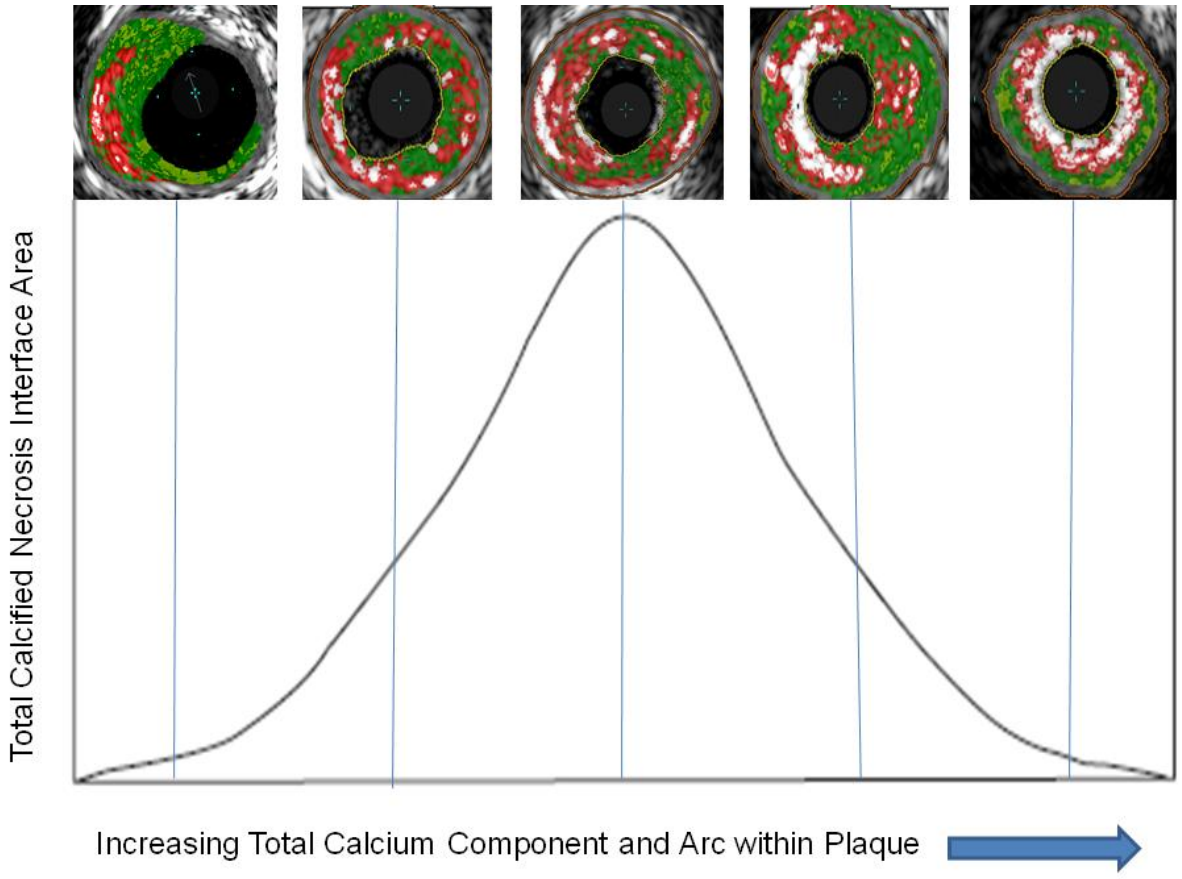

Figure 6.9: Graphical representation of the "bell curve" relationship between increasing calcium within a lesion and the interfacial area between calcium and necrosis as calcium coalesces.

It could be suggested that the development of primitive or nascent calcification, starting as microscopic "spotty" islands in a sea of active necrotic core, is the process highlighted by ^{18}F-NaF on PET CT [*Joshi et al 2013*] and therefore we have suggested a theory that could explain the increased risk of these plaques to rupture and cause events.

Previous biomechanical studies suggest that at the interface between a solid impurity (calcium) and a softer compound (necrosis), the large divergence in material resistance creates local strain concentrations at the poles of the impurity [*Hoshino et al 2009; Vengrenyuk et al 2006; Bluestein et al 2008; Cilla et al 2013; Huang et al 2001; Maldonado et al 2012; Knesi et al 2007*]. Theoretically, should the stress placed on these areas change suddenly, via known plaque rupture triggers, such as increases in blood pressure or localised vasomotor function (sympathetic stimulation), then subsequent tissue de-bonding could occur, separating these tissues and precipitating plaque fissuring/rupture. We have suggested that these points (when seen at the luminal surface/cap) could be called "Stress Interface Mismatch Points (SIMPS)" See Figure 6.10.

The prevalence of these sites within a plaque is difficult to define accurately with IVUS-VH. However, we have attempted to infer the presence of more primitive calcification through the calculation of our two novel markers (PCE and CIA). As previously discussed, as a plaque "heals" and stabilises (PCE ↑ and CIA ↓) this would decrease the prevalence of stress interface mismatch points (SIMPs) between the calcium speckles, as the intermediary necrotic core is replaced by calcium fusing.

A future study may be warranted to explore this theory in more detail with optical coherence tomography analysis. This would more accurately determine the prevalence of point vulnerability where lipid or necrosis meets calcification at thin fibrous caps. In further support of our observational theory for plaque vulnerability, biomechanical analyses using finite element analysis (FEA) models appear to confirm that micro-calcifications can alter the maximal principal stress by up to 32% [*Cilla et al 2013*]. In this paper, the fibrous cap thickness, micro-calcification ratio, eccentricity and angle appear to be the key morphological parameters that play a role in the overall rupture risk of the plaque. 3D FEA has also showed that local stress concentrations could be increased five-fold in the tissue space between micro-calcifications, especially when they were in close proximity to each other [*Maldonado et al 2012; Knesl et al 2007*].

According to the science of linear elastic fracture mechanics, if a system consisting of two edge-bonded wedges of different materials is considered, a stress-singularity occurs at the vertex of the bi-material interface [*Knesl et al 2007*]. The existence of these "stress-singularities" means that micro-failure processes can occur at the interfaces, leading to crack initiation and propagation (described in figure 6.10). Further circumferential stress on the plaque could be generated by segmental coronary endothelial dysfunction, creating imbalances in vasoconstriction and vasodilatation. In addition, circadian pulses in blood pressure or increases in shear stress along the shear points of these weak spots, could be a trigger for the tissue de-bonding and rupture at these sites. Overall, our stress interface mismatch point

theory could explain the importance of plaque calcification patterns in the identification of vulnerable plaques and why "spotty" calcification is associated with increased plaque risk. This has been shown to increase the risk of ACS occurring in a group followed up after coronary artery CT [*Motoyama et al 2009*].

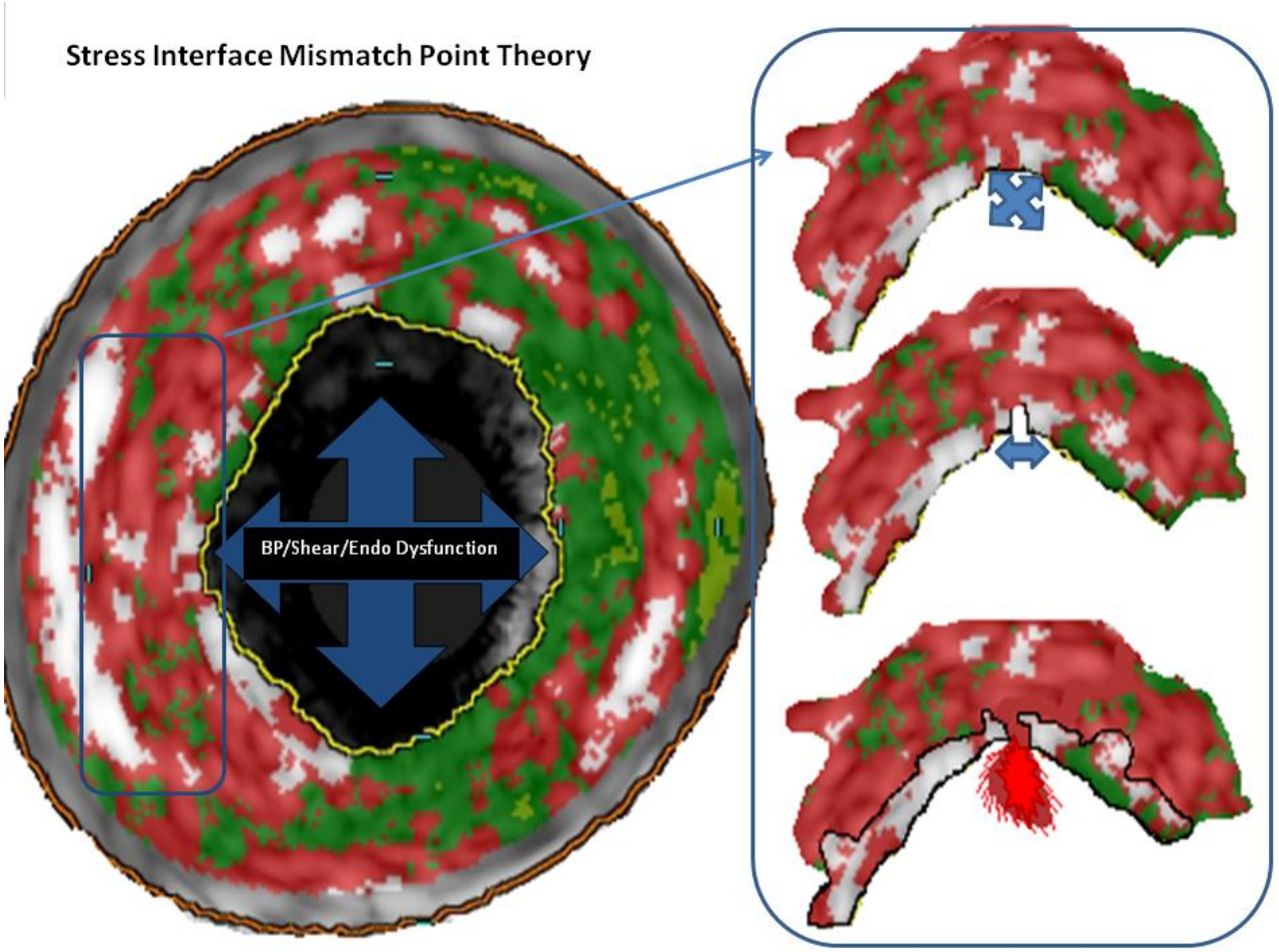

Figure 6.10: Virtual Histology explanation of the Stress Interface Mismatch Point (SIMPS) theory of plaque instability, trigger and rupture based upon evidence from biomechanics and finite element analysis.

6.5 Limitations

This is a single centre, observational study with the inherent limitations of this design. Our theory is observational and experimental in nature and is built upon the detailed scrutiny of both the IVUS and VH images at each individual plaque frame. Although efforts were made to blind the analysing operator to the presentation type, it is occasionally clear when a plaque is a culprit, due to the presence of thrombus and plaque rupture. This is a potential source of bias. Analysis of high-risk ACS culprit plaques required interrogation of IVUS images containing rupture cavities and thrombus at varying stages of progression and therefore we followed previously published guidance by including thrombus (when seen) in the plaque analysis where possible [*Garcia-Garcia et al 2009*]. This can be difficult and previous studies have shown a difference between independent IVUS-VH measurements and measurements performed in a core-lab facility [*Obaid et al 2012; Huisman et al 2010*]. However, we have published our magnitude of measurement variability in high risk ACS plaques, following a previous in-depth study [*Murray et al 2012*]. The inclusion of ratio scores and percentages where DC and NC are involved does merit some discussion as previously in the literature the impact of dense calcium measurement on necrotic core coding from VH has been investigated [*Murray et al 2009; Sales et al 2010*]. It has previously been shown on some of these analyses that dense calcium in VH analysis begets the identification of necrotic core behind the calcium signal. Although this is certainly observed in some situations, it previously did not statistically influence our previous volume measurements [*Murray et al 2014*].

Even if larger arcs of calcium are present this would still lead to a lower NC/DC or CIA compared to a plaque with small speckles of calcium and a large positively remodelled necrotic core. We are aware that VH is a crude surrogate or "window" to the true plaque histopathology (as the algorithm was built around a single pathologists interpretation of "calcifying necrosis"). However, in support of VH, a recent analysis by the Cambridge group comparing VH to conventional histology [*Obaid et al 2013*] revealed that there still appears to be reasonably good diagnostic accuracy for calcified plaque components (92%). Also VH-TCFA was able to detect histological TCFAs with a diagnostic accuracy of between 74-82%.

6.6 Conclusion

Virtual Histology IVUS produces reasonable surrogate measurements for the true histological composition of coronary artery plaques. From this we have found different patterns in site-specific plaque morphologies, both within an individual culprit plaque and between culprit plaques with different clinical presentations. Determining the stage of calcifying necrosis, along with the remodelling index can discriminate between stable and ACS related plaques. These findings could be applied in the future to help detect and stage plaques that have features of a vulnerable phenotype.

CHAPTER VII

STUDY IV

The Intravascular Relationship of Proximal Unstable Plaque Components to the Minimum Lumen Area Stenosis: Implications for Coronary Stent Implantation.

7.1 Introduction

Recent studies have suggested that the angiographically-derived point of maximum stenosis, or minimum lumen diameter (MLD), is not where the majority of unstable plaque is found [*Kaple et al 2008; Tanaka et al 2006*]**.** Furthermore, areas of necrotic-rich plaque tend to exist more proximally than this point. These areas may be hidden within positively remodelled disease at the angiographic proximal reference segment, where relative normality of the vessel is conventionally assumed on angiography [*Legutko et al 2013*]. This has implications for angiographically-guided percutaneous coronary intervention (PCI).

Most of our knowledge about the morphological characteristics of coronary lesions has previously been obtained from necropsy studies at the extreme end of the spectrum [*Burke et al 2001*]. The development of Intravascular Ultrasound (IVUS) with Virtual Histology ™ (VH), using the spectral analysis of the radiofrequency ultrasound backscatter signals to identify specific components of the atherosclerotic plaque, has allowed us *in-vivo*, to delineate the relative contributions of different plaque types to lesions [*Nasu et al 2006; Qian et al 2009; Hong et al 2008; Rodriguez Granillo et al 2006*]. This evidence suggests that there may be multiple variations in the morphology of plaques, rather than the traditionally accepted view that a common pathological mechanism is at play [*Maehara et al 2002*]. The spectrum of coronary heart disease is heterogenous and many IVUS-VH studies suggest that

significant variations exist in the focal point of lipid, necrotic and calcified components of different plaques [*Garcia-Garcia et al 2006; Hong et al 2008; Qian et al 2009; Rodriguez-Granillo et al 2006; Surmely et al 2006; Nakamura et al 2006*]

Moreover, multiple more recent VH studies, including PROSPECT, VIVA and ATHEREMO (*Stone et al 2011; Calvert et al 2011; Garcia-Garcia et al 2014*) have suggested that plaques with a "higher-risk" for future events appear to have the following features: Plaque burden >70%; Minimum Lumen Area (MLA) <4mm^2; Presence of one or more VH-Thin Cap Fibroatheromas (VH-TCFA)

7.2 Study Objectives

We sought to determine the distance between the minimum lumen area (MLA) and the site of maximum necrotic core content (MAX NC) across the spectrum of coronary artery disease by measuring this on motorized (0.5mm/s) Intravascular Ultrasound (IVUS). The aim was to quantify the longitudinal relationship between these sites in:

1. Acute coronary syndrome (ACS) culprit plaques (CP)
2. Stable plaques (SP)
3. Non-culprit plaques - from adjacent plaque/vessels in ACS patients (NCP).

7.2.1 Hypotheses:

1) The most significant necrotic core plaque does not occur at the angiographic MLD/IVUS derived MLA.
2) The longitudinal distance between these sites varies related to clinical presentation.
3) The prevalence of "higher risk" lesions types varies between clinical presentations.

7.3 Methods

These are as decribed in the general methods section and similar to previous chapters. In relation to this specific study, we measured the distance on IVUS pullbacks (at 0.5mm/sec) between the MLA and MAX NC site. Any MAX NC site within 1.5mm (3 frames at a heart rate of 60) of the MLA was rounded down to zero and taken to be part of the MLA lesion. This allowed us to decide whether the MAX NC frame occurs as part of the MLA lesion or not. Anything beyond 1.5mm proximally was taken as measured. Non-culprit plaques were taken distally to a culprit plaque (same vessel) in 16 patients and from a separate vessel in 4 patients.

The proportional presence of the MAX NC plaque frame is displayed in length groups: **1.** At MLA; **2.** 1.5-5mm; **3**. 5-10mm; **4.** 10-15mm and **5.** 15mm+. We have eliminated Nerotic Core or TCFA sites >1.5mm distal to the MLA, as these sites often tend to be part of another lesion developing (as part of diffuse disease) downstream.

7.4 Study specific statistics and power

Simple descriptive statistics have been used to analyse the compositional differences and relative distances between MLA sites and MAX NC sites expressed in mm. On comparing sites a student's t-test was used when the data was normally distributed, however if variances were unequal or a two sided F test was significant a Mann-Whitney U test was performed to ensure statistical significant was met for median values. A P value of <0.05 was taken as indicating a statistically significant result.

To ensure we had significant power to detect a difference we used data from our previous variability and magnitude of measurement error work [*Murray et al 2012*]. We know that the mean total plaque lengths for two different types of plaque are: CP 30.56±11.86 and SP 21.83±10.56. Using these previous results, we were able to determine that 19 plaques in each group are required for 80% power to detect a difference with an alpha of 0.5 (95% CI). We have 70 CP, 35 SP and 20 NC plaques which should ensure adequate statistical power.

7.5 Results

250 lesions sites within 125 vessels were examined from 105 patients (70 ACS and 35 Stable). Patient characteristics across the spectrum of coronary disease studied are displayed in table 7.1. The full details of plaque volume composition across the main groups are displayed within Table 7.2. Further detailed analysis at each individual lesion site is shown in Table 7.3. Although complexity exists when comparing three groups at two separate sites, with regard to plaque components, general signals exist. At the MAX NC site there is greater vessel size, a greater lumen area and greater amounts of necrotic core compared to the MLA. Interestingly, even though angiographically the vessel lumen may appear reasonable, the plaque burden at the proximal MAX NC site always remains >40%. This occurs across all clinical presentations, indicating that there is still a definite lesion present here. With regard to outputs from a VH analysis, there appears to be differences in the absolute area of plaque types. However, when this is corrected for total plaque burden by the percentage composition of plaques (Table 7.2), the only difference that truly exists (as reported before in this thesis) is a greater presence of DC in stable plaques ($p=0.014$).

Table 7.1 – Patient Characteristics

Characteristic	ACS N=70 Culprit Plaque (CP)	ACS N=20 Non-Culprit Plaque (NCP)	Stable Angina N=35 Stable Plaque (SP)
Mean Age (±SD)	59.2 ± 11.0	57.3 ± 9.7	60.1 ± 7.8
Male %	73%	60%	60%
LAD/Diagonal	41%	55%	74% (p<0.05)
Circumflex/OM	25%	35%	12%
Right Coronary	34% (p=0.01)	10%	14%
Mean Trop (±SD)	14.8 ± 27.2	n/a	n/a
Median Trop (IQR)	1.4 (0.1-13.7)	n/a	n/a
Hypertension	51%	44%	59%
Diabetes	24%	21%	18%
Current Smoker	54%	45%	57%
Hypercholesterolaemia	60%	54%	52%
Family History	70%	63%	65%
CKD	3%	0%	1%
Previous MI	16% (P<0.01)	10%	7%

Table 7.2 Simple plaque comparisons across the spectrum of coronary disease

Mean Variable	Culprit (CP) N=70	Non-Culprit (NCP) N=20	Stable (SP) N=35	p-value
Fib Vol (mm^3) Mean (±SEM)	111.0 (±9.6)	59.0 (±9.9)	50.5 (±5.3)	CP>Both (p<0.0001)
FFatty Vol (mm^3) Mean (±SEM)	19.5 (±1.9)	11.1 (±2.4)	9.2 (±1.2)	CP>Both (p<0.0001)
NC Vol (mm^3) Mean (±SEM)	50.9 (±5.9)	25.5 (±7.9)	21.3 (±2.5)	CP>Both (p<0.0001)
DC Vol (mm^3) Mean (±SEM)	20.6 (±3.1)	9.8 (±2.7)	13.5 (±2.0)	CP>NCP (p=0.014)
Fib % Mean (±SEM)	57.2 (±1.2)	59.2 (±1.9)	55.4 (±1.9)	NS
FF % Mean (±SEM)	10.8 (±1.4)	10.5 (±0.8)	9.9 (±0.9)	NS
NC % Mean (±SEM)	23.2 (±1.2)	21.5 (±1.9)	21.7 (±1.2)	NS
DC% Mean (±SEM)	9.1 (±0.8)	8.7 (±1.1)	13.1 (±1.3)	SP>Both (p=0.014)

Table 7.3 – IVUS measurements at MLA and MAX NC site per plaque type

Mean Measurement Variable (±SEM)	Culprit ACS (CP) (N=140)		Stable Culprit (SP) (N=70)		Non-Culprit plaque (N=40)	
	MLA	**Max NC**	**MLA**	**MAX NC**	**MLA**	**MAX NC**
Vessel area	**14.8 (±0.68)**	**18.4 (±0.81)**	**4.0 (±0.42)**	**7.3 (±0.72)**	**12.0 (±0.76)**	**15.13 (±1.1)**
Plaque area	**11.8 (±0.62)**	**12.5 (±0.64)**	**12.7 (±0.74)**	**15.9 (±1.0)**	**8.4 (±0.67)**	**9.1 (±0.70)**
Fibrous Area	**5.3 (±0.36)**	**4.2 (±0.24)**	**8.7 (±0.66)**	**8.1 (±0.94)**	**3.3 (±0.37)**	**2.8 (±0.37)**
Fibro-Fatty Area	**1.2 (±0.12)**	**0.45 (±0.06)**	**66.5 (±2.5)**	**49.0 (±3.4)**	**0.67 (±0.10)**	**0.36 (±0.11)**
NC Area	**2.1 (±0.21)**	**3.8 (±0.31)**	**3.5 (±0.43)**	**2.1 (±0.45)**	**1.4 (±0.18)**	**2.1 (±0.22)**
DC Area	**0.77 (±0.08)**	**1.1 (±0.11)**	**0.66 (±0.10)**	**0.26 (±0.9)**	**0.72 (±0.11)**	**0.99 (±0.09)**
Fibrous %	**58.2 (±1.2)**	**46.0 (±1.3)**	**1.3 (±0.19)**	**1.5 (±0.21)**	**53.7 (±2.9)**	**41.9 (±2.2)**
Fibro-fatty %	**13.0 (±1.4)**	**5.5 (±0.70)**	**0.67 (±0.09)**	**0.65 (0.11)**	**11.2 (±1.3)**	**5.0 (±0.71)**
NC%	**21.4 (±1.3)**	**37.5 (±1.3)**	**58.5 (±2.9)**	**43.3 (±2.9)**	**20.9 (±1.9)**	**34.2 (±1.4)**
DC%	**7.4 (±0.98)**	**11.1 (±0.77)**	**11.1 (±1.6)**	**3.7 (±0.82)**	**11.3 (±1.6)**	**17.3 (±1.7)**

With regard to the longitudinal distance between the MLA and MAX NC site, the distance as measured on IVUS motorized pullback is shown in Table 7.4, both mean and median values for each distance are shown.

Table 7.4 – Differences in distance between MLA and MAX NC site for each plaque type

Distance (mm) **MLA-MAX NC**	**Culprit ACS Plaque** **CP (n=70)**	**Non-culprit Plaque** **NCP (n=20)**	**Stable Plaque** **SP (n=35)**
0mm (@MLA)	2/70 (2.9%)	5/20 (25%)	9/35 (25.7%)
0-5mm	25/70 (35.7%)	6/20 (30%)	6/35 (17.1%)
5-10mm	26/70 (37.1%)	9/20 (45%)	12/35 (34.3%)
10mm +	17/70 (24.3%)	0/20 (0%)	8/35 (22.9%)
Mean (±SD)	7.9mm (±4.9)	4.1mm (±3.0)	6.2mm (±5.4)
Median (IQR)	6.2mm (4.3-18.1)	4.8mm (0-9.7)	5.4mm (0-9.4)

The MAX NC site occurs at the MLA in around one quarter of stable and non-culprit presentations but only 2.9% of culprit presentations. The spread of the MAX NC is displayed graphically in several formats to aid understanding. To determine the statistical differences between these multiple groups both a simple Mann-Whitney U test was performed (between each group separately) and a Bonferroni multiple comparison test was performed. The main result (confirmed by both tests) was that culprit plaque MAX NC is statistically more proximal than that seen in non-Culprit plaque ($p=0.003$). However on comparing stable plaque to non-culprit plaque and culprit plaque to stable plaque no difference was seen statistically between these groups ($p=0.139$ and 0.087 respectively).

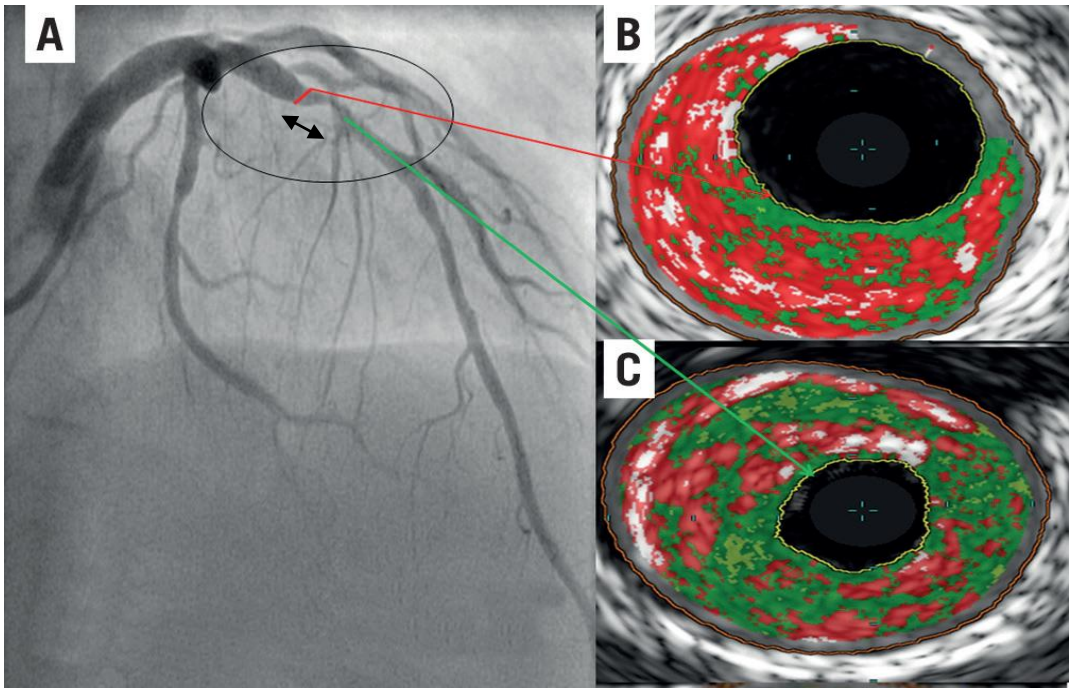

Figure 7.1 – A – Angiogram of Culprit lesion in LAD; B – MAX NC frame; C – MLA frame.

Figure 7.2 is a spread plot detailing individual positions of the MAX NC at pre-defined distances from the MLA and this is again displayed in a histogram for understanding (Figure 7.3). Finally, Figure 7.4 shows our findings per plaque type as it may be seen on a "angiographic-like" side-on representation of an IVUS-VH pullback. This final figure shows the mean differences between plaque types and that culprit plaques appear to have the greatest distance from MAX NC frame to the IVUS MLA. The IVUS MLA is used as a more accurate surrogate for the "angiographically perceived" minimum lumen diameter: **CP** mean 7.9mm (±4.9) Vs **NCP** mean 4.1mm (±3.0) Vs **SP** mean 6.2mm (±5.4). On statistical testing of these differences, individually it is clear that there is a statistical difference between CP and NCP. However, this does not exist between NCP and SP. When comparing CP and stable plaque there is a signal that the distance may be greater in CP, however this does not quite reach statistical significance with $p=0.052$.

Figure 7.2 – Spread plot of distance (mm) from MLA to MAX NC frame per plaque type.

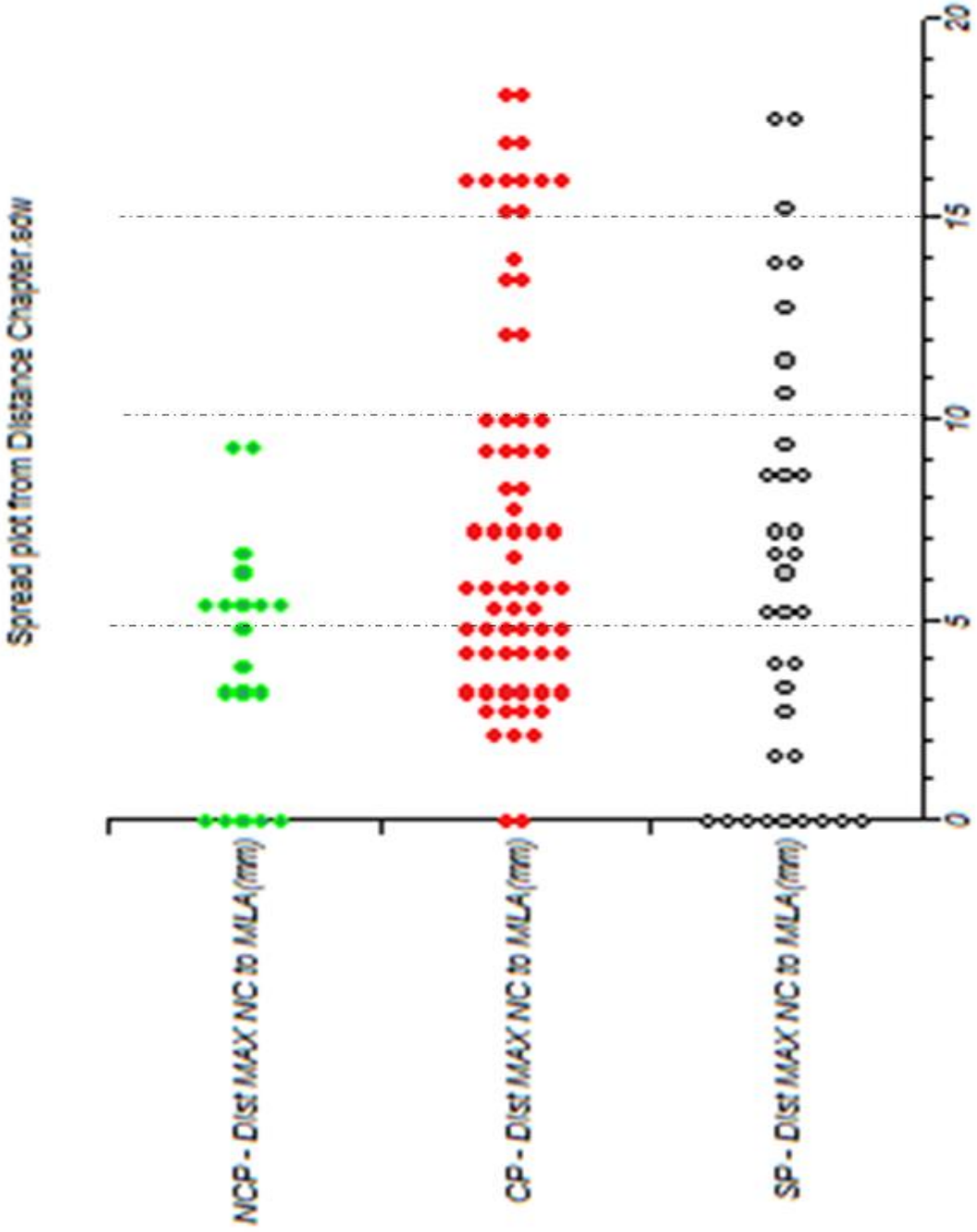

Figure 7.3 – Histogram of distance (mm) and relative percentage of this from MLA to MAX NC frame per plaque type.

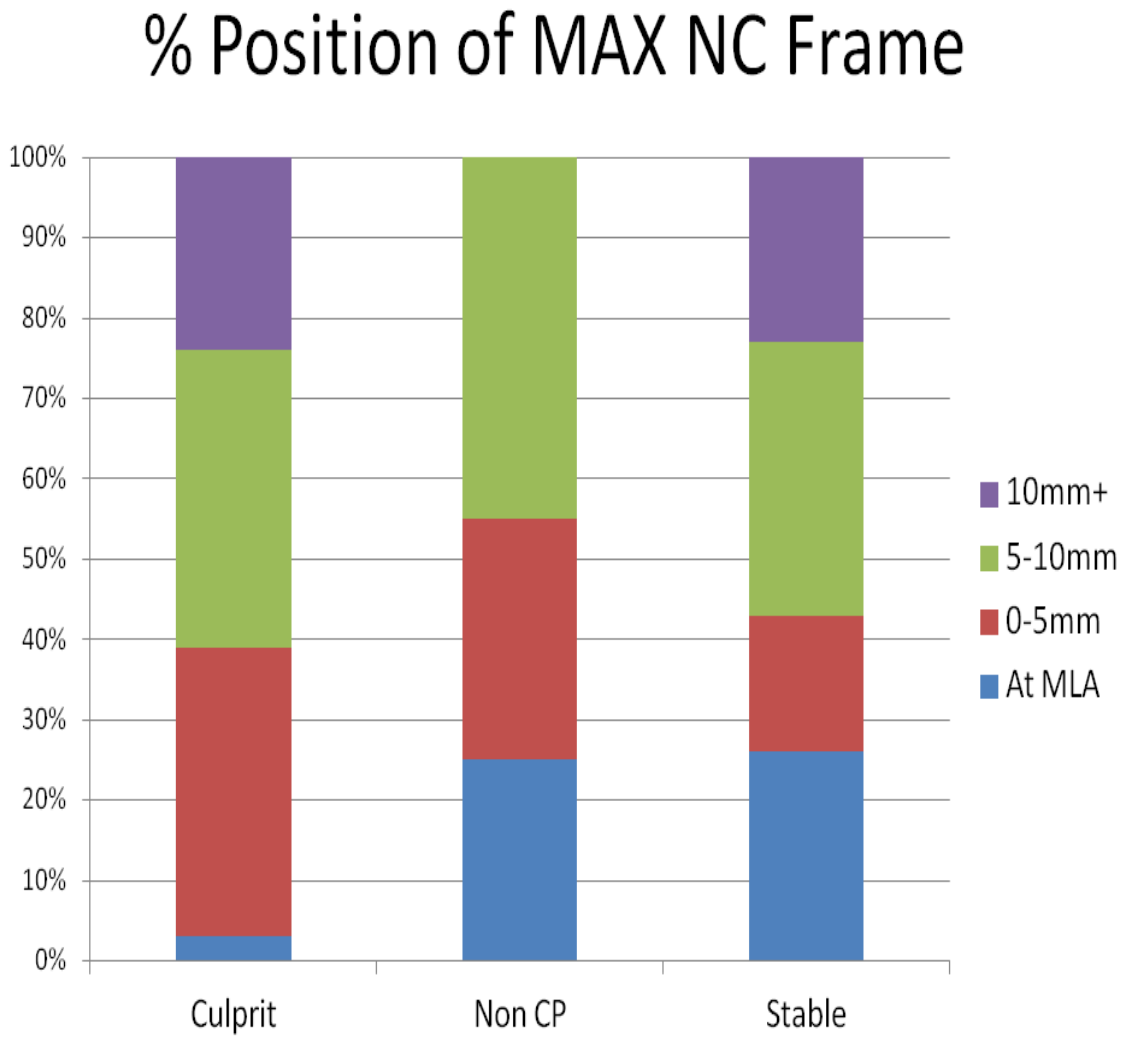

Table 7.5 – Prevalence of "high risk" plaques within the MAX NC frame.

High Risk Plaque within MAX NC Lesion (Prospect/VIVA/Atheroemo Lesions**)**	**CP** (N=70) Prevalence %	**NCP** (N=20) Prevalence %	**SP** (n=35) Prevalence %
PB>70% / MLA<4 / VH-TCFA	35%	20%	19%

Figure 7.4: Schematic showing comparative mean lengths between MAX NC frames and MLA in different plaque

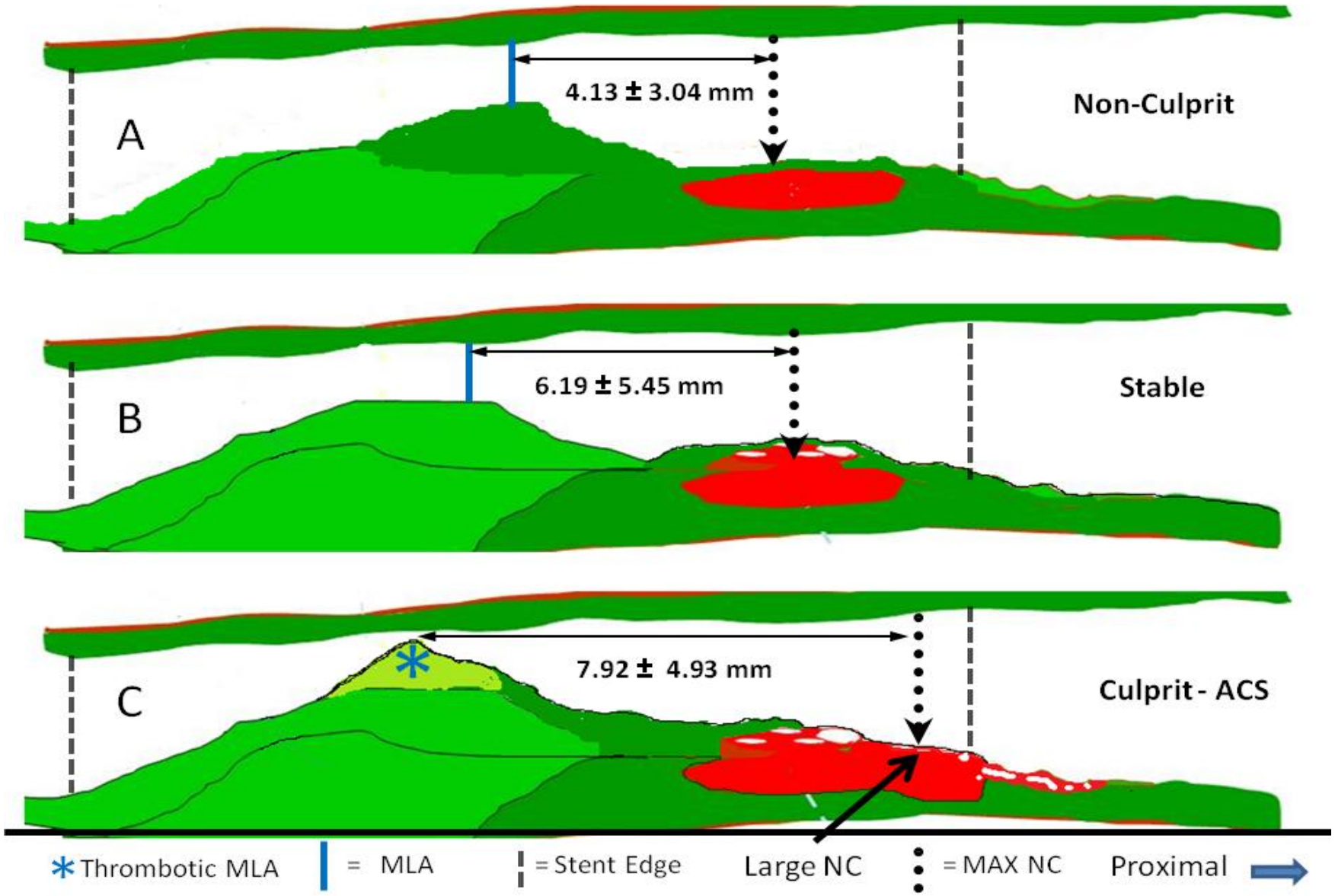

7.6 Discussion

We have reported our original findings detailing the differential distances that exist between proximal unstable plaque components and the minimum lumen site as determined by IVUS-VH. This appears to occur with varying degrees across the spectrum of atherosclerosis. Although this is not an entirely original concept, previous work has concentrated on one type of clinical presentation individually and the implications this has for stent implantation. In 2012, Legutko *et al* have separately addressed STEMI and NSTEMI culprit plaques finding that 50% of stents in STEMI do not cover the most proximal unstable part of the culprit plaque. This was repeated in NSTEMI and 35% of patients still had an uncovered proximal VH-TCFA. Wykrzykowska *et al* in 2012 found that there is a gradient from proximal to distal in terms of the amount of necrotic core plaque that can be found and Sarno *et al* in 2011 suggested that 31% of stents do not cover proximal unstable plaque components. In the study which is most similar to ours, Kaple *et al* in 2008 found in 81 stable patients that the MAX NC site was located at the MLA in 3.3% of patients. They found that 61% of lesions had a proximal MAX NC site by around 4mm. They concluded that the MLA is rarely the site of greatest instability and this is consistent with previous pathological analyses. Our investigation involved a greater amount of patients, vessels and plaque sites than in previous studies in this area and therefore further clarifies the intra-vascular relationship of plaque components to the MLA (perceived angiographic target). Our results suggest that when treating ACS culprit

lesions, the operator placing a stent should be mindful that consideration should be given to extending the stent proximally from the MLA by at least 10mm. This may be less conventional than the current teaching of allowing a 50:50 distribution of stent length coverage either side of the "perceived angiographic" MLA. It has been suggested by other authors (*Legutko and Dudek et al 2012-2013*) that there is a "culprit of the culprit" phenomenon that occurs in unstable plaques, where the necrotic rich rupture site occurs proximally and a thrombotic tail exists and extends into the more distal stable plaque that has a reduced luminal size. This cannot be proven well enough on IVUS due to the limited ability to truly define thrombus.

Further intra-vascular imaging trials into this phenomenon should be conducted, particularly with Optical Coherence Tomography (OCT). This is able to visualize the point of plaque rupture, TCFA, presence of thrombus and length of plaque with much greater accuracy than IVUS [*Prati et al 2013*]. An operator blinded stenting trial, utilising new intra-vascular imaging modalities, should be performed. This might allow further clarification of this hypothesis and confirm with more precision, how far proximal a stent may need to be extended in ACS PCI (to ensure coverage of the rupture site). A future trial would also have to ensure adequate statistical power to compare clinical events during follow up, as it remains unknown whether this practice would alter hard end-points such as stent thrombosis and target vessel revascularisation. There may be a trade-off in risk with regard to increasing the length of stent implanted, although in the most recent trials utilizing IVUS for DES

implantation this does not appear true. This could not be done with any precision based on angiographic analysis alone, as it is impossible to know exactly where the most positively remodelled and necrotic-rich plaque is. It is hoped that recent results showing IVUS use improves outcomes, from studies such as ADAPT-DES [*Witzenbichler et al 2014*] and a recent meta-analysis of over 19,000 patients [*Zhang et al 2012*], may improve the current poor uptake of intra-vascular imaging during PCI.

7.7 Limitations

IVUS measurements and examinations have their own inter-catheter, inter-observer, inter-pullback and intra-observer variabilities. We previously addressed this with an in-depth measurement variability study [*Murray et al 2012*]. These results showed that our maximum measurement variability error for length measurement (calculated by the repeatability co-efficient from the within subjects standard deviation) was 2.81mm for intra-observer and 4.82mm for inter-observers. These maximums must be contemplated particularly where different operators choose different starting frames for pullbacks or when pullback are done repeatedly on lesions. The motorized IVUS pullback at 0.5mm/s has now been eclipsed by rotational IVUS or OCT (in-sheath) pullback devices that suffer less from the effects of jumping and sticking in lesions. A strict policy was adhered to within this study regarding poor mechanical pullbacks. They were either repeated or dismissed as being unsuitable for analysis at an early stage.

Despite being able to state that there appears to be plaques types that differ compositionally along the length of a given plaque, we still have no evidence to support the concept that failing to treat the plaque completely, has a negative effect on hard end-points. We do know that somewhere between 12%-20% of ACS culprit lesion that are treated are subsequently responsible for further events [Prospect trial 2009] Therefore, this part of our work can only hypothesise that misjudgements in plaque positioning and subsequent stent placement may contribute to the rate of these further events.

7.8 Conclusions

The angiographic "culprit" MLD point, when imaged as the MLA point on IVUS-VH, often does not contain the most necrotic or "high-risk" plaque types as defined by virtual histology. These sites lie significantly more proximal in ACS patients compared with non-culprit plaques. This may have implications for stent implantation practices that are currently guided by angiography.

CHAPTER VIII

STUDY V

Observations of angiographically guided stent selection and placement during percutaneous coronary intervention for acute coronary syndromes: The potential influence of IVUS-VH assessment.

8.1 Introduction

Angiographically-guided stent deployment is the conventional, albeit imperfect, approach in the setting of 'real world' percutaneous coronary intervention (PCI). Despite improvements in stent technology with third-generation drug eluting stents, stent thrombosis and target lesion/vessel revascularisation rates (TLR/TVR) have not been abolished [*Stefanini et al 2012; Takebayashi et al 2005*] Whilst multiple factors contribute to the major limitations of PCI, it is well recognised that stent under-sizing, under-deployment, inaccurate stent length selection and poor placement ("geographic miss") can lead to long-term adverse events [*Cutlip et al 1999; Zahn et all 2005; Iakoyou et al 2005; Mauri et al 2008*]. Previous work has also demonstrated that geographic miss is frequent (up to 50% of cases) and can result in both residual stent edge stenoses and an increase in target vessel revascularisation (TVR) [*Suddath et al 2010; Park et al 2013; Claessen et al 2011*]. In the setting of acute coronary syndromes, post-mortem human studies of patients dying as a result of stent thrombosis have described the impact of incomplete stent coverage of necrotic core resulting in delayed endothelialisation, impaired thrombotic homeostasis and acquired late stent malapposition [*Iakovou et al 2005; Palmerini et al 2012*]. The ADAPT-DES study [*Witzenbichler et al 2014*] has suggested that the benefits of IVUS were especially evident in patients with acute coronary syndromes and complex lesions. Further

study is therefore required to understand the mechanistic aspects of how IVUS guidance could improve the placement and deployment of a stent.

We therefore sought to determine the mechanistic nature of stent deployment during routine PCI for ACS in our large-volume, UK-based tertiary centre. Our aim was to analyse the Acute Coronary Syndrome (ACS) culprit plaque with IVUS-VH before and after *angiographically-guided* PCI. The PCI operator was initially blinded to the IVUS images relying solely on the angiographic interpretation. Our aim was to fully describe the mechanistic treatment of ACS lesions and to accurately measure stent architecture, deployment and residual plaque. The prevalence of any abnormalities, detailed stent measurements and compliance with known IVUS criteria for adequate stent deployment [*Russo et al 2009; Chieffo et al 2013; de Jaegere et al 1998]* are reported within this paper.

8.2 Methods

This has been described previously in our general methods section. Further study specific details, measurements and statistics are presented below.

8.2.1 Measurements and Statistics

It is necessary to define what was measured at each stage to understand the subsequent results:

IVUS analysis 1 (pre-intervention): Culprit Plaque Length; Reference vessel dimensions; lumen dimensions; plaque burden; IVUS-VH plaque composition.

IVUS analysis 2 (post-intervention after operator satisfied): Residual plaque length; stent length; residual plaque burden; Minimum stent diameter; Maximum stent diameter; Minimum Stent Lumen Area (MLA); Maximum Stent Lumen Area; Frequency of observed longitudinal geographic miss; Frequency of residual plaque being of "high risk" nature (VH-TCFA); Frequency of stent edge dissection; Frequency of prolapsed material inside stent; Frequency of stent mallapposition.

From these measurements, we were able to calculate some basic criteria known to define good stent deployment and these have been taken from the landmark MUSIC and AVID trials [*Russo et al 2009; de Jaegere et al 1998*].

- **Min/Max Lumen Diameter (Should be >0.7) – marker of uniform stent deployment.**
- **MLA/Av Ref Vessel Lumen Area (Should >0.8) – marker of stent result achieved relative to vessel.**

- **Minimum Stent Area Achieved (should always be >5.5mm^2) – Correlates with better stent outcomes.**

From the above measurements, we have also calculated a new measurement to try and determine by how much the operator under-sizes and under-deploys stents in usual angiographic practice. We have called this the Calculated Under-Deployment Area (CUDA): This is calculated by the following:

- **Minimum stent area achievable (MSAach) = (π/4) × (Diameter of stent chosen)^2**

- **Calculated under deployment area = MSAach – IVUS measured minimum stent area (IVUS MSA).**

Figure 8.1: Worked example of CUDA for illustration purposes

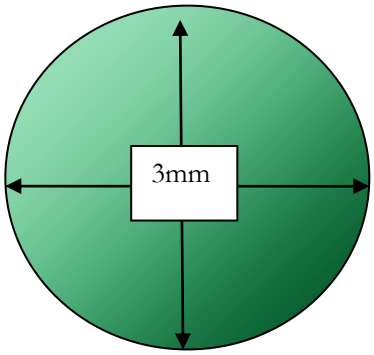

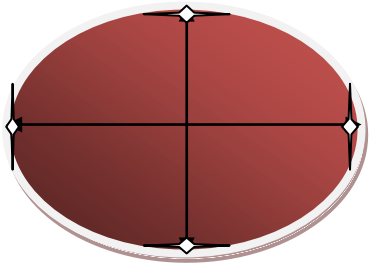

(Stent Chosen 3.0mm diameter) **IVUS Measured MSA**

MSAach (3.14/4) x (3)^2 = (0.79) x (9) = 7.11mm^2 **5.7mm^2**

CUDA = MSAach (7.11) – IVUS MSA (5.7) = 1.41mm^2

8.3 Results

Table 8.1 – Basic characteristics for stent patients imaged

Characteristic	ACS N=54 Culprit Plaque (CP)
Mean Age (±SD)	55.2 ± 11.0
Male %	70%
LAD/Diagonal	61%
Circumflex/OM	20%
Right Coronary	19%
Mean Trop (±SD)	14.8 ± 27.2
Median Trop (IQR)	1.4 (0.1-13.7)
Hypertension	51%
Diabetes	24%
Current Smoker	54%
Hypercholesterolaemia	60%
Family History	70%
CKD	3%
Previous MI	16%

Table 8.2 – Final measured stent data after angiographic guidance

Measured Stent Variable	Result (Mean +/- SD)
Post Stent Residual Plaque Burden (%)	49.20 (±7.45)
Stent Min Lumen Diameter (mm)	2.51 (±0.54)
Stent Max Lumen Diameter (mm)	4.18 (±0.65)
Min/Max Lumen Diameter (Should be > 0.7)	0.61 (±0.13) 21/58 (>0.7) = 36%
Total Plaque Length (Pre-stent with PB>40%) (mm)	31.63 (±12.11)
Stented Length on IVUS (mm)	20.86 (±6.15)
Residual Plaque Length (Post-stent PB>40%)	14.60 (±11.56)
Implanted Stent Diameter (mm)	3.33 (±0.49)
Implanted Stent Length (mm)	20.59 (±8.02)
Minimum Stent Area Achieved (mm^2) (Should be >5.5)	6.79 (±2.43) 38/58 (>5.5) =65.5%
Min Stent Area Achievable (mm^2) (Theoretically for chosen stent size)	8.87 (±2.68)
Calculated Relative Under Deployment Area (mm^2)	2.08 (±1.87)
Av Reference Vessel Lumen Area (mm^2)	10.58 (±2.51)
MLA/Av Ref Vessel Lumen Area (Should >0.8)	0.66 (±0.24) 23/58 (>0.8) = 40%
Maximum Stent Lumen Area (mm^2)	7.83 (±2.38)

Table 8.3 – Relative frequencies of post PCI stent abnormalities

Measured Variable +/- SD	Result
Frequency of Longitudinal Miss (Residual PB > 40%)	25/58 = 43%
Frequency of "unstable" VH-TCFA (in residual plaque)	9/58 = 15.5%
Frequency of Stent Edge Dissection	5/58 = 8.6%
Frequency of Incomplete Stent Apposition	13/58 = 22.4%
Frequency of plaque prolapse/in-stent tissue	3/58 = 5.2%

Figure 8.2 – Histogram showing spread of IVUS MSA (mm^2) in number of stents receiving post-dilatation.

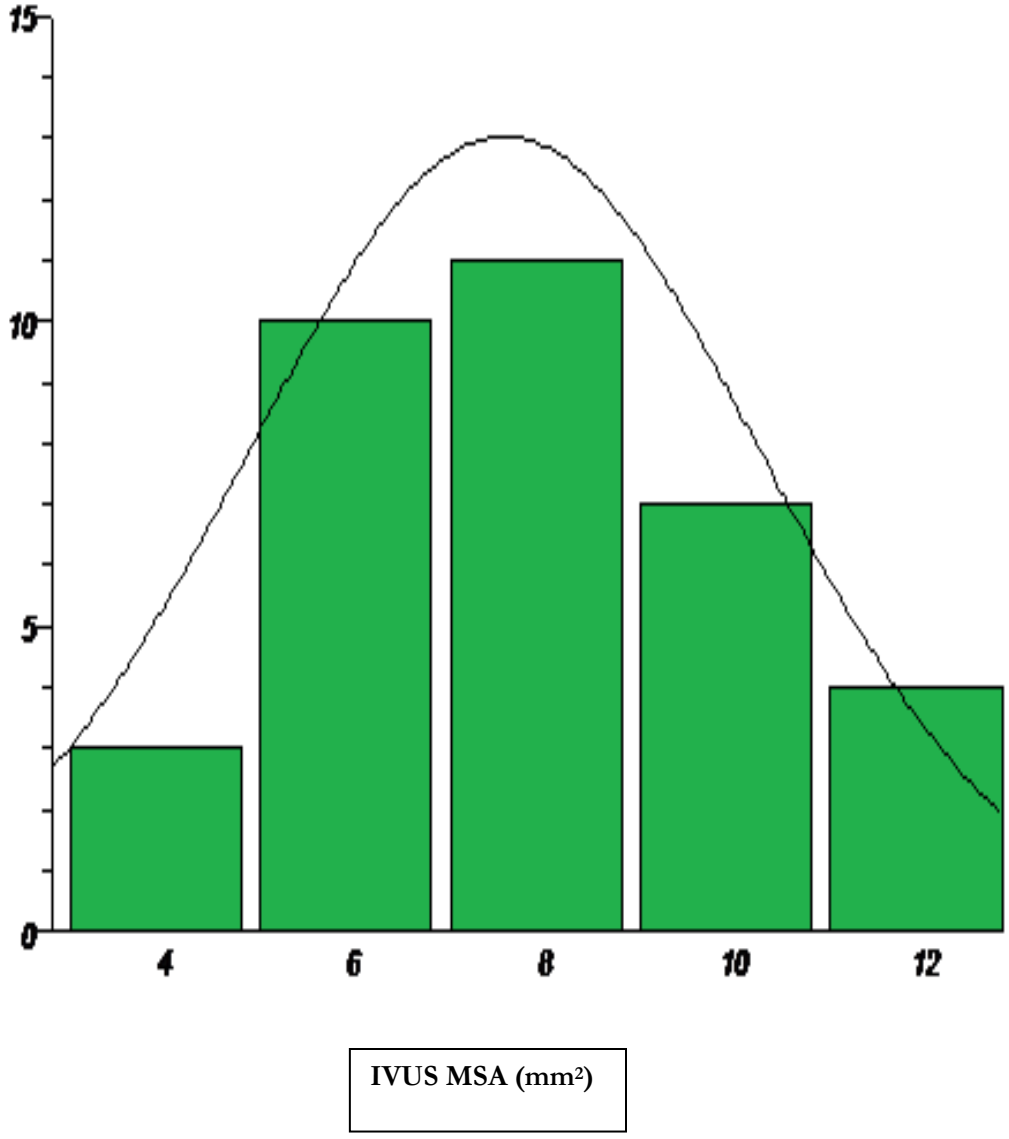

Figure 8.3 – Histogram showing spread of IVUS MSA (mm^2) in number of stents NOT receiving post-dilatation.

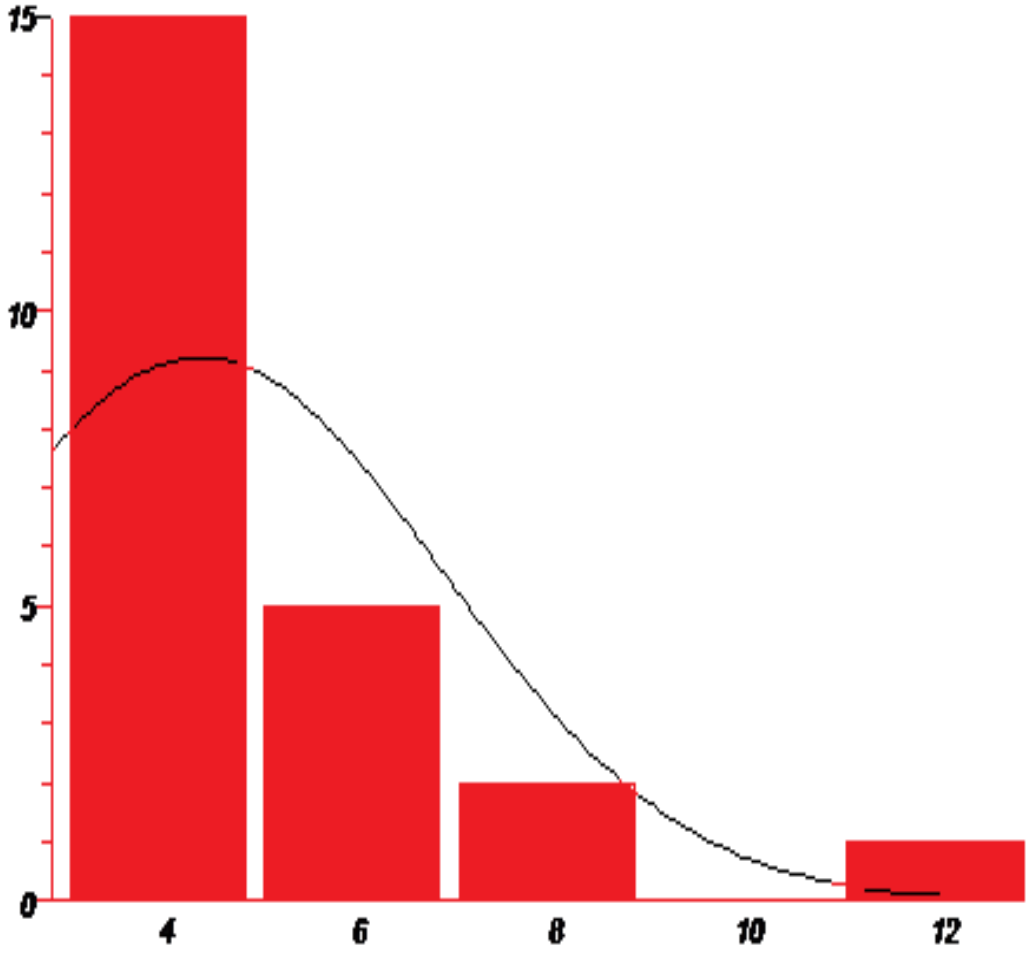

Figure 8.4 – Comparison of min, max and mean (+/- 95% CI) minimum stent area (mm^2) for those stents post-dilated (PD+) and not post-dilated (PD-)

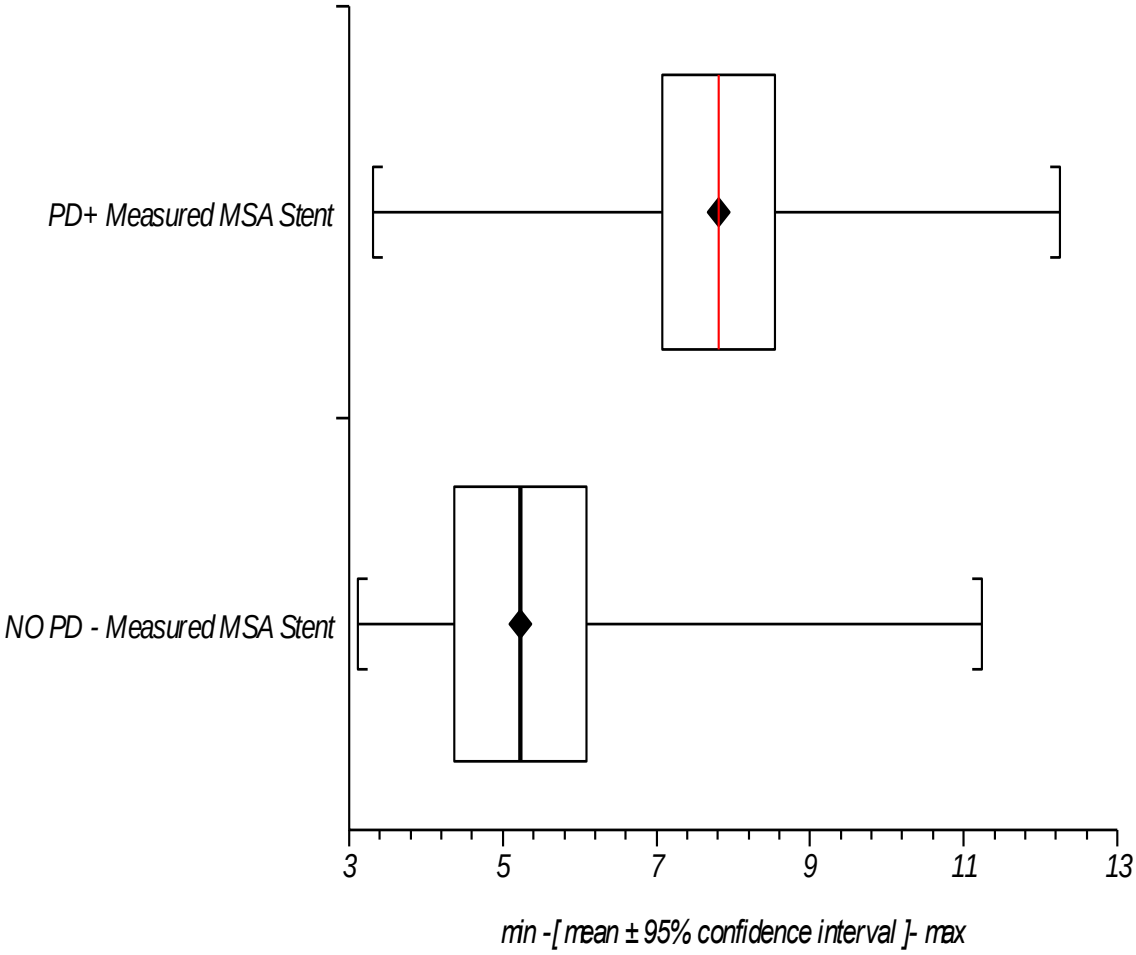

Figure 8.5: Differences in maximum lumen stent area compared between post-dilated stents (PD+) and those with no post-dilatation.

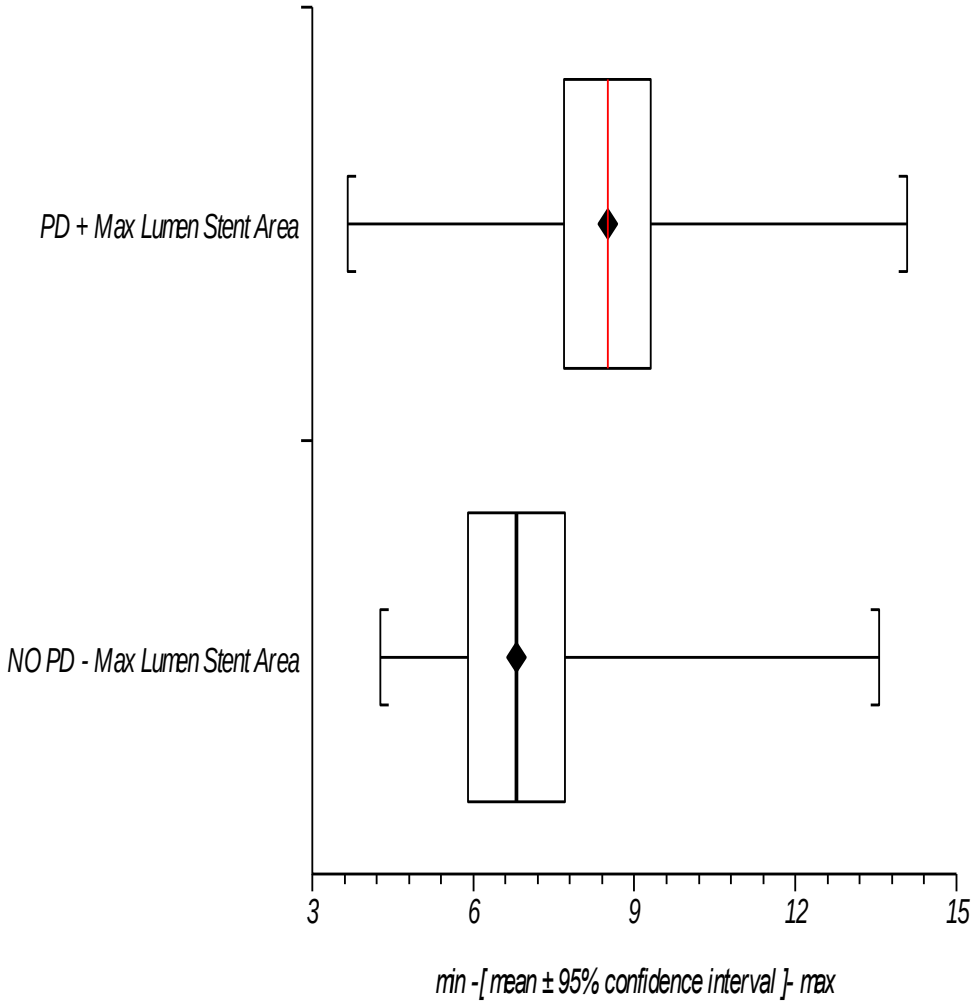

Figure 8.6 – Significant differences in MSA between PD and NO PD with highly significant statistical differences proving the benefits of luminal gain from post-dilatation.

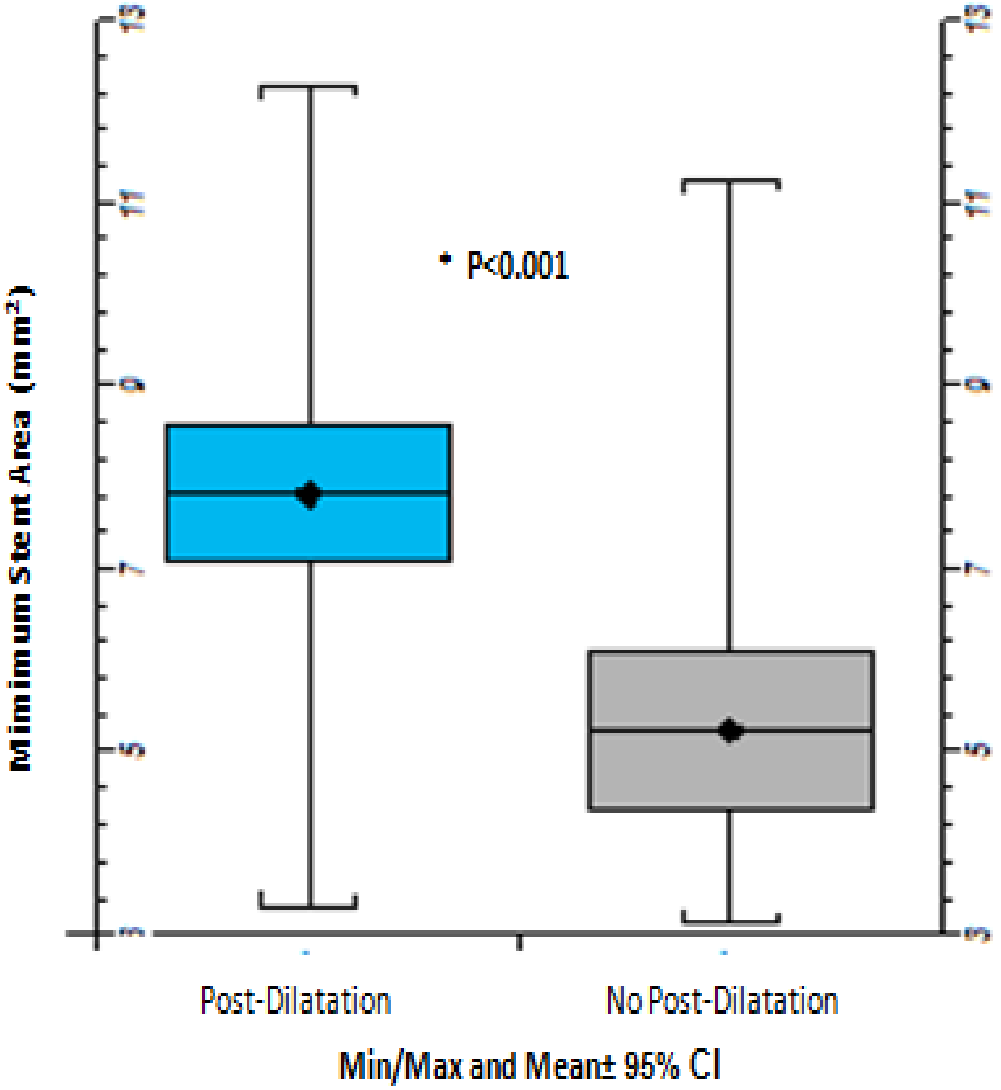

Figure 8.7 – The statistical differences in the calculated under deployment area (mm^2) between those stents with post-dilatation and those without. This shows that even with angiographic post-dilatation, under deployment still exists.

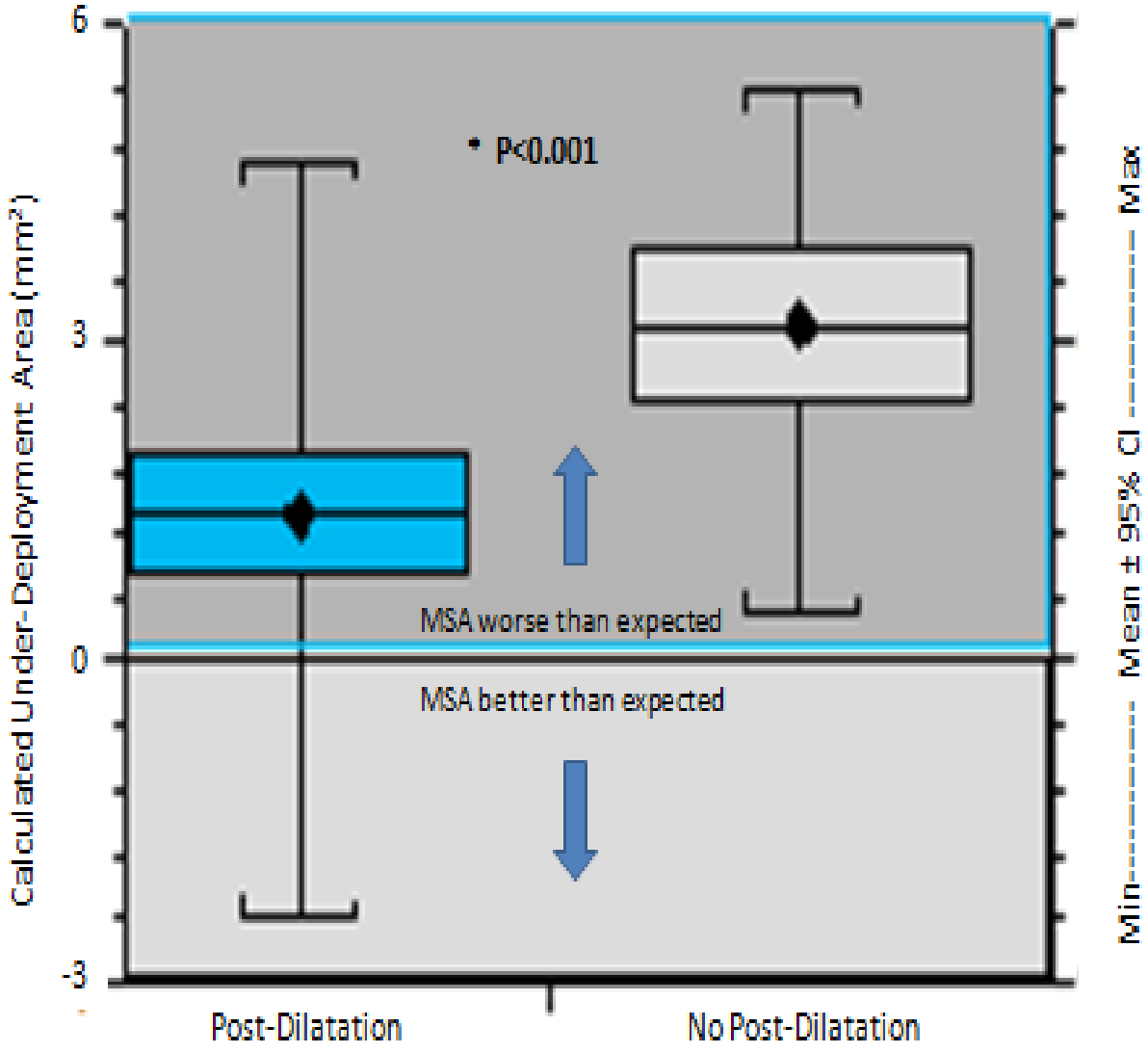

Figure 8.8 Comparisons of "ideal" stent sizes (based on predicted MSA in mm^2) compared to those measured and achieved per stent with and without post-dilatation.

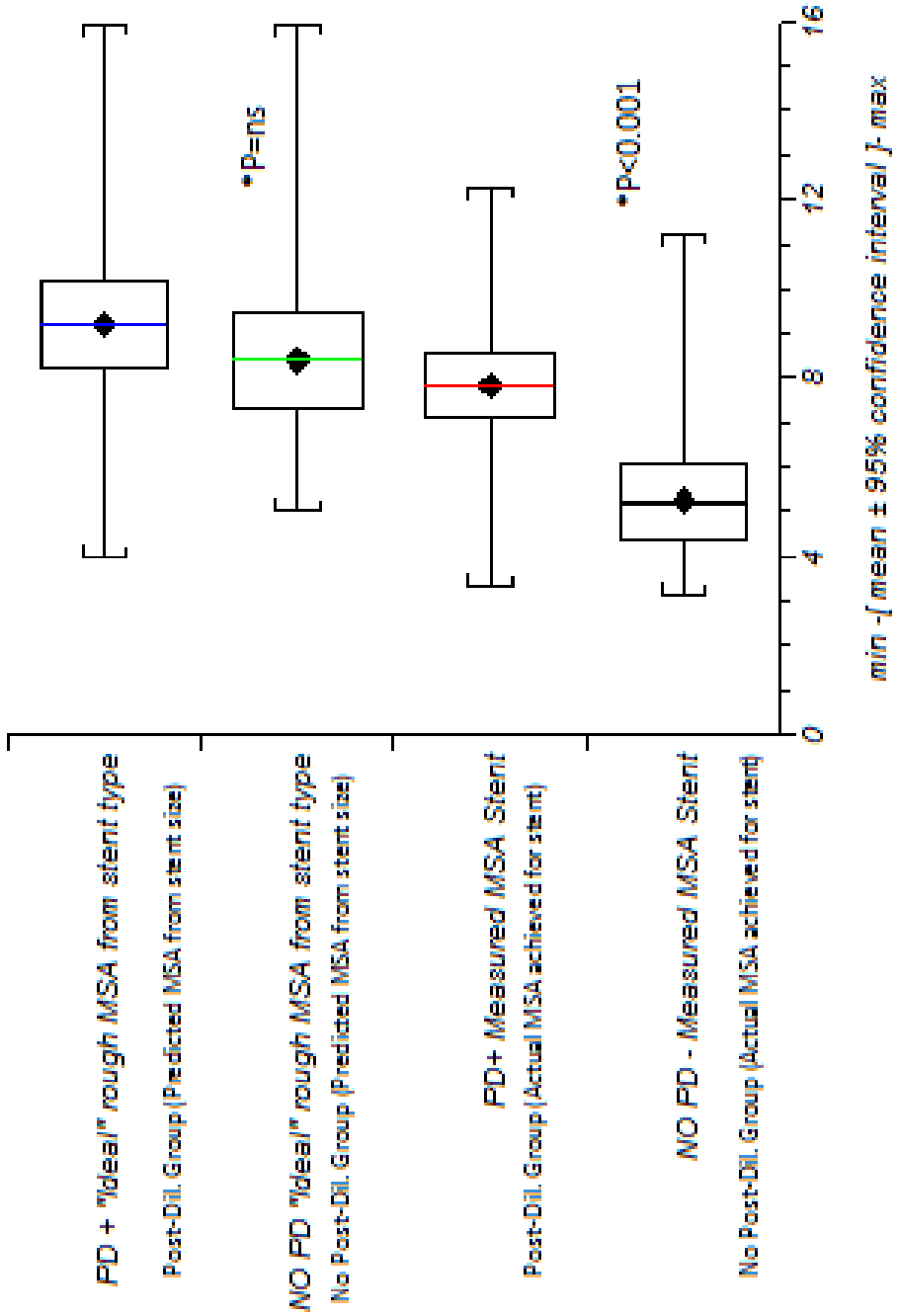

Figure 8.9 – Schematic of stent abnormalities seen with IVUS

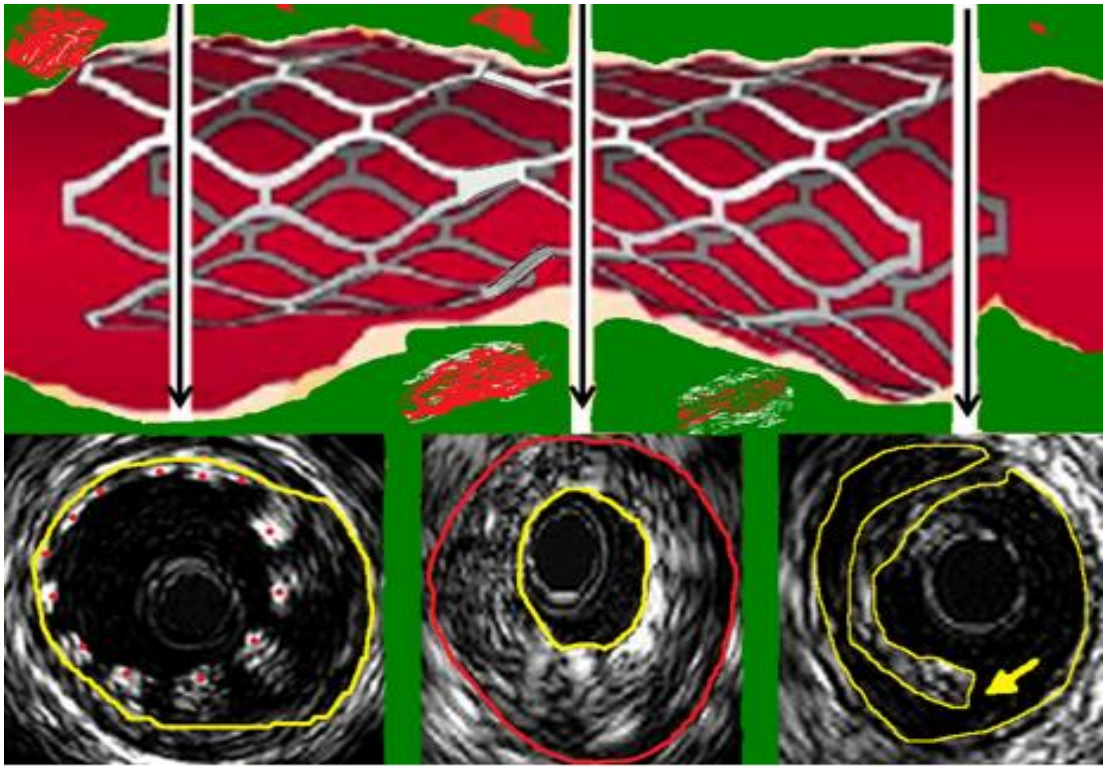

INAPPOSITION UNDER-DEPLOYMENT EDGE TEAR

8.4 Discussion

We have shown that experienced operators in a tertiary cardiac centre, reliant on angiography alone, systematically undersize the vessel and then choose stents that are smaller than they should be. They then go on to deploy those stents inadequately, even despite some good improvements with routine post-dilatation. Although a "excellent" angiographic result is very often achieved and documented, this is not a reflection of what has happened intra-vascularly.

We have also shown that the prevalence of other stent and vessel abnormalities, at the end of a procedure, remains substantial.

In the past, underpowered studies of IVUS-guided PCI in the bare metal stent era, failed to demonstrate superiority to angiography-guided PCI alone [*Parise et al 2011*]. Some of these trials were already influenced by the work from the Milan group, using larger post-dilatation balloons, inflated at high pressure. However, there is evidence now in the DES era to suggest that suboptimal deployment (defined by a cross-sectional minimal stent area <5.5mm^2) is associated with higher TLR and ST rates [*Roy et al 2008; Fuji et al 2005; Claessen et al 2010; Zhang et al 2012*] Recently, the ADAPT-DES (Assessment of Dual Anti-Platelet Therapy with Drug-Eluting Stents) trial [*Witzenbichler et al 2014*] reported that IVUS-Guidance improved clinical outcomes both acutely (<30 Days) and at 1 yr, with a 33% reduction in MI and a 50% reduction in sub-acute and late stent thrombosis. These results are despite 40% more IVUS patients initially presenting with ST elevation myocardial infarction (STEMI). The benefits of IVUS were especially evident in patients with acute coronary syndromes and complex lesions. Overall, In ADAPT-DES, operators who used IVUS pre and post-procedure were found to achieve greater maximal lumen areas for proximal reference lumen area (8.9 vs. 7.6 mm^2), in-stent lumen area (6.3 vs. 5.8 mm^2), and distal reference lumen areas (6.5 vs. 6.1mm^2, P<0.001 for all measures). Greater maximum lumen area is identified as a key procedural factor to reduce risk for stent thrombosis with DES. Based solely on the IVUS evaluation, the

operator changed the PCI strategy in 74 % (2484/3349) of patients to choose (1) a larger stent or balloon (in 38% [943/2484] of cases); (2) higher inflation pressures (in 23% [564/2484] of cases); (3) a longer stent (in 22% [546/2484] of cases); (4) additional post stent dilatation due to incomplete expansion (in 13% [329/2484] or incomplete stent apposition (in 7% [166/2484]); and/or (5) additional stent placement (in 8% [197/2484]). Moreover, a recent large meta-analysis by Zhang *et al* 2012 has shown in 19,619 patients from both randomised and observational studies that a mortality benefit exists for IVUS guided stent implantation. This meta-analysis was then further enhanced [Zhang et al 2013] by the inclusion of three recent studies taking the total number of patients involved to 29,000. As described before, The ADAPT-DES [*Witzenbichler et al 2014*] trial was a prospective multicentre registry study that enrolled approximately 11,000 patients. The outcomes, after IVUS-guided percutaneous coronary intervention (PCI), were compared to the non-IVUS-guided PCI group in 8,575 patients. A significant reduction in the primary endpoint of definite/probable stent thrombosis was evident in patients who underwent PCI under IVUS guidance (vs. angiography guidance) at one-year follow-up (0.52% vs. 1.04%, p=0.011).

In the pre-specified long lesion subset of the RESET (Real Safety and Efficacy of a 3-month Dual Antiplatelet Therapy Following Zotarolimus-eluting Stents Implantation) trial [*Mintz et al 2012*]; 543 patients were enrolled and randomised to either the IVUS or angiography-guided PCI group. IVUS-guided PCI was related to

a significantly lower risk of MACE at one-year follow-up compared to angiographic guidance (4.0% vs. 8.1%, p=0.048). In the AVIO trial, no statistical differences were observed in MACE (16.9% vs. 23.2%) or target lesion revascularisation (TLR, 9.2% vs. 11.9%) between the IVUS and angiography-guided groups [*Chieffo et al 2013*]. However, this final work is from a group known for their "IVUS-like" results using routine bigger post-dilatation balloons at high pressure. This may not be representative of that achieved elsewhere in the world.

Based on the available data, the currently updated meta-analysis includes 14 studies involving 29,029 patients. This confirms the previous findings that IVUS guidance is associated with reductions in death (hazard ratio [HR]: 0.66, 95% confidence interval [CI]: 0.55-0.78, p<0.001), stent thrombosis (HR: 0.57, 95% CI: 0.44-0.73, p<0.001), myocardial infarction (MI) (HR: 0.74, 95% CI: 0.62-0.90, p=0.002) and MACE (HR: 0.86, 95% CI: 0.77-0.95, p=0.003), but also shows the beneficial effect of IVUS guidance in reducing TLR (HR: 0.82, 95% CI: 0.68-0.97, p=0.02). This again suggests that IVUS guided DES implantation could saves lives. Following this important meta-analysis, there have now been three further large meta-analyses published [*Jang et al 2014; Ahn et al 2014; Klersy et al 2013*] each with >20,000 patients confirming the general trend that IVUS-guided DES implantation is associated with lower rates of adverse clinical events.

IVUS can also detect geographical miss, which has been shown to correlate with an increased frequency of TLR and acute MI [*Costa et al 2008*] In addition, late incomplete stent apposition is associated with a higher rate of MI and very late ST during long-term follow-up [*Cook et al 2012*]. This is mainly due to outward vessel remodelling, but acutely inapposed stents, due to stent under-sizing or inadequate deployment, are easily identified by IVUS.

If we examine the data from SYNTAX, it is clear that despite how good we think we are at PCI, we have certainly not done well in the contemporary treatment of complex three vessel disease. The three year MACE rate was 28% with a repeat revascularisation rate of 19.7% and confirmed MI occurring in 7.1%. Also, the IVUS sub-study of the HORIZONS-AMI study showed a post-procedure stent malapposition rate due to inappropriate stent size selection or underexpansion of 35.2% [*Choi SY et al 2011*].

It may be that the lessons learnt from IVUS studies in the 1990s, regarding the use of larger post-dilatation balloons inflated to high pressure, should be re-enforced to Cardiologists of today's DES era. A recent observational study from the UK [*Rana et al 2014*] has also shown that, despite high pressure post-dilatation of stents to standard criteria, only 54% reached the study end-point that defined good deployment. If these contemporary stent results are compared to the data from the 2002 POST Registry [*Uren et al 2002*], there are striking similarities despite 15 years of progress within the field. In 53 stent thrombosis cases imaged as part of the

POST registry, there were approximately: 50% stents expanded less than 80% (from MUSIC criteria); 50% malapposition rate; 50% inflow-outflow disease; 20% thombus; 20% edge tears and 15% plaque protrusion. Overall 94% had an IVUS abnormality, compared with a 30% rate of abnormality on angiography alone. Therefore, it is clear that despite these warnings, we have not moved on from our obsession with the angiogram as the guide to routine stent insertion.

In light of our results, conducted in a high-volume tertiary cardiac centre, angiographically-guided stent procedures, in ACS patients, may be to the detriment of acute and long term stent results. Overall this could be one of the reason that PCI (in a stable setting) does not provide enormous advantages in mortality, yet IVUS-guided comparison studies and meta-analyses (in the DES era) show mortality benefits.

8.5 Conclusions

We have shown that utilizing angiography alone to guide the percutaneous treatment of ACS plaques can lead to several errors in both the initial selection of stent size and length. This data also suggests that symmetrical deployment and insufficient post-dilatation of the stents can lead to inadequate results. Experienced operators in a UK tertiary centre can systematically fail to achieve results that satisfy historical markers of proper stent implantation. This may have implications for subsequent target lesion or target vessel revascularization events, such as in-stent re-stenosis and stent thrombosis. A well-powered randomized trial of IVUS use is now required within the interventional cardiology community, to conclusively prove that these intuitive benfits will lead to a reduction in future MACE.

CHAPTER IX

FINAL SUMMARY AND GENERAL CONCLUSIONS

This body of work started almost eight years ago now and since those intial descriptions, the field has changed and other work has been published. With regard to our findings, we have influenced the field with publications in three main areas so far:

1. From the work carried out in Chapter IV, our initial magnitude of variability study has become a standard in the field. The depth of study given to the possible measurement errors accrued by visibly interrogating IVUS-VH was a first. Moreover, the use of the repeatability co-efficient had never been done before in this line of investigation. Our initial hypothesis with regard to this was statistically proven at the level of agreement between an individual operator and between operators. However, the actual magnitude of measurement variability calculated for some virtual histology variables was found to be greater than initially thought in previously published studies in the literature. This has led to our study being cited related to the calculation of end-points and power for prospective studies in the field. This has included a recent Lancet publication by Joshi *et al* 2014. With regard to the overall thesis title, this measurement variability (even between experienced operators) certainly has an impact on the perceived clinical utility of this tool on percutaneous coronary intervention.

In addition, the time required to analyse and interpret the data in a frame by frame format is significant and is not conducive to immediate results within the catheter lab. This is a major limitation of the technique (yet to be overcome by recent versions). This limits any immediate role the technique has in changing the percutaneous strategy for the operators on the day, in "real-time".

2. Our second main piece of work began in an era where there was still some discussion about which plaque types were seen more often in ACS vs stable patients and our initial hypotheses were based upon this. However, after the publication of Prospect (*Stone and Serruys et al 2011*), which had results that were particularly disappointing, primarily due to the study design (see discussion in Chapter V). It became clear during our work that we had the opportunity to use the data differently to build a risk score, this had not been attempted before in intra-vascular imaging. I therefore began analyzing the IVUS and VH data based upon the statistical concept of logistic regression and ROC curve analysis. This allowed us to filter through the various plaque variables to concentrate on those that are the most important in determining the differences between recently active, acute coronary syndrome plaques and stable angina plaques. Interestingly, when the results were distilled, the purest predictors of a plaque that has recently been "active" were mainly grey-scale IVUS based and not Virtual Histology. One parameter Necrotic Core/Dense

Calcium ratio (NC/DC) did have an influence on the final risk score equation having an AUC of 0.78 with sensitivity, specificity and odds ratio for determining an active plaque of 80%, 70% and 1.56 respectively. By far the main determinants of a high risk plaque were the total plaque burden and remodelling index. These findings were not entirely novel, but the plaque risk score generated was and has now been cited several times in the field. In addition, the methodology we used has now been recreated and applied by other investigators in the field of CT angiography of coronary plaques and in subdivided groups of patients such as diabetics.

3. The work within chapter VI was influenced by the findings from the previous risk score. Of note, the risk score that was previously generated was based upon the total volume of plaque constituents seen within a given culprit plaque. We applied some of these findings to individual plaque areas at different sites within the plaques and also attempted to try and understand better the relationship that had been revealed statistically regarding the increase in dense calcium measurements within stable plaques. It is important to re-iterate here that we did not show any differences in the output from a standard VH analysis between stable and acute coronary syndrome plaques, other than in the relative amount of calcium. Calcium again can be clearly seen on a standard grey-scale analysis and therefore does not necessarily need the VH algorithm for this to influence a coronary intervention. This site-

specific work was exploratory and experimental around the initial hypothesis that different sites within a single plaque have different compositional elements. The initial hypothesis was proven statistically in this work and has allowed us to understand that coronary plaque does changes significantly frame by frame along its length. Given that plaque anatomy can be somewhat heterogenous and unable to be judged (let alone seen in some cases) by basic angiography, these observations bring home the severe limitations of angiography alone. One major finding from this site-specific work was the fact that calcification in ACS related plaques tended to be spottier and nascent or less organized in a fixed arc. It is difficult to find a reliable measure of the spots of calcification seen and therefore we were reduced to using simple calculations (such as NC/DC) that would be able to summarise or assign a value to this phenomenon, to allow it to be compared. There are various flaws within this methodology as highlighted in the discussion and limitations section of that chapter. However, it was always felt that our work was very much observational, exploratory and hypothesis generating rather than definitive in the field. It is hoped that our theories from this work can be taken forward by more established research groups to fully understand the implications of spotty calcification and the possibility of stress interface mismatch points. The Edinburgh research group, led by Prof David Newby have recently found a Positron Emission Tomography (PET) tracer 18 F-NaF that appears to be able to "light up" early or nascent micro-calcifications

within coronary plaques seen on CT scans. This shows early promise in correctly identifying those plaques that have been causative in generating clinically significant acute coronary syndromes. This appears to be the most exciting work in the field at the current time.

Although the rest of the work in the final two chapters of this thesis remains currently unpublished or peer reviewed, ironically this work may highlight the most important role for intra-vascular imaging in PCI. This relates to determining the relationship between the angiographically-percieved narrowest point of the vessel (during an ACS) and the actual place where most of the plaque burden is placed. This appears to be almost universally within the proximal portion of the vessel before the stenosis. Positively remodelled plaque (in keeping with Glagov's original theory) can be present at varying lengths from the narrowest angiographic point and the measured spread of the disease is occasionally greater than an operator might consider for stent length. Although now not a new concept in this field, our hypothesis was to look at the differences across the spectrum of coronary artery disease (stable/culprit and non-culprit) to see if there is a statistical difference and we have shown this with regard to the anatomy of a culprit plaque. The limitations of measuring on a single IVUS pullback have been discussed in our measurement error chapter and this may have cast some doubts on our ability to have millimetre accuracy. Despite this, the work

highlights an important warning for the operator to not become entirely focused on the angiographic "occulo-stenotic reflex" and to consider the possibility that the proximal vessel is heavily diseased and may require the stent to be extended proximally to cover this. Although this work does highlight some important points with regard to the anatomy of a plaque, it again does not appear to provide solid evidence of a role for the virtual histology element of the IVUS output and again points to the fact that simply using the IVUS in standard grey-scale mode tells you much more than you were aware of beyond standard luminography.

Some recent work from studies such as PROSPECT, VIVA and ATHEROEMO has suggested that if you leave disease containing a Virtual Histology TCFA and an MLA <4mm^2 then you are risking a future MACE event. Despite this, there are numerous difficulties with interpreting some of this data and a caution must be highlighted regarding the ability of simple operators to even identify a TCFA or to sub-classify plaques into the subgroups that have been purpoted by the key opinion leaders in this field (*Garcia-Garcia, Calvert, Stone, Serruys et al*). If anything the Virtual Histology part of the IVUS still remains too complicated for the average interventional cardiologist to completely understand and apply to their current practice. Whilst it has given us good surrogate insights into the true anatomy of

different plaque types, it is unlikely (in its current format) to affect routine decision making in the cath lab.

From our observational perspective, we had a final group of hypotheses to be tested and this involved what a PCI operator does in everyday practice when placing stents in ACS lesions. The final chapter of this thesis takes the initial concept of intra-vascular plaque anatomy one step further to explore the mechanistic aspects of PCI in ACS. These blinded observations of intra-vascualar stent placement and expansion generated many interesting results. With regard to our original hypotheses, we were able to quantify the prevalence of stent abnormalities generated and focus on those that have impacted upon outcomes and end-points in other trials. Specifically, we have shown that many stents are asymmetrically expanded, under-sized, under-deployed or mallapposed. Furthermore, many stents do not cover all the plaque anatomy that is part of the active plaque. Some stents also create problems of their own with signs of dissection, plaque prolapse etc. These frequent abnormalities may have implications for future target vessel revascularization and therefore from a theoretical perspective could have been avoided, had IVUS revealed them at an early stage. Although this stent work was again observational and not powered to draw major conclusions, it has given us new insight into what can be expected from routine, angiographically-guided, PCI in ACS lesion. It has provided instructive data

that shows us all where we can improve our practice, particularly in the main areas linked to outcomes (stent MLA etc).

It is sincerely hoped that these final chapters of work can be published in due course, in order to convey to other operators the clear pitfalls of angiographically-guided PCI.

In final summary, although the role of the virtual histology component of this technology does have some limitations, the use of IVUS remains strengthened by this work. Particularly in relation to having direct vision of vessel and plaque anatomy before undertaking the intervention and choosing the equipment sizes. It is also possible to ensure that no immediate complications have arisen from the PCI and the best final stent MLA has been achieved to prevent the spectre of stent thrombosis and re-stenosis. I can say that I have used IVUS and VH in my clinical practice outside this work and found it both intriguing and useful in most cases.

Therefore, to answer the main question posed by this thesis as to whether virtual histology can have an impact on the percutaneous treatment of Acute Coronary Syndromes, I would have to conclude that IVUS alone, in basic grey-scale guise, can provide more than enough information over and above angiography to furnish the operator about the pattern, burden and anatomy of the disease being tackled. The use of the virtual histology aspect of this technology does have some niche advantages in very experienced hands and can provide excellent insight into plaque morphology that may influence lesion based treatments. Unfortunately, due to the

time involved in accurately processing the results, the average cardiologist's lack of in-depth knowledge about VH and the limited impact that the findings from this are likely to have over and above grey-scale IVUS, I feel that it is not ready to be applied to all ACS PCI.

Although throughout this work we have proved some interesting VH hypotheses and shown within the data that certain aspects of VH may help understand the plaque anatomy in more detail, this remains limited to the confines of plaque research. Overall, grey-scale IVUS can probably provide everything that is required to impact on improving the mechanistic aspects of PCI. There are also more sensitive tools becoming used more frequently such as OCT which can provide more detail of the stent after deployment. On the horizon are newer techniques such as IVUS-HD, IVUS-NIRS, OCT-NIRS, OCT-NIRF and CT based plaque characterization that will probably take things further. This may even extend into the non-invasive realm, to allow plaque prevention to occur with medical therapy before the heart "attacks".

As a final point on the benefit of IVUS-guided PCI, several recent studies (including a large updated meta-analysis in over 20,000 patients) appear to suggest that there is a mortality advantage for the use of IVUS guided PCI (in the drug eluting stent era). This has not yet been tested in an adequately powered, prospective randomized controlled trial in an all-comers population. Without this important data IVUS may sadly continue to be confined to the "specialist adjunct techniques" available in PCI.

It is currently used in <10% of procedures in the UK and worldwide. This may unfortunately be to the detriment of some long term stent results and patient outcomes for the immediate future.

Dr Scott W Murray

March 2016

BILBLIOGRAPHY

(1) Abdel-Wahab M, Khattab AA, Liska B, Toelg R, El-Hammady W, Farag N, et al. Relationship between cardiovascular risk as predicted by established risk scores and coronary artery plaque composition as detected by virtual histology intravascular ultrasound analysis: the PREDICT pilot study. EuroIntervention 2008 Jan;3(4):482-9.

(2) Abdel-Wahab M, Khattab AA, Toelg R, Geist V, Liska B, Richardt G. Plaque characteristics of nonobstructive coronary lesions in diabetic patients: an intravascular ultrasound virtual histology analysis. J Cardiovasc Med (Hagerstown) 2010 May;11(5):345-51.

(3) Aboufakher R, Torey J, Szpunar S, Davis T. Peripheral plaque volume changes pre- and post-rotational atherectomy followed by directional plaque excision: assessment by intravascular ultrasound and virtual histology. J Invasive Cardiol 2009 Oct;21(10):501-5.

(4) Adlam D, Joseph S, Robinson C, Rousseau C, Barber J, Biggs M, et al. Coronary optical coherence tomography: minimally invasive virtual

histology as part of targeted post-mortem computed tomography angiography. Int J Legal Med 2013 Sep;127(5):991-6.

(5) Alfonso F, Hernando L, Dutary J. Virtual histology assessment of atheroma at coronary bifurcations: colours at the crossroads? EuroIntervention 2010 Aug;6(3):295-301.

(6) Amano H, Wagatsuma K, Yamazaki J, Ikeda T. Virtual histology intravascular ultrasound analysis of attenuated plaque and ulcerated plaque detected by gray scale intravascular ultrasound and the relation between the plaque composition and slow flow/no reflow phenomenon during percutaneous coronary intervention. J Interv Cardiol 2013 Jun;26(3):295-301.

(7) Ambrosi CM, Moazami N, Rollins AM, Efimov IR. Virtual histology of the human heart using optical coherence tomography. J Biomed Opt 2009 Sep;14(5):054002.

(8) Appleby CE, Bui S, Dzavik V. A calcified neointima--"stent" within a stent. J Invasive Cardiol 2009 Mar;21(3):141-3.

(9) Atary JZ, Bergheanu SC, van der Hoeven BL, Atsma DE, Bootsma M, van der Kley F, et al. Impact of sirolimus-eluting stent implantation

compared to bare-metal stent implantation for acute myocardial infarction on coronary plaque composition at nine months follow-up: a Virtual Histology intravascular ultrasound analysis. Results from the Leiden MISSION! intervention study. EuroIntervention 2009 Nov;5(5):565-72.

(10) Athanasiou LS, Karvelis PS, Tsakanikas VD, Naka KK, Michalis LK, Bourantas CV, et al. A novel semiautomated atherosclerotic plaque characterization method using grayscale intravascular ultrasound images: comparison with virtual histology. IEEE Trans Inf Technol Biomed 2012 May;16(3):391-400.

(11) Baars T, Kleinbongard P, Bose D, Konorza T, Mohlenkamp S, Hippler J, et al. Saphenous vein aorto-coronary graft atherosclerosis in patients with chronic kidney disease: more plaque calcification and necrosis, but less vasoconstrictor potential. Basic Res Cardiol 2012;107(6):303.

(12) Bae JH, Kwon TG, Hyun DW, Rihal CS, Lerman A. Predictors of slow flow during primary percutaneous coronary intervention: an intravascular ultrasound-virtual histology study. Heart 2008 Dec;94(12):1559-64.

(13) Bose D, von BC, Zhou XY, Schmermund A, Philipp S, Sack S, et al. Impact of atherosclerotic plaque composition on coronary microembolization during percutaneous coronary interventions. Basic Res Cardiol 2008 Nov;103(6):587-97.

(14) Bourantas CV, Garcia-Garcia HM, Farooq V, Maehara A, Xu K, Genereux P, et al. Clinical and Angiographic Characteristics of Patients Likely to Have Vulnerable Plaques: Analysis From the PROSPECT Study. JACC Cardiovasc Imaging 2013 Oct 17.

(15) Brodoefel H, Reimann A, Heuschmid M, Tsiflikas I, Kopp AF, Schroeder S, et al. Characterization of coronary atherosclerosis by dual-source computed tomography and HU-based color mapping: a pilot study. Eur Radiol 2008 Nov;18(11):2466-74.

(16) Brodoefel H, Burgstahler C, Heuschmid M, Reimann A, Khosa F, Kopp A, et al. Accuracy of dual-source CT in the characterisation of non-calcified plaque: use of a colour-coded analysis compared with virtual histology intravascular ultrasound. Br J Radiol 2009 Oct;82(982):805-12.

(17) Brown AJ, McCormick LM, Hoole SP, West NE. Coregistered intravascular ultrasound and optical coherence tomography imaging

during implantation of a bioresorbable vascular scaffold. JACC Cardiovasc Interv 2013 Jul;6(7):e41-e42.

(18) Brugaletta S, Garcia-Garcia HM, Serruys PW, de BS, Ligthart J, Gomez-Lara J, et al. NIRS and IVUS for characterization of atherosclerosis in patients undergoing coronary angiography. JACC Cardiovasc Imaging 2011 Jun;4(6):647-55.

(19) Brugaletta S, Garcia-Garcia HM, Diletti R, Gomez-Lara J, Garg S, Onuma Y, et al. Comparison between the first and second generation bioresorbable vascular scaffolds: a six month virtual histology study. EuroIntervention 2011 Apr;6(9):1110-6.

(20) Brugaletta S, Garcia-Garcia HM, Garg S, Gomez-Lara J, Diletti R, Onuma Y, et al. Temporal changes of coronary artery plaque located behind the struts of the everolimus eluting bioresorbable vascular scaffold. Int J Cardiovasc Imaging 2011 Jul;27(6):859-66.

(21) Brugaletta S, Garcia-Garcia HM, Serruys PW, Maehara A, Farooq V, Mintz GS, et al. Relationship between palpography and virtual histology in patients with acute coronary syndromes. JACC Cardiovasc Imaging 2012 Mar;5(3 Suppl):S19-S27.

(22) Brugaletta S, Heo JH, Garcia-Garcia HM, Farooq V, van Geuns RJ, de BB, et al. Endothelial-dependent vasomotion in a coronary segment treated by ABSORB everolimus-eluting bioresorbable vascular scaffold system is related to plaque composition at the time of bioresorption of the polymer: indirect finding of vascular reparative therapy? Eur Heart J 2012 Jun;33(11):1325-33.

(23) Brugaletta S, Garcia-Garcia HM, Shen ZJ, Gomez-Lara J, Diletti R, Sarno G, et al. Morphology of coronary artery lesions assessed by virtual histology intravascular ultrasound tissue characterization and fractional flow reserve. Int J Cardiovasc Imaging 2012 Feb;28(2):221-8.

(24) Brugaletta S, Gomez-Lara J, Garcia-Garcia HM, Heo JH, Farooq V, van Geuns RJ, et al. Analysis of 1 year virtual histology changes in coronary plaque located behind the struts of the everolimus eluting bioresorbable vascular scaffold. Int J Cardiovasc Imaging 2012 Aug;28(6):1307-14.

(25) Calvert PA, Liew TV, Gorenne I, Clarke M, Costopoulos C, Obaid DR, et al. Leukocyte telomere length is associated with high-risk plaques on virtual histology intravascular ultrasound and increased proinflammatory activity. Arterioscler Thromb Vasc Biol 2011 Sep;31(9):2157-64.

(26) Calvert PA, Obaid DR, O'Sullivan M, Shapiro LM, McNab D, Densem CG, et al. Association between IVUS findings and adverse outcomes in patients with coronary artery disease: the VIVA (VH-IVUS in Vulnerable Atherosclerosis) Study. JACC Cardiovasc Imaging 2011 Aug;4(8):894-901.

(27) Cascon-Perez JD, Consuegra L, Pico-Aracil F. Virtual histology of an acute thrombotic occlusive lesion. Rev Esp Cardiol 2009 Jun;62(6):705-6.

(28) Cascon-Perez JD, de la Torre-Hernandez JM, Ruiz-Abellon MC, Martinez-Pascual M, Marmol-Lozano R, Lopez-Candel J, et al. Characteristics of culprit atheromatous plaques obtained in vivo by intravascular ultrasound radiofrequency analysis: results from the CULPLAC study. Am Heart J 2013 Mar;165(3):400-7.

(29) Casella G, Prati F, Klauss V, Coutsoumbas G, Di PG. [Imaging of atherosclerosis]. G Ital Cardiol (Rome) 2009 Dec;10(11-12 Suppl 3):4S-12S.

(30) Cheng JM, Garcia-Garcia HM, de Boer SP, Kardys I, Heo JH, Akkerhuis KM, et al. In vivo detection of high-risk coronary plaques by

radiofrequency intravascular ultrasound and cardiovascular outcome: results of the ATHEROREMO-IVUS study. Eur Heart J 2013 Nov 19.

(31) Chiocchi M, Morosetti D, Chiaravalloti A, Loreni G, Gandini R, Simonetti G. Intravascular ultrasound assisted carotid artery stenting: randomized controlled trial. Preliminary results on 60 patients. J Cardiovasc Med (Hagerstown) 2013 Jan 3.

(32) Choi BJ, Kang DK, Tahk SJ, Choi SY, Yoon MH, Lim HS, et al. Comparison of 64-slice multidetector computed tomography with spectral analysis of intravascular ultrasound backscatter signals for characterizations of noncalcified coronary arterial plaques. Am J Cardiol 2008 Oct 15;102(8):988-93.

(33) Choi SH, Chae A, Chen CH, Merki E, Shaw PX, Tsimikas S. Emerging approaches for imaging vulnerable plaques in patients. Curr Opin Biotechnol 2007 Feb;18(1):73-82.

(34) Choi YH, Hong YJ, Park IH, Jeong MH, Ahmed K, Hwang SH, et al. Relationship between coronary artery calcium score by multidetector computed tomography and plaque components by virtual histology intravascular ultrasound. J Korean Med Sci 2011 Aug;26(8):1052-60.

(35) Claessen BE, Maehara A, Fahy M, Xu K, Stone GW, Mintz GS. Plaque composition by intravascular ultrasound and distal embolization after percutaneous coronary intervention. JACC Cardiovasc Imaging 2012 Mar;5(3 Suppl):S111-S118.

(36) Clementi F, Di LM, Mango R, Luciani G, Trivisonno A, Pizzuto F, et al. Regression and shift in composition of coronary atherosclerotic plaques by pioglitazone: insight from an intravascular ultrasound analysis. J Cardiovasc Med (Hagerstown) 2009 Mar;10(3):231-7.

(37) de Boer SP, Cheng JM, Garcia-Garcia HM, Oemrawsingh RM, van Geuns RJ, Regar E, et al. Relation of genetic profile and novel circulating biomarkers with coronary plaque phenotype as determined by intravascular ultrasound: rationale and design of the ATHEROREMO-IVUS study. EuroIntervention 2013 Aug 26.

(38) de Graaf MA, Broersen A, Kitslaar PH, Roos CJ, Dijkstra J, Lelieveldt BP, et al. Automatic quantification and characterization of coronary atherosclerosis with computed tomography coronary angiography: cross-correlation with intravascular ultrasound virtual histology. Int J Cardiovasc Imaging 2013 Jun;29(5):1177-90.

(39) de Graaf MA, van Velzen JE, de Graaf FR, Schuijf JD, Dijkstra J, Bax JJ, et al. The maximum necrotic core area is most often located proximally to the site of most severe narrowing: a virtual histology intravascular ultrasound study. Heart Vessels 2013 Mar;28(2):166-72.

(40) de la Torre-Hernandez JM, Sainz-Laso F, Colman T. [Virtual histology of a post-angioplasty intramural hematoma]. Rev Esp Cardiol 2006 Mar;59(3):275.

(41) Deftereos S, Giannopoulos G, Kossyvakis C, Pyrgakis VN. Virtual histology. Hellenic J Cardiol 2010 May;51(3):235-44.

(42) Deftereos S, Giannopoulos G, Kossyvakis C, Kaoukis A, Raisakis K, Panagopoulou V, et al. Association of soluble tumour necrosis factor-related apoptosis-inducing ligand levels with coronary plaque burden and composition. Heart 2012 Feb;98(3):214-8.

(43) Deliargyris EN. Intravascular ultrasound virtual histology derived thin cap fibroatheroma now you see it, now you don't.. J Am Coll Cardiol 2010 Apr 13;55(15):1598-9.

(44) Dhawan SS, Corban MT, Nanjundappa RA, Eshtehardi P, McDaniel MC, Kwarteng CA, et al. Coronary microvascular dysfunction is

associated with higher frequency of thin-cap fibroatheroma. Atherosclerosis 2012 Aug;223(2):384-8.

(45) Diethrich EB, Irshad K, Reid DB. Virtual histology and color flow intravascular ultrasound in peripheral interventions. Semin Vasc Surg 2006 Sep;19(3):155-62.

(46) Diletti R, Garcia-Garcia HM, Gomez-Lara J, Brugaletta S, Wykrzykowska JJ, van DN, et al. Assessment of coronary atherosclerosis progression and regression at bifurcations using combined IVUS and OCT. JACC Cardiovasc Imaging 2011 Jul;4(7):774-80.

(47) Diletti R, Serruys PW, Farooq V, Sudhir K, Dorange C, Miquel-Hebert K, et al. ABSORB II randomized controlled trial: a clinical evaluation to compare the safety, efficacy, and performance of the Absorb everolimus-eluting bioresorbable vascular scaffold system against the XIENCE everolimus-eluting coronary stent system in the treatment of subjects with ischemic heart disease caused by de novo native coronary artery lesions: rationale and study design. Am Heart J 2012 Nov;164(5):654-63.

(48) Dohi T, Mintz GS, McPherson JA, de BB, Farhat NZ, Lansky AJ, et al. Non-fibroatheroma lesion phenotype and long-term clinical outcomes: a substudy analysis from the PROSPECT study. JACC Cardiovasc Imaging 2013 Aug;6(8):908-16.

(49) Dolla WJ, House JA, Marso SP. Stratification of risk in thin cap fibroatheromas using peak plaque stress estimates from idealized finite element models. Med Eng Phys 2012 Nov;34(9):1330-8.

(50) Dunphy MP, Strauss HW. Molecular imaging of atherosclerosis. Curr Cardiol Rep 2008 Mar;10(2):121-7.

(51) Egede R, Jensen LO, Hansen HS, Hansen KN, Junker A, Thayssen P. Influence of high-dose lipid lowering treatment compared to low-dose lipid lowering treatment on plaque composition assessed by intravascular ultrasound virtual histology in patients with ST-segment elevation acute myocardial infarction: the VIRHISTAMI trial. EuroIntervention 2013 Feb 22;8(10):1182-9.

(52) Epstein SE, Waksman R, Pichard AD, Kent KM, Panza JA. Percutaneous coronary intervention versus medical therapy in stable coronary artery disease: the unresolved conundrum. JACC Cardiovasc Interv 2013 Oct;6(10):993-8.

(53) Eshtehardi P, McDaniel MC, Suo J, Dhawan SS, Timmins LH, Binongo JN, et al. Association of coronary wall shear stress with atherosclerotic plaque burden, composition, and distribution in patients with coronary artery disease. J Am Heart Assoc 2012 Aug;1(4):e002543.

(54) Frutkin AD, Mehta SK, McCrary JR, Marso SP. Limitations to the use of virtual histology-intravascular ultrasound to detect vulnerable plaque. Eur Heart J 2007 Jul;28(14):1783-4.

(55) Fuchs FS, Zirlik S, Hildner K, Schubert J, Vieth M, Neurath MF. Confocal laser endomicroscopy for diagnosing lung cancer in vivo. Eur Respir J 2013 Jun;41(6):1401-8.

(56) Fuchs M, Heider P, Pelisek J, Poppert H, Eckstein HH. Ex vivo characterization of carotid plaques by intravascular ultrasonography and virtual histology: concordance with real plaque pathomorphology. J Cardiovasc Surg (Torino) 2013 Dec 10.

(57) Fuchs S, Lavi I, Tzang O, Fuchs S, Brosh D, Bental T, et al. Necrotic core and thin cap fibrous atheroma distribution in native coronary artery lesion-containing segments: a virtual histology intravascular ultrasound study. Coron Artery Dis 2011 Aug;22(5):339-44.

(58) Fuchs S, Lavi I, Tzang O, Bessler H, Brosh D, Bental T, et al. Intracoronary monocyte chemoattractant protein 1 and vascular endothelial growth factor levels are associated with necrotic core, calcium and fibrous tissue atherosclerotic plaque components: an intracoronary ultrasound radiofrequency study. Cardiology 2012;123(2):125-32.

(59) Fujii K, Carlier SG, Mintz GS, Wijns W, Colombo A, Bose D, et al. Association of plaque characterization by intravascular ultrasound virtual histology and arterial remodeling. Am J Cardiol 2005 Dec 1;96(11):1476-83.

(60) Funada R, Oikawa Y, Yajima J, Kirigaya H, Nagashima K, Ogasawara K, et al. The potential of RF backscattered IVUS data and multidetector-row computed tomography images for tissue characterization of human coronary atherosclerotic plaques. Int J Cardiovasc Imaging 2009 Jun;25(5):471-8.

(61) Garcia-Garcia HM, Goedhart D, Schuurbiers JC, Kukreja N, Tanimoto S, Daemen J, et al. Virtual histology and remodelling index allow in vivo identification of allegedly high-risk coronary plaques in patients with

acute coronary syndromes: a three vessel intravascular ultrasound radiofrequency data analysis. EuroIntervention 2006 Nov;2(3):338-44.

(62) Garcia-Garcia HM, Gonzalo N, Granada JF, Regar E, Serruys PW. Diagnosis and treatment of coronary vulnerable plaques. Expert Rev Cardiovasc Ther 2008 Feb;6(2):209-22.

(63) Garcia-Garcia HM, Gonzalo N, Regar E, Serruys PW. Virtual histology and optical coherence tomography: from research to a broad clinical application. Heart 2009 Aug;95(16):1362-74.

(64) Garcia-Garcia HM, Mintz GS, Lerman A, Vince DG, Margolis MP, van Es GA, et al. Tissue characterisation using intravascular radiofrequency data analysis: recommendations for acquisition, analysis, interpretation and reporting. EuroIntervention 2009 Jun;5(2):177-89.

(65) Garcia-Garcia HM, Shen Z, Piazza N. Study of restenosis in drug eluting stents: new insights from greyscale intravascular ultrasound and virtual histology. EuroIntervention 2009 May;5 Suppl D:D84-D92.

(66) Garcia-Garcia HM, Gogas BD, Serruys PW, Bruining N. IVUS-based imaging modalities for tissue characterization: similarities and differences. Int J Cardiovasc Imaging 2011 Feb;27(2):215-24.

(67) Gaxiola E. [Detection and treatment of vulnerable plaque]. Arch Cardiol Mex 2007 Oct;77 Suppl 4:S4-84.

(68) Gogas BD, Serruys PW, Diletti R, Farooq V, Brugaletta S, Radu MD, et al. Vascular response of the segments adjacent to the proximal and distal edges of the ABSORB everolimus-eluting bioresorbable vascular scaffold: 6-month and 1-year follow-up assessment: a virtual histology intravascular ultrasound study from the first-in-man ABSORB cohort B trial. JACC Cardiovasc Interv 2012 Jun;5(6):656-65.

(69) Gogas BD, Garcia-Garcia HM, Onuma Y, Muramatsu T, Farooq V, Bourantas CV, et al. Edge vascular response after percutaneous coronary intervention: an intracoronary ultrasound and optical coherence tomography appraisal: from radioactive platforms to first- and second-generation drug-eluting stents and bioresorbable scaffolds. JACC Cardiovasc Interv 2013 Mar;6(3):211-21.

(70) Gonzalez A, Lopez-Rueda A, Gutierrez I, Moniche F, Cayuela A, Bustamante A, et al. Carotid plaque characterization by virtual histology intravascular ultrasound related to the timing of carotid intervention. J Endovasc Ther 2012 Dec;19(6):764-73.

(71) Gonzalo N, Garcia-Garcia HM, Regar E, Barlis P, Wentzel J, Onuma Y, et al. In vivo assessment of high-risk coronary plaques at bifurcations with combined intravascular ultrasound and optical coherence tomography. JACC Cardiovasc Imaging 2009 Apr;2(4):473-82.

(72) Granada JF, Wallace-Bradley D, Win HK, Alviar CL, Builes A, Lev EI, et al. In vivo plaque characterization using intravascular ultrasound-virtual histology in a porcine model of complex coronary lesions. Arterioscler Thromb Vasc Biol 2007 Feb;27(2):387-93.

(73) Guo J, Maehara A, Mintz GS, Ashida K, Pu J, Shang Y, et al. A virtual histology intravascular ultrasound analysis of coronary chronic total occlusions. Catheter Cardiovasc Interv 2013 Feb;81(3):464-70.

(74) Guo J, Maehara A, Guo N, Ashida K, Chirumamilla A, Shang Y, et al. Virtual histology intravascular ultrasound comparison of coronary chronic total occlusions versus non-occlusive lesions. Int J Cardiovasc Imaging 2013 Aug;29(6):1249-54.

(75) Guo S, Wang R, Yang Z, Li K, Wang Q. Effects of atorvastatin on serum lipids, serum inflammation and plaque morphology in patients with stable atherosclerotic plaques. Exp Ther Med 2012 Dec;4(6):1069-74.

(76) Han SH, Puma J, Garcia-Garcia HM, Nasu K, Margolis P, Leon MB, et al. Tissue characterisation of atherosclerotic plaque in coronary artery bifurcations: an intravascular ultrasound radiofrequency data analysis in humans. EuroIntervention 2010 Aug;6(3):313-20.

(77) Haraki T, Hirase H, Ohta M, Uno Y, Sakata K, Kawashiri MA, et al. A patient with significant slow-flow phenomenon during percutaneous coronary intervention for ST elevation myocardial infarction associated with scattered necrotic core by virtual histology intravascular ultrasound. Cardiovasc Interv Ther 2011 Sep;26(3):290-5.

(78) Hernando L, Corros C, Gonzalo N, Hernandez-Antolin R, Banuelos C, Jimenez-Quevedo P, et al. Morphological characteristics of culprit coronary lesions according to clinical presentation: insights from a multimodality imaging approach. Int J Cardiovasc Imaging 2013 Jan;29(1):13-21.

(79) Hikita H, Kuroda S, Oosaka Y, Kawaguchi N, Nakashima E, Sugiyama T, et al. Impact of statin use before the onset of acute myocardial infarction on coronary plaque morphology of the culprit lesion. Angiology 2013 Jul;64(5):375-8.

(80) Hishikawa T, Iihara K, Ishibashi-Ueda H, Nagatsuka K, Yamada N, Miyamoto S. Virtual histology-intravascular ultrasound in assessment of carotid plaques: ex vivo study. Neurosurgery 2009 Jul;65(1):146-52.

(81) Ho HH, Wong CP, Hau WK, Loh KK, Ong PJ. Intravascular ultrasound virtual histology imaging in acute ST-elevation myocardial infarction: A useful clinical tool during primary percutaneous coronary intervention. Acute Card Care 2011 Dec;13(4):245-7.

(82) Ho HH, Foo D, Ong PJ. Intravascular ultrasound-virtual histology imaging in acute myocardial infarction. Postgrad Med J 2011 May;87(1027):384-5.

(83) Hong MK, Mintz GS, Lee CW, Suh J, Kim JH, Park DW, et al. Comparison of virtual histology to intravascular ultrasound of culprit coronary lesions in acute coronary syndrome and target coronary lesions in stable angina pectoris. Am J Cardiol 2007 Sep 15;100(6):953-9.

(84) Hong MK, Mintz GS, Lee CW, Lee JW, Park JH, Park DW, et al. A three-vessel virtual histology intravascular ultrasound analysis of frequency and distribution of thin-cap fibroatheromas in patients with

acute coronary syndrome or stable angina pectoris. Am J Cardiol 2008 Mar 1;101(5):568-72.

(85) Hong MK, Park DW, Lee CW, Lee SW, Kim YH, Kang DH, et al. Effects of statin treatments on coronary plaques assessed by volumetric virtual histology intravascular ultrasound analysis. JACC Cardiovasc Interv 2009 Jul;2(7):679-88.

(86) Hong YJ, Mintz GS, Kim SW, Lee SY, Okabe T, Pichard AD, et al. Impact of plaque composition on cardiac troponin elevation after percutaneous coronary intervention: an ultrasound analysis. JACC Cardiovasc Imaging 2009 Apr;2(4):458-68.

(87) Hong YJ, Jeong MH, Choi YH, Ko JS, Lee MG, Kang WY, et al. Plaque characteristics in culprit lesions and inflammatory status in diabetic acute coronary syndrome patients. JACC Cardiovasc Imaging 2009 Mar;2(3):339-49.

(88) Hong YJ, Ahn Y, Sim DS, Yoon NS, Yoon HJ, Kim KH, et al. Relation between N-terminal pro-B-type natriuretic peptide and coronary plaque components in patients with acute coronary syndrome: virtual histology-intravascular ultrasound analysis. Coron Artery Dis 2009 Dec;20(8):518-24.

(89) Hong YJ, Jeong MH, Choi YH, Ma EH, Ko JS, Lee MG, et al. Age-related differences in virtual histology-intravascular ultrasound findings in patients with coronary artery disease. J Cardiol 2010 Mar;55(2):224-31.

(90) Hong YJ, Jeong MH, Kim SW, Choi YH, Ma EH, Ko JS, et al. Relation between plaque components and plaque prolapse after drug-eluting stent implantation--virtual histology-intravascular ultrasound. Circ J 2010 Jun;74(6):1142-51.

(91) Hong YJ, Jeong MH, Choi YH, Ma EH, Ko JS, Lee MG, et al. Plaque components at coronary sites with focal spasm in patients with variant angina: virtual histology-intravascular ultrasound analysis. Int J Cardiol 2010 Oct 29;144(3):367-72.

(92) Hong YJ, Jeong MH, Choi YH, Ma EH, Cho SH, Ko JS, et al. Gender differences in coronary plaque components in patients with acute coronary syndrome: virtual histology-intravascular ultrasound analysis. J Cardiol 2010 Sep;56(2):211-9.

(93) Hong YJ, Jeong MH, Choi YH, Ma EH, Ko JS, Lee MG, et al. Impact of baseline plaque components on plaque progression in nonintervened

coronary segments in patients with angina pectoris on rosuvastatin 10 mg/day. Am J Cardiol 2010 Nov 1;106(9):1241-7.

(94) Hong YJ, Jeong MH, Choi YH, Cho SH, Hwang SH, Ko JS, et al. Relation between high-sensitivity C-reactive protein and coronary plaque components in patients with acute coronary syndrome: virtual histology-intravascular ultrasound analysis. Korean Circ J 2011 Aug;41(8):440-6.

(95) Hong YJ, Jeong MH, Choi YH, Song JA, Ahmed K, Kim DH, et al. Relationship between microalbuminuria and vulnerable plaque components in patients with acute coronary syndrome and with diabetes mellitus. Virtual histology-intravascular ultrasound. Circ J 2011;75(12):2893-901.

(96) Hong YJ, Jeong MH, Choi YH, Hwang SH, Ko JS, Lee MG, et al. Coronary plaque components assessed by virtual histology-intravascular ultrasound are not associated with neointimal hyperplasia in patients who underwent drug-eluting stent implantation. Int J Cardiol 2011 Jan 21;146(2):275-6.

(97) Hong YJ, Jeong MH, Choi YH, Ko JS, Lee MG, Kang WY, et al. Impact of plaque components on no-reflow phenomenon after stent

deployment in patients with acute coronary syndrome: a virtual histology-intravascular ultrasound analysis. Eur Heart J 2011 Aug;32(16):2059-66.

(98) Hong YJ, Jeong MH, Ahn Y, Kim SW, Bae JH, Hur SH, et al. Effect of pitavastatin treatment on changes of plaque volume and composition according to the reduction of high-sensitivity C-reactive protein levels. J Cardiol 2012 Oct;60(4):277-82.

(99) Hong YJ, Jeong MH, Choi YH, Song JA, Kim DH, Lee KH, et al. Relation between anemia and vulnerable coronary plaque components in patients with acute coronary syndrome: virtual histology-intravascular ultrasound analysis. J Korean Med Sci 2012 Apr;27(4):370-6.

(100) Hong YJ, Jeong MH, Choi YH, Song JA, Jang SY, Yoo JH, et al. Relation between poststenting peristent plaque components and late stent malapposition after drug-eluting stent implantation: virtual histology-intravascular ultrasound analysis. Int J Cardiol 2013 Sep 1;167(5):1882-7.

(101) Hong YJ, Jeong MH, Choi YH, Park SY, Rhew SH, Jeong HC, et al. Comparison of Coronary Plaque Components between Non-Culprit Lesions in Patients with Acute Coronary Syndrome and Target Lesions

in Patients with Stable Angina: Virtual Histology-Intravascular Ultrasound Analysis. Korean Circ J 2013 Sep;43(9):607-14.

(102) Hong YJ, Jeong MH, Choi YH, Song JA, Ahmed K, Lee KH, et al. Positive remodeling is associated with vulnerable coronary plaque components regardless of clinical presentation: virtual histology-intravascular ultrasound analysis. Int J Cardiol 2013 Aug 10;167(3):871-6.

(103) Huisman J, Egede R, Rdzanek A, Bose D, Erbel R, Kochman J, et al. Between-centre reproducibility of volumetric intravascular ultrasound radiofrequency-based analyses in mild-to-moderate coronary atherosclerosis: an international multicentre study. EuroIntervention 2010 Apr;5(8):925-31.

(104) Huisman J, Egede R, Rdzanek A, Bose D, Erbel R, Kochman J, et al. Multicenter assessment of the reproducibility of volumetric radiofrequency-based intravascular ultrasound measurements in coronary lesions that were consecutively stented. Int J Cardiovasc Imaging 2012 Dec;28(8):1867-78.

(105) Hwang DS, Shin ES, Kim SJ, Lee JH, Kim JM, Lee SG. Early differential changes in coronary plaque composition according to plaque

stability following statin initiation in acute coronary syndrome: classification and analysis by intravascular ultrasound-virtual histology. Yonsei Med J 2013 Mar 1;54(2):336-44.

(106) Inoue F, Yamaguchi S, Ueshima K, Fujimoto T, Kagoshima T, Uemura S, et al. Gender differences in coronary plaque characteristics in patients with stable angina: a virtual histology intravascular ultrasound study. Cardiovasc Interv Ther 2010 Jan;25(1):40-5.

(107) Inoue F, Ueshima K, Fujimoto T, An K, Uemura S, Saito Y. Coronary plaque characteristics that indicate distal embolization during percutaneous coronary intervention in patients with stable angina-virtual histology intravascular ultrasound study. Cardiovasc Interv Ther 2013 Jul;28(3):227-34.

(108) Ivanovic M, Rancic M, Rdzanek A, Filipjak KJ, Opolski G, Cvetanovic J. Virtual histology study of atherosclerotic plaque composition in patients with stable angina and acute phase of acute coronary syndromes without ST segment elevation. Srp Arh Celok Lek 2013 May;141(5-6):308-14.

(109) Izumiya Y, Kojima S, Kojima S, Araki S, Usuku H, Matsubara J, et al. Long-term use of oral nicorandil stabilizes coronary plaque in patients with stable angina pectoris. Atherosclerosis 2011 Feb;214(2):415-21.

(110) Jang JS, Jin HY, Seo JS, Yang TH, Kim DK, Park YA, et al. Meta-analysis of plaque composition by intravascular ultrasound and its relation to distal embolization after percutaneous coronary intervention. Am J Cardiol 2013 Apr 1;111(7):968-72.

(111) Jim MH, Hau WK, Ko RL, Siu CW, Ho HH, Yiu KH, et al. Virtual histology by intravascular ultrasound study on degenerative aortocoronary saphenous vein grafts. Heart Vessels 2010 May;25(3):175-81.

(112) Joan MM, Moya BG, Agusti FP, Vidal RG, Arjona YA, Alija MP, et al. Utility of intravascular ultrasound examination during carotid stenting. Ann Vasc Surg 2009 Sep;23(5):606-11.

(113) Kaneda H. Re: coronary plaque composition of culprit/target lesions according to the clinical presentation: a virtual histology intravascular ultrasound analysis. Eur Heart J 2007 Jul;28(14):1784.

(114) Kang SJ, Mintz GS, Park DW, Lee SW, Kim YH, Lee CW, et al. Tissue characterization of in-stent neointima using intravascular ultrasound radiofrequency data analysis. Am J Cardiol 2010 Dec 1;106(11):1561-5.

(115) Kaple RK, Maehara A, Mintz GS. Characteristics of high-risk atherosclerotic plaque using intravascular ultrasound-derived virtual histology. Expert Opin Med Diagn 2008 May;2(5):565-76.

(116) Kaple RK, Maehara A, Sano K, Missel E, Castellanos C, Tsujita K, et al. The axial distribution of lesion-site atherosclerotic plaque components: an in vivo volumetric intravascular ultrasound radio-frequency analysis of lumen stenosis, necrotic core and vessel remodeling. Ultrasound Med Biol 2009 Apr;35(4):550-7.

(117) Kashiwagi M, Tanaka A, Kitabata H, Ozaki Y, Komukai K, Tanimoto T, et al. Comparison of diagnostic accuracy between multidetector computed tomography and virtual histology intravascular ultrasound for detecting optical coherence tomography-derived fibroatheroma. Cardiovasc Interv Ther 2013 Oct 23.

(118) Kashyap VS, Lakin RO, Feiten LE, Bishop PD, Sarac TP. In vivo assessment of endothelial function in human lower extremity arteries. J Vasc Surg 2013 Nov;58(5):1259-66.

(119) Kato K, Yasutake M, Yonetsu T, Kim SJ, Xing L, Kratlian CM, et al. Intracoronary imaging modalities for vulnerable plaques. J Nippon Med Sch 2011;78(6):340-51.

(120) Kawaguchi R, Oshima S, Jingu M, Tsurugaya H, Toyama T, Hoshizaki H, et al. Usefulness of virtual histology intravascular ultrasound to predict distal embolization for ST-segment elevation myocardial infarction. J Am Coll Cardiol 2007 Oct 23;50(17):1641-6.

(121) Kawamoto T, Okura H, Koyama Y, Toda I, Taguchi H, Tamita K, et al. The relationship between coronary plaque characteristics and small embolic particles during coronary stent implantation. J Am Coll Cardiol 2007 Oct 23;50(17):1635-40.

(122) Kawano T, Honye J, Takayama T, Yokoyama S, Chiku M, Ando H, et al. Compositional analysis of angioscopic yellow plaques with intravascular ultrasound radiofrequency data. Int J Cardiol 2008 Mar 28;125(1):74-8.

(123) Kiesslich R, Goetz M, Neurath MF. Virtual histology. Best Pract Res Clin Gastroenterol 2008;22(5):883-97.

(124) Kim JH, Jeong MH, Hong YJ, Lee KH, Kim IS, Choi YH, et al. Low density lipoprotein-cholesterol/high density lipoprotein-cholesterol ratio predicts plaque vulnerability in patients with stable angina. Korean Circ J 2012 Apr;42(4):246-51.

(125) Kim KH, Kim WH, Park HW, Song IG, Yang DJ, Seo YH, et al. Impact of plaque composition on long-term clinical outcomes in patients with coronary artery occlusive disease. Korean Circ J 2013 Jun;43(6):377-83.

(126) Kim SW, Mintz GS, Hong YJ, Pakala R, Park KS, Pichard AD, et al. The virtual histology intravascular ultrasound appearance of newly placed drug-eluting stents. Am J Cardiol 2008 Nov 1;102(9):1182-6.

(127) Kim SW, Hong YJ, Mintz GS, Lee SY, Doh JH, Lim SH, et al. Relation of ruptured plaque culprit lesion phenotype and outcomes in patients with ST elevation acute myocardial infarction. Am J Cardiol 2012 Mar 15;109(6):794-9.

(128) Kim WH, Park HW, Kim KH, Song IG, Yang DJ, Lee CS, et al. Fibro-Fatty Component is Important for the Long-Term Clinical Events in Patients Who Have Undergone Primary Percutaneous Coronary Intervention. Korean Circ J 2012 Jan;42(1):33-9.

(129) Kimura S, Inagaki H, Haraguchi G, Sugiyama T, Miyazaki T, Hatano Y, et al. Relationships of Elevated Systemic Pentraxin-3 Levels With High-Risk Coronary Plaque Components and Impaired Myocardial Perfusion After Percutaneous Coronary Intervention in Patients With ST-Elevation Acute Myocardial Infarction. Circ J 2013 Oct 16.

(130) Ko YG, Le VC, Kim BH, Shin DH, Kim JS, Kim BK, et al. Correlations between coronary plaque tissue composition assessed by virtual histology and blood levels of biomarkers for coronary artery disease. Yonsei Med J 2012 May;53(3):508-16.

(131) Kojima S, Kojima S, Maruyoshi H, Nagayoshi Y, Kaikita K, Sumida H, et al. Hypercholesterolemia and hypoadiponectinemia are associated with necrotic core-rich coronary plaque. Int J Cardiol 2011 Mar 17;147(3):371-6.

(132) Konig A, Klauss V. Virtual histology. Heart 2007 Aug;93(8):977-82.

(133) Konig A, Kilian E, Rieber J, Schiele TM, Leibig M, Sohn HY, et al. Assessment of early atherosclerosis in de novo heart transplant recipients: analysis with intravascular ultrasound-derived radiofrequency analysis. J Heart Lung Transplant 2008 Jan;27(1):26-30.

(134) Kono K, Fujii H, Miyoshi N, Kawamori H, Shite J, Hirata K, et al. Coronary plaque morphology using virtual histology-intravascular ultrasound analysis in hemodialysis patients. Ther Apher Dial 2011 Feb;15(1):44-50.

(135) Kono K, Fujii H, Nakai K, Goto S, Shite J, Hirata K, et al. Composition and plaque patterns of coronary culprit lesions and clinical characteristics of patients with chronic kidney disease. Kidney Int 2012 Aug;82(3):344-51.

(136) Kovarnik T, Mintz GS, Skalicka H, Kral A, Horak J, Skulec R, et al. Virtual histology evaluation of atherosclerosis regression during atorvastatin and ezetimibe administration: HEAVEN study. Circ J 2012;76(1):176-83.

(137) Kovarnik T, Kral A, Skalicka H, Mintz GS, Kralik L, Chval M, et al. The prediction of coronary artery disease based on non-invasive examinations and heme oxygenase 1 polymorphism versus virtual histology. J Invasive Cardiol 2013 Jan;25(1):32-7.

(138) Kovarnik T, Kral A, Skalicka H, Skalicka L, Dostal O, Kralik L, et al. Prediction of coronary vessel involvement on the basis of atherosclerosis risk factor analysis. Bratisl Lek Listy 2013;114(7):413-7.

(139) Kroner ES, van Velzen JE, Boogers MJ, Siebelink HM, Schalij MJ, Kroft LJ, et al. Positive remodeling on coronary computed tomography as a marker for plaque vulnerability on virtual histology intravascular ultrasound. Am J Cardiol 2011 Jun 15;107(12):1725-9.

(140) Kubo T, Matsuo Y, Hayashi Y, Yamano T, Tanimoto T, Ino Y, et al. High-sensitivity C-reactive protein and plaque composition in patients with stable angina pectoris: a virtual histology intravascular ultrasound study. Coron Artery Dis 2009 Dec;20(8):531-5.

(141) Kubo T, Maehara A, Mintz GS, Doi H, Tsujita K, Choi SY, et al. The dynamic nature of coronary artery lesion morphology assessed by serial virtual histology intravascular ultrasound tissue characterization. J Am Coll Cardiol 2010 Apr 13;55(15):1590-7.

(142) Kubo T, Maehara A, Mintz GS, Garcia-Garcia HM, Serruys PW, Suzuki T, et al. Analysis of the long-term effects of drug-eluting stents on coronary arterial wall morphology as assessed by virtual histology intravascular ultrasound. Am Heart J 2010 Feb;159(2):271-7.

(143) Kubo T, Nakamura N, Matsuo Y, Okumoto Y, Wu X, Choi SY, et al. Virtual histology intravascular ultrasound compared with optical

coherence tomography for identification of thin-cap fibroatheroma. Int Heart J 2011;52(3):175-9.

(144) Kuchulakanti P, Rha SW, Cheneau E, Satler L, Pichard A, Kent K, et al. Identification of "vulnerable plaque" using virtual histology in angiographically benign looking lesion of proximal left anterior descending artery. Cardiovasc Radiat Med 2003 Oct;4(4):225-7.

(145) Kwon JE, Mintz GS, Kim SW, Oh MS, Min YJ, Kim HK, et al. Relationship between coronary artery plaque composition by virtual histology intravascular ultrasound analysis and brachial-ankle pulse wave velocity in patients with coronary artery disease. Coron Artery Dis 2011 Dec;22(8):565-9.

(146) Kwon TG, Seo YH, Lee CS, Yang DJ, Song IG, Park HW, et al. Discrepancy of calcium detection between gray scale intravascular ultrasound and spectral analysis of radiofrequency data. Int J Cardiol 2013 Sep 10;167(6):2611-6.

(147) Layland J, Wilson AM, Lim I, Whitbourn RJ. Virtual histology: a window to the heart of atherosclerosis. Heart Lung Circ 2011 Oct;20(10):615-21.

(148) Leach C, Bach RG. Atherosclerotic coronary plaque in a patient with the metabolic syndrome: assessment by lesion physiology and intravascular ultrasound virtual histology. J Cardiometab Syndr 2006;1(3):225-7.

(149) Lee CH, Hau WK, Tai BC, Chan MY, Saw B, Phua QH, et al. Adiponectin profile in Asian patients undergoing coronary revascularization and its association with plaque vulnerability: IDEAS-ADIPO study. Obesity (Silver Spring) 2012 Dec;20(12):2451-7.

(150) Lee CS, Seo YH, Yang DJ, Kim KH, Park HW, Yuk HB, et al. Positive Vascular Remodeling in Culprit Coronary Lesion is Associated With Plaque Composition: An Intravascular Ultrasound-Virtual Histology Study. Korean Circ J 2012 Nov;42(11):747-52.

(151) Lee IS, Bourantas CV, Muramatsu T, Gogas BD, Heo JH, Diletti R, et al. Assessment of plaque evolution in coronary bifurcations located beyond everolimus eluting scaffolds: serial intravascular ultrasound virtual histology study. Cardiovasc Ultrasound 2013;11:25.

(152) Lee JH, Youn TJ, Yoon YE, Park JJ, Hong SJ, Chun EJ, et al. Coronary artery stenosis in moyamoya disease: tissue characterization by 256-slice

multi-detector CT and virtual histology. Circulation 2013 May 21;127(20):2063-5.

(153) Lee MG, Jeong MH, Kim DH, Lee KH, Park KH, Sim DS, et al. Can metabolic syndrome predict the vulnerable plaque in patients with stable angina pectoris? Virtual histology-intravascular ultrasound analysis. J Cardiol 2012 May;59(3):266-74.

(154) Lee SW, Hau WK, Kong SL, Chan KK, Chan PH, Lam SC, et al. Virtual histology findings and effects of varying doses of atorvastatin on coronary plaque volume and composition in statin-naive patients: the VENUS study. Circ J 2012;76(11):2662-72.

(155) Lee WS, Kim SW, Ryu WS. Progression and observational frequency of atheromatous plaques in autopsied coronary arteries. Korean Circ J 2009 Oct;39(10):399-407.

(156) Legutko J, Jakala J, Mintz GS, Wizimirski M, Rzeszutko L, Partyka L, et al. Virtual histology-intravascular ultrasound assessment of lesion coverage after angiographically-guided stent implantation in patients with ST Elevation myocardial infarction undergoing primary percutaneous coronary intervention. Am J Cardiol 2012 May 15;109(10):1405-10.

(157) Li XM, Huang CX, Wang TS, Zhuang SW, Zhou H, Tian B. Comparison of coronary plaque composition among patients with acute coronary syndrome and stable coronary artery disease. Chin Med J (Engl) 2008 Mar 20;121(6):534-9.

(158) Lin QF, Luo YK, Zhao ZW, Cai W, Zhen XC, Chen LL. Atherosclerotic plaque identification by virtual histology intravascular ultrasound in a rabbit abdominal aorta model of vulnerable plaque. Exp Biol Med (Maywood) 2013 Nov 1;238(11):1223-32.

(159) Lindsey JB, House JA, Kennedy KF, Marso SP. Diabetes duration is associated with increased thin-cap fibroatheroma detected by intravascular ultrasound with virtual histology. Circ Cardiovasc Interv 2009 Dec;2(6):543-8.

(160) Liu HL, Zhang J, Ma DX, Luo JP, Yang SL, Han W, et al. Coronary plaque characterization of nonculprit or nontarget lesions assessed by analysis of in vivo intracoronary ultrasound radio-frequency data. Chin Med J (Engl) 2009 Mar 20;122(6):622-6.

(161) Liu Y, Liu XB, Qian JY, Li CG, Dai YX, Huang ZY, et al. [Virtual histology intravascular ultrasound assessment of coronary

atherosclerotic plaques in diabetic patients]. Zhonghua Xin Xue Guan Bing Za Zhi 2010 Jun;38(6):497-502.

(162) Loland KH, Bleie O, Strand E, Ueland PM, Nordrehaug JE, Garcia-Garcia HM, et al. Effect of folic acid supplementation on levels of circulating Monocyte Chemoattractant Protein-1 and the presence of intravascular ultrasound derived virtual histology thin-cap fibroatheromas in patients with stable angina pectoris. PLoS One 2013;8(7):e70101.

(163) Lopez-Rueda A, Gonzalez GA, Aguilar PM, Gutierrez J, I, Mayol DA. Intravascular ultrasound and virtual histology of basilar artery atherosclerotic lesion. A case report. Interv Neuroradiol 2011 Dec;17(4):472-6.

(164) Maehara A, Cristea E, Mintz GS, Lansky AJ, Dressler O, Biro S, et al. Definitions and methodology for the grayscale and radiofrequency intravascular ultrasound and coronary angiographic analyses. JACC Cardiovasc Imaging 2012 Mar;5(3 Suppl):S1-S9.

(165) Marso SP, Frutkin AD, Mehta SK, House JA, McCrary JR, Klauss V, et al. Intravascular ultrasound measures of coronary atherosclerosis are

associated with the Framingham risk score: an analysis from a global IVUS registry. EuroIntervention 2009 Jun;5(2):212-8.

(166) Matsuo K, Ueda Y, Tsujimoto M, Hao H, Nishio M, Hirata A, et al. Ruptured plaque and large plaque burden are risks of distal embolisation during percutaneous coronary intervention: evaluation by angioscopy and virtual histology intravascular ultrasound imaging. EuroIntervention 2013 Jun 22;9(2):235-42.

(167) Mazurek T, Kochman J, Kobylecka M, Wilimski R, Filipiak KJ, Krolicki L, et al. Inflammatory activity of pericoronary adipose tissue may affect plaque composition in patients with acute coronary syndrome without persistent ST-segment elevation - PVAT in NSTE-ACS: preliminary results. Kardiol Pol 2013 Dec 2.

(168) Mercado N, Moe TG, Pieper M, House JA, Dolla WJ, Seifert L, et al. Tissue characterisation of atherosclerotic plaque in the left main: an in vivo intravascular ultrasound radiofrequency data analysis. EuroIntervention 2011 Jul;7(3):347-52.

(169) Michalak M, Huczek Z, Filipiak KJ, Roik MF, Kochman J, Opolski G. Periprocedural myocardial damage during percutaneous coronary

intervention: a point-of-care platelet testing and intravascular ultrasound/virtual histology study. Kardiol Pol 2013;71(4):325-33.

(170) Missel E, Mintz GS, Carlier SG, Sano K, Qian J, Kaple RK, et al. Necrotic core and its ratio to dense calcium are predictors of high-risk non-ST-elevation acute coronary syndrome. Am J Cardiol 2008 Mar 1;101(5):573-8.

(171) Missel E, Mintz GS, Carlier SG, Qian J, Shan S, Castellanos C, et al. In vivo virtual histology intravascular ultrasound correlates of risk factors for sudden coronary death in men: results from the prospective, multi-centre virtual histology intravascular ultrasound registry. Eur Heart J 2008 Sep;29(17):2141-7.

(172) Mitani Y, Ohashi H, Sawada H, Ikeyama Y, Hayakawa H, Takabayashi S, et al. In vivo plaque composition and morphology in coronary artery lesions in adolescents and young adults long after Kawasaki disease: a virtual histology-intravascular ultrasound study. Circulation 2009 Jun 2;119(21):2829-36.

(173) Mohlenkamp S, Bose D, Mahabadi AA, Heusch G, Erbel R. On the paradox of exercise: coronary atherosclerosis in an apparently healthy marathon runner. Nat Clin Pract Cardiovasc Med 2007 Jul;4(7):396-401.

(174) Movsesiants MI, Ivanov VA, Trunin IV. [Intravascular ultrasound investigation with virtual hystology in the study of coronary artery lesions]. Kardiologiia 2009;49(12):58-61.

(175) Murray SW, Palmer ND. Intravascular ultrasound and virtual histology interpretation of plaque rupture and thrombus in acute coronary syndromes. Heart 2009 Sep;95(18):1494.

(176) Murray SW, Palmer ND. What is behind the calcium? The relationship between calcium and necrotic core on virtual histology analyses. Eur Heart J 2009 Jan;30(1):125-6.

(177) Murray SW, Stables RH, Palmer ND. Virtual histology imaging in acute coronary syndromes: useful or just a research tool? J Invasive Cardiol 2010 Feb;22(2):84-91.

(178) Murray SW, Stables RH, Hart G, Palmer ND. Defining the magnitude of measurement variability in the virtual histology analysis of acute coronary syndrome plaques. Eur Heart J Cardiovasc Imaging 2013 Feb;14(2):167-74.

(179) Musialek P. Virtual histology intravascular ultrasound evaluation of atherosclerotic carotid artery stenosis: time for fully quantitative image analysis. J Endovasc Ther 2013 Aug;20(4):589-94.

(180) Nakamura R, Ito K, Koide M, Taniguchi T, Irie H, Kinoshita N, et al. [Coronary artery plaque assessment using Volcano Therapeutics' Virtual Histology intravascular ultrasound and temperature guide wire]. J Cardiol 2006 Aug;48(2):85-92.

(181) Nakamura T, Kubo N, Ako J, Momomura S. Angiographic no-reflow phenomenon and plaque characteristics by virtual histology intravascular ultrasound in patients with acute myocardial infarction. J Interv Cardiol 2007 Oct;20(5):335-9.

(182) Nakamura T, Kubo N, Funayama H, Sugawara Y, Ako J, Momomura S. Plaque characteristics of the coronary segment proximal to the culprit lesion in stable and unstable patients. Clin Cardiol 2009 Aug;32(8):E9-12.

(183) Nakamura T, Ogita M, Ako J, Momomura S. Gender differences of plaque characteristics in elderly patients with stable angina pectoris: an intravascular ultrasonic radiofrequency data analysis. Int J Vasc Med 2010;2010:134692.

(184) Nakazawa G, Finn AV, Virmani R. Virtual histology: does it add anything? Heart 2007 Aug;93(8):897-8.

(185) Nasu K, Tsuchikane E, Katoh O, Vince DG, Virmani R, Surmely JF, et al. Accuracy of in vivo coronary plaque morphology assessment: a validation study of in vivo virtual histology compared with in vitro histopathology. J Am Coll Cardiol 2006 Jun 20;47(12):2405-12.

(186) Nasu K, Tsuchikane E, Katoh O, Vince DG, Margolis PM, Virmani R, et al. Impact of intramural thrombus in coronary arteries on the accuracy of tissue characterization by in vivo intravascular ultrasound radiofrequency data analysis. Am J Cardiol 2008 Apr 15;101(8):1079-83.

(187) Nasu K, Tsuchikane E, Katoh O, Fujita H, Surmely JF, Ehara M, et al. Plaque characterisation by Virtual Histology intravascular ultrasound analysis in patients with type 2 diabetes. Heart 2008 Apr;94(4):429-33.

(188) Nasu K, Tsuchikane E, Katoh O, Tanaka N, Kimura M, Ehara M, et al. Effect of fluvastatin on progression of coronary atherosclerotic plaque evaluated by virtual histology intravascular ultrasound. JACC Cardiovasc Interv 2009 Jul;2(7):689-96.

(189) Nasu K, Terashima M, Habara M, Ko E, Ito T, Yokota D, et al. Impact of cholesterol metabolism on coronary plaque vulnerability of target vessels: a combined analysis of virtual histology intravascular ultrasound and optical coherence tomography. JACC Cardiovasc Interv 2013 Jul;6(7):746-55.

(190) Nozue T, Yamamoto S, Tohyama S, Umezawa S, Kunishima T, Sato A, et al. Treatment with statin on atheroma regression evaluated by intravascular ultrasound with Virtual Histology (TRUTH Study): rationale and design. Circ J 2009 Feb;73(2):352-5.

(191) Nozue T, Yamamoto S, Tohyama S, Fukui K, Umezawa S, Onishi Y, et al. Impacts of conventional coronary risk factors, diabetes and hypertension, on coronary atherosclerosis during statin therapy: subanalysis of the TRUTH study. Coron Artery Dis 2012 Jun;23(4):239-44.

(192) Nozue T, Yamamoto S, Tohyama S, Fukui K, Umezawa S, Onishi Y, et al. Impact of diabetes mellitus on coronary atherosclerosis and plaque composition under statin therapy - subanalysis of the TRUTH study -. Circ J 2012;76(9):2188-96.

(193) Nozue T, Yamamoto S, Tohyama S, Umezawa S, Kunishima T, Sato A, et al. Statin treatment for coronary artery plaque composition based on intravascular ultrasound radiofrequency data analysis. Am Heart J 2012 Feb;163(2):191-9.

(194) Nozue T, Yamamoto S, Tohyama S, Fukui K, Umezawa S, Onishi Y, et al. Comparison of arterial remodeling and changes in plaque composition between patients with progression versus regression of coronary atherosclerosis during statin therapy (from the TRUTH study). Am J Cardiol 2012 May 1;109(9):1247-53.

(195) Nozue T, Yamamoto S, Tohyama S, Fukui K, Umezawa S, Onishi Y, et al. Comparison of change in coronary atherosclerosis in patients with stable versus unstable angina pectoris receiving statin therapy (from the Treatment With Statin on Atheroma Regression Evaluated by Intravascular Ultrasound With Virtual Histology [TRUTH] study). Am J Cardiol 2013 Apr 1;111(7):923-9.

(196) Nozue T, Yamamoto S, Tohyama S, Fukui K, Umezawa S, Onishi Y, et al. Effects of serum n-3 to n-6 polyunsaturated fatty acids ratios on coronary atherosclerosis in statin-treated patients with coronary artery disease. Am J Cardiol 2013 Jan 1;111(1):6-11.

(197) Nozue T, Fukui K, Yamamoto S, Kunishima T, Umezawa S, Onishi Y, et al. Time course of statin-induced changes in coronary atherosclerosis using intravascular ultrasound with virtual histology. Coron Artery Dis 2013 Sep;24(6):481-6.

(198) Nozue T, Fukui K, Yamamoto S, Kunishima T, Umezawa S, Onishi Y, et al. C-reactive protein and future cardiovascular events in statin-treated patients with angina pectoris: the extended TRUTH study. J Atheroscler Thromb 2013;20(9):717-25.

(199) Nozue T, Yamamoto S, Tohyama S, Fukui K, Umezawa S, Onishi Y, et al. Impacts of age on coronary atherosclerosis and vascular response to statin therapy. Heart Vessels 2013 Jun 30.

(200) Nozue T, Yamamoto S, Tohyama S, Fukui K, Umezawa S, Onishi Y, et al. A predictor of atheroma progression in patients achieving very low levels of low-density lipoprotein cholesterol. Am J Cardiovasc Dis 2013;3(4):255-63.

(201) Nozue T, Yamamoto S, Tohyama S, Fukui K, Umezawa S, Onishi Y, et al. Comparison of effects of serum n-3 to n-6 polyunsaturated fatty acid ratios on coronary atherosclerosis in patients treated with pitavastatin or

pravastatin undergoing percutaneous coronary intervention. Am J Cardiol 2013 Jun 1;111(11):1570-5.

(202) Obaid DR, Calvert PA, McNab D, West NE, Bennett MR. Identification of coronary plaque sub-types using virtual histology intravascular ultrasound is affected by inter-observer variability and differences in plaque definitions. Circ Cardiovasc Imaging 2012 Jan;5(1):86-93.

(203) Obaid DR, Calvert PA, Gopalan D, Parker RA, Hoole SP, West NE, et al. Atherosclerotic plaque composition and classification identified by coronary computed tomography: assessment of computed tomography-generated plaque maps compared with virtual histology intravascular ultrasound and histology. Circ Cardiovasc Imaging 2013 Sep;6(5):655-64.

(204) Ogasawara D, Shite J, Shinke T, Watanabe S, Otake H, Tanino Y, et al. Pioglitazone reduces the necrotic-core component in coronary plaque in association with enhanced plasma adiponectin in patients with type 2 diabetes mellitus. Circ J 2009 Feb;73(2):343-51.

(205) Ogita M, Funayama H, Nakamura T, Sakakura K, Sugawara Y, Kubo N, et al. Plaque characterization of non-culprit lesions by virtual histology

intravascular ultrasound in diabetic patients: impact of renal function. J Cardiol 2009 Aug;54(1):59-65.

(206) Ohshima K, Ikeda S, Watanabe K, Yamane K, Izumi N, Ishibashi K, et al. Relationship between plaque composition and no-reflow phenomenon following primary angioplasty in patients with ST-segment elevation myocardial infarction--analysis with virtual histology intravascular ultrasound. J Cardiol 2009 Oct;54(2):205-13.

(207) Ohshima K, Ikeda S, Kadota H, Yamane K, Izumi N, Kawazoe H, et al. Cavity volume of ruptured plaque is an independent predictor for angiographic no-reflow phenomenon during primary angioplasty in patients with ST-segment elevation myocardial infarction. J Cardiol 2011 Jan;57(1):36-43.

(208) Ohshima K, Ikeda S, Kadota H, Yamane K, Izumi N, Ohshima K, et al. Impact of culprit plaque volume and composition on myocardial microcirculation following primary angioplasty in patients with ST-segment elevation myocardial infarction: virtual histology intravascular ultrasound analysis. Int J Cardiol 2013 Aug 10;167(3):1000-5.

(209) Okubo M, Kawasaki M, Ishihara Y, Takeyama U, Yasuda S, Kubota T, et al. Tissue characterization of coronary plaques: comparison of

integrated backscatter intravascular ultrasound with virtual histology intravascular ultrasound. Circ J 2008 Oct;72(10):1631-9.

(210) Otake H, Shite J, Shinke T, Watanabe S, Tanino Y, Ogasawara D, et al. Relation between plasma adiponectin, high-sensitivity C-reactive protein, and coronary plaque components in patients with acute coronary syndrome. Am J Cardiol 2008 Jan 1;101(1):1-7.

(211) Papadopoulou SL, Brugaletta S, Garcia-Garcia HM, Rossi A, Girasis C, Dharampal AS, et al. Assessment of atherosclerotic plaques at coronary bifurcations with multidetector computed tomography angiography and intravascular ultrasound-virtual histology. Eur Heart J Cardiovasc Imaging 2012 Aug;13(8):635-42.

(212) Papaioannou TG, Schizas D, Vavuranakis M, Katsarou O, Soulis D, Stefanadis C. Quantification of new structural features of coronary plaques by computational post-hoc analysis of virtual histology-intravascular ultrasound images. Comput Methods Biomech Biomed Engin 2012 Sep 13.

(213) Paramo JA, Rodriguez Ja JA, Orbe J. Integrating soluble biomarkers and imaging technologies in the identification of vulnerable atherosclerotic patients. Biomark Insights 2007;1:165-73.

(214) Park JP, Lee BK, Shim JM, Kim SH, Lee CW, Kang DH, et al. Relationship between multiple plasma biomarkers and vulnerable plaque determined by virtual histology intravascular ultrasound. Circ J 2010 Feb;74(2):332-6.

(215) Park JS, Choi SY, Zheng M, Yang HM, Lim HS, Choi BJ, et al. Epicardial adipose tissue thickness is a predictor for plaque vulnerability in patients with significant coronary artery disease. Atherosclerosis 2013 Jan;226(1):134-9.

(216) Pawlowski T, Mintz GS, Kulawik T, Gil RJ. Virtual histology intravascular ultrasound evaluation of the left anterior descending coronary artery in patients with transient left ventricular ballooning syndrome. Kardiol Pol 2010 Oct;68(10):1093-8.

(217) Philipp S, Bose D, Wijns W, Marso SP, Schwartz RS, Konig A, et al. Do systemic risk factors impact invasive findings from virtual histology? Insights from the international virtual histology registry. Eur Heart J 2010 Jan;31(2):196-202.

(218) Prasad A, Cipher DJ, Prasad A, Mohandas A, Roesle M, Brilakis ES, et al. Reproducibility of intravascular ultrasound virtual histology analysis. Cardiovasc Revasc Med 2008 Apr;9(2):71-7.

(219) Pu J, Mintz GS, Brilakis ES, Banerjee S, Abdel-Karim AR, Maini B, et al. In vivo characterization of coronary plaques: novel findings from comparing greyscale and virtual histology intravascular ultrasound and near-infrared spectroscopy. Eur Heart J 2012 Feb;33(3):372-83.

(220) Pundziute G, Schuijf JD, Jukema JW, Decramer I, Sarno G, Vanhoenacker PK, et al. Head-to-head comparison of coronary plaque evaluation between multislice computed tomography and intravascular ultrasound radiofrequency data analysis. JACC Cardiovasc Interv 2008 Apr;1(2):176-82.

(221) Pundziute G, Schuijf JD, Jukema JW, Decramer I, Sarno G, Vanhoenacker PK, et al. Evaluation of plaque characteristics in acute coronary syndromes: non-invasive assessment with multi-slice computed tomography and invasive evaluation with intravascular ultrasound radiofrequency data analysis. Eur Heart J 2008 Oct;29(19):2373-81.

(222) Pundziute G, Schuijf JD, Jukema JW, van Werkhoven JM, Nucifora G, Decramer I, et al. Type 2 diabetes is associated with more advanced coronary atherosclerosis on multislice computed tomography and

virtual histology intravascular ultrasound. J Nucl Cardiol 2009 May;16(3):376-83.

(223) Pundziute G, Schuijf JD, van Velzen JE, Jukema JW, van Werkhoven JM, Nucifora G, et al. Assessment with multi-slice computed tomography and gray-scale and virtual histology intravascular ultrasound of gender-specific differences in extent and composition of coronary atherosclerotic plaques in relation to age. Am J Cardiol 2010 Feb 15;105(4):480-6.

(224) Qian J, Maehara A, Mintz GS, Margolis MP, Biro S, Stone GW, et al. Relation between individual plaque components and overall plaque burden in the prospective, multicenter virtual histology intravascular ultrasound registry. Am J Cardiol 2009 Aug 15;104(4):501-6.

(225) Qian J, Maehara A, Mintz GS, Margolis MP, Lerman A, Rogers J, et al. Impact of gender and age on in vivo virtual histology-intravascular ultrasound imaging plaque characterization (from the global Virtual Histology Intravascular Ultrasound [VH-IVUS] registry). Am J Cardiol 2009 May 1;103(9):1210-4.

(226) Qian JY. Detection of vulnerable plaques rather than the culprit lesions in patients with acute coronary syndrome using virtual histology

intravascular ultrasound imaging. Chin Med J (Engl) 2009 Mar 20;122(6):610-1.

(227) Raber L, Heo JH, Radu MD, Garcia-Garcia HM, Stefanini GG, Moschovitis A, et al. Offline fusion of co-registered intravascular ultrasound and frequency domain optical coherence tomography images for the analysis of human atherosclerotic plaques. EuroIntervention 2012 May 15;8(1):98-108.

(228) Ramcharitar S, Gonzalo N, van Geuns RJ, Garcia-Garcia HM, Wykrzykowska JJ, Ligthart JM, et al. First case of stenting of a vulnerable plaque in the SECRITT I trial-the dawn of a new era? Nat Rev Cardiol 2009 May;6(5):374-8.

(229) Rdzanek A, Kochman J, Pietrasik A, Wilczynska J, Rancic M, Opolski G. The prevalence of potentially unstable coronary lesions in patients with coronary artery disease--virtual histology study. Kardiol Pol 2008 Mar;66(3):244-50, discussion.

(230) Ribamar CJ, Jr., Abizaid A, Sousa A, Siqueira D, Chamie D, Feres F, et al. Serial greyscale and radiofrequency intravascular ultrasound assessment of plaque modification and vessel geometry at proximal and

distal edges of bare metal and first-generation drug-eluting stents. EuroIntervention 2012 Jun 20;8(2):225-34.

(231) Rieber J. [Intravascular imaging and its integration into coronary angiography]. Dtsch Med Wochenschr 2012 Apr;137(14):726-31.

(232) Rodriguez-Granillo GA, Aoki J, Ong AT, Valgimigli M, van Mieghem CA, Regar E, et al. Methodological considerations and approach to cross-technique comparisons using in vivo coronary plaque characterization based on intravascular ultrasound radiofrequency data analysis: insights from the Integrated Biomarker and Imaging Study (IBIS). Int J Cardiovasc Intervent 2005;7(1):52-8.

(233) Rodriguez-Granillo GA, Garcia-Garcia HM, Mc Fadden EP, Valgimigli M, Aoki J, de FP, et al. In vivo intravascular ultrasound-derived thin-cap fibroatheroma detection using ultrasound radiofrequency data analysis. J Am Coll Cardiol 2005 Dec 6;46(11):2038-42.

(234) Rodriguez-Granillo GA, Bruining N, Mc FE, Ligthart JM, Aoki J, Regar E, et al. Geometrical validation of intravascular ultrasound radiofrequency data analysis (Virtual Histology) acquired with a 30 MHz boston scientific corporation imaging catheter. Catheter Cardiovasc Interv 2005 Dec;66(4):514-8.

(235) Rodriguez-Granillo GA, Serruys PW, McFadden EP, van Mieghem CA, Goedhart D, Bruining N, et al. First-in-man prospective evaluation of temporal changes in coronary plaque composition by in vivo intravascular ultrasound radiofrequency data analysis: an Integrated Biomarker and Imaging Study (IBIS) substudy. EuroIntervention 2005 Nov;1(3):282-8.

(236) Rodriguez-Granillo GA, Serruys PW, Garcia-Garcia HM, Aoki J, Valgimigli M, van Mieghem CA, et al. Coronary artery remodelling is related to plaque composition. Heart 2006 Mar;92(3):388-91.

(237) Rodriguez-Granillo GA, McFadden EP, Valgimigli M, van Mieghem CA, Regar E, de Feyter PJ, et al. Coronary plaque composition of nonculprit lesions, assessed by in vivo intracoronary ultrasound radio frequency data analysis, is related to clinical presentation. Am Heart J 2006 May;151(5):1020-4.

(238) Rogers JH, Wegelin J, Harder K, Valente R, Low R. Assessment of FFR-negative intermediate coronary artery stenoses by spectral analysis of the radiofrequency intravascular ultrasound signal. J Invasive Cardiol 2006 Oct;18(10):448-53.

(239) Ryou HS, Kim S, Kim SW, Cho SW. Construction of healthy arteries using computed tomography and virtual histology intravascular ultrasound. J Biomech 2012 Jun 1;45(9):1612-8.

(240) Sakata K, Kawashiri MA, Ino H, Matsubara T, Uno Y, Yasuda T, et al. Intravascular ultrasound appearance of scattered necrotic core as an index for deterioration of coronary flow during intervention in acute coronary syndrome. Heart Vessels 2012 Sep;27(5):443-52.

(241) Sales FJ, Falcao BA, Falcao JL, Ribeiro EE, Perin MA, Horta PE, et al. Evaluation of plaque composition by intravascular ultrasound "virtual histology": the impact of dense calcium on the measurement of necrotic tissue. EuroIntervention 2010 Aug;6(3):394-9.

(242) Samady H, Eshtehardi P, McDaniel MC, Suo J, Dhawan SS, Maynard C, et al. Coronary artery wall shear stress is associated with progression and transformation of atherosclerotic plaque and arterial remodeling in patients with coronary artery disease. Circulation 2011 Aug 16;124(7):779-88.

(243) Sanchez-Elvira G, Coma-Canella I, Artaiz M, Paramo JA, Barba J, Calabuig J. Characterization of coronary plaques with combined use of

intravascular ultrasound, virtual histology and optical coherence tomography. Heart Int 2010 Dec 31;5(2):e12.

(244) Sangiorgi G, Bedogni F, Sganzerla P, Binetti G, Inglese L, Musialek P, et al. The Virtual histology In CaroTids Observational RegistrY (VICTORY) study: a European prospective registry to assess the feasibility and safety of intravascular ultrasound and virtual histology during carotid interventions. Int J Cardiol 2013 Oct 3;168(3):2089-93.

(245) Sangiorgi GM, Clementi F, Cola C, Biondi-Zoccai G. Plaque vulnerability and related coronary event prediction by intravascular ultrasound with virtual histology: "it's a long way to tipperary"? Catheter Cardiovasc Interv 2007 Aug 1;70(2):203-10.

(246) Sanidas EA, Maehara A, Mintz GS, Kashiyama T, Guo J, Pu J, et al. Angioscopic and virtual histology intravascular ultrasound characteristics of culprit lesion morphology underlying coronary artery thrombosis. Am J Cardiol 2011 May 1;107(9):1285-90.

(247) Sanidas EA, Mintz GS, Maehara A, Cristea E, Wennerblom B, Iniguez A, et al. Adverse cardiovascular events arising from atherosclerotic lesions with and without angiographic disease progression. JACC Cardiovasc Imaging 2012 Mar;5(3 Suppl):S95-S105.

(248) Sanon S, Patel R, Eshelbrenner C, Sanon VP, Alhaddad M, Oliveros R, et al. Acute coronary syndrome in patients with diabetes mellitus: perspectives of an interventional cardiologist. Am J Cardiol 2012 Nov 6;110(9 Suppl):13B-23B.

(249) Sarno G, Onuma Y, Garcia Garcia HM, Garg S, Regar E, Thuesen L, et al. IVUS radiofrequency analysis in the evaluation of the polymeric struts of the bioabsorbable everolimus-eluting device during the bioabsorption process. Catheter Cardiovasc Interv 2010 May 1;75(6):914-8.

(250) Sarno G, Garg S, Gomez-Lara J, Garcia Garcia HM, Ligthart J, Bruining N, et al. Intravascular ultrasound radiofrequency analysis after optimal coronary stenting with initial quantitative coronary angiography guidance: an ATHEROREMO sub-study. EuroIntervention 2011 Mar;6(8):977-84.

(251) Sato T, Kameyama T, Noto T, Nozawa T, Inoue H. Impact of preinterventional plaque composition and eccentricity on late-acquired incomplete stent apposition after sirolimus-eluting stent implantation: an intravascular ultrasound radiofrequency analysis. Coron Artery Dis 2012 Nov;23(7):432-7.

(252) Satoh S, Mori E, Takenaka K, Mori T, Inoue H, Numaguchi K, et al. Relationships between inflammatory mediators and coronary plaque composition in patients with stable angina investigated by ultrasound radiofrequency data analysis. Cardiovasc Interv Ther 2011 Sep;26(3):193-201.

(253) Saunamaki KI. Virtual histology and the hunt for the vulnerable plaque. Eur Heart J 2006 Dec;27(24):2914-5.

(254) Sawada T, Shite J, Shinke T, Watanabe S, Otake H, Matsumoto D, et al. [Relationship between high sensitive C-reactive protein and coronary plaque component in patients with acute coronary syndrome: Virtual Histology study]. J Cardiol 2006 Sep;48(3):141-50.

(255) Sawada T, Shite J, Garcia-Garcia HM, Shinke T, Watanabe S, Otake H, et al. Feasibility of combined use of intravascular ultrasound radiofrequency data analysis and optical coherence tomography for detecting thin-cap fibroatheroma. Eur Heart J 2008 May;29(9):1136-46.

(256) Sawada T, Shite J, Shinke T, Otake H, Tanino Y, Ogasawara D, et al. Low plasma adiponectin levels are associated with presence of thin-cap fibroatheroma in men with stable coronary artery disease. Int J Cardiol 2010 Jul 23;142(3):250-6.

(257) Sawada T, Emoto T, Motoji Y, Hashimoto M, Kageyama H, Terashita D, et al. Possible association between non-invasive parameter of flow-mediated dilatation in brachial artery and whole coronary plaque vulnerability in patients with coronary artery disease. Int J Cardiol 2013 Jul 1;166(3):613-20.

(258) Schoenenberger AW, Urbanek N, Toggweiler S, Stuck AE, Resink TJ, Erne P. Ultrasound-assessed non-culprit and culprit coronary vessels differ by age and gender. World J Cardiol 2013 Mar 26;5(3):42-8.

(259) Seo YH, Lee CS, Yuk HB, Yang DJ, Park HW, Kim KH, et al. Hypercholesterolemia and in-vivo coronary plaque composition in patients with coronary artery disease: a virtual histology - intravascular ultrasound study. Korean Circ J 2013 Jan;43(1):23-8.

(260) Shin ES, Garcia-Garcia HM, Serruys PW. A new method to measure necrotic core and calcium content in coronary plaques using intravascular ultrasound radiofrequency-based analysis. Int J Cardiovasc Imaging 2010 Apr;26(4):387-96.

(261) Shin ES, Garcia-Garcia HM, Ligthart JM, Witberg K, Schultz C, van der Steen AF, et al. In vivo findings of tissue characteristics using iMap

IVUS and Virtual Histology IVUS. EuroIntervention 2011 Mar;6(8):1017-9.

(262) Shin ES, Garcia-Garcia HM, Garg S, Serruys PW. A comparison between plaque-based and vessel-based measurement for plaque component using volumetric intravascular ultrasound radiofrequency data analysis. Int J Cardiovasc Imaging 2011 Apr;27(4):491-7.

(263) Shin ES, Garcia-Garcia HM, Garg S, Park J, Kim SJ, Serruys PW. The assessment of Shin's method for the prediction of creatinine kinase-MB elevation after percutaneous coronary intervention: an intravascular ultrasound study. Int J Cardiovasc Imaging 2011 Jul;27(6):883-92.

(264) Shin ES, Garcia-Garcia HM, Garg S, Ligthart J, Thuesen L, Dudek D, et al. Assessment of the serial changes of vessel wall contents in atherosclerotic coronary lesion with bioresorbable everolimus-eluting vascular scaffolds using Shin's method: an IVUS study. Int J Cardiovasc Imaging 2011 Oct;27(7):931-7.

(265) Shin ES, Garcia-Garcia HM, Sarno G, Thuesen L, Dudek D, Ormiston JA, et al. Reproducibility of Shin's method for necrotic core and calcium content in atherosclerotic coronary lesions treated with bioresorbable everolimus-eluting vascular scaffolds using volumetric intravascular

ultrasound radiofrequency-based analysis. Int J Cardiovasc Imaging 2012 Jan;28(1):43-9.

(266) Shin ES, Garcia-Garcia HM, Okamura T, Serruys PW. Effect of statins on coronary bifurcation atherosclerosis: an intravascular ultrasound virtual histology study. Int J Cardiovasc Imaging 2012 Oct;28(7):1643-52.

(267) Simsek C, Garcia-Garcia HM, van Geuns RJ, Magro M, Girasis C, van MN, et al. The ability of high dose rosuvastatin to improve plaque composition in non-intervened coronary arteries: rationale and design of the Integrated Biomarker and Imaging Study-3 (IBIS-3). EuroIntervention 2012 Jun 20;8(2):235-41.

(268) Siqueira DA, Sousa AG, Costa Junior JR, da Costa RA, Staico R, Tanajura LF, et al. Correlation between plaque composition as assessed by virtual histology and C-reactive protein. Arq Bras Cardiol 2013 Jul;101(1):78-86.

(269) Sonka M, Downe RW, Garvin JW, Lopez J, Kovarnik T, Wahle A. IVUS-based assessment of 3D morphology and virtual histology: prediction of atherosclerotic plaque status and changes. Conf Proc IEEE Eng Med Biol Soc 2011;2011:6647-50.

(270) Stone GW, Mintz GS. Letter by Stone and Mintz regarding article, "unreliable assessment of necrotic core by virtual histology intravascular ultrasound in porcine coronary artery disease". Circ Cardiovasc Imaging 2010 Sep;3(5):e4.

(271) Sudarski S, Fink C, Sueselbeck T, Kayed H, Schoenberg SO, Borggrefe M, et al. Quantitative analysis of coronary plaque composition by dual-source CT in patients with acute non-ST-elevation myocardial infarction compared to patients with stable coronary artery disease correlated with virtual histology intravascular ultrasound. Acad Radiol 2013 Aug;20(8):995-1003.

(272) Sukiennik A, Radomski M, Rychter M, Kubica J. Usefulness of optical coherence tomography in the assessment of atherosclerotic culprit lesions in acute coronary syndromes. Comparison with intravascular ultrasound and virtual histology. Cardiol J 2008;15(6):561-3.

(273) Surmely JF, Nasu K, Fujita H, Terashima M, Matsubara T, Tsuchikane E, et al. Coronary plaque composition of culprit/target lesions according to the clinical presentation: a virtual histology intravascular ultrasound analysis. Eur Heart J 2006 Dec;27(24):2939-44.

(274) Surmely JF, Nasu K, Fujita H, Terashima M, Matsubara T, Tsuchikane E, et al. Association of coronary plaque composition and arterial remodelling: a virtual histology analysis by intravascular ultrasound. Heart 2007 Aug;93(8):928-32.

(275) Suter Y, Schoenenberger AW, Toggweiler S, Jamshidi P, Resink T, Erne P. Intravascular ultrasound-based left main coronary artery assessment: comparison between pullback from left anterior descending and circumflex arteries. J Invasive Cardiol 2009 Sep;21(9):457-60.

(276) Taguchi I, Oda K, Yoneda S, Kageyama M, Kanaya T, Toyoda S, et al. Evaluation of serial changes in tissue characteristics during statin-induced plaque regression using virtual histology-intravascular ultrasound studies. Am J Cardiol 2013 May 1;111(9):1246-52.

(277) Taki A, Hetterich H, Roodaki A, Setarehdan SK, Unal G, Rieber J, et al. A new approach for improving coronary plaque component analysis based on intravascular ultrasound images. Ultrasound Med Biol 2010 Aug;36(8):1245-58.

(278) Taki A, Roodaki A, Setarehdan SK, Avansari S, Unal G, Navab N. An IVUS image-based approach for improvement of coronary plaque characterization. Comput Biol Med 2013 May 1;43(4):268-80.

(279) Tan A, Hau W, Ho HH, Maralani HG, Loo G, Khoo SM, et al. Obstructive Sleep Apnea and Coronary Plaque Characteristics. Chest 2013 Oct 31.

(280) Thim T, Hagensen MK, Wallace-Bradley D, Granada JF, Kaluza GL, Drouet L, et al. Unreliable assessment of necrotic core by virtual histology intravascular ultrasound in porcine coronary artery disease. Circ Cardiovasc Imaging 2010 Jul;3(4):384-91.

(281) Tian J, Gu X, Sun Y, Ban X, Xiao Y, Hu S, et al. Effect of statin therapy on the progression of coronary atherosclerosis. BMC Cardiovasc Disord 2012;12:70.

(282) Timaran CH, Rosero EB, Martinez AE, Ilarraza A, Modrall JG, Clagett GP. Atherosclerotic plaque composition assessed by virtual histology intravascular ultrasound and cerebral embolization after carotid stenting. J Vasc Surg 2010 Nov;52(5):1188-94.

(283) Timmins LH, Suever JD, Eshtehardi P, McDaniel MC, Oshinski JN, Samady H, et al. Framework to Co-register Longitudinal Virtual Histology-Intravascular Ultrasound Data in the Circumferential Direction. IEEE Trans Med Imaging 2013 Nov;32(11):1989-96.

(284) Toggweiler S, Suter Y, Schoenenberger AW, Kaspar M, Jamshidi P, Erne P. Differences in coronary artery plaques between target and non-target vessels. J Invasive Cardiol 2009 Nov;21(11):584-7.

(285) Toggweiler S, Urbanek N, Schoenenberger AW, Erne P. Analysis of coronary bifurcations by intravascular ultrasound and virtual histology. Atherosclerosis 2010 Oct;212(2):524-7.

(286) Toi T, Taguchi I, Yoneda S, Kageyama M, Kikuchi A, Tokura M, et al. Early effect of lipid-lowering therapy with pitavastatin on regression of coronary atherosclerotic plaque. Comparison with atorvastatin. Circ J 2009 Aug;73(8):1466-72.

(287) Tsui PT, Lau CL. Severe plaque prolapse after stenting a lesion with large areas of necrotic core. BMJ Case Rep 2009;2009:bcr2006104190.

(288) Tsujita K, Sakamoto K, Kojima S, Kojima S, Takaoka N, Nagayoshi Y, et al. Coronary plaque component in patients with vasospastic angina: a virtual histology intravascular ultrasound study. Int J Cardiol 2013 Oct 3;168(3):2411-5.

(289) Tsurumi A, Tsurumi Y, Hososhima O, Matsubara N, Izumi T, Miyachi S. Virtual histology analysis of carotid atherosclerotic plaque: plaque

composition at the minimum lumen site and of the entire carotid plaque. J Neuroimaging 2013 Jan;23(1):12-7.

(289) Uren NG, Schwarzacher SP, Metz JA, Lee DP, Honda Y, Yeung AC, Fitzgerald PJ, Yock PG; POST Registry Investigators Predictors and outcomes of stent thrombosis: an intravascular ultrasound registry. Eur Heart J. 2002 Jan; 23(2):124-32.

(290) Valgimigli M, Rodriguez-Granillo GA, Garcia-Garcia HM, Malagutti P, Regar E, de JP, et al. Distance from the ostium as an independent determinant of coronary plaque composition in vivo: an intravascular ultrasound study based radiofrequency data analysis in humans. Eur Heart J 2006 Mar;27(6):655-63.

(291) Valgimigli M, Rodriguez-Granillo GA, Garcia-Garcia HM, Vaina S, de JP, de FP, et al. Plaque composition in the left main stem mimics the distal but not the proximal tract of the left coronary artery: influence of clinical presentation, length of the left main trunk, lipid profile, and systemic levels of C-reactive protein. J Am Coll Cardiol 2007 Jan 2;49(1):23-31.

(292) van Velzen JE, Schuijf JD, de Graaf FR, Nucifora G, Pundziute G, Jukema JW, et al. Plaque type and composition as evaluated non-

invasively by MSCT angiography and invasively by VH IVUS in relation to the degree of stenosis. Heart 2009 Dec;95(24):1990-6.

(293) van Velzen JE, de Graaf FR, Jukema JW, de Grooth GJ, Pundziute G, Kroft LJ, et al. Comparison of the relation between the calcium score and plaque characteristics in patients with acute coronary syndrome versus patients with stable coronary artery disease, assessed by computed tomography angiography and virtual histology intravascular ultrasound. Am J Cardiol 2011 Sep 1;108(5):658-64.

(294) Van HJ, De MG, Ennekens G, Van HP, Herman A, Vrints C. Validation of in vivo plaque characterisation by virtual histology in a rabbit model of atherosclerosis. EuroIntervention 2009 May;5(1):149-56.

(295) Virmani R, Nakazawa G. Animal models and virtual histology. Arterioscler Thromb Vasc Biol 2007 Jul;27(7):1666-8.

(296) Voros S, Rinehart S, Qian Z, Joshi P, Vazquez G, Fischer C, et al. Coronary atherosclerosis imaging by coronary CT angiography: current status, correlation with intravascular interrogation and meta-analysis. JACC Cardiovasc Imaging 2011 May;4(5):537-48.

(297) Voros S, Rinehart S, Qian Z, Vazquez G, Anderson H, Murrieta L, et al. Prospective validation of standardized, 3-dimensional, quantitative coronary computed tomographic plaque measurements using radiofrequency backscatter intravascular ultrasound as reference standard in intermediate coronary arterial lesions: results from the ATLANTA (assessment of tissue characteristics, lesion morphology, and hemodynamics by angiography with fractional flow reserve, intravascular ultrasound and virtual histology, and noninvasive computed tomography in atherosclerotic plaques) I study. JACC Cardiovasc Interv 2011 Feb;4(2):198-208.

(298) Waksman R, Legutko J, Singh J, Orlando Q, Marso S, Schloss T, et al. FIRST: Fractional Flow Reserve and Intravascular Ultrasound Relationship Study. J Am Coll Cardiol 2013 Mar 5;61(9):917-23.

(299) Wang TS, Li XM, Zhuang SW, Tian B, Jin C, Wang S, et al. [Comparison of coronary plaque composition between patients with acute coronary syndrome and stable coronary artery disease]. Zhonghua Xin Xue Guan Bing Za Zhi 2008 Nov;36(11):994-8.

(300) Wentzel JJ, Schuurbiers JC, Lopez NG, Gijsen FJ, van der Giessen AG, Groen HC, et al. In vivo assessment of the relationship between shear

stress and necrotic core in early and advanced coronary artery disease. EuroIntervention 2013 Mar 7.

(301) Wood FO, Badhey N, Garcia B, Abdel-Karim AR, Maini B, Banerjee S, et al. Analysis of saphenous vein graft lesion composition using near-infrared spectroscopy and intravascular ultrasonography with virtual histology. Atherosclerosis 2010 Oct;212(2):528-33.

(302) Wu X, Maehara A, Mintz GS, Kubo T, Xu K, Choi SY, et al. Virtual histology intravascular ultrasound analysis of non-culprit attenuated plaques detected by grayscale intravascular ultrasound in patients with acute coronary syndromes. Am J Cardiol 2010 Jan 1;105(1):48-53.

(303) Wykrzykowska JJ, Mintz GS, Garcia-Garcia HM, Maehara A, Fahy M, Xu K, et al. Longitudinal distribution of plaque burden and necrotic core-rich plaques in nonculprit lesions of patients presenting with acute coronary syndromes. JACC Cardiovasc Imaging 2012 Mar;5(3 Suppl):S10-S18.

(304) Wykrzykowska JJ, Diletti R, Gutierrez-Chico JL, van Geuns RJ, van der Giessen WJ, Ramcharitar S, et al. Plaque sealing and passivation with a mechanical self-expanding low outward force nitinol vShield device for the treatment of IVUS and OCT-derived thin cap fibroatheromas

(TCFAs) in native coronary arteries: report of the pilot study vShield Evaluated at Cardiac hospital in Rotterdam for Investigation and Treatment of TCFA (SECRITT). EuroIntervention 2012 Dec 20;8(8):945-54.

(305) Xu Y, Mintz GS, Tam A, McPherson JA, Iniguez A, Fajadet J, et al. Prevalence, distribution, predictors, and outcomes of patients with calcified nodules in native coronary arteries: a 3-vessel intravascular ultrasound analysis from Providing Regional Observations to Study Predictors of Events in the Coronary Tree (PROSPECT). Circulation 2012 Jul 31;126(5):537-45.

(306) Xu ZS, Lee BK, Park DW, Lee SW, Kim YH, Lee CW, et al. Relation of plaque size to compositions as determined by an in vivo volumetric intravascular ultrasound radiofrequency analysis. Int J Cardiovasc Imaging 2010 Feb;26(2):165-71.

(307) Yamada K, Yoshimura S, Kawasaki M, Enomoto Y, Takano K, Asano T, et al. Prediction of silent ischemic lesions after carotid artery stenting using virtual histology intravascular ultrasound. Cerebrovasc Dis 2011;32(2):106-13.

(308) Yamada R, Okura H, Kume T, Neishi Y, Kawamoto T, Miyamoto Y, et al. Target lesion thin-cap fibroatheroma defined by virtual histology intravascular ultrasound affects microvascular injury during percutaneous coronary intervention in patients with angina pectoris. Circ J 2010 Aug;74(8):1658-62.

(309) Yamamoto M, Takano M, Okamatsu K, Murakami D, Inami S, Xie Y, et al. Relationship between thin cap fibroatheroma identified by virtual histology and angioscopic yellow plaque in quantitative analysis with colorimetry. Circ J 2009 Mar;73(3):497-502.

(310) Yamamoto Y, Otani H, Iwasaka J, Park H, Sakuma T, Kamihata H, et al. Comparison of neointimal morphology of in-stent restenosis with sirolimus-eluting stents versus bare metal stents: virtual histology-intravascular ultrasound analysis. Cardiovasc Interv Ther 2011 Sep;26(3):186-92.

(311) Yang DJ, Lee MS, Kim WH, Park HW, Kim KH, Kwon TG, et al. The impact of glucose control on coronary plaque composition in patients with diabetes mellitus. J Invasive Cardiol 2013 Mar;25(3):137-41.

(312) Yang HB, Zhao XY, Zhao YT, Zhang JY, Li L. [Effects of domestic rosuvastatin on coronary plaque in patients with mild-to-moderate

coronary artery stenosis as evaluated by virtual histology-intravascular ultrasound]. Zhonghua Yi Xue Za Zhi 2012 Jun 12;92(22):1550-2.

(313) Yu E, Calvert PA, Mercer JR, Harrison J, Baker L, Figg NL, et al. Mitochondrial DNA damage can promote atherosclerosis independently of reactive oxygen species through effects on smooth muscle cells and monocytes and correlates with higher-risk plaques in humans. Circulation 2013 Aug 13;128(7):702-12.

(314) Yun KH, Mintz GS, Farhat N, Marso SP, Taglieri N, Verheye S, et al. Relation between angiographic lesion severity, vulnerable plaque morphology and future adverse cardiac events (from the Providing Regional Observations to Study Predictors of Events in the Coronary Tree study). Am J Cardiol 2012 Aug 15;110(4):471-7.

(315) Zhao XY, Wang XF, Zhang JY, Du YY, Yang HB. Effect of the composition of atherosclerotic plaques and rate of platelet aggregation on elevation of serum levels of cardiac troponin T after percutaneous coronary interventions. J Interv Cardiol 2012 Oct;25(5):433-8.

(316) Zhao XY, Wang XF, Li L, Zhang JY, Du YY, Yao HM. Plaque characteristics and serum pregnancy-associated plasma protein A levels

predict the no-reflow phenomenon after percutaneous coronary intervention. J Int Med Res 2013 Apr;41(2):307-16.

(317) Zhao Z, Witzenbichler B, Mintz GS, Jaster M, Choi SY, Wu X, et al. Dynamic nature of nonculprit coronary artery lesion morphology in STEMI: a serial IVUS analysis from the HORIZONS-AMI trial. JACC Cardiovasc Imaging 2013 Jan;6(1):86-95.

(318) Zheng M, Choi SY, Tahk SJ, Lim HS, Yang HM, Choi BJ, et al. The relationship between volumetric plaque components and classical cardiovascular risk factors and the metabolic syndrome a 3-vessel coronary artery virtual